

**Site-Directed Mutagenesis of the *Campylobacter jejuni* Fur Box and the
Iron- and Oxygen-Responsive Regulation of *fumC***

Thesis submitted for the degree of

Doctor of Philosophy

at the University of Leicester

by

Ran Ren M.Sc., B.Sc.

Department of Genetics

University of Leicester

December 2011

Site-Directed Mutagenesis of the *Campylobacter jejuni* Fur Box and the Iron- and Oxygen-Responsive Regulation of *fumC*
Ran Ren M.Sc., B.Sc.

For the foodborne enteric pathogen *Campylobacter jejuni*, regulation of iron homeostasis is tightly controlled by the ferric uptake regulator Fur. Fur regulates iron-responsive gene expression by binding to the Fur box sequence and a 19 bp Fur box is positioned within the promoter region of the outer membrane haem receptor gene *chuA*. The fumarase *fumC* Fur box-like sequence shows three mismatches to the consensus sequence and this variation is predicted to be key to the contrasting iron regulation and Fur-Fur box binding affinity between *chuA* and *fumC*. The aims of this study were to determine the functionally important bases in the *C. jejuni* Fur box that are essential for Fur-Fur box interaction and to assess the interplay of iron and oxygen in the modulation of *fumC* expression.

Site-directed mutagenesis of the 1st, 7th, 10th, 13th and 19th positions was carried out for the *chuA* and *fumC* Fur boxes and their interaction with Fur was determined *in vitro* and *in vivo*. Two Fur dimers were determined to bind to the Fur box, and although the 1st, 7th, 13th and 19th positions were found to facilitate the interaction of Fur with the Fur box, the architecture of the promoter region is likely to play a more significant role in Fur regulation. *fumC* encodes the only fumarase in *C. jejuni* and it is essential for cell growth and for maintaining a functional tricarboxylic acid cycle. Further characterisation of *chuA* and *fumC* expression in response to iron and oxygen indicated that both genes are controlled by Fur as well as the peroxide response regulator PerR, and the RacR-RacS two-component system. These observations illustrate the necessity for *C. jejuni* to cooperatively regulate essential gene expressions using its rather limited set of regulators thus allowing it to adapt to various conditions encountered during transmission and colonisation.

Acknowledgements

I would like to take this opportunity to firstly thank Prof. Ketley for his supervision and for providing me with an opportunity to work on this interesting and challenging project. I am also grateful for his endless encouragement and support, and for his witty personality (well, depends on if you get him or not) that inspired me to work for him and made this learning experience more enjoyable.

I would like to acknowledge all the members of laboratory 121 for being there to lend assistance and advice whenever I needed it and for providing me with a supportive and friendly environment to work in. In particular, I would like to thank Dr Haigh for sharing his endless knowledge on pretty much everything (including how to calculate the curvature of the earth), Mrs Hardy for her willingness to help (whether it's work related or not), Dr Johnson for ordering material, Dr Miller for been an AMAZING flatmate and Dr Purves for putting up with my constant harassment about RNA work.

I also need to acknowledge the members of my thesis committee Dr Meacock and Dr Morrissey and my external examiner Prof. Le Brun from the University of East Anglia for their helpful suggestions. Many thanks go to Dr Shearer and Dr van Vliet from the Institute of Food Research; Dr Badge, Dr Bravo and Dr Rahbari from the University of Leicester and Dr Wösten from the Utrecht University for their assistance on RACE, running sequencing gels and RacR/S purification respectively. Thanks also go to my project students Mr Caudle and Mr Gittins for their contributions toward this study.

I need to finally thank the International Office of the University of Leicester and my parents Mr Ren and Mrs Li for their financial support and my wife Mrs Wu for looking after me and constantly listen to me moaning about my work and life in general.

Contents

Abstract	I
Acknowledgements	II
Contents	III
Figures and tables	IX
Abbreviations	XV

Chapter 1: Introduction	1
1.1 Regulation of gene expression	2
1.1.1 Negative gene regulation - the lactose (lac) operon	4
1.1.2 Positive gene regulation - the L-arabinose (ara) operon	9
1.1.3 TCS - the EnvZ-OmpR osmolarity regulatory system	15
1.2 Iron acquisition, Fur and the Fur regulon	21
1.2.1 Iron and iron limitation in host	21
1.2.2 Mechanisms of bacterial iron acquisition and iron storage	25
1.2.2.1 Ferrous iron uptake	25
1.2.2.2 Siderophore-mediated ferric iron uptake	28
1.2.2.3 Ferric iron uptake from transferrin/lactoferrin	37
1.2.2.4 Direct haem uptake and haem uptake from haemoproteins	39
1.2.2.5 Iron and haem storage	41
1.2.3 Fur and the functional role of Fur as a global transcriptional regulator	44
1.2.3.1 Fur as an iron-dependent repressor and its role in iron homeostasis	44
1.2.3.2 Structure-function relationships of Fur	50
1.2.3.3 The Fur box and models of Fur-Fur box interaction	59
1.2.3.4 Fur as a transcriptional activator	64
1.2.3.5 Transcriptional regulation by <i>apo</i> -Fur	67
1.2.3.6 Fur as a global regulator	70
1.2.3.7 Fur homologues and DtxR	73

1.3 The biology of <i>C. jejuni</i>	78
1.3.1 Historic perspective and the genus <i>Campylobacter</i>	78
1.3.2 Physical and genetic characteristics of <i>C. jejuni</i>	80
1.3.3 Transmission and epidemiology	83
1.3.4 Pathogenesis and virulence factors	86
1.3.4.1 Motility	86
1.3.4.2 Chemotaxis	88
1.3.4.3 Adhesion	88
1.3.4.4 Invasion	89
1.3.4.5 Toxin production	90
1.3.5 Gene regulation in <i>C. jejuni</i>	91
1.3.5.1 Sigma factors	91
1.3.5.2 Transcriptional regulators	93
1.4 Iron homeostasis and gene regulation by the <i>C. jejuni</i> Fur	95
1.4.1 Iron acquisition and storage systems in <i>C. jejuni</i>	95
1.4.1.1 Ferrous iron uptake	95
1.4.1.2 Siderophore-mediated ferric iron uptake	97
1.4.1.3 Iron acquisition from host iron-containing compounds	101
1.4.1.4 TonB and iron storage proteins	102
1.4.2 <i>C. jejuni</i> Fur homologues and their function in gene regulation	104
1.4.2.1 Fur _{Cj} and fur _{Cj} regulation	104
1.4.2.2 Iron and Fur _{Cj} -mediated gene regulation in <i>C. jejuni</i>	106
1.4.2.3 Characterisation of the Fur _{Cj} box	109
1.4.2.4 PerR _{Cj} and oxidative stress response	112
1.5 Research aims	115
Chapter 2: Material and methods	117
2.1 Microbial analysis	117
2.1.1 Bacterial growth media, antibiotics and supplements	117

Contents

2.1.2 Bacterial strains used	118
2.1.3 Bacterial growth conditions	119
2.1.4 Strain maintenance and recovery	120
2.1.5 Preparation of electrocompetent <i>E. coli</i>	120
2.1.6 Preparation of electrocompetent <i>C. jejuni</i>	121
2.1.7 <i>C. jejuni</i> growth assay	121
2.2 DNA analysis	122
2.2.1 Extraction and purification of <i>C. jejuni</i> chromosomal DNA	122
2.2.2 <i>C. jejuni</i> natural transformation	122
2.2.3 Extraction and purification of plasmid DNA	123
2.2.4 Plasmids used	123
2.2.5 Nucleic acid quantification	127
2.2.6 Transformation of electrocompetent <i>E. coli</i>	128
2.2.7 Transformation of electrocompetent <i>C. jejuni</i>	128
2.2.8 DNA purification by ethanol precipitation	128
2.2.9 DNA purification by phenol/chloroform extraction	129
2.2.10 Agarose gel electrophoresis	129
2.2.11 DNA purification from agarose gel	130
2.2.12 Standard polymerase chain reaction (PCR)	130
2.2.13 Primers used	132
2.2.14 PCR product purification	137
2.2.15 Automated DNA sequencing	137
2.2.16 Restriction of DNA	138
2.2.17 Ligation of DNA	138
2.2.18 Standard mutagenesis and complementation	139
2.2.19 Site-directed mutagenesis	139
2.2.20 β -galactosidase assay	140
2.2.21 Polyacrylamide gel electrophoresis (PAGE)	141
2.2.22 Transfer DNA from polyacrylamide gel onto membrane (Southern	142

Contents

blot)	
2.2.23 Detection of DNA by anti-DIG-antibodies	142
2.2.24 Electrophoretic mobility shift assay	143
2.2.25 Sequencing PAGE	144
2.2.26 Manual DNA sequencing	145
2.2.27 DNase I footprinting assay	145
2.3 RNA analysis	146
2.3.1 Extraction and purification of <i>C. jejuni</i> total RNA	146
2.3.2 Formaldehyde agarose gel electrophoresis	147
2.3.3 Transfer RNA from agarose gel onto membrane (northern blot)	147
2.3.4 RNA detection by RNA-DNA hybridisation	148
2.3.5 Complementary DNA (cDNA) synthesis by reverse transcriptase (RT)	149
2.3.6 Primer extension	150
2.3.7 RACE	150
2.4 Protein analysis	152
2.4.1 Expression and purification of recombinant Fur _{Cj}	152
2.4.2 Expression and purification of recombinant <i>C. jejuni</i> RacR and RacS-HK	153
2.4.3 Protein buffer exchange	154
2.4.4 Protein concentration	154
2.4.5 SDS-PAGE	154
2.4.6 SDS-PAGE gel visualisation and drying	155
2.4.7 Transfer protein from SDS-PAGE gel onto membrane (western blot)	156
2.4.8 Detection of protein by anti-His-antibody	156
2.4.9 Protein identification	157
2.4.10 Protein quantification	157
2.4.11 Phosphorylation assay	157
2.4.12 Fumarase activity assay	158
2.5 Bioinformatics	159

Chapter 3: Site-directed mutagenesis of the <i>chuA</i> and <i>fumC</i> Fur boxes	161
3.1 Introduction	161
3.2 Aims	163
3.3 Results	165
3.3.1 Site-directed mutagenesis	165
3.3.2 Purification of the recombinant Fur _{Cj} protein	167
3.3.3 EMSA	170
3.3.4 β-galactosidase assay	177
3.3.5 Construction of the <i>C. jejuni</i> 480 fur _{Cj} mutant	186
3.3.6 Verification of <i>fumC</i> iron regulation by northern blot	196
3.3.7 Identification of the transcriptional start site	200
3.3.8 DNase I footprinting assay	208
3.3.9 Further characterisation of the Fur _{Cj} box	216
3.4 Discussions	220
3.4.1 Fur _{Cj} -Fur _{Cj} box interaction	220
3.4.2 The location of Fur _{Cj} binding	222
3.4.3 Functional important bases of the Fur _{Cj} box	225
3.4.4 Interpretation of the Fur _{Cj} box	228
Chapter 4: The iron- and oxygen-responsive regulation of <i>fumC</i>	233
4.1 Introduction	233
4.1.1 Regulation of fumarase genes in <i>E. coli</i>	233
4.1.2 <i>fumC</i> regulation and the function of FumC in other bacteria	236
4.1.3 Regulation of <i>fumC</i> in <i>C. jejuni</i>	237
4.2 Aims	239
4.3 Results	240
4.3.1 Iron-responsive regulation of 81116 <i>racR</i>	240
4.3.2 Iron- and oxygen-responsive gene regulation	243

4.3.3 Expression and purification of recombinant NCTC 11168 RacR and RacS-HK	249
4.3.4 Phosphorylation of RacR by RacS-HK	253
4.3.5 Interaction of RacR and the <i>fumC</i> and <i>aspA</i> promoters	253
4.3.6 Construction of the <i>C. jejuni</i> NCTC 11168 <i>fumC</i> mutant	260
4.3.7 The effects of the <i>fumC</i> mutant on growth rate and fumarase activities	262
4.4 Discussion	269
4.4.1 NCTC 11168 <i>fumC</i> and its functional importance	269
4.4.2 The iron and oxygen responsive regulation of <i>fumC</i> and <i>racR</i>	271
4.4.2.1 Factors affect <i>fumC</i> expression	271
4.4.2.2 Regulation of <i>fumC</i> expression under high iron conditions	273
4.4.2.3 Regulation of <i>fumC</i> expression under low iron conditions	276
4.4.2.4 Possible post-transcriptional and translational regulation of <i>fumC</i>	279
4.4.3 The interaction of RacR with RacS-HK and RacR regulated promoters	280
4.4.4 The regulation of <i>chuA</i> by PerR _{Cj} and RacR	282
Chapter 5: General discussion	284
5.1 Fur _{Cj} -Fur _{Cj} box interaction	284
5.2 Regulation of <i>chuA</i> expression	290
5.3 Regulation of <i>fumC</i> expression	293
5.4 The RacR-RacS TCS	294
5.5 Final remarks	295
Bibliography	298

Figures and tables

List of figures

- | | | |
|------|---|----|
| 1.1 | A simple illustration of the bacterial transcriptional regulatory networks and the modulation of gene expressions by transcriptional regulators | 3 |
| 1.2 | The negative regulation of the <i>lac</i> operon in response to lactose availability | 5 |
| 1.3 | Ribbon illustrations of the LacI monomer (a) and the tetramer-DNA complex (b) and the illustration of the allosteric changes of the LacI dimer between the induced (left) and repressed states (c) | 7 |
| 1.4 | An illustration of the regulation of the <i>ara</i> operon in the absence and presence of L-arabinose by AraC and the domains of the AraC monomer | 11 |
| 1.5 | Ribbon illustrations of the AraC monomer N-terminal domain in the presence of L-arabinose (a) and the representation of the C-terminal DNA-binding domain in explicit water (b) | 13 |
| 1.6 | An illustration of the <i>E. coli</i> EnvZ-OmpR two-component system and the transcriptional regulation of <i>ompF</i> and <i>ompR</i> under different osmolarity | 17 |
| 1.7 | Ribbon illustrations of the EnvZ dimerisation subdomain (a), the EnvZ catalytic subdomain bound to an ATP analogue AMP-PNP (b) and the OpmR effector domain (c) | 19 |
| 1.8 | An illustration of iron acquisition systems of Gram-negative bacteria including: ferrous iron uptake (a), siderophore-mediated ferric iron uptake (b), iron uptake from transferrin/lactoferrin (c) and direct haem uptake and haem uptake from haemoproteins (d) | 26 |
| 1.9 | Structures of siderophore metal-chelating functional groups: α -hydroxycarboxylate (a), catecholate (b) and hydroxamate (c) and structures of the siderophores ferrichrome (d) and enterobactin (e) | 29 |
| 1.10 | Ribbon illustrations of the <i>E. coli</i> ferric citrate OM receptor FecA (a), the <i>E. coli</i> siderophore PBP FhuD bound to ferrichrome coloured in yellow (b) and the <i>E. coli</i> vitamin B ₁₂ ABC permease complex BtuCD (c) | 32 |
| 1.11 | The regulatory potential of Fur in response to iron availability | 46 |

1.12	The expression of <i>fur</i> in <i>E. coli</i> (a) and <i>H. pylori</i> (b)	49
1.13	The ribbon illustration of the Fur _{Pa} dimer with bound zinc atoms and α helices 1 and 4 indicated (a) and stereo views of the electron density surrounded both zinc atoms (b and c)	52
1.14	The ribbon illustration of the Fur _{Vc} dimer with bound zinc atoms and the α helix 4 indicated (a) and stereo views of the electron density surrounded both zinc atoms (b and c)	56
1.15	The ribbon illustration of the Fur _{Hp} dimer with bound zinc atoms indicated (a) and the geometry of the three zinc-binding sites (b)	58
1.16	An illustration of iron sparing response mediated by the interplay between Fur and RyhB	66
1.17	Electron micrographs of <i>C. jejuni</i> exhibiting the spiral rod-shape (a) and coccoid forms (b)	82
1.18	The routes and outcomes of <i>C. jejuni</i> infection	84
1.19	An overview of the different stages of <i>C. jejuni</i> colonisation and virulence factors expressed at each stage	87
1.20	Iron acquisition systems of <i>C. jejuni</i> including: ferrous iron uptake, siderophore-mediated ferric iron uptake and iron uptake from host iron-containing compounds	96
3.1	A brief outline of the stages carried out in the characterisation of the putative Fur _{Cj} -binding site using <i>chuA</i> and <i>fumC</i> Fur _{Cj} boxes as models	166
3.2	The <i>C. jejuni</i> NCTC 11168 <i>chuA</i> and <i>fumC</i> promoter regions under investigation	168
3.3	A SDS-PAGE analysis of the purified recombinant Fur _{Cj}	171
3.4	Standard (a) and competitive (b) EMSA of 1.55 fmol DIG-labelled <i>chuA</i> and <i>fumC</i> promoter regions containing the wild-type and triple mutated Fur _{Cj} boxes with the purified Fur _{Cj} protein	172
3.5	Standard EMSA of 1.55 fmol labelled <i>chuA</i> promoter regions containing mutated Fur _{Cj} boxes with the purified Fur _{Cj} protein	175

3.6	Standard EMSA of 1.55 fmol labelled <i>fumC</i> promoter regions containing mutated Fur _{Cj} boxes with the purified Fur _{Cj} protein	176
3.7	β-galactosidase assay of the <i>chuA</i> wild-type promoter region with controls under high iron (40 μM FeSO ₄) and low iron (20 μM Desferal) conditions	180
3.8	β-galactosidase assay of the <i>chuA</i> wild-type and mutated promoter regions with controls under high iron (40 μM FeSO ₄) and low iron (20 μM Desferal) conditions	181
3.9	β-galactosidase assay of the <i>fumC</i> wild-type and mutated promoter regions with controls under high iron (40 μM FeSO ₄) and low iron (20 μM Desferal) conditions	183
3.10	β-galactosidase assay of the original (pRR23) and extended (pRR42) <i>fumC</i> wild-type promoter regions with controls under high iron (40 μM FeSO ₄) and low iron (20 μM Desferal) conditions for different amount of time i.e. 5 and 16 hours	185
3.11	The mutated <i>fur_{Cj}</i> genes and flanking regions of NCTC 11168 <i>fur_{Cj}</i> mutant strains AV17 and AV41	188
3.12	Verification of the 81-176 <i>fur_{Cj}</i> mutant by PCR	190
3.13	Verification of the 480 <i>fur_{Cj}</i> mutant by PCR	193
3.14	Verification of the RR1 transformants by PCR using M13F and SKanR primers	195
3.15	Northern blot analysis of the iron- and Fur _{Cj} -responsive regulation of <i>fumC</i>	197
3.16	Northern blot analysis of the iron-, Fur _{Cj} - and RacR _{Cj} -responsive regulation of <i>fumC</i>	197
3.17	Illustration of different approaches used to identify the transcriptional start sites for <i>chuA</i> and <i>fumC</i>	201
3.18	Comparison of <i>chuA</i> and <i>fumC</i> cDNA synthesised from the TAP treated and untreated RNA	205
3.19	Organisation of the <i>chuA</i> and <i>fumC</i> promoter regions	207
3.20	DNase I footprinting assays for <i>chuA</i> wild-type and <i>chuA10/13/19</i>	210

	promoters along with corresponding sequencing ladders	
3.21	DNase I footprinting assays for <i>chuA</i> wild-type and mutated promoters along with corresponding sequencing ladders	212
3.22	DNase I footprinting assays for <i>fumC</i> wild-type and <i>fumC10/13/19</i> promoters along with corresponding sequencing ladders	214
3.23	DNase I footprinting assays for <i>fumC</i> wild-type and mutated promoters along with corresponding sequencing ladders	215
3.24	Standard EMSA of 1.55 fmol labelled <i>chuA</i> promoter regions containing the wild-type and mutated Fur _{Cj} boxes with the purified Fur _{Cj} protein	217
3.25	β-galactosidase assay of the <i>chuA</i> wild-type and mutated promoter regions with controls under high iron (40 μM FeSO ₄) and low iron (20 μM Desferal) conditions	219
3.26	<i>chuA</i> and <i>fumC</i> promoter regions investigated in this study	224
4.1	Northern blot analysis of the iron-responsive regulation of 81116 <i>racR</i>	242
4.2	Northern blot analysis of the iron-responsive regulation of <i>fumC</i> , <i>racR</i> , <i>chuA</i> and <i>chuZ</i> under 3% oxygen	244
4.3	Northern blot analysis of the iron-responsive regulation of <i>fumC</i> , <i>racR</i> , <i>chuA</i> and <i>chuZ</i> under 7% oxygen	246
4.4	Northern blot analysis of the iron-responsive regulation of <i>fumC</i> , <i>racR</i> , <i>chuA</i> and <i>chuZ</i> under 11% oxygen	248
4.5	The predicted transmembrane domains (red) and the histidine kinase domain (blue) of NCTC 11168 RacS	250
4.6	SDS-PAGE analysis of the purified recombinant RacR (25.6 KDa, a) and RacS-HK (28.3KDa, b) proteins	252
4.7	SDS-PAGE and western blot analysis of the concentrated recombinant RacR and RacS-HK	254
4.8	<i>in vitro</i> phosphorylation of NCTC 11168 RacR and RacS-HK analysed by SDS-PAGE	255
4.9	Standard EMSA of 1.55 fmol labelled <i>fumC</i> (a) and <i>aspA</i> (b) promoter	257

	regions with purified <i>C. jejuni</i> NCTC 11168 RacR, RacS-HK and ATP	
4.10	DNase I footprinting assays for the <i>fumC</i> and <i>aspA</i> promoters along with corresponding sequencing ladders	259
4.11	Illustration of the mutagenesis strategies used to create a NCTC 11168 <i>fumC</i> mutant (RR2)	261
4.12	Verification of the NCTC 11168 <i>fumC</i> mutant (RR2) by PCR	263
4.13	Growth assays of the wild-type NCTC 11168 and RR2 (<i>fumC</i> mutant)	265
4.14	Growth assay of RR2 (<i>fumC</i> mutant)	266
4.15	Fumarase activity assays of the wild-type NCTC 11168, RR2, AV17 and AB3 under different high iron (40 μ M FeSO ₄) and low iron (20 μ M Desferal) conditions along with BSA controls	268
4.16	Transcriptional regulation of <i>fumC</i> by several regulators in response to oxygen and potentially iron availability	274
5.1	Iron-responsive repression of <i>chuA</i> at different oxygen concentrations by Fur _{Cj} and RacR	291
5.2	Regulation of the <i>aspA</i> promoter by the RacR-RacS TCS in response to low oxygen conditions	296

List of tables

1.1	Different interpretations of the consensus Fur box and proposed modes of Fur-DNA interaction	61
1.2	Sequence alignment of the Fur _{Ec} box and the putative Fur _{Cj} box	111
2.1	Bacterial stains used in this study	118
2.2	Plasmids used in this study	127
2.3	Reagents used in various types and volumes of PCR	131
2.4	Cycle conditions used in various types of PCR	131
2.5	Primers used in this study	137
3.1	Sequence alignment of the Fur _{Ec} box, the putative Fur _{Cj} box and the predicated <i>C. jejuni</i> <i>chuA</i> and <i>fumC</i> Fur _{Cj} boxes	162

Figures and tables

- 3.2 Illustration of the mutational change at the 10th, 13th and 19th positions of the *chuA* and *fumC* putative Fur_{Cj} boxes 164
- 3.3 Partial sequence alignments between wild-type (top stand) and mutated Fur_{Cj} boxes (bottom stand) performed using Clone Manager software 169
- 3.4 Summary of the approaches used to create the *C. jejuni* 480 *furCj* mutant strain 191
- 5.1 Illustration of the Fur_{Cj} protected regions observed for the wild-type *chuA* and the *fumC*10/13/19 promoters 286

Abbreviations

+1 site	Transcriptional start site
ABC	ATP-binding cassette
AHT	Anhydrotetracycline
Ala	Alanine
Amp	Ampicillin
Aps	Ammonium persulphate
Arg	Arginine
Asp	Aspartate
ATP	Adenosine triphosphate
<i>Bj</i>	<i>Bradyrhizobium japonicum</i>
<i>Bs</i>	<i>Bacillus subtilis</i>
BSA	Bovine serum albumin
cAMP	Cyclic adenosine monophosphate
Cap	Catabolite activator protein
cDNA	Complementary DNA
CDT	Cytolethal distending toxin
CEB	<i>Campylobacter</i> electroporation buffer
<i>Cj</i>	<i>Campylobacter jejuni</i>
CM	Cytoplasmic membrane
Cm	Chloramphenicol
CSPD	Disodium 3-(4-methoxy Spiro{1,2-dioxetane-3,2'-(5' -chloro)tricyclo[3.3.1.1 ^{3,7}]decan}-4-yl) phenyl phosphate
Cys	Cysteine
DEPC	Diethyl pyrocarbonate
dH ₂ O	Distilled water
DIG	Digoxigenin
DMF	Dimethylformamide
dNTPs	Deoxynucleotide triphosphates

Abbreviations

DTT	Dithiothreitol
DtxR	Diphtheria toxin regulator
<i>Ec</i>	<i>Escherichia coli</i>
EDTA	Ethylenediamine tetraacetic acid
EMSA	Electrophoretic mobility shift assay
FAM	Fluorescein amidite
FeSO ₄	Iron (II) sulphate heptahydrate
Fur	Ferric uptake regulator
Glu	Glutamine
GTG	Glycerol tolerant gel
His	Histidine
HK	Histidine kinases domain
<i>Hp</i>	<i>Helicobacter pylori</i>
HTH	Helix-turn-helix
IPTG	Isopropyl-β-D-1-thiogalactoside
IR	Intermediate regulator
Kan	Kanamycin
LB	Luria-Bertani
LOS	Lipooligosaccharide
MBS	Metal binding site
MH	Mueller-Hinton
MOPS	3-(N-morpholino) propanesulfonic acid
mRNA	Messenger RNA
MRS	Mur responsive sequence
MSC	Multi-cloning site
Mur	Manganese uptake regulator
<i>Ng</i>	<i>Neisseria gonorrhoeae</i>
<i>Nm</i>	<i>Neisseria meningitidis</i>
Nramp1	Natural resistance-associated macrophage protein 1

Abbreviations

NRPS	Nonribosomal peptide synthetases
Nur	Nickel uptake regulator
OD	Optical density
OM	Outer membrane
ONPG	2-nitrophenyl- β -D-galactopyranoside
<i>Pa</i>	<i>Pseudomonas aeruginosa</i>
PAGE	Polyacrylamide gel electrophoresis
PBP	Periplasmic binding protein
PBS	Phosphate buffered saline
PCR	Polymerase chain reaction
PerR	Peroxide regulon regulator
PMF	Proton motive force
PNACL	Protein nucleic acid chemistry laboratory
Pol	Polymerase
RACE	Rapid amplification of cDNA ends
<i>Rl</i>	<i>Rhizobium leguminosarum</i>
rpm	Revolutions per minute
RT	Reverse transcriptase
<i>Sc</i>	<i>Streptomyces coelicolor</i>
SDS	Sodium dodecyl sulphate
<i>Se</i>	<i>Salmonella enterica</i>
spp	Species
sRNA	Small RNA
SSC	Saline sodium citrate
TA	Tris-acetate
TAE	Tris-acetate-EDTA
TAP	Tobacco acid pyrophosphatase
TB	Tris-boric acid
TCA	Tricarboxylic acid

Abbreviations

TCS	Two-component system
TMEDA	N,N,N',N'-tetramethylethylene diamine
Tri	Trimethoprim
UTR	Un-translated region
<i>Va</i>	<i>Vibrio alginolyticus</i>
VAIN	Variable atmosphere incubator
Van	Vancomycin
<i>Vc</i>	<i>Vibrio cholerae</i>
v/v	Volume/volume
w/v	Weight/volume
X-gal	5-bromo-4-chloro-3-indoyl- β -D-galactoside
Zur	Zinc uptake regulator

Chapter 1: Introduction

Campylobacter jejuni is a causative agent for zoonose, and since its initial definitive association with a patient with diarrhoea in Brussels (Dekeyser *et al.*, 1972), *C. jejuni* has rapidly emerged as the most common cause of bacterial gastroenteritis and a major public health concern in the developed world. Although its unusual DNA base composition, metabolism and culture requirements have hindered early progress in understanding this organism, with the completion of the *C. jejuni* NCTC 11168 genome sequence (Parkhill *et al.*, 2000), many important aspects of epidemiology and pathophysiology of *C. jejuni* infection have been revealed in the past decade.

A key determinant of *C. jejuni* pathogenesis, and indeed of all pathogenic bacteria, is the ability to effectively regulate the expression of genes involved in host induced adaptation responses, which allows *C. jejuni* to successfully colonise the avian and human gastrointestinal tract and causes disease in the human host. Transcriptional regulation of iron metabolism genes by the ferric uptake regulator (Fur) is an example of such adaptive response regulation where the *C. jejuni* Fur (Fur_{Cj}) plays crucial roles in controlling cellular iron homeostasis and other cellular processes that are essential for *C. jejuni* survival (Palyada *et al.*, 2004; Holmes *et al.*, 2005). Characterisation of the Fur_{Cj} binding site, the Fur_{Cj} box, as well as the interaction between Fur_{Cj} and the Fur_{Cj} box are important for understanding the regulatory function of Fur_{Cj} and are addressed in detail in this research.

1.1 REGULATION OF GENE EXPRESSION

In order to adapt to and survive in a wide range of environmental conditions as well as compete effectively with other organisms, bacteria have evolved numerous systems for sensing and responding to changes in their environment. When facing suboptimal or stressful conditions such as limitation of nutrients, temperature fluctuations and oxidative or osmotic stresses, the expression of bacterial genes participating in response to the physiological and environmental demands must be coordinated by highly sophisticated and regulated global regulatory networks. These regulatory networks are mediated through the activation or inhibition of transcription initiation by transcriptional regulators, sigma factors and corresponding signal transduction pathways. Alternatively, it is increasingly evident that elevation and repression of messenger RNA (mRNA) translation by post-transcriptional regulation are also critical determinants of gene expression. Together, these regulatory mechanisms help bacteria to adjust to the surrounding environment, modulating cellular metabolism to optimise the utilisation of limited nutrients and improving the probability of survival and establishing colonisation in various niches (Snyder and Champness, 2003).

At the heart of any transcriptional regulatory network in bacteria is the transcriptional regulator which effectively functions as a molecular switch that converts environmental input signals to output responses (Figure 1.1). A major system for bacteria to detect extracellular signals is mediated by the two-component signal transduction systems (or two-component systems, TCSs) that activate transcriptional regulators by a short, or in

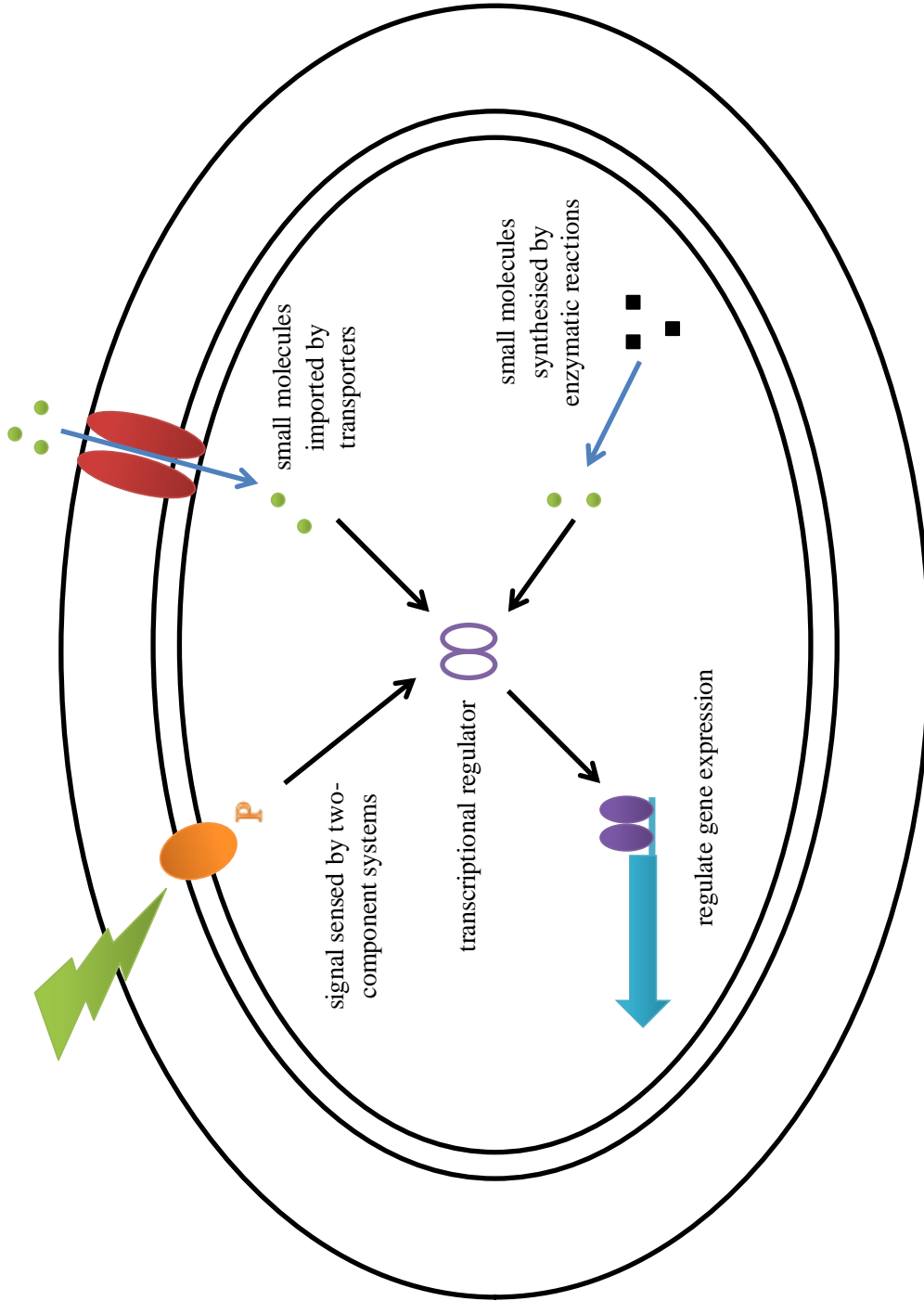


Figure 1.1: A simple illustration of the bacterial transcriptional regulatory networks and the modulation of gene expressions by transcriptional regulators. Transcriptional regulators sense extracellular signals through TCSs or by binding to imported small molecules and sense intracellular signals by binding to synthetic small molecules. Input signals trigger the allosteric responses of transcriptional regulators and allow them to interact with their target promoters and control their expression according to the input signals (adapted from Sechasayee *et al.*, 2006).

some cases, relatively long phosphorelays. Alternatively, bacteria sense extracellular or intercellular signals by the interaction of transcriptional regulators with small molecules that in most cases are either internalised by specific transport systems or synthesised internally by enzymatic reactions (Seshasayee *et al.*, 2006). The interactions of exogenous or endogenous signals with transcriptional regulators subsequently trigger the allosteric responses of the regulators and allow their DNA-binding domains to interact with the target promoters and either negatively or positively regulate the level of transcription (Snyder and Champness, 2003).

1.1.1 Negative gene regulation - the lactose (*lac*) operon

The *Escherichia coli lac* operon model originally proposed by Jacob and Monod a half century ago is the paradigm of gene regulation and allosteric behaviour and a cogent depiction of how the concentration of metabolites in environment affects the coordinate transcription of a set of structural genes (Jacob and Monod, 1961). The first gene of the operon encodes the LacI repressor and in the absence of lactose, LacI binds with a high affinity to the operator 1 (O_1) sequence located at the 5' end of the *lacZ* gene (Figure 1.2). This interaction dramatically compromises but does not eliminate the transcription of the downstream structural genes *lacZ*, *lacY* and *lacA*, which code for β -galactosidase, the *lac* permease and thiogalactoside transacetylase respectively that are required for lactose metabolism (Wilson *et al.*, 2007).

When lactose becomes available, the inducer allolactose is synthesised by the basal

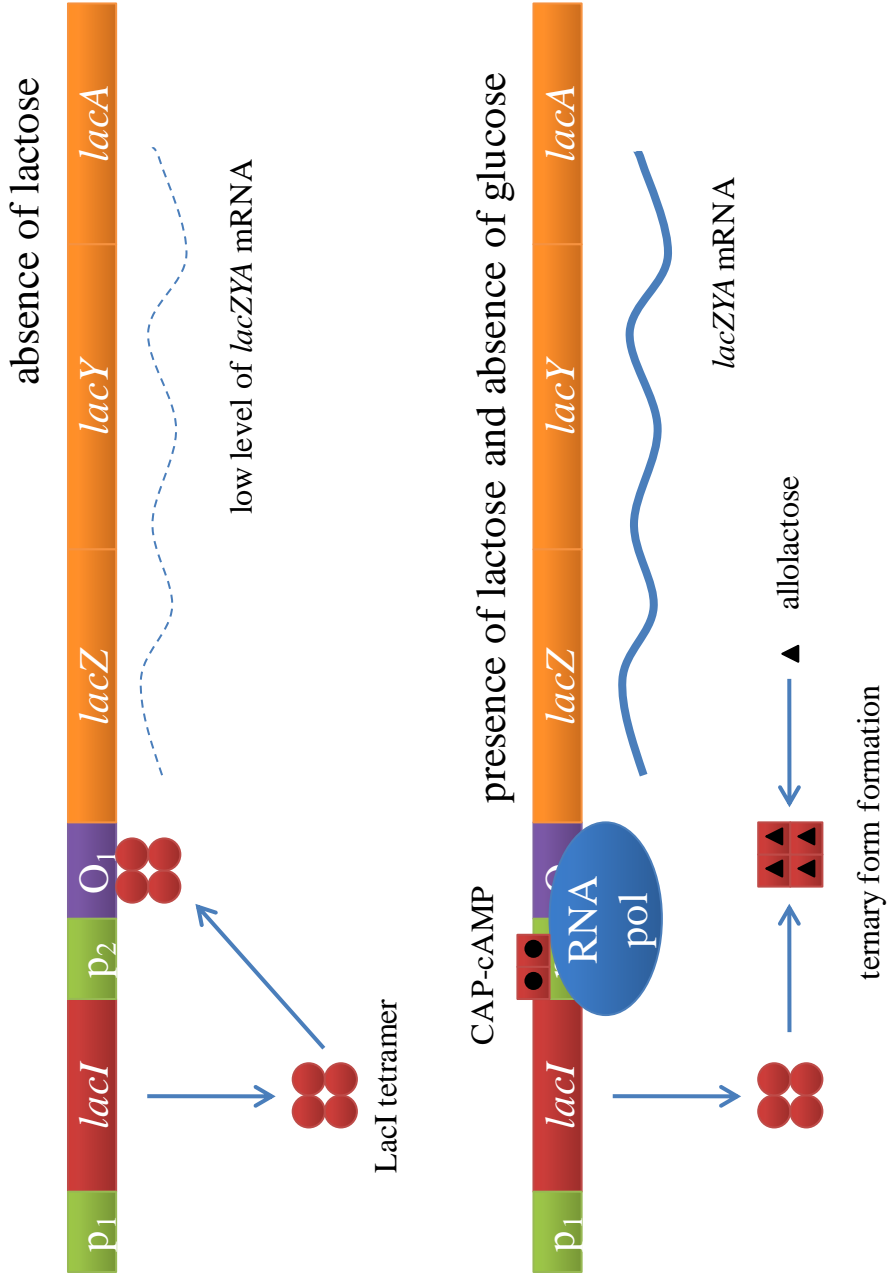


Figure 1.2: The negative regulation of the *lac* operon in response to lactose availability (adapted from Wilson *et al.*, 2007). See text for details.

level of β -galactosidase in the cell and it binds to the LacI repressor to lower its affinity to the operator. However the downstream structural genes are only fully transcribed in the absence of glucose where high levels of cyclic adenosine monophosphate (cAMP) are produced by adenylyl cyclase and bound to the catabolite activator protein (Cap). The Cap-cAMP complex subsequently binds to the Cap-binding site upstream from the *lacZ* promoter (p_1) and this in turn enhances the affinity of the RNA polymerase (pol) towards the promoter (Wilson *et al.*, 2007).

The key component of *lac* operon regulation, the LacI repressor, is a tetrameric protein consisting of identical 37 kDa monomers. The three-dimensional structure of the repressor reveals that each monomer contains a C-terminal tetramerisation domain and a hinge region that connects the N-terminal headpiece with the core sugar binding domain (Figure 1.3.a). The headpiece contains a classic helix-turn-helix (HTH) motif and it flexes independently from the core domain. In the presence of the operator sequence, the hinge region undergoes coil to helix transition allowing it to make specific contacts with the minor groove of the DNA and allows the headpiece to fit into the major groove of the operator sequence. The core domain belongs to the periplasmic binding protein superfamily and consists of two structurally similar N- and C-terminal subdomains. The two subdomains are hinged together by three linkers that form a cleft at the subdomains interface. The effector ligand such as allolactose or isopropyl- β -D-1-thiogalactoside (IPTG) binds to this cleft through hydrogen bond formation and van de Waals contacts. The dimeric state of the repressor is held together by an extensive monomer-monomer

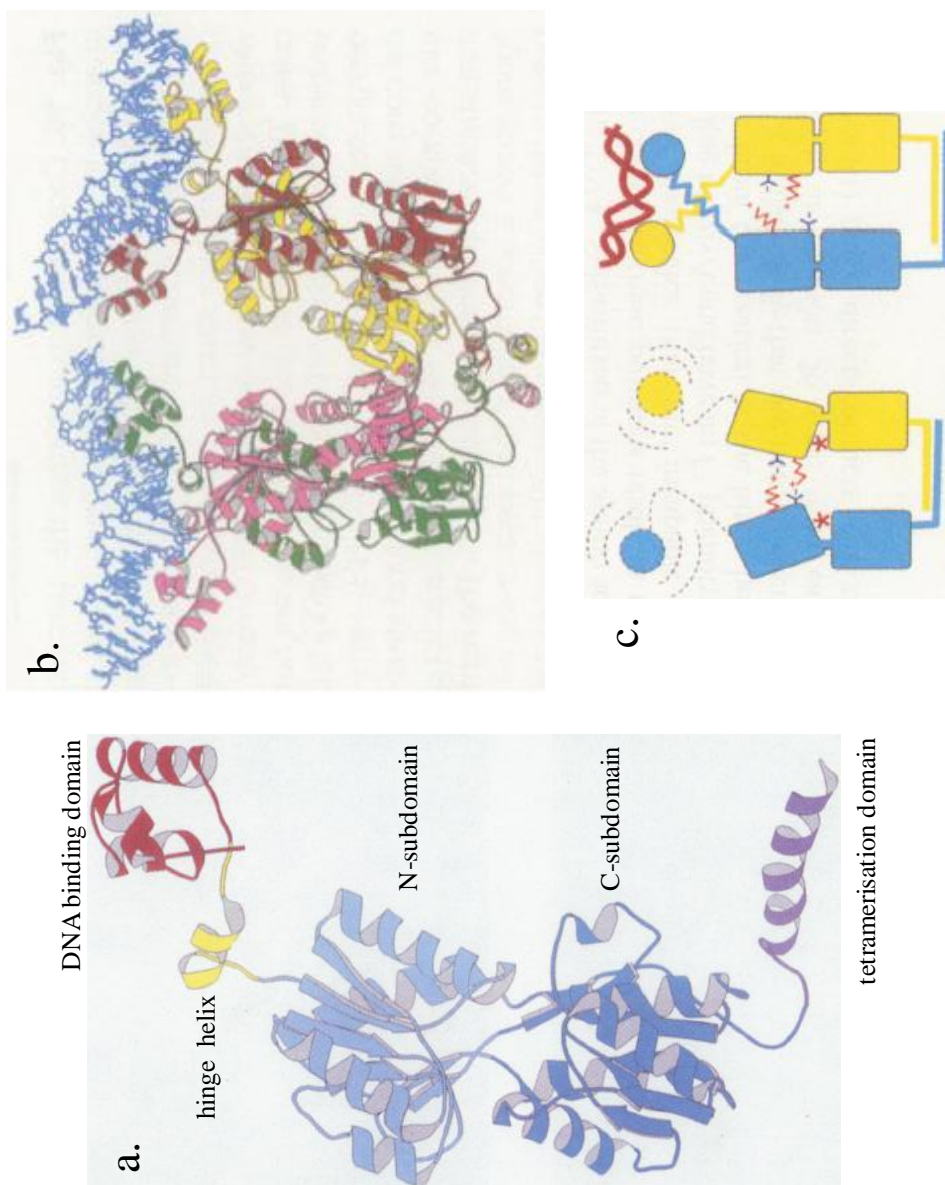


Figure 1.3: Ribbon illustrations of the LacI monomer (a) and the tetramer-DNA complex (b) and the illustration of the allosteric changes of the LacI dimer between the induced (left) and repressed states (c). See text for more details (taken from Lewis *et al.*, 1996).

interface between the core domains of two monomers and it forms the functional operator binding unit. The tetrameric structure of the LacI repressor formed by the association of C-terminal tetramerisation domains does not maintain the point of group symmetry and it is essentially viewed as a V-shaped dimer of dimers where each dimer interacts with an operator and bends the DNA molecules away from the repressor (Figure 1.3.b, Lewis *et al.*, 1996)

The allosteric change of the LacI dimer occurs primarily at the interface between two N-terminal subdomains which results in a small structural change between the N- and C-terminal subdomains of each monomer and the signal of this change is propagated to the headpieces via the hinge helices. As illustrated in Figure 1.3.c, in the induced state, the binding of an effector changes the subdomain's interface by a small hinge motion which allows the formation of a number of electrostatic interactions across the N-terminal subdomains. This change in the dimer interface displaces the first amino acid residue of the core domain, which disrupts the interactions between the hinge helices and reduces the affinity of the DNA-binding domain for the operator. The electrostatic interactions that hold the dimer together are broken in the repressed state and the N-terminal subdomains move closer resulting in the reformation of the hinge helices interaction and the headpieces-operator complex (Lewis *et al.*, 1996).

Aside from the primary operator sequence, the *lac* operon also contains two auxiliary operators located 92 bp upstream and 401 bp downstream from O₁. These three

operators share a high degree of sequence similarity and these auxiliary operators are required for the maximal level of repression. Although the allosteric transition of the LacI repressor occurs in the dimeric state, the formation of LacI tetramer allows it to interact with two operators simultaneously and creates a repression loop. The V-shaped LacI tetramer bends the operator sequence away from the repressor and creates a wrapping away loop. Alternatively, a simple loop also forms when the tetramer adapts to a conformation where the DNA-binding domain of each dimer is located at the opposite ends of the LacI tetramer (Friedman *et al.*, 1995). Both repression loop formations mediate supercoiling of the promoter region and further enhance the repression of the structural genes in the operon (Wilson *et al.*, 2007).

1.1.2 Positive gene regulation - the L-arabinose (*ara*) operon

Another well studied regulatory system in *E. coli* is the *ara* operon where the structural genes involved in the utilisation of L-arabinose, a five-carbon sugar, are positively (and negatively) regulated by AraC. The four-gene operon consists of the activator coding gene *araC* which is transcribed from its own promoter *pC* and followed by the structural genes *araB*, *araA* and *araD* which are divergently transcribed from *araC* by the *pBAD* promoter. *araB*, *araA* and *araD* encode the L-arabinose kinase, L-arabinose isomerase and D-xylulose-5-phosphate epimerase respectively. These enzymes are involved in enzymatic reactions to convert L-arabinose to D-xylulose-5-phosphate, which can be subsequently fed into the pentose phosphate pathway (Englesberg, 1961).

The AraC protein contains a C-terminal DNA-binding domain and is linked to the N-terminal dimerisation and L-arabinose-binding domain by a linker. The N-terminal domain also contains an N-terminal arm which plays a key role in determining the ligand-dependent DNA-binding properties of the protein and renders the AraC protein with both the ability to induce and repress transcription (Soisson *et al.*, 1997). The negative and positive regulation of the *araBAD* genes by AraC is explained by the switch mechanism illustrated in Figure 1.4.

In the absence of the inducer, L-arabinose, the two N-terminal arms of the AraC dimer interact with the corresponding DNA-binding domains and orientate them to form contact with the two widely separated O₂ and I₁ binding sites located upstream from pC and pBAD respectively. This allows the formation of a repression loop which prevents the interaction of RNA pol with this region and hence represses the transcription of *araBAD* as well as the *araC* gene. The negative autoregulation of *araC* is also mediated by the direct binding of AraC dimer to the O₁ pair of binding sites that partially overlap the pC RNA pol binding site. In the presence of L-arabinose, the N-terminal arms are repositioned by the binding of the inducer with the L-arabinose binding domain and the arms are held over the L-arabinose binding pockets by the bound sugar molecules. In this structure, the DNA-binding domains are less constrained and the repositioning of the arms provides the DNA-binding domains with the freedom to reorient and bind to the direct repeat I₁ and I₂ binding sites (Saviola *et al.*, 1998). The binding of the AraC protein stimulates both the interactions of RNA pol to pBAD and pC and the formation

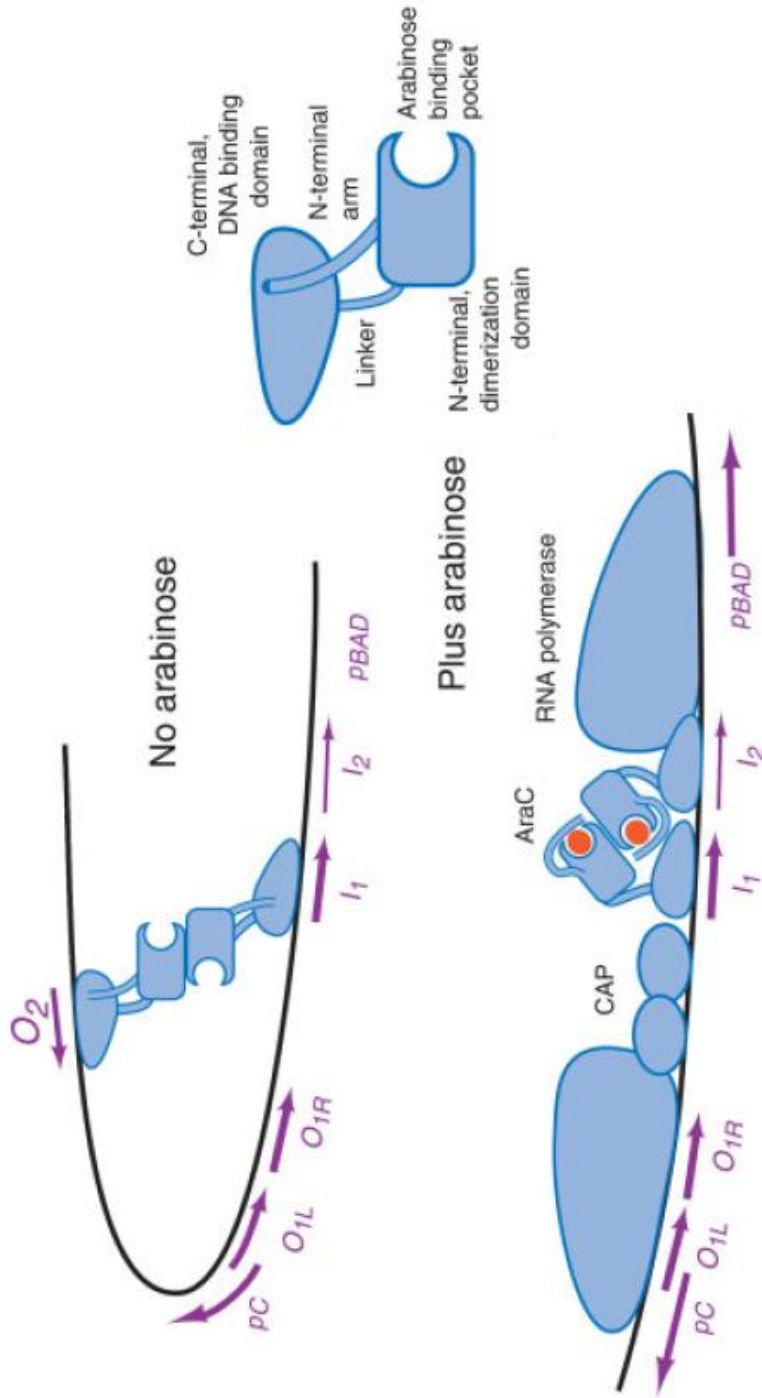


Figure 1.4: An illustration of the regulation of the *ara* operon in the absence and presence of L-arabinose by AraC and the domains of the AraC monomer. See text for more details (taken from Schleif, 2003).

of open complexes in the promoters (Zhang *et al.*, 1996).

Like in the *lac* operon, the transcription of the structural genes in the *ara* operon is only fully induced in the absence of glucose by the Cap-cAMP complex. The Cap-binding site is located between I₁ and O₁ binding sites and serves the divergently oriented pC and pBAD promoters. The binding of Cap-cAMP complex dimer facilitates the opening of the repression loop and the Cap dimer also interacts with the C-terminal domain of the RNA pol α subunit and stimulates the binding of RNA pol to the promoters (Zhang and Schleif, 1998).

Due to the insolubility and the inability to yield crystals, the full structure of the AraC protein is still unknown, however the crystal structure of the N-terminal domain in the presence and absence of L-arabinose (Soisson *et al.*, 1997; Weldon *et al.*, 2007) and the solution structure of the C-terminal domain have been determined (Rodgers and Schleif, 2009). The N-terminal domain consists of nine β strands which form an antiparallel β barrel and two α helices that are packed against the barrel (Figure 1.5.a). A single L-arabinose molecule binds into the barrel and is stabilised by hydrogen bonds formed between the side chains of the barrel and the sugar hydroxyl groups. A 12 residue-long N-terminal arm forms direct and indirect contact with the sugar molecule and completely encloses the L-arabinose in the β barrel (Soisson *et al.*, 1997). The N-terminal domain of AraC also contains 10 amino acid residues which form part of the mutable and flexible linker that links the N-terminal domain with the DNA-binding

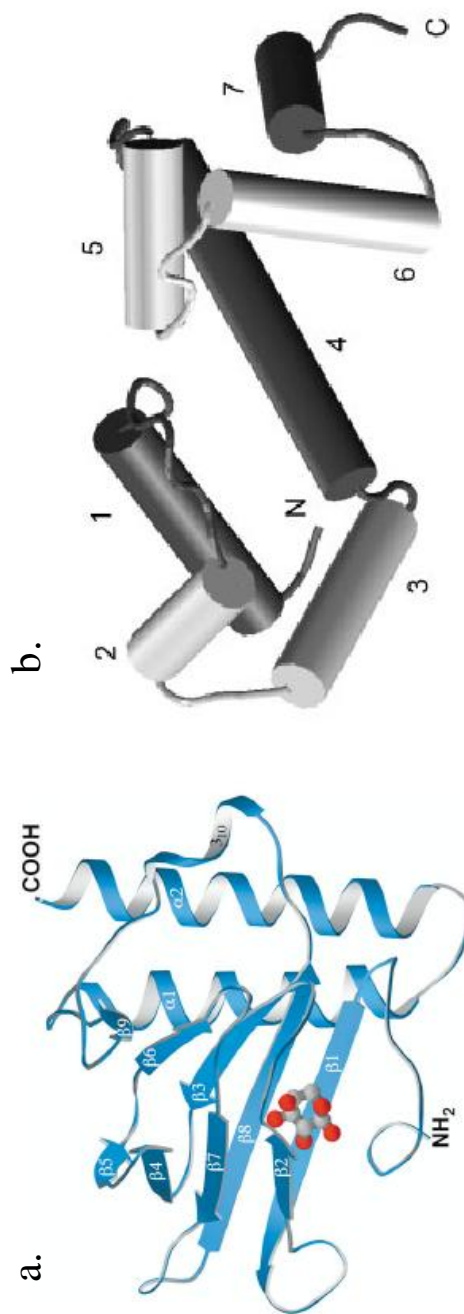


Figure 1.5: Ribbon illustrations of the AraC monomer N-terminal domain in the presence of L-arabinose (a, taken from Soisson *et al.*, 1997) and the representation of the C-terminal DNA-binding domain in explicit water (b, taken from Rodgers and Schleif, 2009).

domain (Eustance *et al.*, 1994).

In the induced form the two N-terminal domain monomers are associated by an antiparallel coiled-coil form between the α helices of each monomer and are held together by a network of hydrogen bonds formed by leucine residues anchored at the end of the coiled-coil. In the *apo* form, the core of the N-terminal domain monomer is virtually identical to the induced form but the N-terminal arm is unstructured in this state due to the absence of the bound sugar molecule. This distortion of the arm exposes the β barrel surface and allows it to act as an oligomerisation interface. The binding of two *apo* N-terminal monomers at the oligomerisation interface allows the side chain of the tyrosine (Tyr) 31 residue to occupy the β barrel of the adjacent monomers (Soisson *et al.*, 1997). This protein aggregation however does not occur at physiological concentrations of AraC and mutation of the Tyr31 does not affect the regulatory function of AraC (Weldon *et al.*, 2006).

The DNA-binding domain of AraC is a well folded seven- α helix structure in the absence of DNA (Figure 1.5.b) and contains two subdomains (α 2-3 and α 5-6) bearing the HTH motif. The two subdomains are weakly interconnected that allows each subdomain to rotate significantly from each other (Rodgers and Schleif, 2009). Mutational studies of the I_1 half binding site demonstrated that the two DNA-recognition helices of the subdomains bind specifically to the adjacent major grooves but not to the middle minor groove (Niland *et al.*, 1996) and the formation of

this AraC-DNA complex significantly distorts the AraC DNA-binding domain and the operator sequence (Rodgers and Schleif, 2009).

1.1.3 TCS - the EnvZ-OmpR osmolarity regulatory system

As shown in Figure 1.1, TCSs are one of the major mechanisms for environmental signal recognition and signal responsive gene regulation in bacteria. A typical simple TCS consists of a signal sensing transmembrane histidine (His) kinase and a cytoplasmic response regulator, usually a transcriptional regulator that is activated by the histidine kinase through a signal phospho-transfer event. Bacteria and some lower eukaryotes also possess more elaborate versions of TCSs that contain additional phosphotransferases and phosphate receivers. These systems sense and responded to environmental signals through multiple phosphotransfer events known as phosphorelays to enable inter connection and amplification between (different) signalling pathways (Stock *et al.*, 2000).

The prototypical example of the simple TCSs is the *E. coli* EnvZ-OmpR regulatory system which regulates outer membrane (OM) pore expression in response to changing osmolarity. Effective osmolarity sensing and response allows bacteria to maintain an optimal osmotic pressure inside the cell and changing osmolarity also serves as an environmental cue for pathogenic bacteria to differentially express genes on entering the host (Snyder and Champness, 2003). *E. coli* expresses two porin proteins, OmpF and OmpC, which form pores with different size cutoffs and allow small hydrophilic

molecules to diffuse across the membrane at different rates according to the surrounding osmolarity. The regulation of porin expression occurs at the transcriptional level by a connected signal transduction pathway which consist of the osmosensing histidine kinase EnvZ and its cognate response regulator OmpR (Figure 1.6). EnvZ senses the surrounding osmolarity by the N-terminal periplasmic sensor domain and transduces the information across the inner membrane to the C-terminal cytoplasmic domain which is joined to the N-terminal by two transmembrane segments. The C-terminal domain can be further divided into a dimerisation subdomain which contains a conserved His residue and a catalytic subdomain that contains the adenosine triphosphate (ATP)-binding site (Pratt and Silhavy, 1995).

Under high osmolarity, EnvZ first undergoes autophosphorylation where the γ -phosphoryl group of the bound ATP is transferred to the His residue by the catalytic subdomain. EnvZ then transfers this high energy phosphoryl group from the His residue to the conserved aspartate (Asp) residue on the N-terminal regulatory domain of OmpR. The phosphorylated N-terminal domain enhances the DNA-binding ability of the OmpR C-terminal effector domain and allows it to activate the transcription of *ompC* while down regulating the expression of *ompF*. OmpC trimers form smaller pores than OmpF and hence significantly reduce the rate of diffusion under high osmolarity. EnvZ also possesses phosphatase activity that promotes dephosphorylation of OmpR under low osmolarity and allows OmpR to function as a transcriptional activator of *ompF* (Pratt and Silhavy, 1995). In addition, the expression of *ompF*, but not *ompC*, is also

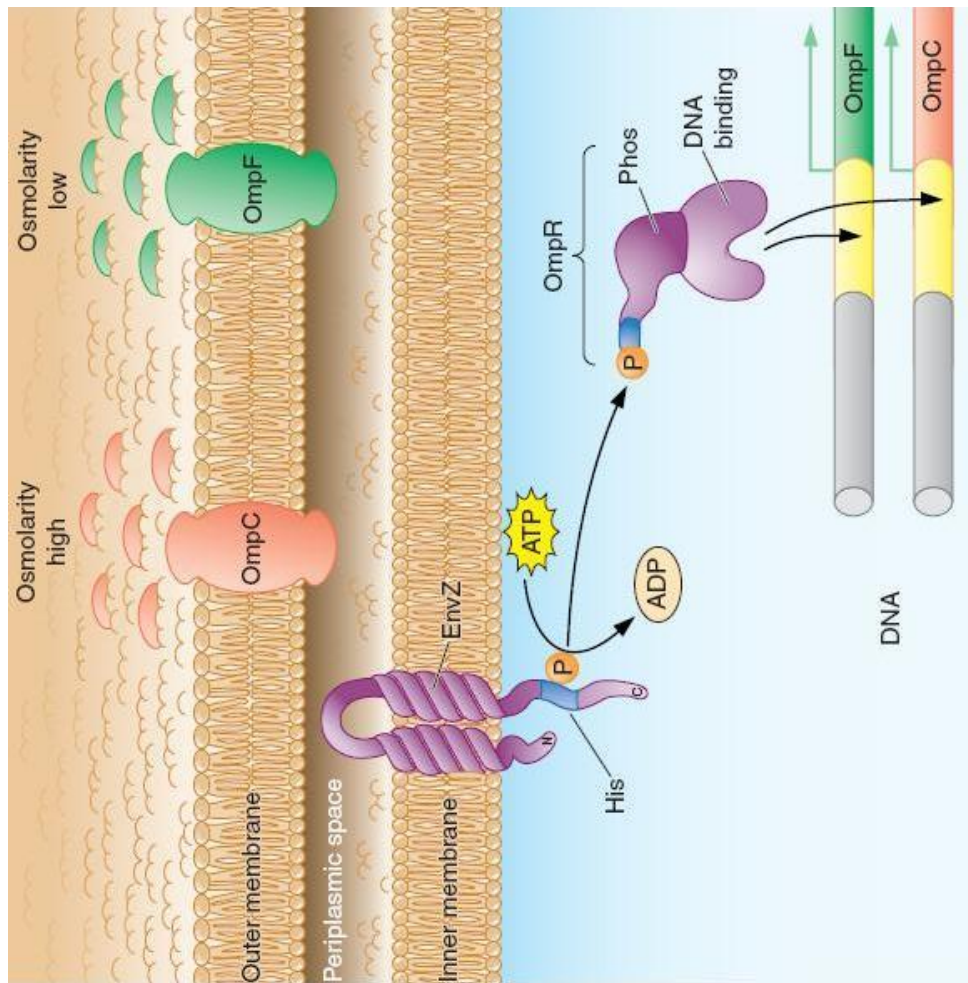


Figure 1.6: An illustration of the *E. coli* EnvZ-OmpR two-component system and the transcriptional regulation of *ompF* and *ompR* under different osmolarity. See text for more details (taken from <http://www.uic.edu/labs/kenney/>).

post-transcriptionally regulated by MicF in response to environmental and internal stress stimuli. Transcribed divergently upstream from *ompC*, *micF* encodes a non-translated small RNA (sRNA, Beisel and Storz, 2010) that binds to *ompF* mRNA and regulates *ompF* expression by inducing RNA degradation (Delihias and Forst, 2001).

In a typical TCS, the ATP-dependent autophosphorylation of the histidine kinase is a bimolecular reaction between homodimers where phosphorylation of the conserved His residue from one histidine kinase monomer is catalysed by the second monomer (Stock *et al.*, 2000). The dimerisation subdomains of an EnvZ homodimer are comprised of two identical antiparallel HTH subunits which interact along the helical axis to form a four-helix bundle structure called the H box (Figure 1.7.a). The outer helix of each subunit contains several conserved amino acid residues including the essential His243 residue which is the functional site of autophosphorylation and phosphate transfer reactions. The His side chain protrudes out from the H box that allows access of the catalytic subdomain and the response regulator OmpR. Several other essential residues are located in the inter-subunit surfaces of the four-helix bundle which indicates that dimer formation is the functional state of the histidine kinase (Tomomori *et al.*, 1999).

The EnvZ catalytic subdomain monomer has an α/β sandwich fold core consisting of five antiparallel β sheets (stands B, D, E, G and F) and three α helices (helices 1, 2 and 4) followed by a polypeptide loop extending away from the core structure which forms part of the ATP-binding site (Figure 1.7.b). The bound AMP-PNP molecule is

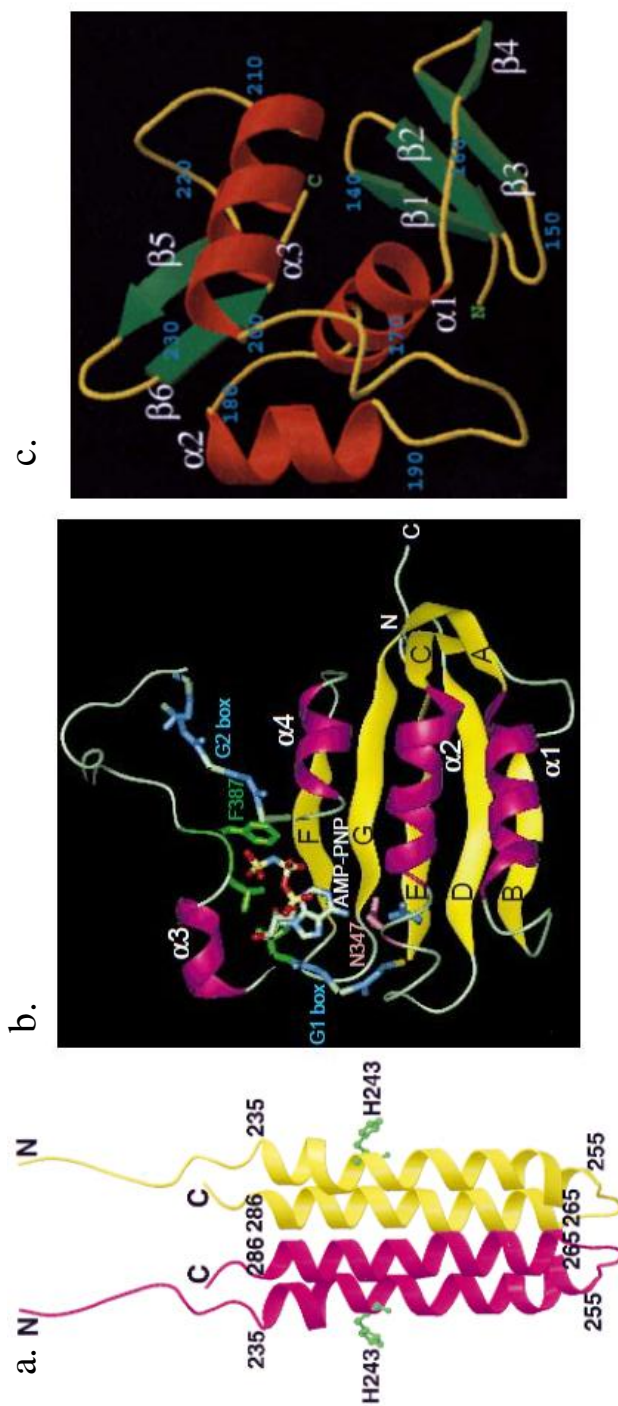


Figure 1.7: Ribbon illustrations of the EnvZ dimerisation subdomain (a, taken from Tomomori et al., 1999), the EnvZ catalytic subdomain bound to an ATP analogue AMP-PNP (b, taken from Tanaka et al., 1998) and the OpmR effector domain (c, taken from Kondo et al., 1997).

surrounded by α helix 3 and the polypeptide loop and its triphosphate side chain is exposed to the protein surface that allows the transfer of γ -phosphoryl group to the His residue in the dimerisation subdomain. The ATP-binding site encloses several highly conserved regions termed the N, G1, F and G2 boxes, in which the G1 and G2 boxes and N box are essential for the kinase and ATP-dependent autophosphorylation activities of EnvZ respectively (Tanaka *et al.*, 1998).

The N-terminal regulatory domain of OmpR contains the conserved Asp55 residue and the phosphorylation states of this residue affect the activity of the C-terminal effector domain. The OmpR effector domain contains a four-strand β sheet connected to a β hairpin by three α helices (Figure 1.7.c). α helices 2 and 3 are joined by a long ten-residue loop (the α loop) that together forms a winged HTH DNA-binding motif. Mutational studies indicate that α helix 3 and the loop connecting β strands 5 and 6 contribute to the DNA-binding activities of OmpR, whereas the α loop interacts with the α subunit of RNA pol and effectively regulate transcription (Martínez-Hackert, 1997). Under high osmolarity, phosphorylated OmpR dimer binds in a hierarchical manner to multiple binding sites called F and C sites located in the *ompF* and *ompR* promoters respectively and functions as either a transcriptional activator or a repressor depending on the sites of interaction (Maeda and Mizuno, 1990; Rampersaud *et al.*, 1994). Each binding site consists of a tandemly arranged 10 bp half binding sites and evidence from DNA affinity cleaving experiments indicate that phosphorylated OmpR asymmetrically interacts with *ompF*'s F1 site with each recognition helix forming contacts with the

major groove of each half binding site (Harrison-McMonagle, 1999).

1.2 IRON ACQUISITION, FUR AND THE FUR REGULON

The ability to effectively regulate cellular gene expression in a coordinated manner is essential for pathogenic bacteria to adapt and survive in the various hostile environments encountered during transmission and colonisation. Sensing and adjusting to the animal internal environment requires global regulatory systems that simultaneously regulate the expression of an array of virulence genes that allow pathogenic bacteria to adapt to the host and cause disease (Snyder and Champness, 2003). Regulation of iron homeostasis and other cellular processes by the global regulator Fur is an example of such adaptive responses and Fur-mediated gene regulation as well as the mechanisms involved in iron acquisition are closely linked to bacterial virulence and pathogenesis (Litwin and Calderwood, 1993; Wooldridge and Williams, 1993; Carpenter *et al.*, 2009b).

1.2.1 Iron and iron limitation in host

Iron is a versatile transition metal which has a great redox potential span ranging from -300 to + 700 mV between the reduced ferrous (Fe^{2+}) state and the oxidised ferric (Fe^{3+}) state (Andrews *et al.*, 2003). When incorporated into proteins, iron, either alone or in a more complex iron-sulphur cluster or haem group, serves as a biocatalyst for a broad spectrum of redox and electron transfer reactions. Many iron-containing proteins participate in major biological processes such as electron transport, energy metabolism,

peroxide reduction, respiration, amino acid and DNA synthesis, nitrogen fixation and photosynthesis, therefore iron is an essential micronutrient for virtually all living organisms (Andrews *et al.*, 2003; Wandersman and Delepelaire, 2004). The exceptions to this absolute iron requirement are *Lactobacillus plantarum*, which uses manganese and cobalt instead of iron for cellular functions (Weinberg, 1997), as well as pathogenic bacteria *Borrelia burgdorferi* and *Treponema pallidum* (Posey and Gherardini, 2000).

Although iron is one of the most abundant elements in nature, the availability of the biologically relevant ferrous form is limited in the natural environment. Under aerobic conditions, ferrous iron is oxidised to the ferric form and produces reactive oxygen species such as superoxide anions and hydroxyl radicals through the Haber-Weiss and Fenton reactions (Wandersman and Delepelaire, 2004). Ferric iron is insoluble under aerobic, aqueous and physiological pH conditions and reactive oxygen species especially hydroxyl radicals are biotoxic, leading to cellular compound damage such as DNA breaks, lipid peroxidation and protein denaturation (Schaible and Kaufmann, 2004). In the animal host, the majority of free iron is complexed within metalloproteins which protect the host from iron induced oxidative damage and also provide a non-specific innate defence mechanism that limits the availability of iron sources to invading pathogenic bacteria (Ratledge and Dover, 2000).

Human and animal hosts obtain iron directly through their diet and it is absorbed in the ferrous form by divalent metal ion transporter 1 in the gut (Fleming *et al.*, 1998). When

circulating in the bloodstream, extracellular ferric iron is bound to a high affinity iron-chelating glycoprotein transferrin which contains two homologous lobes, each with single ferric iron binding capacity (Wandersman and Delepelaire, 2004). Transferrin in humans is only 30% saturated with allows it to effectively scavenge any surplus iron present in the blood during infection. Cellular iron uptake is achieved by transferrin receptor 1 and 2 which each bind to *holo*-transferrin and the resulting complex is then internalised by endocytosis. The acidic environment in the endosome reduces the transferrin-bound ferric iron and the released ferrous iron is then transported to the cytoplasm where it is stored in ferritin in its ferric form (Hentze *et al.*, 2004). When acquired with a sufficient amount of iron, ferritin reforms into haemosiderin, which is an insoluble amalgam of degraded protein and ferric hydroxide (Weinberg, 2009). Lactoferrin is another iron-binding protein that is commonly found in lymph and mucosal secretions such as tears and saliva and it is structurally and functionally related to transferrin. However unlike transferrin, lactoferrin retains its high affinity for iron under the low pH conditions that usually occur at the site of infections (Wooldridge and Williams, 1993). Lactoferrin also releases an N-terminal peptide lactoferricin by acidic proteolysis, which has a broad range of antimicrobial activities (Bellamy *et al.*, 1992).

Haem is the most abundant iron source in the animal host and dietary haem is transported to the cytosol by the haem carrier protein 1 and the gene product of haem responsive gene 1 (Yanatori *et al.*, 2010). Haem is mostly bound intracellularly by haemoproteins such as haemoglobin and myoglobin (Wooldridge and Williams, 1993).

Haemoglobin released into the plasma as a result of erythrocyte lysis forms a complex with haptoglobin, which is then taken up by reticuloendothelial macrophages through haemoglobin scavenger receptor CD163-mediated endocytosis (Hentze *et al.*, 2004). Haem dissociated from haemoglobin is sequestered due to its toxicity by haemopexin in the plasma and it is then transported to the liver where haem is removed from haemopexin by hepatic parenchymal cells. Serum albumin also binds haem though with a low affinity and haem complexed with albumin is removed from the circulation by *apo*-haemopexin (Wooldridge and Williams, 1993).

Under the influence of cytokines, the level of free iron in the mammalian host is further reduced during microbial invasion in a set of reactions collectively known as hypoferremia. Synthesis of transferrin, lactoferrin and haemopexin elevates during inflammation, removing any free iron and haem liberated into plasma as a result of infection. Degranulation of leukocytes also occurs at the site of infection which further increases the local concentration of lactoferrin to chelate iron and remove iron from transferrin which has a reduced affinity to iron at low pH (Litwin and Calderwood, 1993). During extracellular microbial invasion, interleukin-6 promotes the secretion of peptide hormone hepcidin which diminishes iron release from reticuloendothelial macrophages and duodenal enterocytes by inactive cellular iron exporter protein ferroportin (Weinberg, 2009). By contrast, during intracellular infection, interferon- γ enhances the function of ferroportin and represses the expression of transferrin receptor 1 in macrophages which reduces the intracellular iron level. Interferon- γ also induces

the expression of natural resistance-associated macrophage protein 1 (Nramp1) which depletes iron from the phagosome and withholds iron from invading microorganisms (Ganz, 2009).

1.2.2 Mechanisms of bacterial iron acquisition and iron storage

Despite facing the elaborate iron withdrawal mechanisms in human and animal hosts as well as the poor solubility and toxicity nature of iron, bacteria have evolved highly specific and adaptive iron acquisition systems. These systems are capable of effectively obtaining various forms of environmental iron such as ferrous iron and ferric iron as well as iron from host iron-containing proteins under iron restricted conditions (Figure 1.8).

1.2.2.1 Ferrous iron uptake

Although iron is predominately present in its ferric state under aerobic conditions, ferrous iron can be directly utilised by bacteria grown under anaerobic and microaerobic conditions. In addition, many bacteria such as *E. coli* (Cowart, 2002), *Helicobacter pylori* (Worst *et al.*, 1988), *Listeria monocytogenes* (Cowart and Foster, 1986) and *Pseudomonas aeruginosa* (Cox, 1986) are capable of synthesising extracellular ferric iron reductases which facilitate the solubilisation of extracellular ferric iron or ferric iron bound to transferrin. In general, ferrous iron passively diffuses through the OM porins of Gram-negative bacteria and is then actively transported through the cytoplasmic membrane (CM) by the Feo system (Figure 1.8.a, Cartron *et al.*, 2006). The

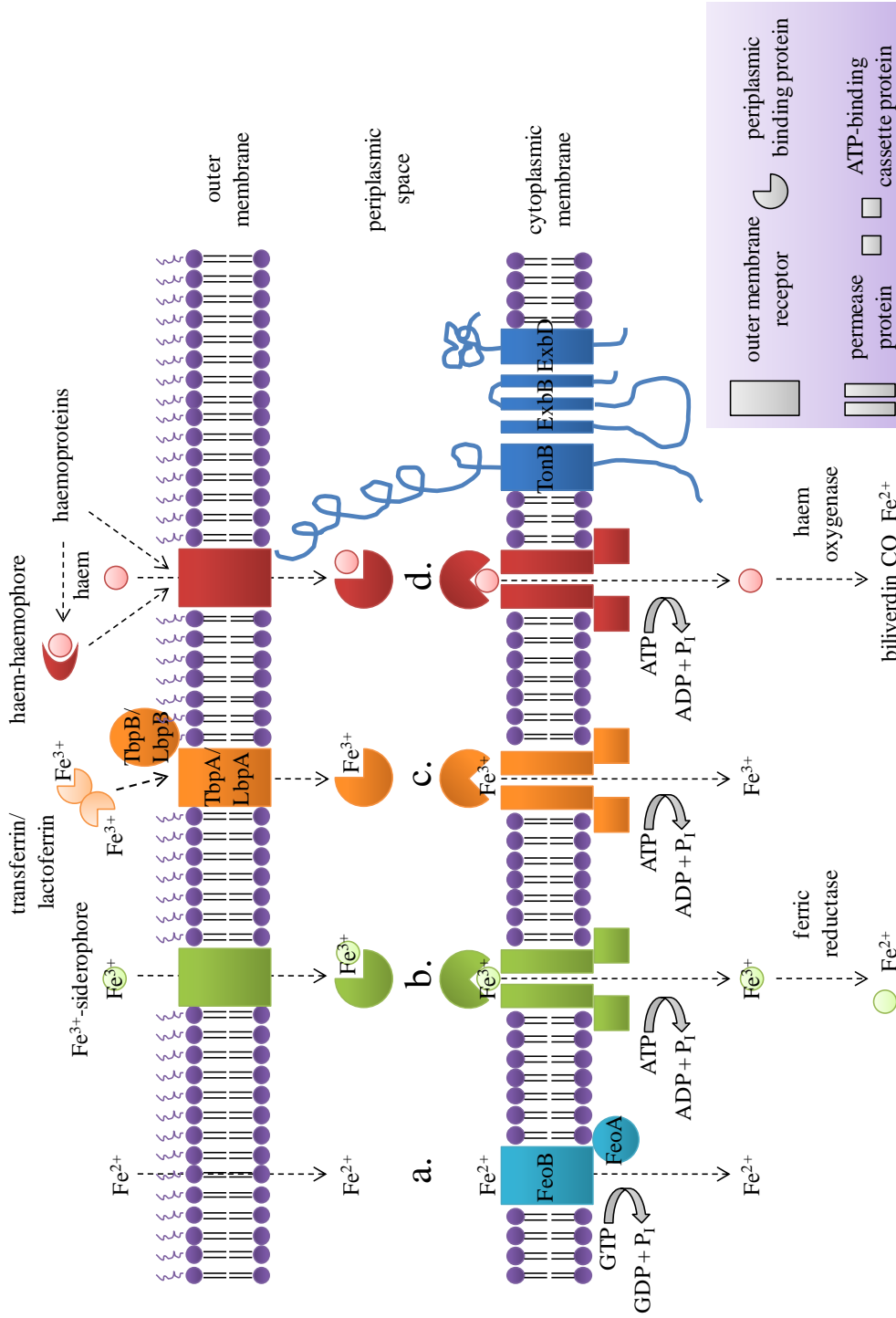


Figure 1.8: An illustration of iron acquisition systems of Gram-negative bacteria including: ferrous iron uptake (a), siderophore-mediated ferric iron uptake (b), iron uptake from transferrin/lactoferrin (c) and direct haem uptake and haem uptake from haemoproteins (d). The energy required for iron and haem uptake through the outer membrane receptor is transduced from the cytoplasmic membrane by the TonB/ExbB/ExbD protein complex (adapted from Krewulak and Vogel, 2008).

E. coli three-gene operon *feoABC* encodes an example of such systems which are iron repressed and anaerobically induced (Hantke, 1987; Kammler *et al.*, 1993).

FeoB is the cytoplasmic ferrous iron permease which consists of a C-terminal transmembrane domain and a hydrophilic N-terminal domain. The C-terminal domain contains two opposite orientated Gate motifs with conserved residues such as cysteine (Cys) that are predicted to be involved in metal binding during iron transport (Cartron *et al.*, 2006). The C-terminal domain contains a G-protein region that possesses GTPase activity and is essential for FeoB transport activity (Marlovitis *et al.*, 2002). In *H. pylori*, Feo activity is ATP-dependent which indicates FeoB may possess GTPase as well as ATPase activity (Velayudhan *et al.*, 2000). FeoA is a small hydrophilic protein probably located in the cytosol and it weakly resembles the SH₃ domain of the diphtheria toxin regulator protein DtxR (see 1.2.3.7). Commonly found in eukaryotic signalling proteins, the SH₃ domain plays a role in protein-protein interactions and therefore by analogy, FeoA potentially interacts with FeoB and facilitates FeoB-dependent ferrous iron uptake (Cartron *et al.*, 2006). FeoC is a small protein that has only been found in the Feo system of γ -proteobacteria. It contains a winged HTH DNA-binding motif in the N-terminal and C-terminal iron-sulphur binding residues which indicates a potential role for FeoC as a transcriptional regulator that controls the expression the *feoABC* operon (Cartron *et al.*, 2006).

The iron transport activity of FeoB is particularly important for facultative anaerobic

pathogens and is an essential requirement for their adaptation under host oxygen limited conditions. The ability to colonise the mouse intestine was severely impeded in *E. coli* and *Salmonella enterica feo* mutants (Stojiljkovic *et al.*, 1993; Tsolis *et al.*, 1996). In microaerophilic *H. pylori*, FeoB-mediated ferrous iron uptake is the major iron acquisition pathway and FeoB is required for colonisation of the mouse gastric mucosa as well as for normal growth (Velayudhan *et al.*, 2000).

1.2.2.2 Siderophore-mediated ferric iron uptake

The most common strategies for iron uptake in bacteria involves the utilisation of low molecular weight extracellular ferric chelators called siderophores which are elaborated and secreted by bacteria and fungi in response to iron restriction (Neilands, 1995). More than 500 siderophores have been characterised and they usually consist of a peptide backbone with incorporated metal-chelating functional groups such as α -hydroxycarboxylate, catecholate and hydroxamate groups (Figure 1.9.a-c) that together form hexadentate octahedral complexes with ferric iron (Andrews *et al.*, 2003). Each functional group donates two oxygen ligands which are capable of forming strong ionic interactions with ferric iron and allow siderophores to chelate ferric iron with high affinity (Miethke and Marahiel, 2007). Siderophores are classified by their functional groups and structures of a fungal hydroxamate siderophore ferrichrome and an *E. coli* catecholate siderophore enterobactin are shown in Figure 1.9.d-e.

Siderophores are synthesised from common precursors such as citrate, amino acids and

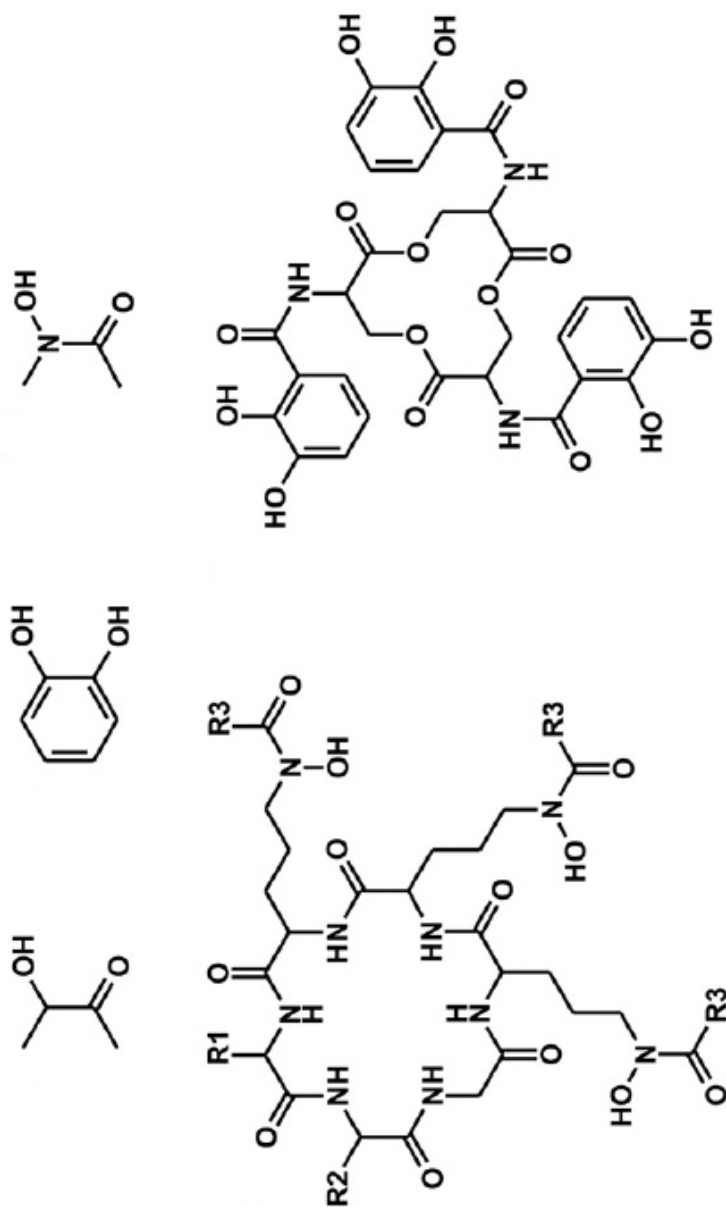


Figure 1.9: Structures of siderophore metal-chelating functional groups: α -hydroxycarboxylate (a), catecholate (b) and hydroxamate (c) and structures of the siderophores ferrichrome (d) and enterobactin (e), taken from Krewulak and Vogel, 2008).

dihydroxybenzoate and the biosynthetic processes are either catalysed by nonribosomal peptide synthetases (NRPS) or by other NRPS-independent enzymatic reactions (Miethke and Marahiel, 2007). Genes encoding the siderophore biosynthetic enzymes are often clustered with genes involved in siderophore uptake and are together induced by iron limitation (Wandersman and Delepelaire, 2004). Once synthesised, siderophores are secreted from the cell through specific transporters such as the *E. coli* membrane protein Ent that belongs to a superfamily of proton motive force (PMF)-dependent membrane efflux pumps and mediates the secretion of enterobactin (Furrer *et al.*, 2002). In addition, many bacteria such as *E. coli* are capable of utilising exogenous siderophores such as ferrichrome as well as enterobactin and related compounds synthesised endogenously by themselves (Chu *et al.*, 2010).

Ferri-siderophores are too large to diffuse freely across the bacterial OM and therefore for Gram-negative bacteria, OM receptors are required to recognise and transport ferri-siderophores into the periplasmic space. The energy required for this process is harnessed from the electrochemical charge gradient across the CM which is delivered to the OM by the energy transducing TonB/ExbB/ExbD protein complex (Figure 1.8.b). Gram-positive bacteria on the other hand do not require TonB-dependent OM receptors for ferri-siderophore uptake due to the lack of the OM (Andrews *et al.*, 2003). Many bacteria possess multiple OM receptors, each displaying a high ligand affinity and specificity. *E. coli* K-12, for example, possesses at least five OM receptors, FepA, CirA, FecA, FhuA and FhuE, which allow the uptake of ferric-bound enterobactin,

enterobactin degraded products, citrate, ferrichrome and rhodotorulic acid respectively (Miethke and Marahiel, 2007). All OM receptors share the same overall structure which consists of a C-terminal transmembrane barrel domain composed of 22 antiparallel β strands connected by 10 periplasmic and 11 extracellular loops (Figure 1.10.a). The N-terminal cork domain has a four-strand β sheet structure with surrounding loops and helices and is kept inside the periplasmic end of the barrel by hydrogen bonds and salt bridges (Krewulak and Vogel, 2008). The cork domain also contains apices that function in siderophore binding (Krewulak and Vogel, 2008) and the periplasmic located N-terminal TonB box essential for TonB-dependent ferri-siderophore uptake (Postle, 1993). In the case of *E. coli* FecA, an additional periplasmic signalling domain transmits a ferric dicitrate-binding signal to the cytoplasmic sigma factor FecI which in turn facilitates the transcription of the ferric dicitrate uptake operon *fecABCDE* (Braun *et al.*, 2003).

The mechanisms of ferri-siderophore transport have been revealed by comparative structural analyses of the ligand free and ferri-siderophore bound FecA and FhuA. Conformational changes of extracellular loops 7 and 8 of the FecA barrel domain have been determined which fold inward over the siderophore binding pocket in the presence of ferric dicitrate (Sauter and Braun, 2004). Similar conformational changes have also been observed for extracellular loops 3 and 11 of the FhuA barrel domain in the presence of ferrichrome (Ferguson *et al.*, 1998) and deletion of these loops completely abolished the ferri-siderophore binding and transporting abilities of FecA and FhuA (Sauter and

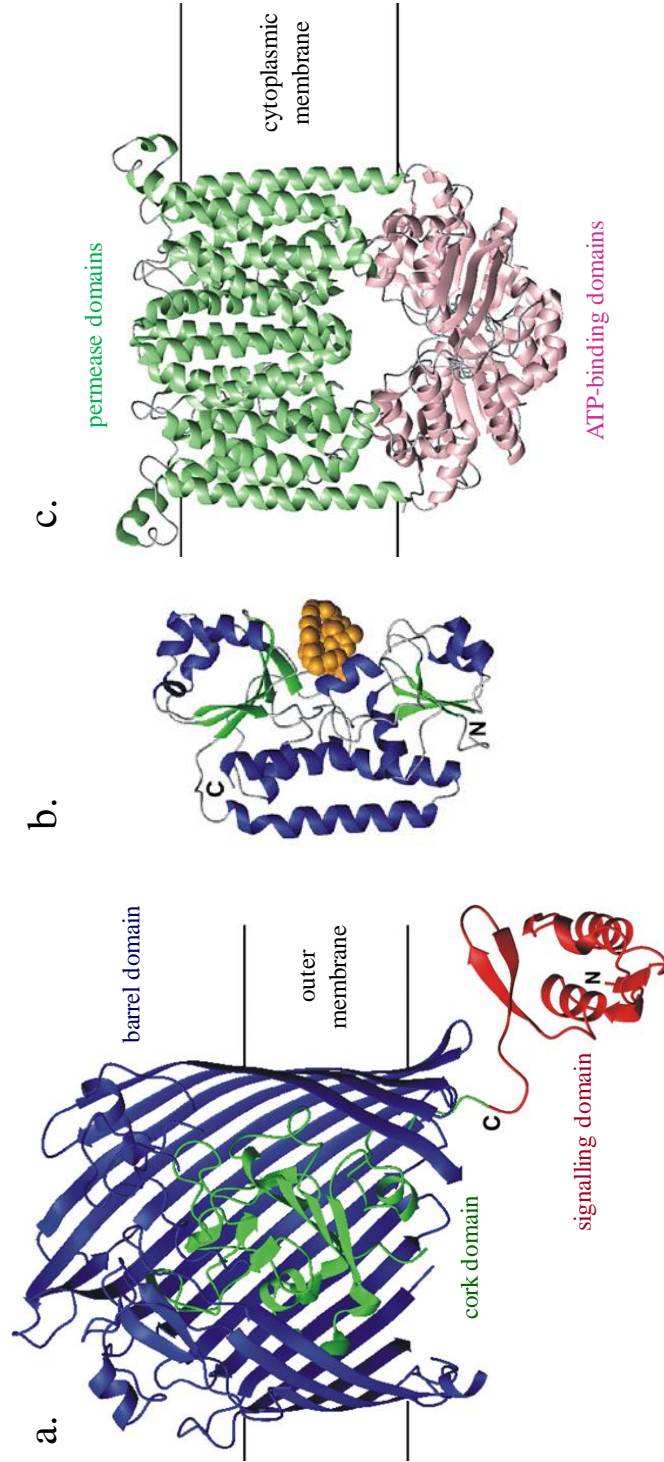


Figure 1.10: Ribbon illustrations of the *E. coli* ferric citrate OM receptor FecA (a), the *E. coli* siderophore PBP FhuD bound to ferrichrome coloured in yellow (b) and the *E. coli* vitamin B₁₂ ABC permease complex BtuCD (c). β -strands that form the front section of the FecA barrel domain have been removed for easy visualisation (taken from Krewulak and Vogel, 2008).

Braun, 2004; Endriss and Braun, 2004). A switch helix in the FhuA cork domain also unwinds when bound to ferrichrome and a similar helix partial unwinding is also observed in the ferric dicitrate bound FecA cork domain (Ferguson *et al.*, 1998; Ferguson *et al.*, 2002). The unwinding of the switch helix leads to a conformational and positional change of the TonB box which signals the binding of a ferri-siderophore to the TonB/ExbB/ExbD protein complex (Noinaj *et al.*, 2010).

ExbB and ExbD are both CM proteins with three and one transmembrane domains respectively and together they transduce the PMF generated at the CM and deliver the energy required for ferri-siderophore transport to the OM receptor via the TonB protein (Figure 1.8). TonB has a single N-terminal transmembrane domain anchored in the CM, a proline rich central domain that spans across the periplasmic space and a periplasmic C-terminal domain consists of one α helix and a three-strand β sheet (Krewulak and Vogel, 2008; Chang *et al.*, 2001). TonB forms a complex with both ExbB and ExbD in a ratio of 1 TonB: 7 ExbB: 2 ExbD (Higgs *et al.*, 2002) and this transmembrane domain-dependent complex formation is essential for TonB activity (Jaskula *et al.*, 1994). Many bacteria have more than one TonB/ExbB/ExbD system. For instance *Vibrio cholerae* has two *tonB* genes associated with a set of *exbBD* genes whereas five potential TonB/ExbB/ExbD coding regions have been identified in *Pseudomonas syringae* (Wandersman and Delepelaire, 2004).

Structural analyses of the TonB-FhuA complex reveal a physical interaction between the

three-strand β sheet of the TonB C-terminal domain and the FhuA TonB box which together forms an interprotein β sheet structure. This interaction leads to a repositioning of the TonB C-terminal α helix and allows the conserved arginine (Arg) residue 166 of TonB to form an electrostatic interaction with the FhuA cork domain. The Arg166 residue is proposed to facilitate the energy transfer from TonB to the cork domain, leading to a structural movement of the cork domain that is necessary for ferri-siderophore translocation to the periplasmic space (Pawelek *et al.*, 2006). The exact movement of the cork domain remains uncertain and it has been postulated that the cork domain undergoes a conformational change that creates a small channel between the cork and the inner barrel wall where the translocation may occur or alternatively the cork domain may partially or completely exit the barrel during ferri-siderophore transport (Noinaj *et al.*, 2010).

Transport of the ferri-siderophore across the periplasmic space is mediated by the siderophore periplasmic binding protein (PBP) which collects and delivers the ferri-siderophore to a cognate ATP-binding cassette (ABC) permease complex in the CM. The ferri-siderophore uptake system in Gram-positive bacteria closely resembles the ABC permease systems found in the CM of Gram-negative bacteria with the exception that the siderophore-binding protein is presented as a lipoprotein tethered to the external surface of the CM (Chu *et al.*, 2010). Unlike OM receptors which have high specificity to individual siderophores, siderophore PBP and cognate ABC permeases are capable of transporting individual classes of siderophores. *E. coli* K-12, for example,

possesses the three siderophore PBPs FepB, FhuD and FecB, which specifically recognise ferric-bound catecholates, hydroxamates and citrates, respectively (Miethke and Marahiel, 2007). The crystal structure of *E. coli* FhuD bound to various hydroxamate type siderophores has been determined and reveals a two-domain structure with each domain composed of a five-strand β sheet sandwiched between layers of α helices (Figure 1.10.b) and the overall structure moves in a Venus flytrap like motion upon ligand binding and releasing (Clarke *et al.*, 2000; 2002). The ligand-binding site is located in the hydrophobic domain interface and ligand specificity is achieved by hydrogen bonding between the hydroxamate functional groups with conserved residues on the binding site. The two domains of FhuD are connected by a long α helix which imposes rigidity on the structure and abolishes the broad ligand associated conformational changes usually seen with other PBP involved in haem or sugar transport (Köster, 2001). Molecular dynamics simulation of FhuD reveals a 6° closure of the C-terminal upon ferrichrome release and this motion is speculated to allow the ferrichrome CM permease FhuB to distinguish between the ligand free and ferrichrome-bound FhuD (Krewulak *et al.*, 2005).

The ABC permease complex is a four-domain structure consisting of two transmembrane domains that form a ferri-siderophore transport channel on the CM and two cytoplasmic nucleotide-binding domains which provide the energy for the transporting process by hydrolysing ATP (Figure 1.8). ABC permease complexes are general assembled from separate subunits and the stoichiometry of these subunits varies.

The permease domains for the *E. coli* ferri-enterobactin transporter for instance are composed of two independent subunits FepD and FepG whereas the ferri-hydroxamate permease is formed by a large two-domain subunit FhuB. The ATP-binding domains for these permeases are assembled by a dimer of FepC and FhuC subunits respectively (Krewulak and Vogel *et al.*, 2008). In addition, the *E. coli* vitamin B₁₂ permease domains are composed of two copies of the same BtuC subunits and the BtuCD complex has shown sequence, design and functional similarities to the siderophore ABC permease complexes (Lewinson *et al.*, 2010). Each BtuC subunit is composed of ten transmembrane helices where helix 5 and 10 from each subunit form a cavity that opens up to the periplasmic space and the cavity is closed from the cytoplasm by helix 4 and 5 (Figure 1.8.a). The ATP-binding protein BtuD contains conserved Walker motifs and Q-loop that are essential for ATP-binding and hydrolysis. The mechanism of ligand transport is proposed by direct contact of the ligand-bound PBP BtuF with the BtuC dimer which facilitates ligand release and BtuD ATP binding. Subsequent ATP hydrolysis triggers a conformational change of the permease that allows ligand transport into the cytoplasm (Locher *et al.*, 2002).

On entering the cytoplasm, siderophore-bound iron is liberated from the complex by one of two general mechanisms. The first method comprises of the reduction of ferric iron resulting in spontaneous release of the reduced iron due to the relative low affinity of siderophore functional groups for ferrous iron (Miethke and Marahiel, 2007). *E. coli* cytoplasmic protein FhuF is an example of a ferric reductase that has substrate

specificity for a set of ferri-hydroxamates. FhuF is iron-regulated and contains an unusual iron-sulphur cluster at the C-terminal that mediates the electron transfer of the ferri-hydroxamate substrates (Matzanke *et al.*, 2004). The alternative iron release mechanism involves intracellular hydrolysis of the ferri-siderophore leading to complex instability and subsequent release of the bound iron, usually by ferric reductase or other iron-binding proteins (Miethke and Marahiel, 2007). An example of such an enzyme with siderophore catabolic function is the *E. coli* esterase Fes, which is encoded by the enterobactin uptake gene cluster and regulated by iron. Fes has a high specificity for ferri-enterobactin and hydrolyses the trilactone backbone of enterobactin into linear trimers, dimers and monomers of 2,3-dihydroxybenzoylserine (Brickman and McIntosh, 1992). In *E. coli* Fes is required for ferri-enterobactin utilisation and it also functions as a ferri-enterobactin-specific ferric reductase (Andrews *et al.*, 2003).

1.2.2.3 Ferric iron uptake from transferrin/lactoferrin

Many pathogenic bacteria such as *Neisseria* species (spp) and *Haemophilus* spp are also able to extract ferric iron from host glycoprotein transferrin and lactoferrin at the cell surface and transport it across the OM using TbpA/TbpB and LbpA/LbpB receptor complexes respectively (Figure 1.8.c, Cornelissen, 2003; Beddek and Schryvers, 2010). Both TbpA and TbpB are surface exposed, iron regulated proteins that are capable of independently binding transferrin (Cornelissen, 2003). TbpA is an integral OM protein structurally related to previously described TonB-dependent ferri-siderophore OM receptors in 1.2.2.2 and its ability to transport ferric iron across the OM is supported by

the inability of TbpA-deficient *Neisseria gonorrhoeae* strains to grow with transferrin as a sole iron source both *in vitro* and *in vivo* (Cornelissen *et al.*, 1992; 1998). The topology model of *N. gonorrhoeae* TbpA reveals large surface loops that are essential for transferrin binding and subsequent iron extraction (Boulton *et al.*, 2000). TbpB is a bi-lobed lipoprotein that contains high-affinity transferrin binding residues at the N-terminal lobe (Moraes *et al.*, 2009). TbpB has a higher preference for *holo*- over *apo*-transferrin due to its ability to discriminate conformational differences between the two ligand forms and this ability has been suggested to enhance the affinity of TbpA for *holo*-transferrin and the rate of *apo*-transferrin release (Cornelissen, 2003). Although TbpB is not essential for transferrin utilisation in *Neisseria meningitidis* and *N. gonorrhoeae* (Irwin *et al.*, 1993; Anderson *et al.*, 1994), TbpB-defective strain of *Actinobacillus pleuropneumoniae*, a causative agent of pneumonia in pig, is avirulent and ineffective in colonisation (Baltes *et al.*, 2002).

The lactoferrin OM receptor complex LbpA/LbpB is functionally and structurally homologous to the TbpA/TbpB complex and is found in several species of the *Neisseriaceae* and *Moraxellaceae* families (Gary-Owen and Schryvers, 1996). In addition, LbpB also protects *N. meningitidis* from the bactericidal effects of lactoferricin and this function is mediated by the clusters of negatively charged residues in the C-terminal lobe (Beddek and Schryvers, 2010). Transport of ferric iron released from transferrin and lactoferrin across the periplasmic space and into the cytoplasm is dependent on the PBP FbpA and the cognate ABC permease complex FbpBC

respectively (Cornelissen, 2003; Beddek and Schryvers, 2010). Structural analysis of *Haemophilus influenzae* FbpA reveals a typical two-domain structure linked by two antiparallel β stands and a 20° domain closure upon ferric iron binding (Bruns *et al.*, 1997; 2001). FbpA also bears resemblance to a single transferrin lobe (Bruns *et al.*, 1997) and possesses similar ferric iron coordination residues and ligand binding affinity that have been seen with transferrin (Nowalk *et al.*, 1994).

1.2.2.4 Direct haem uptake and haem uptake from haemoproteins

Another alternative mechanism to siderophores for microbial iron acquisition *in vivo* is the direct utilisation of host haem and haemoproteins as iron and haem sources (Genco and Dixon, 2001). Exotoxins such as haemolysins, cytolysins and proteases are secreted by extracellular pathogens which liberate haem and haemoglobin from erythrocytes and the free haem and haem complexed with host haemoproteins can then be transported by bacteria using receptor- or haemophore-mediated uptake systems (Figure 1.8.d). The receptor-mediated systems in Gram-negative bacteria involve direct binding of haem or haemoproteins by TonB-dependent OM receptors and the haem is then transported into the cell by haem-specific PBP and ABC permease complexes (Tong and Guo, 2009). Many ligand specific OM receptors have been identified and some examples including haem-specific receptor HutA of *V. cholerae* (Occhino *et al.*, 1998) and HumR of *Yersinia pestis* (Thompson *et al.*, 1999); haemoglobin-specific receptor HmbR of *N. meningitidis* (Stojiljkovic *et al.*, 1996); haem and haemoglobin receptor ChuA of *E. coli* (Torres and Payne, 1997) and PhuR of *P. aeruginosa* (Ochsner *et al.*, 2000) and

haemoglobin and haemoglobin-haptoglobin receptors HgpA, B and C of *H. influenzae* (Morton *et al.*, 1999). *N. gonorrhoeae* and *N. meningitidis* also possess haemoglobin and haemoglobin-haptoglobin receptor HpuB with associated OM lipoprotein HpuA and the HpuBA complex is an analogue to the bipartite transferrin receptor TbpA/TbpB complex described in 1.2.2.3 (Chen *et al.*, 1998; Lewis *et al.*, 1998). Gram-positive bacteria also possess receptor-mediated haem uptake systems such as the *Staphylococcus aureus* cell surface receptors IsdB and IsdH which bind haemoglobin and haemoglobin-haptoglobin respectively. Haem is removed from the bound haemoglobin by surface protein IsdA and transferred to the cell wall protein IsdC prior to passing through the membrane mediated by the translocation protein complex IsdDEF (Mazmanian *et al.*, 2003).

Several Gram-negative bacteria also secrete extracellular haemophores which bind haem or extract haem from haemoproteins and shuttle them back to the OM for uptake by specific TonB-dependent OM haemophore receptors (Tong and Guo, 2009). Two types of such systems have been reported, one is the *Serratia marcescens* haemophore HasA and its cognate receptor HasR. Secreted by the HasDEF protein complex, HasA has a high affinity to haem and functions to capture haem or extract haem from haemoglobin and present it to HasR. HasR also acts as a low affinity OM receptor for haem and haemoglobin and the energy required for haem transport through HasR is depended on HasB, a TonB-like protein (Létoffé *et al.*, 2004). HxuA of *H. influenzae* is another type of haemophore which is secreted by HuxB and forms a complex with

haem-haemopexin. HxuC is the cognate OM receptor for HxuA and is also required for haem and haem-albumin uptake processes (Morton *et al.*, 2007). The majority of haem transported into the cytoplasm is rapidly catabolised by haem oxygenase which catalyses the oxidation of haem into ferrous iron, biliverdin and carbon monoxide (Li and Stocker, 2009). Haem oxygenase has been isolated from both Gram-negative and positive bacteria such as ChuS of *E. coli* (Suits *et al.*, 2005), HemO of *N. meningitidis* (Zhu *et al.*, 2000) and IsdG/I of *S. aureus* (Skaar *et al.*, 2004).

1.2.2.5 Iron and haem storage

When acquired by specific iron uptake systems and liberated from siderophore and haem, ferrous iron is either incorporated directly into metalloenzymes to fulfil their biological roles, or if in excess, iron is deposited in the ferric form in iron storage proteins which can then be used as intracellular iron sources when exogenous iron supplies are restricted. Iron storage proteins also protect the bacterial cell against oxidative stress induced by iron overload (Smith, 2004). Three iron storage proteins have been characterised in bacteria including the bacterial ferritin (referring to as ferritin from here onward), bacterioferritin and Dps. Both ferritin and bacterioferritin are tetracosameric spheres usually assembled by identical subunits surrounding a central iron storage cavity. Ferroxidase residues are found in the centre of each subunit which act as iron-binding ligands and use oxygen to catalyse the oxidation of bound ferrous iron into diferric intermediates for subsequent storage in the central cavity (Le Brun *et al.*, 2010). The ferroxidase centre of ferritin closely resembles that of the eukaryotic

ferritin H-chain centre and it functions as a gated iron pore. Bacterioferritin ferroxidase centre on the other hand is quite distinct from the H-chain eukaryotic ferritin and it acts as a true catalytic centre (Le Brun *et al.*, 2010). In addition, all known bacterioferritins also contain additional haem groups located at the subunit interfaces near the central cavity that play an essential role in facilitating iron release from the bacterioferritin central cavity (Yasmin *et al.*, 2011). Dps is a stress-induced non-specific DNA-binding protein with a dodecameric structure and contains non-conserved ferroxidase residues (Smith, 2004).

Inactivation of the *E. coli* ferritin encoding gene *ftnA* results in a reduction of stationary phase cellular iron content and a reduced growth rate under iron-restricted conditions which demonstrates the iron storage function of FtnA and the ability for *E. coli* to use FtnA stored iron as an intracellular iron source (Abdul-Tehrani *et al.*, 1999). Iron stored in *H. pylori* ferritin Pfr on the other hand does not serve as an iron source, Pfr rather functions in protecting the cell from iron overload and is essential for the colonisation of gastric mucosa in animal models (Waidner *et al.*, 2002). The *E. coli* bacterioferritin Bfr catalyses the oxidation of bound ferrous iron using hydrogen peroxide and hence reduces the formation of hydroxyl radicals, though no phenotypes have been associated with the *bfr* mutant (Bou-abdallah *et al.*, 2001). Unlike the *E. coli* Bfr, the *N. gonorrhoeae* bacterioferritin is assembled by non-identical A and B subunits. The exact ratio of subunit A and B is unknown, however the subunit B is essential for protecting the cell against oxidative stress and iron stored in the *N. gonorrhoeae* bacterioferritin

can be utilised by the cell during iron deprivation (Chen and Morse, 1999). The synthesis of *E. coli* Dps is induced during stationary phase by nutrient starvation or oxidative stress. Dps utilises hydrogen peroxide as the ferrous oxidant during iron binding and therefore protects Dps-bound DNA from hydroxyl radicals (Zhao *et al.*, 2002). The Dps of *Porphyromonas gingivalis* is another example of an iron- and DNA-binding protein which increases bacterial survival during infection of endothelial cells. The mechanism Dps uses to protect the cell against hydroxyl radicals is not mediated by DNA-binding, but rather by decomposing hydrogen peroxide during the oxidation of ferrous iron, a mechanism also used by *E. coli* Bfr. The significance of *P. gingivalis* Dps-DNA interaction is unclear and Dps-bound iron cannot be used as an iron source (Ueshima *et al.*, 2003).

Although not identified in most organisms, haem storage proteins have also been identified in bacteria that acquire exogenous haem and these proteins were originally considered as haem oxygenases (Wandersman and Delepelaire, 2004). The oligomeric protein ShuS of *Shigella dysenteriae* is an experimentally characterised haem storage protein that consists of 18 identical subunits each with a single haem molecule binding capacity. ShuS also functions as a DNA-binding protein that protects DNA from haem-induced oxidative damage (Wilks, 2001). The haem-transporting protein HemS of *Yersinia enterocolitica* shares 64% sequence identity with ShuS, it protects the cell from haem toxicity effects and also has been proposed as a haem storage protein (Stojiljkovic and Hantke, 1994). HmuS of *Y. pestis* and PhuS of *P. aeruginosa* are other candidates

that have been hypothesised to involve in haem storage (Tong and Guo, 2009).

1.2.3 Fur and the functional role of Fur as a global transcriptional regulator

Due to the necessity and toxicity of iron, many bacteria effectively regulate their iron acquisition and storage genes in response to iron availability. This enables bacteria to maintain a balanced level of intracellular iron required for biological functions and at the same time avoid unnecessary stress and damage to the cell due to excess iron. In most Gram-negative bacteria and AT-rich Gram-positive bacteria, iron homeostasis is regulated by the Fur protein. Fur also functions as a global regulator in controlling genes involved in metabolism, oxidative stress, acid tolerance and virulence factors (Hantke, 2001; Lee and Helmann, 2007; Carpenter *et al.*, 2009b).

1.2.3.1 Fur as an iron-dependent repressor and its role in iron homeostasis

The first connection between iron homeostasis and Fur was noted back in 1978 when constitutive expression of ferri-enterobactin and ferrichrome uptake systems were observed for a *S. enterica* mutant grown in iron-rich media (Ernst *et al.*, 1978). This strain was named *fur*, for iron uptake regulation (Ernst *et al.*, 1978). The *E. coli fur* (*fur_{Ec}*) mutant isolated three years later showed constitutive expression of the OM iron-acquisition receptor genes *cir*, *fhuA* and *fecA* which were otherwise strongly repressed by iron in the wild-type strain (Hantke, 1981). The *fur_{Ec}* mutant was subsequently complemented (Hantke, 1982), the *fur_{Ec}* gene cloned (Hantke, 1984) and sequenced (Schäffer *et al.*, 1985) and the Fur_{Ec} protein purified (Wee *et al.*, 1988).

Fur_{Ec} is a 17 kDa His-rich metalloprotein (Schäffer *et al.*, 1985) consisting of an N-terminal DNA-binding domain with a winged HTH motif and a C-terminal dimerisation domain (Stojiljkovic and Hantke, 1995). Fur_{Ec} functions as a homodimer (Bagg and Neilands, 1987b) where each subunit binds to a single ferrous iron atom (Bagg and Neilands, 1987a). Other divalent cations such as cobalt, manganese and zinc also activate Fur_{Ec} *in vitro*, although the level of cobalt and manganese present *in vivo* are usually insufficient to be physiologically relevant for Fur_{Ec} function (Bagg and Neilands, 1987b; de Lorenzo *et al.*, 1987; Mills and Marletta, 2005) whereas the intercellular zinc concentration is tightly regulated to prevent it from displacing native metals in Fur_{Ec} (Waldron and Robinson, 2009). Binding of the iron corepressor induces a conformational change in the Fur_{Ec} protein (Coy and Neilands, 1991) which allows the N-terminal domain to recognise and bind to a 19 bp operator sequence termed the Fur_{Ec} box (de Lorenzo *et al.*, 1987). The Fur_{Ec} box is found in the promoter region of Fur_{Ec}-repressed genes, often overlapping the -10 and -35 regions of the promoter (de Lorenzo *et al.*, 1987), thus interaction of Fur_{Ec} with the Fur_{Ec} box prevents the access of RNA pol to the promoter resulting in transcriptional repression of the target genes (Figure 1.11.a, Bagg and Neilands, 1987a).

The affinity of Fur_{Ec} for ferrous iron is approximately 10 μ M (Bagg and Neilands, 1987a) which is comparable to the estimated amount of free iron in the cytosol (Keyser and Imlay, 1996) and iron-binding leads to an approximate 1000-fold increase in the

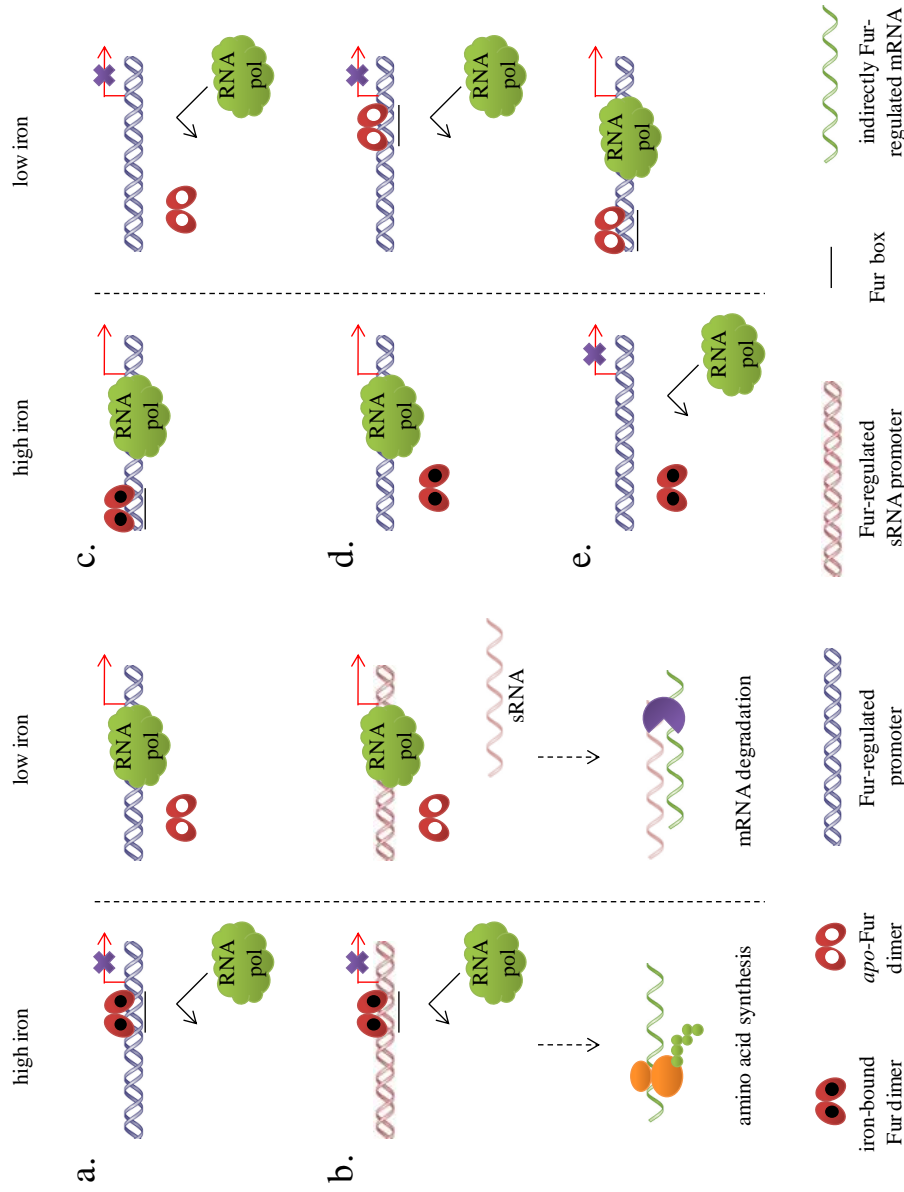


Figure 1.11: The regulatory potential of Fur in response to iron availability. In most cases, Fur dimer in its iron-bound form binds to the Fur box that overlaps the Fur-regulated promoter and inhibits transcription initiation by blocking the access of RNA pol to the promoter (a). Iron-bound Fur dimer also activates gene expression either indirectly by repressing the intermediate sRNA synthesis which in turn allows the expression of sRNA-repressed genes (b) or directly by binding to the Fur box upstream of the Fur-regulated promoter which recruits and/or enhances RNA pol binding to the promoter (c). Both transcriptional gene repression and activation by *apo-Fur* have been characterised in *H. pylori* (d and e respectively). Whether *apo-Fur_{Hp}* functions as a monomer or a dimer is uncertain and it is illustrated as a dimer in here for simplicity (adapted from Carpenter *et al.*, 2009).

affinity of Fur_{Ec} for the Fur_{Ec} box (Andrews *et al.*, 2003). These characteristics make Fur_{Ec} an ideal candidate for monitoring and responding to physiologically relevant fluctuations in intracellular free iron levels (Andrews *et al.*, 2003). Under iron-restricted conditions, the affinity of Fur_{Ec} for iron is insufficient to populate the Fur_{Ec} iron-binding site, which causes derepression of iron acquisition genes and allows accumulation of intracellular iron. However when the iron level exceeds cellular demands, Fur_{Ec} coupled with iron prevents further iron intake by down regulating these iron acquisition genes thus protecting the cell from iron-induced oxidative stress (Andrews *et al.*, 2003; Lee and Helmann *et al.*, 2007).

Not surprisingly, all known *E. coli* iron acquisition systems are Fur_{Ec} and iron-repressed and some examples include enterobactin biosynthesis genes *entABCDEFG* (Brickman *et al.*, 1990; McHugh *et al.*, 2003), ferri-enterobactin uptake genes *fepABCDEG* (Brickman *et al.*, 1990; Hantke, 1981), the ferri-enterobactin esterase gene *fes* (Hunt *et al.*, 1994), aerobactin biosynthesis genes *iucABCD* (de Lorenzo *et al.*, 1987), the ferri-aerobactin uptake gene *iutA* (de Lorenzo *et al.*, 1987), ferrichrome uptake genes *fhuABCD* (Hantke, 1981), ferric dicitrate uptake genes *fecABCDE* (Enz *et al.*, 2000), *fec* operon regulator genes *fecI* and *fecR* (Hantke, 1981; Enz *et al.*, 2000; Braun *et al.*, 2003), the ferri-rhodotorulic acid uptake gene *fhuE* (McHugh *et al.*, 2003), the TonB/ExbB/ExbD system coding genes (McHugh *et al.*, 2003) as well as ferrous iron uptake genes *feoABC* (Kammler *et al.*, 1993).

Fur_{Ec} also represses its own expression (Figure 1.12.a) under iron-rich conditions as indicated by a direct binding of Fur_{Ec} to the *fur*_{Ec} promoter located in the intergenic region between *fur*_{Ec} and the upstream flavodoxin coding gene *fldA* (de Lorenzo *et al.*, 1988b). Fur autoregulation is the most common mechanism of *fur* regulation which allows Fur to effectively regulate its expression according to intracellular iron levels (Carpenter *et al.*, 2009b). In addition to autoregulation, Fur_{Ec} expression is positively influenced by peroxide-sensing regulator OxyR and superoxide regulators SoxRS in response to oxidative stress (Zheng *et al.*, 1999). OxyR activates the *fur*_{Ec} promoter in response to hydrogen peroxide and when exposed to superoxide-mediated stress, *fur*_{Ec} can also be co-transcribed with *fldA* from the SoxRS-regulated *fldA* promoter (Zheng *et al.*, 1999). In fact, the estimated number of Fur_{Ec} molecules per cell doubles under oxidative stress and this link between *fur*_{Ec} expression and oxidative stress further illustrates the essential role of Fur_{Ec} in iron homeostasis (Zheng *et al.*, 1999). Furthermore, a putative Cap-binding site has been identified in the *fldA-fur*_{Ec} intergenic region indicating potential cAMP responsive *fur*_{Ec} regulation (de Lorenzo *et al.*, 1988b).

Since the discovery of Fur_{Ec}, Fur orthologues have been identified in many Gram-negative bacteria such as *H. pylori* (Bereswill *et al.*, 1998), *N. meningitidis* (Thomas and Sparling, 1994), *P. aeruginosa* (Prince *et al.*, 1993), *V. cholerae* (Litwin *et al.*, 1992) and *Y. pestis* (Staggs and Perry, 1991), and in AT-rich Gram-positive bacteria such as *Bacillus subtilis* (Bsat *et al.*, 1998) and *L. monocytogenes* (Ledala *et al.*, 2007). All these proteins show a high degree of homology with Fur_{Ec}. Like in *E. coli* (McHugh

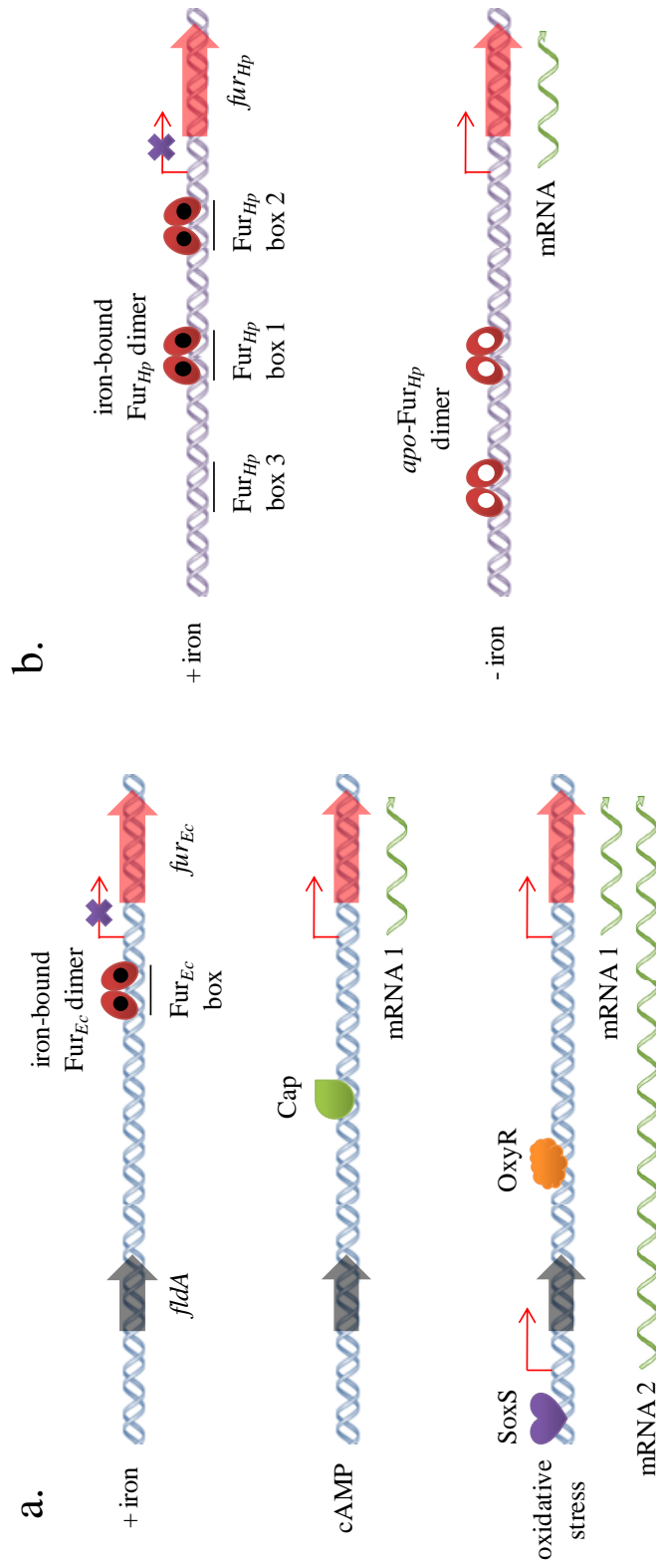


Figure 1.12: The expression of *fur* in *E. coli* (a) and *H. pylori* (b). *fur_{Ec}* is repressed by its own gene product under iron-rich conditions but it is activated by Cap and OxyR in response to cAMP and exposure to hydrogen peroxide respectively. Under superoxide-mediated stress, *fur_{Ec}* is activated by SoxS from a distal promoter, resulting in the production of a multicistronic mRNA also contains transcript of the upstream *fldA* gene. *fur_{Hp}* is repressed by *Fur_{Hp}* binding to the *Fur_{Hp}* boxes 1 and 2 under iron-rich conditions and activated by *apo-Fur_{Hp}* binding to *Fur_{Hp}* boxes 1 and 3 under iron-restricted conditions. For easy visualisation, the length of *Fur* genes and *Fur* promoter regions are not drawn in proportion and *apo-Fur_{Hp}* is illustrated as a dimer for simplicity (adapted from Gilbreath *et al.*, 2011).

et al., 2003), genetic analyses of these Fur regulons indicate the majority of Fur- and iron-repressed genes in these bacteria are associated with iron homeostasis (Ochsner and Vasil, 1996; Baichoo *et al.*, 2002; Grifantini *et al.*, 2003; Mey *et al.*, 2005; Danielli *et al.*, 2006; Gao *et al.*, 2008; Ledala *et al.*, 2010).

1.2.3.2 Structure-function relationships of Fur

Initial characterisation of the tertiary structure of Fur_{Ec} illustrated a rigid, α helix-rich structure (Saito and Williams, 1991) where each monomer possesses a regulatory iron site (Saito *et al.*, 1991a; 1991b) and a C-terminal structural zinc site (Jacquamet *et al.*, 1998; Althaus *et al.*, 1999). Binding of iron or other divalent cations to the regulatory site is essential for allosteric activation of Fur_{Ec} (Coy and Neilands, 1991) while zinc binding to the structural site induces C-terminal domain structural stability and dimerisation (Pecqueur *et al.*, 2006). Spectroscopic and molecular modelling analyses reveal that iron is bound to the regulatory site in a hexa-coordinated environment (Adrait *et al.*, 1999; Jabour and Hamed, 2009) whereas zinc is coordinated in the structural site in a tetrahedral geometry (Jacquamet *et al.*, 1998). Fur_{Ec} contains four Cys residues that are commonly associated with metal ligands in other proteins (O'Halloran, 1993) and are grouped in Cys92-X₂-Cys95 (X_n where n represents the number of amino acids) and Cys134-X₄-Cys139 motifs (Schäffer *et al.*, 1985). Mutational and chemical modification studies demonstrate that Cys92 and Cys95 are essential for Fur_{Ec} activity and structural zinc coordination, whereas Cys134 and Cys139 are dispensable and potentially involved in oxidative stress sensing (Coy *et al.*,

1994; Gonzalez de Peredo *et al.*, 1999; Pecqueur *et al.*, 2006). The *B. subtilis* Fur (Fur_{Bs}) also possesses two metal-binding sites and contains four Cys residues that are all required for Fur_{Bs} activity, stability (Bast and Helmann, 1999) and potentially function as zinc ligands (Lee and Helmann, 2007).

Early binding studies of both Fur_{Ec} and Fur_{Bs} have indicated that both proteins, either in the metal-bound form or in the *apo* form (in this report, *apo*-Fur is referred to as Fur protein complexed with a structural zinc but not with any bound regulatory metals) were able to bind DNA with high affinities (Althaus *et al.*, 1999; Bsat and Helmann, 1999). In both cases, *apo*-Fur binding was likely to be caused by metal contamination (Lee and Helmann, 2007) and in fact, the ability for *apo*-Fur_{Ec} to bind DNA was abolished when possible contaminating metals were removed by EDTA (Mills and Marletta, 2005). *apo*-Fur regulation is however physiologically relevant in some bacteria such as *H. pylori* and is described in detail in 1.2.3.5.

The first crystal structure of the Fur complexed with two zinc atoms per monomer was resolved in *P. aeruginosa* (Fur_{Pa}) which confirmed the originally predicted dimeric protein structure (Figure 1.13.a, Pohl *et al.*, 2003). Each monomer consists of four α helices (helix 1-4) followed by a two-stranded antiparallel β sheet that together form the N-terminal DNA-binding domain, while the C-terminal dimerisation domain is composed of three antiparallel β strands (strand 3-5) with a distal terminal α helix (helix 5, Pohl *et al.*, 2003). Strand 3-5 from both monomers form a six-strand β sheet that

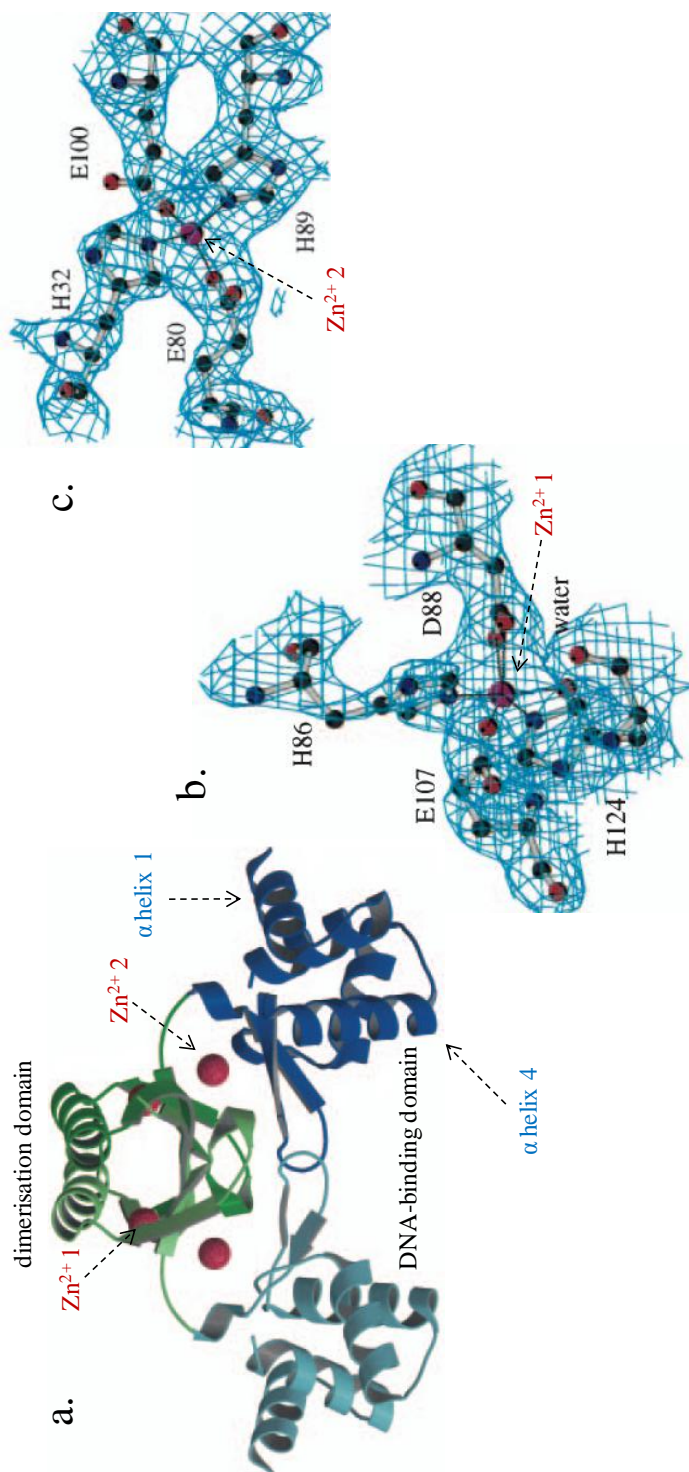


Figure 1.13: The ribbon illustration of the Fur_{P α} dimer with bound zinc atoms and α helices 1 and 4 indicated (a) and stereo views of the electron density surrounded both zinc atoms (b and c, taken from Pohl *et al.*, 2003).

connects the two monomers together and the dimeric structure is further strengthened by numerous hydrophobic and hydrophilic interactions between helix 5 of each monomer (Phol *et al.*, 2003). Asp103 and Arg109 of each monomer also form salt bridges that facilitate dimerisation (Phol *et al.*, 2003) as reduced DNA-binding affinity has been observed with an Asp103 mutant (Barton, 1997).

The N-terminal domain exhibits a typical winged HTH motif and helix 4 of each Fur_{Pa} dimer are proposed to come in contact with two major grooves on the DNA molecule separated by a single helix turn (Phol *et al.*, 2003). In addition, helix 1 is also involved in DNA recognition as mutation of alanine (Ala) residue 10 in helix 1 caused a partial unfolding of the N-terminal domain and the DNA-binding activity of Fur_{Pa} was subsequently abolished (Barton *et al.*, 1996). In a comparative analysis of apo-Fur_{Ec}, Fur_{Ec} monomer and the N-terminal domain, the folding of helix 2, 3 and 4 were unaffected by the state of the C-terminal whereas helix 1 was unstructured in apo-Fur_{Ec} (Pecqueur *et al.*, 2006). This observation led to the conclusion that helix 1 is associated with the activation state of the Fur_{Ec} protein and, like Fur_{Pa}, helix 1 formation is triggered by binding of the iron cofactor and it functions in facilitating DNA recognition and interaction (Pecqueur *et al.*, 2006).

The structure of Fur_{Pa} reveals the presence of two metal binding sites (MBSs) per monomer (Figure 1.13): MBS1_{Pa} is located in the dimerisation domain and coordinates the zinc atom 1 in a distorted octahedral geometry with the side chains of His86, Asp88

(a symmetrical bidentate), glutamine (Glu) residue 107 and His124 and a water molecule; MBS2_{Pa} connects the two domains and the zinc atom 2 is coordinated by the side chains of His32, Glu80, His89 and Glu100 in a tetrahedral geometry. Fur_{Pa} only possesses one of the four Cys residues seen with Fur_{Ec}, and it does not function as a metal ligand (Pohl *et al.*, 2003). Iron substitution analysis of the zinc-bound Fur_{Pa} revealed that zinc atom at MBS1_{Pa} but not MBS2_{Pa} could be replaced by iron and thus MBS1_{Pa} and MBS2_{Pa} were proposed to function as regulatory iron and structural zinc sites respectively (Pohl *et al.*, 2003). This proposal however was contradicted with the observation of several mutational studies. For instance, the iron-responsiveness of Fur_{Pa} was retained for a His86 and Asp88 (MBS1_{Pa} ligands) mutant but not for a His98 (an MBS2_{Pa} ligand) mutant (Lewin *et al.*, 2002) and the iron-responsive ability was also abolished for a *fur_{Bs}* mutant containing altered His97 (corresponds to His98 of Fur_{Pa}, Bsat and Helmann, 1999). The MBS2_{Pa} site proposed by Pohl *et al.* (2003) is therefore currently reassigned by Lee and Helmann (2007) as the regulatory iron site, while MBS1_{Pa} plays a subsidiary role that remains to be elucidated and unlike Fur_{Ec}, Fur_{Pa} may lack a structural zinc site (Lewin *et al.*, 2002). This view is further supported by free energy calculations of Fur_{Ec} and Fur_{Pa} which proposes the coordination of iron in MBS2_{Pa} in an octahedral environment with His87 as an additional putative iron ligand (Ahmad *et al.*, 2009), and also supported by the crystal structure of the *V. cholerae* Fur (Fur_{Vc}, Sheikh and Taylor, 2009).

Purified Fur_{Vc} complexed with zinc atoms also possesses two MBSs per monomer

(Figure 1.14). The zinc atom 1 in MBS1_{Vc} is tetra-coordinated by the side chains of His87, Asp89, Glu108 and His125 which are the equivalent of ligands found in MBS1_{Pa} (Sheikh and Taylor, 2009). Mutation of His87 and His125 of *Vibrio alginolyticus* Fur (Fur_{Va}, which shares 94% sequence identity to Fur_{Vc}) resulted in a two-fold reduction of Fur_{Va} activity (Liu *et al.*, 2007) which by analogy, suggests the auxiliary role of MBS1_{Vc} in Fur_{Vc} activity (Sheikh and Taylor, 2009). MBS2_{Vc} coordinates the zinc atom 2 in a tetrahedral environment by the side chains of His33, Glu81, His88 and His90 where His88 is substituted by Glu100 (equivalent of Glu101 in Fur_{Vc}) in MBS2_{Pa}. A His90 mutant of Fur_{Vc} demonstrated that His90 is essential for iron sensing (Lam *et al.*, 1994) and Fur_{Va} activity was also abolished in His33 and His90 mutants (Liu *et al.*, 2007), which together indicates the crucial role of MBS2_{Vc} as the regulatory iron site (Sheikh and Taylor, 2009). In addition, Glu101 of Fur_{Vc} is also proposed to function as the fifth metal ligand in coordinating iron in an octahedral environment in MBS2_{Vc} (Sheikh and Taylor, 2009).

Fur_{Vc} contains four conserved Cys residues grouped in two Cys-X₂-Cys motifs, and interestingly unlike Fur_{Ec}, they are not involved in metal coordination but instead Cys93 and Cys133 form a disulphide bridge that stabilises the dimeric protein structure (Sheikh and Taylor, 2009). Comparison of the overall structure between Fur_{Vc} and Fur_{Pa}, which share 50% sequence identity, revealed a 30° rotation of the DNA-binding domain relative to the C-terminal domain of zinc-bound Fur_{Vc} such that the distance between the two helix 4s in the Fur_{Vc} dimer is closer than that seen with Fur_{Pa} (Sheikh and Taylor,

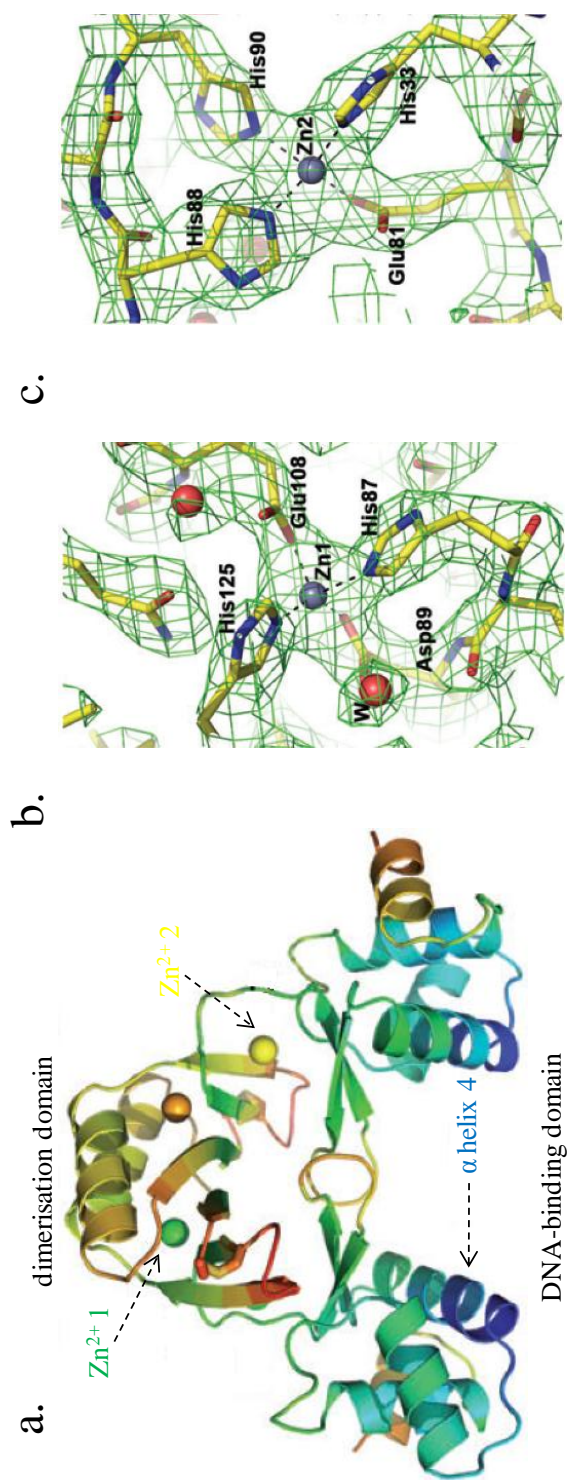


Figure 1.14: The ribbon illustration of the Fur_c dimer with bound zinc atoms and the α helix 4 indicated (a) and stereo views of the electron density surrounded both zinc atoms (b and c, taken from Sheikh and Taylor, 2009).

2009). The authors suggested that binding of zinc to MBS2_{Vc} is inadequate for the N-terminal domain to fold into an optimal position for DNA-binding and an efficient DNA-binding is only achieved by coordinating iron in MBS2_{Vc} (Sheikh and Taylor, 2009).

The crystal structure of the *H. pylori* Fur (Fur_{Hp}) containing two amino acid substitutions has been recently resolved which shows several unique features when compared with Fur_{Pa} and Fur_{Vc}. Each Fur_{Hp} monomer (Figure 1.15) possesses a ten-residue extension at the start of the N-terminal domain, an additional α helix 6 at the end of the C-terminal domain and three MBSs (Dian *et al.*, 2011). MBS1_{Hp} is located in the C-terminal and it tetra-coordinates the zinc atom 1 by the side chains of two Cys-X₂-Cys motifs consisting Cys102, Cys105, Cys142 and Cys145. Binding of zinc to MBS1_{Hp} stabilises the dimeric protein structure which reflects the role of MBS1_{Hp} as the structural zinc site (Dian *et al.*, 2011). MBS2_{Hp} has equivalent location to MBS2_{Pa} and MBS2_{Vc}, but unlike in these bacteria, coordination of the zinc atom 2 in MBS2_{Hp} adopts different geometries between each Fur_{Hp} monomer. In one monomer, the zinc atom 2 is coordinated in a tetrahedral environment by the side chains of His42, Glu90, His97 and His99, whereas the zinc atom 2 in the second monomer is octa-coordinated by the additional side chain of Glu110. MBS3_{Hp} is locationally equivalent to MBS1_{Pa} and MBS1_{Vc} and it coordinates the zinc atom 3 in a tetrahedral environment by the side chains His96, Asp98, Glu117 and His134 (Dain *et al.*, 2011).

Functional analyses of MBS2_{Hp} and MBS3_{Hp} demonstrated that MBS2_{Hp} is essential for DNA-binding activity and the metal-induced allosteric activation of Fur_{Hp} whereas MBS3_{Hp} is dispensable for DNA-binding, though its disruption significantly reduces the affinity of DNA-binding. Based on these observations, MBS2_{Hp} is proposed to function as a primary regulatory iron site where metallation of this site mediates Fur_{Hp}-DNA interaction and this DNA-binding is further strengthened by the binding of a second metal ion to MBS3_{Hp} under excess metal conditions (Dian *et al.*, 2011). The assigned roles of MBS2_{Hp} and MBS3_{Hp} are further supported by an independent mutation study, which also demonstrated the subsidiary role of both sites involved in maintaining Fur_{Hp} oligomerisation (Carpenter *et al.*, 2010). The unique structural features observed for Fur_{Hp} are likely to reflect its diverse regulatory potential (see 1.2.3.4 and 1.2.3.5) and the distinct metal coordination schemes adopted by Fur_{Ec}, Fur_{Pa}, Fur_{Vc} and Fur_{Hp} may lead to variations in the mechanisms of metal-sensing and gene regulation among these Fur orthologues (Danielli and Scarlato, 2010).

1.2.3.3 The Fur box and models of Fur-Fur box interaction

A 31 bp Fur_{Ec} protected region containing a dyad symmetrical element was first observed in a DNase I footprinting analysis of the iron-regulated *E. coli iucA* promoter and a 19 bp Fur_{Ec} box consensus sequence was derived from the alignment of this symmetrical element with the *fhuA* and *fepA* promoter regions (de Lorenzo *et al.*, 1987). This sequence was subsequently observed in an alignment of more than 30 iron-regulated promoters (Stojilkovic *et al.*, 1994) and when cloned downstream of a

heterologous promoter, it was sufficient to induce iron regulation *in vivo* (Calderwood and Mekalanos, 1988). Although the Fur_{Ec} box has since been used as the gold standard for identification of Fur-binding sites in many bacterial species, several models of Fur-Fur box interaction have been proposed based on this sequence (Table 1.1).

Due to the dimeric nature of Fur_{Ec}, it was originally proposed that each Fur_{Ec} monomer recognises and binds to each half of the palindromic sequence (the 9-1-9 model) resembling the mechanism of classical bacterial repressors (Ptashne, 2004). This model however was not compatible with the observation that after the initial Fur_{Ec} binding to the *iucA* Fur_{Ec} box, multiple Fur_{Ec} dimers polymerised along regions that did not resemble the consensus Fur_{Ec} box sequence (de Lorenzo *et al.*, 1987; Escolar *et al.*, 2000). Despite the rigidity of the Fur_{Ec} protein, the unique protection pattern obtained from hydroxyl radical footprinting studies also indicated that Fur_{Ec} wraps the *iucA* promoter region in a helical manner (de Lorenzo *et al.*, 1988a) and this phenomenon has also been directly observed by electron and atomic force microscopy (Fréchon and Le Cam, 1994; Le Cam *et al.*, 1994).

Attempts to resolve these contrasting features, have led to the reinterpretation of the palindromic Fur_{Ec} box as tandem hexameric repeats arranged in a head to head to tail motif (the 6-6-1-6 model, Escolar *et al.*, 1998; Escolar *et al.*, 1999). High affinity Fur_{Ec} binding was achieved using a minimum of three synthetic hexamers and the AT nucleotides in each hexamer were predicted to be important Fur_{Ec} recognition sites

model name	interpretation of the Fur box	model of Fur-DNA interaction	reference
9-1-9 model	<p><u>GATAATGATAATCATTATC</u> <u>CTATTACTATTAGTAATAG</u></p>		de Lorenzo <i>et al.</i> , 1987
6-6-1-6 model	<p><u>GATAATGATAATCATTATC</u> <u>CTATTACTATTAGTAATAG</u></p>	undetermined	Escolar <i>et al.</i> , 1998
(6-1-6) ₂ model	<p><u>GATAATGATAATCATTATC</u> <u>CTATTACTATTAGTAATAG</u></p>		Lavrrar <i>et al.</i> , 2002
(7-1-7) ₂ model	<p><u>tGATAATGATAATCATTATCa</u> <u>aCTATTACTATTAGTAATAGt</u></p>		Baichoo and Helmann, 2002
(9-1-9) ₂ model	<p><u>aatGATAATGATAATCATTATCatt</u> <u>ttaCTATTACTATTAGTAATAGtaa</u></p>		Chen <i>et al.</i> , 2007

Table 1.1: Different interpretations of the consensus Fur box and proposed modes of Fur-DNA interaction. The numbers 6, 7 and 9 used in model names represent the number of nucleotides in each tandem repeat recognised by a Fur monomer and the actual nucleotide sequences are underlined by orange arrows. The number 1 represents the single nucleotide separating two repeats while subscripted number 2 represents the presence of tandem repeats on both strands of the Fur-binding site.

(Escolar *et al.*, 1998). An array of such repeats was also identified in the natural *iucA* promoter where the ability of Fur_{Ec} to extend outside the initial binding site was dependent on these short repeats (Escolar *et al.*, 2000). Although this model could possibly explain the phenomenon of Fur_{Ec} polymerisation along otherwise functionally unrelated DNA, the mechanism of how each Fur_{Ec} dimer binds to the DNA and how many repeats are needed to interact with a Fur_{Ec} dimer remain difficult to explain.

During an electrophoretic mobility shift assay (EMSA) investigation of the *E. coli* *febD-entS* promoter region which contains two overlapping Fur_{Ec} boxes, a hierarchy of distinct shifts was detected and the sequence determined from each shift has revealed a new model of Fur_{Ec}-DNA interaction [the (6-1-6)₂ model] that combines features of the two previous models (Lavrrar *et al.*, 2002). The consensus sequence was reinterpreted as two overlapping inverted hexameric repeats in which each set of repeats interacts with one Fur_{Ec} dimer on each face of the DNA helix (Lavrrar *et al.*, 2002). The addition of consecutive hexameric sets then allows more dimers to polymerise along the DNA molecule and the protein-protein interaction between each dimer also facilitates Fur_{Ec} to form complexes with less conserved regions outside the Fur_{Ec} box (Lavrrar *et al.*, 2002; Lavrrar and McIntosh, 2003).

A similar reinterpretation was also made for the Fur_{Bs} box and a 7-1-7 heptamer motif rather than the (6-1-6)₂ model was concluded to be the minimum recognition site for Fur_{Bs} (Baichoo and Helmann, 2002). DNA target site comparisons have also indicated

the presence of this core 7-1-7 repeat in the recognition site of the Fur_{Bs} homologues PerR_{Bs} (peroxide regulon regulator, see 1.2.3.7) and Zur_{Bs} (zinc uptake regulator, see 1.2.3.7), and a single change in each heptamer was sufficient to alter the recognition pattern between Fur_{Bs}, PerR_{Bs} and Zur_{Bs} (Fuangthong and Helmann, 2003). Despite minor base differences, both (6-1-6)₂ and (7-1-7)₂ interpretations revealed the same method of Fur binding that has close resemblance to the mechanism of DtxR-DNA interaction (White *et al.*, 1998; Pohl *et al.*, 1999) and is also in agreement with the model predicted from the crystal structure of Fur_{Pa} (Pohl *et al.*, 2003).

A recent re-examination of Fur binding site clusters using information theory models constructed from experimentally confirmed Fur_{Ec} binding sites has led to the proposal of yet another interpretation of the consensus Fur_{Ec} box sequence, the (9-1-9)₂ model (Chen *et al.*, 2007). A 9-1-9 motif was predicated as the minimum Fur_{Ec} dimer binding site and *E. coli* genome scans with this model have revealed all known Fur_{Ec}-repressed genes involved in iron metabolism (Chen *et al.*, 2007). This predicted model also correlates with confirmed Fur binding sites in *P. aeruginosa* and *B. subtilis* indicating a conserved Fur-DNA recognition mechanism between these bacteria and *E. coli* (Chen *et al.*, 2007).

Despite different views on each interpretation of the Fur box, a good correlation between the presence of the consensus sequence and the corresponding iron-responsive gene regulation (predominately gene repression) is generally accepted and observed in

numerous bacteria (Panina *et al.*, 2001; Rodionov *et al.*, 2006). Genome searching with a consensus Fur box sequence has been an effective approach to identify candidates for Fur-regulated genes in *B. Subtilis* (Baichoo *et al.*, 2002), *N. meningitidis* (Grifantini *et al.*, 2003) and *Y. pestis* (Gao *et al.*, 2008). However it is also important to know that not all Fur-regulated genes bearing a Fur binding site resemble the conventional Fur_{Ec} box consensus sequence as a genome scan with the Fur_{Ec} box failed to identify candidate Fur boxes in several members of the δ -proteobacteria such as *Desulfovibrio* spp, *Desulfuromonas* spp and *Geobacter* spp (Rodionov *et al.*, 2004). The *Bradyrhizobium japonicum* Fur (Fur_{Bj}) binding site is another such example in that it contains three imperfect direct hexameric repeats that poorly match the Fur_{Ec} box and just two of the three repeats were sufficient to both bind a Fur_{Bj} dimer and repress transcription (Freidman and O'Brian, 2003). These observations suggest that the consensus Fur_{Ec} box sequence may not completely represent the target site for bacterial Fur as a whole and the basis for target set specificity among different bacteria is likely to reflect variation in their genomic base composition, Fur structure and the mechanisms of Fur regulation (Lee and Helmann, 2007).

1.2.3.4 *Fur as a transcriptional activator*

Although Fur_{Ec} was originally described as a transcriptional repressor, several iron-induced Fur_{Ec}-activated genes have also been identified including the aconitase coding gene *acnA*, *bfr*, *ftnA*, succinate dehydrogenase coding operon *sdhCDAB* and *sodB* which encodes a iron-dependent superoxide dismutase (Hantke, 2001; McHugh *et*

al., 2003). The exact involvement of Fur_{Ec} in the regulation of these genes was initially puzzling but was later supported by the discovery of a non-coding regulatory RNA RhyB (Massé and Gottesman, 2002). RhyB is a 90-nucleotide long Fur_{Ec}-repressed sRNA transcribed under iron-limiting conditions and part of RhyB is complementary to these Fur_{Ec}-activated transcripts. RhyB forms complexes with these target transcripts in a RNA chaperone Hfq-dependent manner and subsequently triggers mRNA degradation by recruiting RNase E (Figure 1.11.b, Massé and Gottesman, 2002; Massé *et al.*, 2003). RhyB homologues have also been indentified in other bacterial species such as *Shigella* spp, *Yersinia* spp and *Salmonella* spp (Massé and Gottesman, 2002) and *P. aeruginosa* possesses two alternative sRNAs PrrF1 and PrrF2 which are functional analogues to RhyB, but share no sequence homology with RhyB (Wilderman *et al.*, 2004).

Global analysis of the *E. coli* RhyB regulon revealed that the expression of 58 proteins either participating in iron storage or requiring iron for their function are directly regulated by RhyB (Massé *et al.*, 2005). This illustrates the involvement of RhyB, along with Fur_{Ec}, in a cellular adaptive response called iron sparing (Figure 1.16, Massé and Arguin, 2005). When the intracellular free iron level is sufficiently high, Fur_{Ec} directly down regulates extracellular iron acquisition and indirectly, via *ryhB* repression, promotes intracellular iron sequestration which together protects the cell from iron-induced toxic effects. However when the cellular iron content falls below a critical level, derepressed RyhB prevents the synthesis of nonessential iron-containing and storage proteins, thus “spares” the available iron for essential cellular functions (Massé

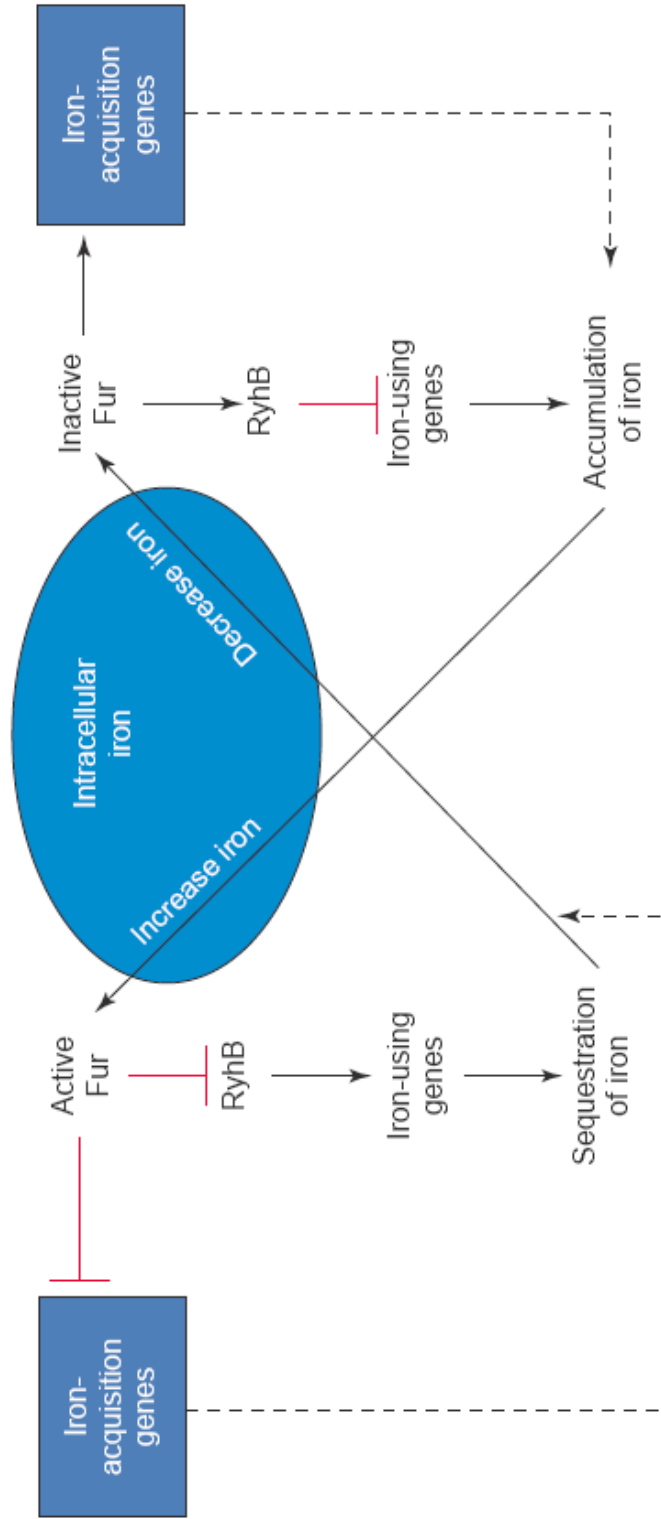


Figure 1.16: An illustration of iron sparing response mediated by the interplay between Fur and RyhB. When the intracellular iron level is sufficiently high, Fur prevents further iron uptake by directly repressing iron acquisition genes while at the same time promotes intracellular iron sequestration by indirectly activating the expression of iron storage and usage proteins via RyhB. However when the amount of intracellular iron falls back to a critical level, derepressed RyhB down regulates iron storage and non-essential iron-containing proteins thus allowing the available iron to be utilised more effectively (taken from Massé and Arguin, 2005).

and Arguin, 2005). The ability for Fur_{Ec} to effectively regulate iron acquisition and storage genes through iron sparing further emphasises its role in iron homeostasis (Lee and Helmann, 2009) and also explains the 70% reduction in iron content previously seen with a *fur*_{Ec} mutant (Abdul-Tehrani *et al.*, 1999).

As well as indirect Fur activation, evidence has suggested that some Fur proteins can also function as a direct transcriptional activator (Figure 1.11.c). In *N. meningitidis*, the promoters of three metalloprotein coding genes *pan1*, *norA* and *norB* are positively regulated by Fur_{Nm} in a iron-dependent manner. Transcriptional activation is mediated by direct binding of iron-bound Fur_{Nm} to the operator sequences located upstream of these iron regulated promoters. Fur_{Nm} binding presumably facilitates RNA pol activity and deletion of the operator sequence in the *norB* promoter abolished this iron- and Fur_{Nm}-responsive gene regulation both *in vitro* and *in vivo* (Delany *et al.*, 2004). Similarly in *H. pylori*, iron-bound Fur_{Hp} was shown to activate the transcription of iron-sulphur cluster synthase coding gene *nifS* by binding to an operator sequence 300 bp upstream from the *nifS* start codon (Alamuri *et al.*, 2006). Most recently, the expression of a type III secretion system regulator HilD in *S. enterica* has also been linked to Fur_{Se} activation in an operator sequence-binding-dependent manner (Teixidó *et al.*, 2011).

1.2.3.5 Transcriptional regulation by apo-Fur

Although Fur has been generally considered as a transcriptional regulator that represses

or activates gene expression in its iron-bound form, characterisation of Fur regulation in *H. pylori* indicated that Fur_{Hp} functions beyond this classic paradigm (Figure 1.11.d-e, Danielli and Scarlato, 2010). DNase I footprinting assay and EMSA studies of the *pfr* and *sodB* promoters revealed that apo-Fur_{Hp} binds directly to the operator sequences overlapping the -10 and -35 regions of these promoters and iron decreases the efficiency of apo-Fur_{Hp} binding (Delany *et al.*, 2001; Ernst *et al.*, 2005). The concept of direct DNA-binding by apo-Fur_{Hp} *in vitro* is controversial as it is questionable whether or not Fur could actually be found in an experimental setting without its metal co-factor (Carpenter *et al.*, 2009b). However transcriptional analyses of both *pfr* and *sodB* promoters in a wild-type background have shown that both genes were induced by iron but repressed under iron-depleted conditions. Furthermore, both genes were also constitutively and iron-independently expressed in a *fur*_{Hp} mutant, which in combination with the data from DNA-binding analyses indicates Fur_{Hp} directly represses the expression of *pfr* and *sodB* in its apo form in response to iron limitation (Delany *et al.*, 2001; Ernst *et al.*, 2005).

apo-Fur_{Hp} can also function as a direct transcriptional activator in a operator sequence-binding-dependent manner and the only example to date involves the autoregulation of *fur*_{Hp} (Figure 1.12.b, Delany *et al.*, 2002; 2003). *fur*_{Hp} is transcribed from its own promoter which consists of three operator sequences. Operator 1 overlaps the -35 region and displays the highest binding affinity for both Fur_{Hp} and apo-Fur_{Hp}. Operator 2 overlaps the -10 region and operator 3 is located upstream from the other

operators (Delany *et al.*, 2002; 2003). Under iron-rich conditions, Fur_{Hp} binds to both operators 1 and 2 and classically represses the expression of *fur*_{Hp}. When iron becomes scarce, Fur_{Hp} bound to operator 1 is replaced by apo-Fur_{Hp}, which also binds to operator 3 and together facilitates the expression of *fur*_{Hp}. In addition, when the Fur_{Hp} concentration falls below a certain level, operator 1 is freed from Fur_{Hp} regulation. This allows operator 1 to function as an UP element for RNA pol thus enhancing transcription from the *fur*_{Hp} promoter (Delany *et al.*, 2002; 2003).

To date, the ability of Fur to regulate gene expression in its apo form has only been studied in detail in *H. pylori*, thus relatively little is known about the apo-Fur_{Hp} recognition site and it is currently unknown whether apo-Fur_{Hp} functions as a dimer or a monomer (Carpenter *et al.*, 2009b). Sequence comparison between *pfr* and *sodB* promoters has failed to identify a consensus apo-Fur_{Hp} box sequence (Delany *et al.*, 2001; Ernst *et al.*, 2005) and homology to the proposed Fur_{Hp} box was also not evident (Merrell *et al.*, 2003). However, a single base substitution of the apo-Fur_{Hp} binding site in the *sodB* promoter resulted in altered apo-Fur_{Hp}-dependent regulation indicating apo-Fur_{Hp} binds to its recognition site in a base-specific manner (Carpenter *et al.*, 2009a). In an *in vivo* complementation study, the ability for *E. coli*, *P. aeruginosa* and *V. cholerae fur* genes to complement Fur_{Hp} and apo-Fur_{Hp} regulation when presented *in trans* in a *fur*_{Hp} mutant was investigated. Although Fur_{Ec} and Fur_{Vc} were able to complement the Fur_{Hp} regulation of the aliphatic amidase coding gene *amiE*, apo-Fur_{Hp} regulation of *pfr* was unable to be complemented by any of the Fur orthologues

indicating Fur_{Hp} contains unique structural and functional features (Miles *et al.*, 2010a).

The crystal structure of Fur_{Hp} described in 1.2.3.2 reveals an additional N-terminal extension that is only conserved among *Helicobacter* spp and an additional MBS when compared to Fur_{Pa} and Fur_{Vc} (Carpenter *et al.*, 2010; Dian *et al.*, 2011). Fur_{Hp} displays a dense hydrogen bonding network that connects the N-terminal extension with α helices 2 and 3. The authors suggested that in the absence of a metal cofactor, this hydrogen bonding network stabilises the DNA-binding domain in its active conformation thus allowing apo-Fur_{Hp} to bind to its target operator sites (Dian *et al.*, 2011). In addition, mutagenesis of conserved amino acids of Fur_{Hp} revealed that Glu90 and His134, which function as metal ligands in MBS2_{Hp} and MBS3_{Hp} respectively, are also required for apo-Fur_{Hp} regulation (Carpenter *et al.*, 2010) conferring the link between the unique Fur_{Hp} structure and its regulatory potential.

1.2.3.6 Fur as a global regulator

In addition to its role in controlling iron homeostasis, analyses of Fur regulons in many bacteria demonstrate the role of Fur as a global regulator in controlling genes involved in the production of toxins and virulence factors, oxidative stress responses, acid tolerance responses, chemotaxis and cellular metabolic pathways (Ochsner and Vasil, 1996; Baichoo *et al.*, 2002; Grifantini *et al.*, 2003; McHugh *et al.*, 2003; Mey *et al.*, 2005; Danielli *et al.*, 2006; Gao *et al.*, 2008; Ledala *et al.*, 2010). While these are too numerous to be discussed exhaustively here, a few well studied examples are briefly

illustrated.

In many pathogenic bacteria, Fur regulates virulence genes (aside from iron-acquisition genes) that are essential for bacterial pathogenesis. In *E. coli* for example, Fur_{Ec} negatively controls the production of haemolysin Hly (Fréchon and Le Cam, 1994), Shiga-like toxins SltA and SltB (Calderwood and Mekalanos, 1987), adhesin Iha (Rashid *et al.*, 2006) and fimbrial adhesin CFA/I (Karjalainen *et al.*, 1991). In *V. cholerae*, the production of haemolysin and an OM virulence determinant IrgA (an Iha homologue) is also negatively regulated by Fur_{Vc} (Stoebner and Payne, 1988; Litwin and Calderwood, 1994). In *P. aeruginosa*, Fur_{Pa} affects biofilm formation (Banin *et al.*, 2005) and it indirectly regulates the synthesis of exotoxin ToxA (Ochsner *et al.*, 1995) and enzymes involved in quorum sensing (Oglesby *et al.*, 2008). In *N. gonorrhoeae*, Fur_{Ng} regulates the repression of 11 *opa* genes which encode OM proteins involved in host cell adherence and invasion (Sebastian *et al.*, 2002), and the production of vacuolating cytotoxin VacA in *H. pylori* is also indirectly regulated by Fur_{Hp} (Gancz *et al.*, 2006). The essential role of Fur in controlling bacterial pathogenesis is also demonstrated by colonisation studies of *fur* mutants. The *H. pylori fur*_{Hp} mutant for instance is less effective in mouse colonisation (Bury-Mone *et al.*, 2004) and it is easily out-competed by the wild-type strain in a gerbil infection model (Gancz *et al.*, 2006; Miles *et al.*, 2010b). Additionally, *fur* mutants of *S. aureus* (Horsburgh *et al.*, 2001), *L. monocytogenes* (Rea *et al.*, 2004) and *V. cholerae* (Mey *et al.*, 2005) also exhibit significant defects or attenuation in colonisation using murine infection models.

Another functional role for Fur is to regulate cellular processes that are essential for bacterial survival in sub-optimal conditions such as under oxidative and acidic stresses. Under oxidative stress, many bacteria produce the catalase Kat and superoxide dismutase Sod to neutralise reactive oxygen species (Touati, 2000). In *E. coli*, the expression of manganese-containing SodA is negatively regulated by Fur_{Ec} (Privalle and Fridovich, 1993) while *sodB* is indirectly activated by Fur_{Ec} via RhyB (Massé and Gottesman, 2002). In *N. gonorrhoeae*, Fur_{Ng} directly activates the expression of *sod* (Sebastian *et al.*, 2002) and in *H. pylori*, *sodB* is repressed by apo-Fur_{Hp} (Ernst *et al.*, 2005). *E. coli* produces two hydroperoxidases encoded by *katG* and *katK* and their expression is activated by Fur_{Ec} (Hoerter *et al.*, 2005). The expression of *kat* in *P. aeruginosa* (Hassett *et al.*, 1996), *S. aureus* (Horsburgh *et al.*, 2001) and *Y. pestis* (Gao *et al.*, 2008) is also activated by Fur whereas the catalase-peroxidase coding gene *katG* is repressed by Fur in all *Mycobacterium* spp (Zahrt *et al.*, 2001). In addition, Fur_{Se} regulates the expression of the flavohaemoglobin coding gene *hmp* and the Nramp1 homologue coding gene *mntH* in *S. enterica* which the gene products protect the bacteria from nitric oxide- and hydrogen peroxide-induced stresses respectively (Crawford and Goldberg, 1998; Kehres *et al.*, 2002).

The involvement of Fur in acid tolerance responses are best studied in *S. enterica* and *H. pylori*. In *S. enterica*, Fur_{Se} controls the expression of several acid tolerance response genes at pH 5.8 which mainly protect the cell from organic acid stress but only play a

minor role in inorganic acid stress (Foster, 1991; Bearson *et al.*, 1998). The *fur_{Se}* mutant is unable to induce these acid tolerance response genes at pH 5.8 and is more sensitive to acid when compared to the wild-type (Foster, 1991). Interestingly, iron availability does not affect the acid tolerance response and an iron-blind *Fur_{Se}* mutant still exhibits an acid tolerance phenotype (Hall and Foster, 1996). When *H. pylori* is exposed to low pH, the number of *Fur_{Hp}* regulated genes increases significantly. Such genes include the glucose transporter coding gene *gluP*, the Holliday junction endodeoxyribonuclease coding gene *rnvC*, the flagellar biosynthetic protein coding gene *fliP* and *amiE* (Gancz *et al.*, 2006). *AmiE* in particular has been shown to contribute to acid resistance by producing ammonia from aliphatic amides (van Vliet *et al.*, 2003).

1.2.3.7 *Fur* homologues and *DtxR*

The *Fur* family of proteins is widespread within the bacterial world, as approximately 800 *Fur*-like proteins have been identified and most of these proteins are likely to function as metal-dependent transcriptional regulators (Lee and Helmann, 2007). However it is important to appreciate that metal-dependence and metal-specificity varies markedly for these *Fur*-like proteins and many proteins originally annotated as ferric uptake regulators may sense cellular or environmental signals other than metal ions (Lee and Helmann, 2007).

Like iron, zinc is also an essential but toxic trace element required for many bacteria and bacterial zinc homeostasis is usually achieved by *Zur* (Hantke, 2005). In *E. coli*,

Zur_{Ec} represses the zinc uptake system ZnuACB in response to zinc sufficiency by binding to the bidirectional promoter region of *znuA* and *znuBC* (Patzner and Hantke, 2000). Binding of Zur_{Ec} to the *znuC* promoter is dependent on the occupancy of both the structural and regulatory zinc sites of Zur_{Ec} with zinc atoms and Zur_{Ec} binds zinc with a high affinity such that at equilibrium, there is no free zinc in the cell (Outten and O'Halloran, 2001; Outten *et al.*, 2001). In *B. subtilis*, Zur_{Bs} represses the zinc uptake system operon *ycdHI-yceI* (Gaballa *et al.*, 2002) and DNA-binding and sequence alignment investigations indicated that Zur_{Ec} and Zur_{Bs} recognise palindromic operator sequences that have resembles to the consensus Fur_{Ec} box sequence (Gaballa and Helmann, 2002; Panina *et al.*, 2003). Zur_{Bs} also represses the expression of a ribosomal protein YtiA (Akanuma *et al.*, 2006) and a folate biosynthesis protein YciA (Lee and Helmann, 2007) under zinc-rich conditions where the alternative zinc-dependent versions of these proteins are expressed. Additionally in a recent characterisation of the Zur regulon in *Y. pestis*, 154 Zur_{Yp} regulated genes were identified suggesting a role for Zur_{Ye} as a global regulator (Li *et al.*, 2009).

In *Rhizobium leguminosarum*, the manganese-uptake operon *sitABCD* is repressed in response to manganese sufficiency by the manganese uptake regulator Mur (Diaz-Mireles *et al.*, 2004). Mur_{Rl} does not contain a structural zinc site, but instead it complexes with two manganese atoms per dimer (Bellini and Hemmings, 2006) and binds to a unique Mur_{Rl} responsive sequence (MRS) in the *sitABCD* operon promoter (Diaz-Mireles *et al.*, 2005). MRS is significantly different from the consensus Fur_{Ec} box

sequence and it is also found in the *sitABCD* operon promoter regions of many other members of the Rhizobiales and Rhodobacterales (Johnston *et al.*, 2007). Interestingly, Mur_{RI} is able to functionally complement the iron-responsive regulation of the *E. coli* bacterioferritin-associated ferredoxin in a *fur_{Ec}* mutant background (Wexler *et al.*, 2003) and recognises a synthetic Fur_{Ec} box suggesting that Mur and Fur may share an overlapping DNA-recognition specificity (Bellini and Hemmings, 2006).

In several member of the α -proteobacteria such as *R. leguminosarum*, Fur is functionally replaced by other global iron regulators such as RirA and Irr (Johnston *et al.*, 2007). RirA is a member of the Rrf2 protein family that functions as a repressor under high iron conditions by interacts with an iron-sulphur cluster (Todd *et al.*, 2002). Irr on the other hand belongs to the Fur superfamily though it represses gene expression in its *apo* form and the repressive effect is released when Irr interacts with haem under high iron conditions (Todd *et al.*, 2006). Although RirA and Irr collectively control the expression of genes that would otherwise be regulated by a Fur orthologue and iron, RirA and Irr sense iron as functions of the intercellular concentration of iron-sulphur cluster and haem respectively (Jonston *et al.*, 2007).

Under nickel-rich conditions, the *Streptomyces coelicolor* nickel transport operon *nikABCDE* is negatively regulated by the nickel uptake regulator Nur (Ahn *et al.*, 2006). Nur_{Sc} also represses the expression of the iron-containing Sod coding gene *sodF* and indirectly regulates the expression of the nickel-containing Sod gene *sodN* (Ahn *et al.*,

2006). Nur_{Sc} exhibits 27% sequence identity with Fur_{Ec} and contains a structural zinc site and a regulatory metal site that has high specificity for nickel both *in vitro* and *in vivo* (Ahn *et al.*, 2006). Recent resolved crystal structure of Nur_{Sc} revealed that unlike Fur, Nur_{Sc} possesses two horizontal β sheets 1 and 2 in the DNA-binding domain that do not interact with DNA and this unique structure allows Nur_{Sc} to recognise and bind to a palindromic operator sequence consisting of two hexameric repeats separated by 5 bp (An *et al.*, 2009).

Another well studied Fur-like protein is PerR, and unlike many metal-sensing Fur proteins, the regulatory metal site of PerR has evolved to function as a metal-based sensor for peroxide (Lee and Helmann, 2007). First characterised in *B. subtilis*, PerR_{Bs} is a major peroxide stress response regulator and functions as a functional replacement of the *E. coli* peroxide sensor OxyR (Bsat *et al.*, 1998). Examples of the PerR_{Bs}-repressed genes include the Dps-like protein coding gene *mrgA* (Chen and Helmann, 1995), *katA* (Chen *et al.*, 1995), alkyl hydroperoxidase coding genes *ahpCF* (Bsat *et al.*, 1996), haem biosynthesis coding genes *hemAXCDBL* (Chen *et al.*, 1995) as well as *fur_{Bs}* and *perR_{Bs}* (Fuangthong *et al.*, 2002). All these PerR_{Bs}-regulated genes are derepressed under hydrogen peroxide-induced stress or under both iron and manganese limitation (Fuangthong *et al.*, 2002), and the *perR_{Bs}* mutant is highly resistant to peroxides (Bsat *et al.*, 1998).

PerR_{Bs} is a homodimer that contains a structural zinc site and it is activated by binding

of iron or manganese to the regulatory metal site thus creating two forms of PerR_{BS} with different sensitivities to peroxide (Herbig and Helmann, 2001). The zinc site coordinates a zinc atom by the side chains of four Cys residues in the dimerisation domain and this site plays a structural role by locking together three β strands that are involved in dimeric protein formation (Traoré *et al.*, 2006). The metal site connects the dimerisation domain with the DNA-binding domain and it penta-coordinates an iron atom by the side chains of His37, Asp85, His91, His93 and Asp104 (Lee and Helmann, 2006). Interaction of His37 with the bound iron allows the two domains to adopt a caliper-like conformation that is essential for operator sequence-binding (Jacquamet *et al.*, 2009). Oxidative stress sensing is also mediated by His37 and His91 where hydrogen peroxide causes rapid oxidation of both residues. Oxidation leads to 2-oxo-His formation which weakens the iron affinity to the regulator site thus resulting in protein inactivation (Lee and Helmann, 2006). This type of metal-catalysed protein oxidation seen with PerR_{BS} is unique and differs from the mechanism used by OxyR where protein inactivation is induced by disulphide bond formation as a direct result of oxidation of the Cys thiolates (Zheng *et al.*, 1998).

Finally, in many GC-rich Gram-positive bacteria such as members of *Brevibacterium* spp (Oguiza *et al.*, 1995), *Streptomyces* spp (Günther-Seeboth and Schupp, 1995) and *Mycobacterium* spp (Doukhan *et al.*, 1995), global iron regulation is mediated by another family of iron-dependent regulators collectively named as DtxR after the first member to be characterised (Fourel *et al.*, 1989). DtxR shares many functional and

structural similarities with Fur. For instance, DtxR regulates a spectrum of cellular processes similar to those regulated by Fur including siderophore biosynthesis, iron acquisition, oxidative stress responses as well as toxin production (i.e. diphtheria toxin, Hantke, 2001). Also like Fur, DtxR is a dimeric metal-dependent repressor that consists of a DNA-binding domain and a dimerisation domain and it negatively regulates gene expression by a mechanism consisting of two DtxR dimers interacting with the opposite faces of a palindromic operator sequence (White *et al.*, 1998; Pohl *et al.*, 1999). However, DtxR is not a Fur-like protein as both proteins display no sequence similarity and DtxR also possesses a third β sheet-rich SH₃-like domain that modulates metal binding and protein activation (Pohl *et al.*, 1999).

1.3 THE BIOLOGY OF *C. JEJUNI*

As stated in 1.2.3, Fur plays crucial roles in controlling cellular iron homeostasis and the expression of other virulence factors that are essential for pathogenic bacteria to establish colonisation and cause disease in their hosts. This is also true for *C. jejuni*, an important and prevalent enteric pathogen. Effective gene regulation by Fur_{Cj} and indeed other transcriptional and translational regulators allow *C. jejuni* to successfully thrive during the commensal relationship with avian species, within the disease-susceptible human host and in natural environments encountered during transmission (Wösten *et al.*, 2008).

1.3.1 Historic perspective and the genus *Campylobacter*

The first possible description of *Campylobacter* was in 1886 when a noncultureable *Vibrio*-like spiral organism was identified in the colon of diarrhoeic infants (Escherich, 1886; Butzler, 2004). Several early recognised isolations of campylobacters were associated with ovine (McFadyean and Stockman, 1913; Skirrow, 2006) and bovine epizootic abortions (Smith and Taylor, 1919) and the name *Vibrio fetus* was initially proposed (Smith and Taylor, 1919). *V. fetus* and other emerging *Vibrio*-like organisms (Jones *et al.*, 1931; Doyle, 1948; Florent, 1953; Bryans *et al.*, 1960; Debruyne *et al.*, 2008) were subsequently re-grouped into the new genus of *Campylobacter* due to their low GC content, microaerobic growth requirement and nonfermentative metabolism (Sebald and Véron, 1963; Véron and Chatelain, 1973). Despite several incidences of human associated infections (Levy, 1946; Vinzent *et al.*, 1947; King, 1957), understanding of this new found genus was limited due to the lack of sufficiently selective culture techniques and therefore *Campylobacter* had largely remained as a cause of veterinary disease. Advances in epidemiological research became possible when a faecal filtration method (Dekeyser *et al.*, 1972; Butzler *et al.*, 1973) and appropriate growth supplements (Skirrow, 1977) were developed. Several new species have since been discovered and *C. jejuni* has rapidly been recognised as one of the most important human enteropathogens.

Phylogenetic and molecular characterisation of the *Campylobacter coli* 23S rRNA gene has positioned *Campylobacter* in the epsilon subdivision of the *Proteobacteria* (Trust *et al.*, 1994). Within the 18 species that have been validated in this genus (Debruyne *et al.*,

2008), *C. jejuni* and *C. coli* are the most important human enteric pathogens and *C. jejuni* alone accounts for 80-90% of the *Campylobacter* enteric infections (Ketley 1997). The genus type species *Campylobacter fetus* on the other hand is primarily linked to veterinary infections causing ovine and bovine infectious infertility and abortions (Debruyne *et al.*, 2008). Although infrequent, *Campylobacter lari*, *Campylobacter upsaliensis* and *Campylobacter hyointestinalis* have also been associated with human and animal intestinal infections or similar disease manifestations (Ketley 1997; Debruyne *et al.*, 2008). *Campylobacter sputorum*, *Campylobacter concisus*, *Campylobacter curvus*, *Campylobacter rectus*, *Campylobacter gracilis*, *Campylobacter showae* and *Campylobacter hominis* are mostly isolated from the human oral cavity and require hydrogen for active growth (On, 2001; Debruyne *et al.*, 2008). *Campylobacter lanienae*, *Campylobacter insulaenigrae*, *Campylobacter canadensis* and *Campylobacter helveticus* are rarely isolated from human and animal sources and their pathogenic properties remain uncharacterised (Debruyne *et al.*, 2008).

1.3.2 Physical and genetic characteristics of *C. jejuni*

Just 0.2-0.8 μm wide and 0.5-5 μm long, *C. jejuni* is a relatively small, rod-shaped Gram-negative microorganism. It is highly motile with a corkscrew-like motion that is facilitated by its spirally curved morphology and a polar unsheathed flagellum situated at one or both ends of the cell (Ketley, 1997). *C. jejuni* is catalase, oxidase and hippurate hydrolysis positive, but lipase and lecithinase negative. Unable to oxidase or ferment carbohydrates, *C. jejuni* utilises amino acids and tricarboxylic acid (TCA) cycle

intermediates instead as its primary energy sources (Snelling *et al.*, 2005). The microaerophilic *C. jejuni* requires an oxygen concentration of 3-15%, a carbon dioxide concentration of 3-5% and 42 °C for active growth. The thermophilic characteristic of *C. jejuni* reflects the adoption of the avian intestinal tract as its natural niche (Ketley, 1997). Upon exposure to oxidative, temperature and acidic stresses, *Campylobacter* is able to change from its normal spiral shape into a viable non-culturable coccoid form (Figure 1.17). This dormant state allows the cell to survive under prolonged sub-optimal growth conditions encountered during transmission between host organisms (Rollins and Colwell, 1986; Chaveerach *et al.*, 2003).

The circular chromosomes of *C. coli* and *C. jejuni* are approximately 1.6-1.7 Mb in length, which is relatively small compared to other enteropathogens such as *E. coli* (van Vliet and Ketley, 2001). The GC ratio of *Campylobacter* DNA averages 30% and this high AT content coupled with differences in base methylation and codon usage compared to *E. coli* make molecular genetic studies of *Campylobacter* sometimes difficult (Ketley, 1997). The first sequenced *C. jejuni* strain NCTC 11168 does not contain any plasmid and has a 1.64 Mb long genome encoding for 1643 genes which make it amongst the densest prokaryotic genomes sequenced to date (Parkhill *et al.*, 2000; Gundogdu *et al.*, 2007). The NCTC 11168 genome has virtually no insertion or phage-associated sequences, has very few repeat sequences and contains several hypervariable tracts. Most of these hypervariable tracts are found in genes responsible for the biosynthesis of surface structures such as the capsule, lipooligosaccharide (LOS)

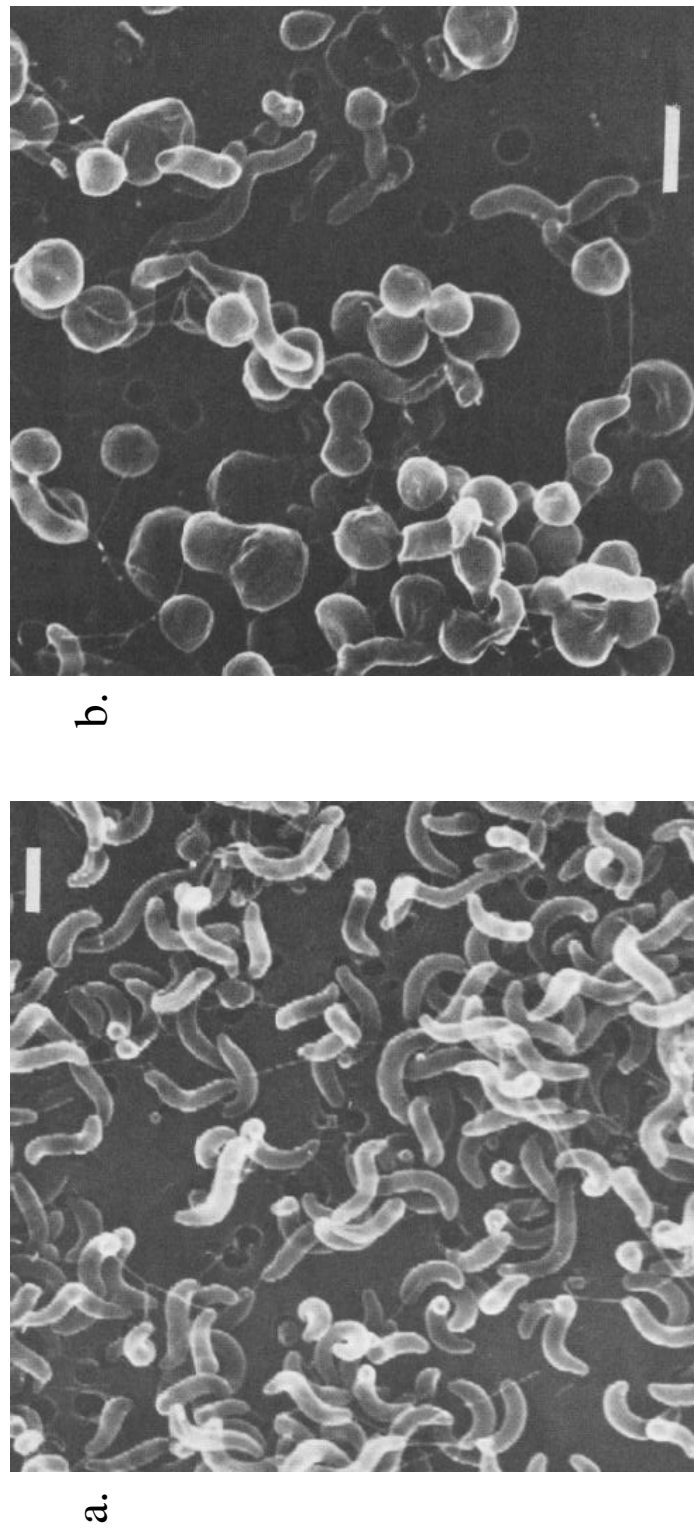


Figure 1.17: Electron micrographs of *C. jejuni* exhibiting the spiral rod-shape (a) and coccoid forms (b, taken from Rollins and Colwell, 1986). The white scale bar in each photo represents 1 μm .

and flagellum and they may play important roles in *Campylobacter* survival and generating genetic diversity (Parkhill *et al.*, 2000). Other sequenced *C. jejuni* strains such as 81-176 (Hofreuter *et al.*, 2006) and 81116 (Pearson *et al.*, 2007) also share similar genomic characteristics with NCTC 11168 with the exception that 81-176 contains two plasmids pVir and pTet that have roles in pathogenesis (Bacon *et al.*, 2002; Batchelor *et al.*, 2004).

1.3.3 Transmission and epidemiology

C. jejuni frequently colonises the avian gastrointestinal tract and is also considered to be part of the normal intestinal flora of a broad range of other domestic and wild animals (van Vliet and Ketley, 2001). Although a commensal in animal hosts, when present in humans, *C. jejuni* may cause acute gastroenteritis and is the most common isolated cause of bacterial gastroenteritis in the world with the numbers of recorded cases much higher than those due to any other enteric pathogen, including the frequently reported *Salmonella* spp and *E. coli* (Wooldridge and Ketley, 1997). Human infection is usually acquired by consumption of faecally contaminated or undercooked meat, unpasteurised milk or contaminated water (Figure 1.18, Wilson *et al.*, 2008). *C. jejuni* infects approximately 1% of the population in the UK and USA annually, causing substantial clinical costs and loss of working hours, and is therefore considered a major public health and economic burden (Snelling *et al.*, 2005).

The infectious dose of *C. jejuni*-induced gastroenteritis is around 500-800 bacteria with

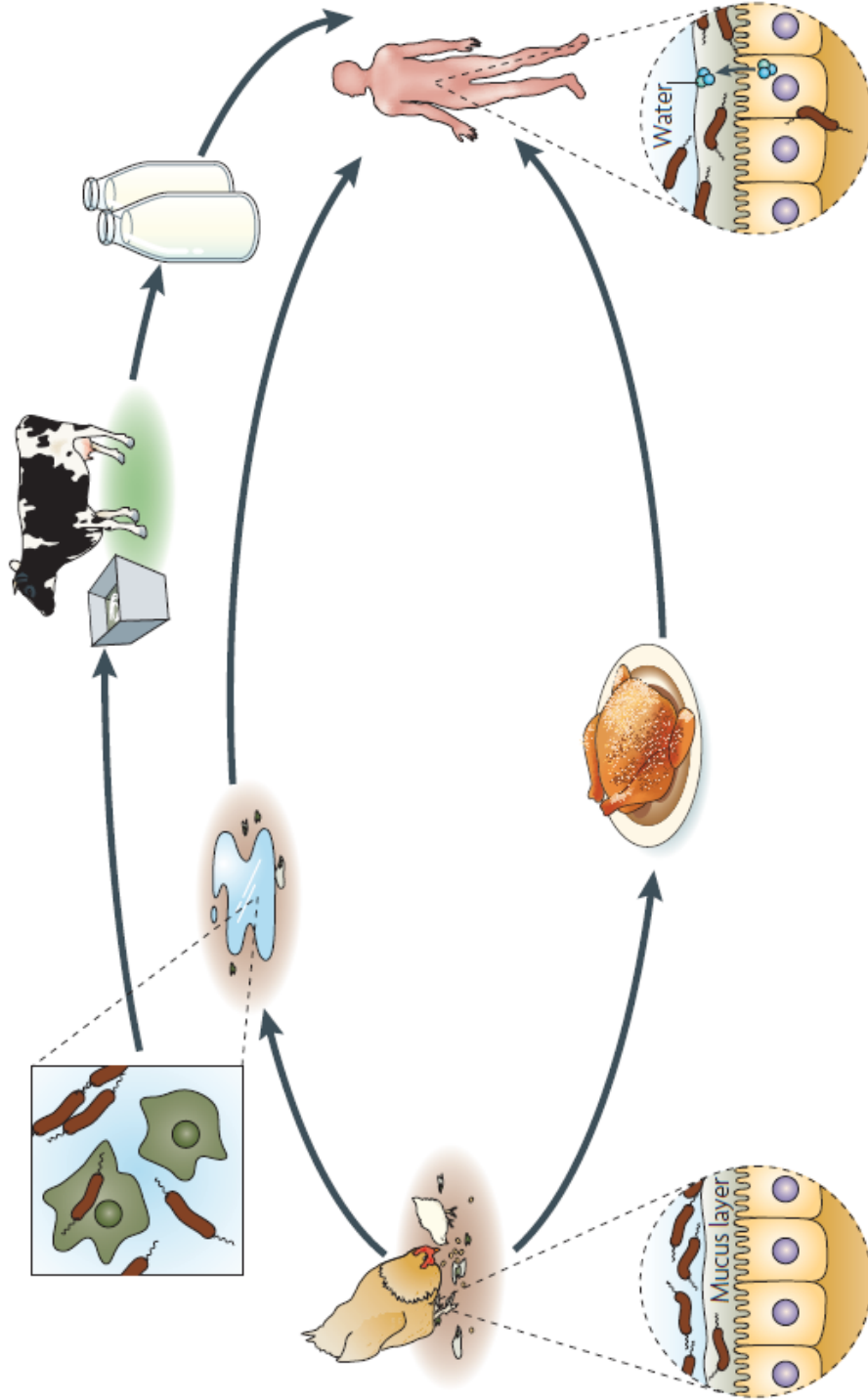


Figure 1.18: The routes and outcomes of *C. jejuni* infection. *C. jejuni* is a commensal bacterium for chicken and it frequently colonises the mucosal layer of the chicken gastrointestinal tract. Human infection is often acquired through consumption of faecally contaminated meat as well as directly from contaminated water and unpasteurised milk. When present in humans, *C. jejuni* invades the intestinal epithelial layer and causes diarrhoea (taken from Young *et al.*, 2007).

an average incubation period of 3.2 days and the disease manifestations are dependent on socio-economic status (Blaser and Engberg, 2008). In industrialised countries, infection with *C. jejuni* is seasonal and often leads to inflammatory diarrhoea with severe cramping amongst young adults with low asymptomatic carriage rates. By contrast, infection in developing countries is not seasonal and is mostly restricted to children. The clinical symptoms are usually milder watery, non-inflammatory diarrhoea with a high rate of asymptomatic carriage. The differences in these symptoms are due to higher rates of exposure to the bacteria in developing countries and early infection in childhood may result in different immune responses (Ketley, 1997; van Vliet and Ketley, 2001).

The disease is usually self-limiting and symptoms usually last for about a week, although bacterial shedding can persist once clinical symptoms have ceased. Complications following infection are uncommon, but previous infections with *C. jejuni* have been linked to the development of a serious neuromuscular paralysis known as Guillian-Barré syndrome (GBS) or the related Miller-Fisher syndrome (Ketley, 1997; van Vliet and Ketley, 2001; Blaser and Engberg, 2008). GBS is the most common cause of acute, temporary paralysis due to autoimmune inflammatory polyradiculoneuropathy and is commonly preceded by *C. jejuni* enteritis. GBS pathogenesis is believed to be caused by the sialylated *C. jejuni* cell surface LOS that mimic human gangliosides and trigger demyelination of gangliosides by host auto-antibodies produced in response to infection (Jacobs *et al.*, 2008).

1.3.4 Pathogenesis and virulence factors

The symptoms of *C. jejuni* infection directly result in epithelial cell damage caused by several putative virulence factors (Figure 1.19) expressed by the bacteria when establishing colonisation of the host intestinal tract. Some of these essential factors include motility, chemotaxis, adhesion, invasion and toxin production (Ketley, 1997).

1.3.4.1. Motility

Motility is achieved by the expression of polar flagella that endow *C. jejuni* with a characteristic darting motility, which is required for penetrating the intestinal mucus layer on colonisation (van Vliet and Ketley, 2001). The *C. jejuni* flagellar filament is composed of two different flagellins FlaA and FlaB (Logan *et al.*, 1987). Both *flaA* and *flaB* genes have been shown to be essential for flagellar production and a reduction in mobility and colonisation was observed in a *flaA* mutant (Wassenaar *et al.*, 1991; 1993; 1994). The flagellar filament is heavily glycosylated (Guerry *et al.*, 2006) and this glycol-modification allows *C. jejuni* to escape attacks from the host immune system (Szymanski and Wren, 2005). In addition, two other proteins, FlgP and FlgQ, have been identified to be essential for flagellar motility though their functional roles are currently unknown (Sommerlad and Hendrixson, 2007). Motility and flagellar expression are also important for subsequent adhesion and invasion as a reduction in mobility resulting from paralysed flagella led to decreased adhesion and no invasion (Yao *et al.*, 1994).

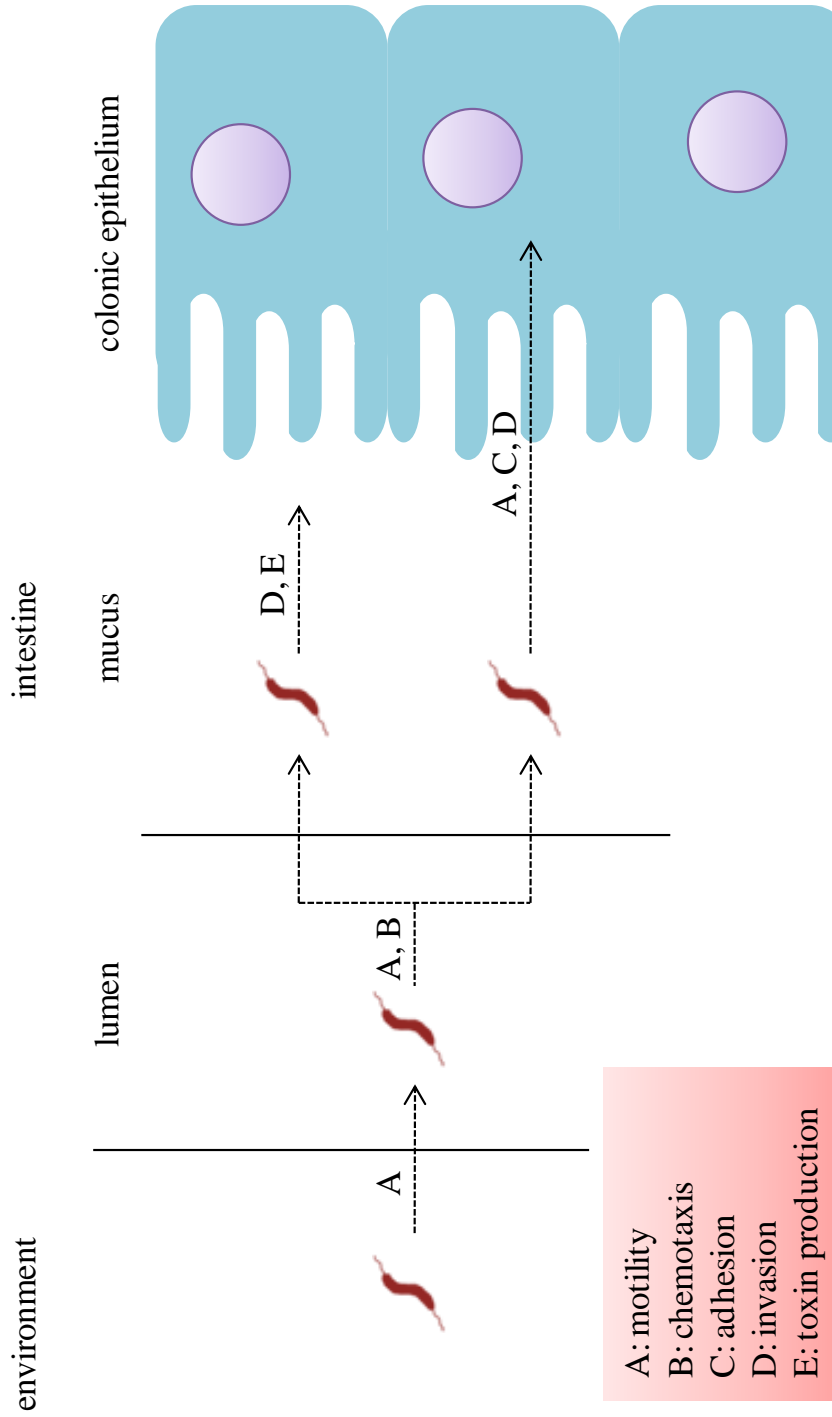


Figure 1.19: An overview of the different stages of *C. jejuni* colonisation and virulence factors expressed at each stage (adapted from van Vliet and Ketley, 2001).

1.3.4.2 Chemotaxis

Chemotaxis is the ability of bacteria to detect and direct their movement according to certain chemical gradients and chemotactic movement has been shown to be essential for *C. jejuni* colonisation (Takata *et al.*, 1992). *C. jejuni* is attracted to mucins, L-serine and L-fucose, but repelled by bile acids (Hugdahl *et al.*, 1988). The chemotactic protein *cheY* was identified from motile, non-adherent and non-invasive *C. jejuni* mutants that showed duplication in *cheY* and colonisation of mice (Yao *et al.*, 1997). A hyperadherent and hyperinvasive phenotype was observed for *cheY* mutant though the ability to establish colonisation and cause disease was abolished (Yao *et al.*, 1997). Several other components of the chemotaxis system have been identified in *C. jejuni* including *cheA*, *cheB*, *cheR*, *cheV*, *cheW* and *cheZ*, which together with *cheY* control the flagellar rotation in response to environmental stimuli by transduction of signals from specific transmembrane chemoreceptors to flagellar motors (Marchant *et al.*, 2002; Korolik and Ketley, 2008).

1.3.4.3 Adhesion

Upon infection, *C. jejuni* must cross the mucus layer on the intestinal cell surface and attach to the epithelial cells (Ketley, 1997). Adhesion by bacterial pathogens is usually mediated by fimbrial structures, however fimbrial-associated adhesins have not been identified in *C. jejuni* (Wassenaar and Blaser, 1999) and adhesive properties have instead been attributed to other proteins such as PEB1 and CadF (Larson *et al.*, 2008). PEB1 is a putative binding component of an ABC transport system expressed from

peb1A. Inactivation of *peb1A* led to a significant reduction of *in vitro* adherence and invasion of HeLa cells and *in vivo* colonisation, which marked its role in *C. jejuni* adherence to epithelial cells (Pei *et al.*, 1998). Many bacteria are also capable of binding to extracellular matrix components such as fibronectin during the initial phase of infection and in *C. jejuni*, this is mediated by CadF (Konkel *et al.*, 1997). Mutational studies on *cadF* have showed a reduction in fibronectin binding and invasion of INT 407 cells (Monteville and Konkel, 2002; Monteville *et al.*, 2003), and the ability to colonise chickens was abolished (Ziprin *et al.*, 1999). Apart from CadF, fibronectin binding has also been proposed for *C. jejuni* flagellin and LOS (Moser and Schröder, 1997).

1.3.4.4 Invasion

Invasion is an important pathogenic mechanism for *C. jejuni* as the invasion of epithelial cells would be expected to disrupt the normal absorptive capacity of the host intestine and induce inflammation, which together leads to diarrhoea (Wassenaar and Blaser, 1999). Interaction with host cells via biochemical crosstalk is a common strategy that facilitates invasive bacterial pathogens to stimulate signalling cascades in both the bacteria and the host, which trigger rearrangements of the host cytoskeleton and cause internalisation of the pathogen (Kopecko *et al.*, 2001). Invasive properties and mechanisms of *C. jejuni* have been characterised in a variety of tissue culture cell lines, in particular with INT-407, HEP-2 and Caco-2 and invasiveness was shown to be strain-dependent (Wooldridge and Ketley, 1997). Two distinct mechanisms of *C. jejuni*

invasion have been proposed, which either employ a microtubule-dependent mechanism seen with highly invasive *C. jejuni* 81-176 strain or in a microfilament-dependent fashion that is demonstrated by most of the *C. jejuni* strains tested (Crushell *et al.*, 2004). *C. jejuni* secretes several type III secretion Cia proteins, where CiaB in particular is required for the invasion of cultured epithelial cells (Konkel *et al.*, 1999a; 1999b). A *ciaB* mutant is motile (Konkel *et al.*, 2004) but exhibits reduced chick colonisation levels (Ziprin *et al.*, 2001) and inactivation of *ciaB* prevents the secretion of other Cia proteins (Konkel *et al.*, 1999a). *C. jejuni* does not encode a type III secretion system (Parkhill *et al.*, 2000) and Cia proteins are secreted through the flagellar secretion apparatus instead in a *C. jejuni*-host cell contact- or mucin-dependent manner (Konkel *et al.*, 2004; Rivera-Amill *et al.*, 2001). Aside from Cia proteins, the flagellar secretion apparatus also secretes FlaC, which shares limited homology with FlaA and FlaB (Song *et al.*, 2004). FlaC is not required for flagella formation or motility but it is required for invasion (Song *et al.*, 2004).

1.3.4.5 Toxin production

Despite the importance of invasion, the level of invasion detected *in vitro* is normally low and invasion itself might not be the sole response to the cytopathic effects associated with *C. jejuni* infection (Wooldridge and Ketley, 1997). Toxin production is a common virulence factor employed by many enteric pathogens and has been proposed as another important determinant for *C. jejuni* pathogenesis (van Vliet and Ketley, 2001). A variety of toxic activities have been characterised in *C. jejuni* including: a

70-kDa toxin active only on HeLa cells; a cytotoxin active on both HeLa and Vero cells; a second cytotoxin showing hemolytic effects; a shiga-like toxin; a hepatotoxin and the best characterised cytolethal distending toxin CDT (Wassenaar, 1997). *C. jejuni* CDT is a tripartite toxin encoded by the *cdtABC* operon, which is required for CDT cytotoxicity (Whitehouse *et al.*, 1998). CDT is composed of CdtB, as the enzymatically active subunit, and CdtA and CdtC, as the heterodimeric subunit that is required for translocation of CdtB (Lara-Tejero and Galán, 2001). The nuclease activities of CdtB effectively cause the target cells to undergo cytodistension and arrest at the G₂-phase of the cell cycle, which ultimately results in cell death (Lara-Tejero and Galán, 2001).

1.3.5 Gene regulation in *C. jejuni*

C. jejuni lacks many responsive regulators such as the sigma factor RpoS (σ^{38}) which regulates stress responses in many Gram-negative bacteria (Parkhill *et al.*, 2000). However considerable variation in gene expression have been observed by transcription profiling of *C. jejuni* cultured under a range of sub-optimal growth conditions indicating that regulation of genes involved in adaptive responses is essential for the lifestyle of *C. jejuni* (Wösten *et al.*, 2008). The *C. jejuni* genome contains approximately 650-750 putative promoters and they are regulated by at least 37 transcriptional regulators including three sigma factors and 34 specific regulators (Wösten *et al.*, 2008).

1.3.5.1 Sigma factors

The main sigma factor in *C. jejuni* is RpoD, which belongs to the σ^{70} family of

housekeeping sigma factors and it regulates most *C. jejuni* promoters (Wösten *et al.*, 2008). RpoD contains two regions, the 2.4 and 4.2 segments, which recognise the -10 and -35 promoter regions respectively (Dombroski *et al.*, 1992). The 2.4 segment is highly conserved among *E. coli*, *B. subtilis* and *C. jejuni*, and an alignment of 175 *C. jejuni* promoter regions revealed that RpoD recognises a hexameric -10 region with the consensus sequence TATAAT. The 4.2 segment on the other hand is less conserved thus resulting in the absence of a consensus -35 promoter region in *C. jejuni* (Wösten *et al.*, 1998; Petersen *et al.*, 2003). However, *C. jejuni* does possess a consensus sequence for the -16 region (Wösten *et al.*, 1998; Petersen *et al.*, 2003), which is an essential transcriptional element for many promoters in Gram-positive bacteria and for *E. coli* promoters lacking a -35 region (Voskuil *et al.*, 1995).

FliA is another alternative sigma factor belonging to the σ^{70} family and it regulates 14 genes (Carrillo *et al.*, 2004) encoding for proteins involved in flagella assembly and flagellin subunit glycosylation (Logan *et al.*, 2002). Consistent with its function, a *fliA* mutant is nonmotile and FliA activity is tightly controlled by the anti-sigma factor FlgM (Wösten *et al.*, 2008). The third *C. jejuni* sigma factor is RpoN, which belongs to the well conserved σ^{54} family and a *rpoN* mutant is nonmotile and without flagella indicating the essential role of RpoN in motility (Wösten *et al.*, 2008). In fact, the protein products of 15 out of 23 genes regulated by RpoN are involved in flagella assembly which includes components of the basal body, the flagellar hook protein FlgE, FlaB as well as FlgM (Carrillo *et al.*, 2004; Wösten *et al.*, 2004).

1.3.5.2 Specific transcriptional regulators

Ten of the specific transcriptional regulators in *C. jejuni* are response regulators of TCSs and seven of their cognate kinase sensor proteins have also been identified. All but one of the response regulators belong to the OmpR family (see 1.1.3) and well studied examples include PhosR, DccR and RacR (Wösten *et al.*, 2008). PhosR forms a TCS with the cognate kinase sensor PhosS which senses the availability of phosphate in the environment. Phosphorylated PhosR regulates gene expression by binding to an operator sequence called the *pho* box located at the -35 region of twelve PhosR regulated genes. Examples of these genes include an alkaline phosphatase coding gene *phoA* and a P_i transport system coding operon *pstSCAB* (Wösten *et al.*, 2006). The DccR-DccS system regulates a putative type I secretion system in response to an unknown stimulus. An 81-167 strain defective in this system is viable but shows a reduced ability to colonise immunocompetent mice and 1-day-old chicks (MacKichan *et al.*, 2004).

Another well studied TCS is the RacR-RacS system which regulates the expression of eleven genes including *racR* itself. Like OmpR, RacR acts as both a repressor and an activator and these RacR regulated genes are expressed in response to changing growth temperature in a RacR-dependent manner. The 81116 *racR* mutant grows at a slower rate at 42 °C and it also shows reduced ability to colonise the alimentary tract of chickens (Brás *et al.*, 1999). The only *C. jejuni* response regulator that does not belong

to the OmpR family is FlgR which instead belongs to the NtrC family. FlgR forms a TCS with the cognate kinase sensor FlgS and functions in concert with RpoN to regulate the same set of RpoN-controlled genes in response to an unknown stimulus (Wösten *et al.*, 2004). Consistent with the *rpoN* mutant phenotype, inactivation of *flgS* or *rpoN* results in a nonmotile *C. jejuni* phenotype that lacks flagella (Jagannathan *et al.*, 2001).

Aside from TCSs, *C. jejuni* also possesses several other regulators such as NssR, CmeR and two Fur_{Cj} homologues (Wösten *et al.*, 2008). NssR is a nitrosative stress response regulator that positively regulates the expression of Cgb, a single-domain protein involved in the scavenging and detoxification process (Elders *et al.*, 2004). The mechanism of nitrite and nitric oxide sensing by NssR is currently unknown and NssR represents the only recognised member of the Cap/Fnr regulator family in *C. jejuni* (Wösten *et al.*, 2008). CmeR is the sole representation of the TetR regulator family in *C. jejuni* and it represses the *cmeABC* operon which encodes an efflux pump involved in multidrug resistance (Lin *et al.*, 2002; Lin *et al.*, 2005a). CmeR is essential for *C. jejuni* colonisation and CmeABC is required for bile resistance suggesting that bile salts are one of the substrates that activate CmeR (Lin *et al.*, 2005b). Fur_{Cj} and Fur homologue PerR_{Cj} are the best characterised transcriptional regulators in *C. jejuni* and their roles in controlling iron homeostasis and oxidative stress response respectively in *C. jejuni* are described in 1.4.2.

1.4 IRON HOMEOSTASIS AND GENE REGULATION BY THE *C. JEJUNI* FUR

1.4.1 Iron acquisition and storage systems in *C. jejuni*

As a successful coloniser of the avian and human gastrointestinal tracts, *C. jejuni* have evolved a range of highly adaptive iron uptake systems (Figure 1.20) which enable the acquisition of nutritional iron from various sources in the animal host. These iron acquisition systems are essential for *C. jejuni* during commensal and pathogenic colonisation and therefore play importance roles in *C. jejuni* survival and pathogenesis (Stintzi *et al.*, 2008; Miller *et al.*, 2009; Gilbreath *et al.*, 2011).

1.4.1.1 Ferrous iron uptake

Ferrous iron is an important iron source for enteric pathogens surviving in the oxygen-reduced intestinal environment and direct utilisation of ferrous iron by FeoB has been characterised in *C. jejuni* strains NCTC 11168, 81-176 and ATCC 43431 (Naikare *et al.*, 2006). The NCTC 11168 *feoB* homologue is located upstream, in an operon, from a *feoA* homologue and both genes share various degrees of identity with the *E. coli* and *H. pylori feoBA* systems (Parkhill *et al.*, 2000; Naikare *et al.*, 2006). No *feoC* homologue has been identified and several sequenced strains such as *C. jejuni* RM1221 carry a non-functional *feoB* gene with frameshift mutations and premature translational stops (Fouts *et al.*, 2005). Mutational analysis of NCTC 11168, 81-176 and ATCC 43431 *feoB* show reduced ferrous iron transport into the cytoplasm and an accumulation of ferrous iron in the periplasmic space. The ability to persist in intestinal cells is reduced for the 81-176 *feoB* mutant, whereas the NCTC 11168 mutant is outcompeted

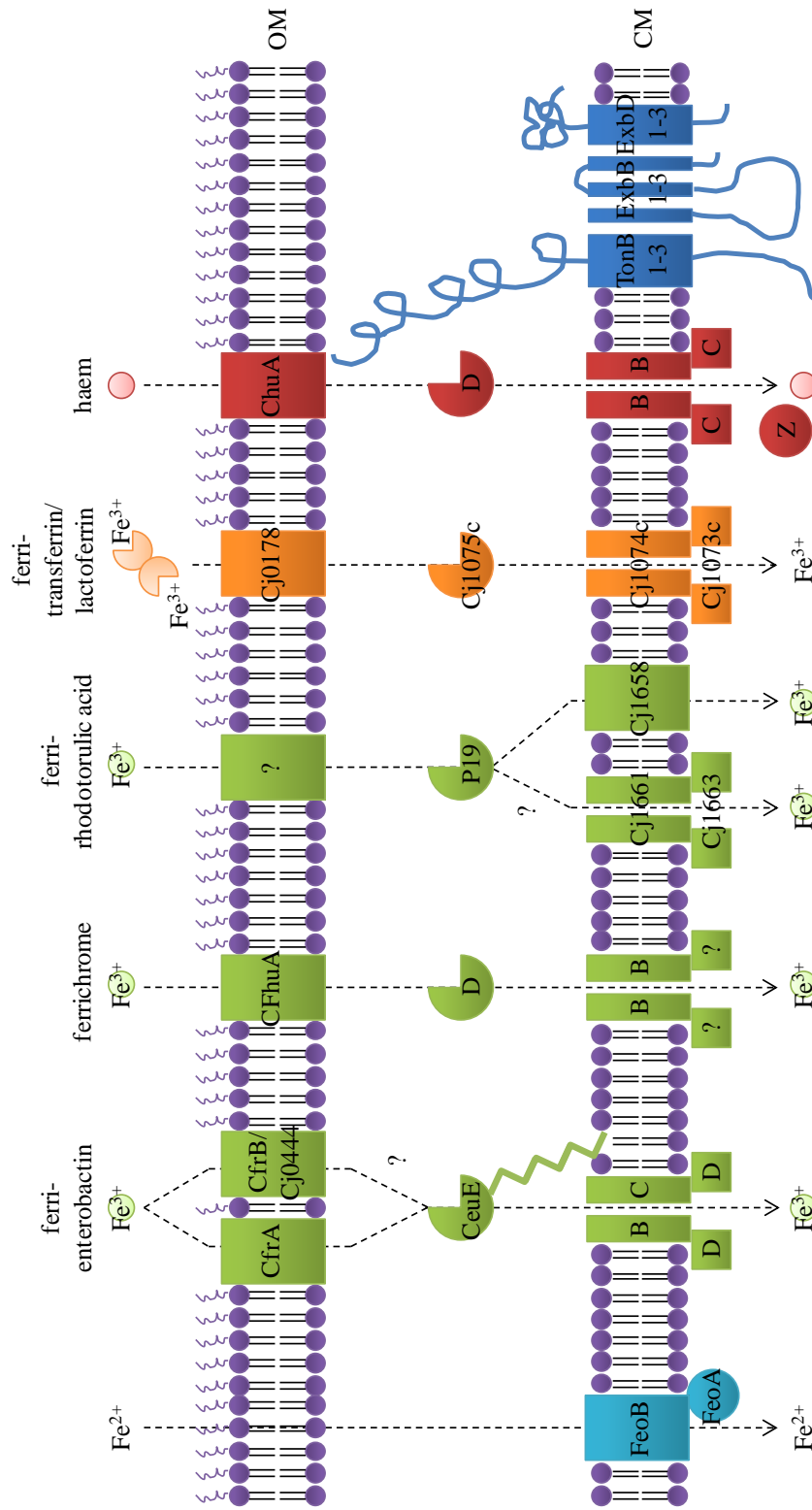


Figure 1.20: Iron acquisition systems of *C. jejuni* including: ferrous iron uptake, siderophore-mediated ferric iron uptake and iron uptake from host iron-containing compounds. The energy required for iron and haem uptake through the OM receptor is transduced from the CM by one of the three TonB/ExbB/ExbD protein complexes (adapted from Miller *et al.*, 2009).

by the wild-type for colonisation of the rabbit ileal loop (Naikare *et al.*, 2006). Furthermore colonisation of the chick caecum and piglet intestinal tract is also significantly compromised in all three *feoB* mutants, which indicate the functional importance of *C. jejuni* FeoB in ferrous iron uptake and pathogenesis (Naikare *et al.*, 2006). The ability to utilise ferrous iron is not affected in *C. jejuni* M129 and F38011 *feoB* mutants (Raphael and Joens, 2003) therefore implying that both strains as well as RM1221 may possess *feoB* homologues or alternative FeoB-independent ferrous iron acquisition systems (Miller *et al.*, 2009).

1.4.1.2 Siderophore-mediated ferric iron uptake

Although siderophore production activity in several *C. jejuni* strains has been documented in an early characterisation of cellular responses to iron limitation (Field *et al.*, 1986), no genes associated with siderophore biosynthesis have been identified from genome analysis of sequenced *C. jejuni* strains (Parkhill *et al.*, 2000; Hofreuter *et al.*, 2006). However, *C. jejuni* possesses specific uptake systems for several exogenous ferri-siderophores including ferri-enterobactin (Palyada *et al.*, 2004), ferrichrome (Galindo *et al.*, 2001) and ferri-rhodotorulic acid (Stintzi *et al.*, 2008). In addition, stress hormone noradrenaline also facilitates *C. jejuni* iron uptake in a siderophore-like and OM receptor-dependent manner (Cogan *et al.*, 2007).

An analogue to the *E. coli* Fep system, the *C. jejuni* ferri-enterobactin uptake system consists of an OM receptor CfrA (Palyada *et al.*, 2004), a PBP CeuE (Park and

Richardson, 1995) and an ABC permease complex CeuBCD (Parkhill *et al.*, 2000). NCTC 11168 *cfrA* is transcribed independently from the downstream *ceuBCDE* locus which forms a transcriptional unit (Parkhill *et al.*, 2000). When compared with FepA of *E. coli*, NCTC 11168 CfrA contains many conserved structural motifs but also shows substantial sequence variation in the putative ligand binding site which could affect the ligand binding affinity of CfrA (Carswell *et al.*, 2008). CeuE is an atypical siderophore PBP which contains a signal sequence resembling that of a lipoprotein (Park and Richardson, 1995) and compared to FhuD of *E. coli*, the ligand binding site of CeuE is more hydrophilic and positively charged (Müller *et al.*, 2006). The unusual structural characteristics of CfrA and CeuE would potentially provide *C. jejuni* with a broader range of siderophore binding than that provided by orthologous *E. coli* siderophore transporters (Gilbreath *et al.*, 2011). Mutational studies of NCTC 11168 *cfrA* and *ceuE* revealed that both genes are required to establish chick intestinal colonisation and although CfrA is essential for enterobactin-mediated iron acquisition, the ability to utilise ferri-enterobactin as a sole iron source is only partially affected by the CeuE mutant, indicating a degree of functional redundancy shared among iron transporters in *C. jejuni* (Palyada *et al.*, 2004; Ridley *et al.*, 2006). In addition, noradrenaline also facilitates cellular iron uptake in a CfrA-dependent manner as noradrenaline-mediated growth in iron restricted conditions is abolished in NCTC 11168 *cfrA* mutant (R. Haigh, personal communication). By contrast, both CfrA and CeuE of *C. coli* are dispensable in ferri-enterobactin utilisation (Richardson and Park, 1996; Guerry *et al.*, 1997) and the ability to colonise the chick intestinal tract is not compromised in a *ceuE* mutant

(Cawthraw *et al.*, 1996). CfrA is conserved amongst a large subset of *C. jejuni* isolates with the exception of strains such as 81-176 and 81116. Both strains however encode a functional TonB-dependent siderophore OM receptor Cj0444 for which the gene homologue in NCTC 11168 is present as a pseudogene (Parkhill *et al.*, 2000; Hofreuter *et al.*, 2006; Pearson *et al.*, 2007). Recently, the NCTC 11168 Cj0444 homologue has been characterised in several *C. coli* and *C. jejuni* isolates as a second ferri-enterobactin OM receptor and consequently named CfrB (Xu *et al.*, 2010). The ability to utilise ferri-enterobactin is greatly impaired in several *C. coli* strains and abolished in *C. jejuni* JL11 carrying a *cfrB* mutation. In addition, *cfrB* presented *in trans* is able to complement the ability to utilise ferri-enterobactin in a NCTC 11168 *cfrA* mutant and mutation of *cfrB* greatly reduces colonisation in the chick infection model (Xu *et al.*, 2010). Interestingly, 81-176 carrying a functional copy of *cfrB* and *ceuBCD* is unable to utilise ferri-enterobactin (Zeng *et al.*, 2009), suggesting the potential presence of a *ceuBCD* homologue or a novel ABC permease complex in *C. jejuni* that facilitates CfrB-mediated iron acquisition (Xu *et al.*, 2010).

A comparative study of *C. jejuni* RM129 OM receptor profiles identified the expression of a three-gene operon *cfhuABD* in the presence of Hep-2 epithelial cells, which was proposed to encode a putative ferrichrome uptake system (Galindo *et al.*, 2001). The iron regulated *cfhuABD* operon has an unusually high GC content compared with the surrounding genome and encodes an OM receptor CfhuA, a PBP CfhuD and a CM permease CfhuB, where each protein displays sequence homology with its counterpart

in the *E. coli* ferrichrome system Fhu (Galindo *et al.*, 2001). Although in this study *cfhuA* homologues were identified by PCR in six of the eleven *C. jejuni* isolates, the *cfhuABD* operon has not been identified in any of the sequenced *C. jejuni* strains (Parkhill *et al.*, 2000; Fouts *et al.*, 2005; Hofreuter *et al.*, 2006; Pearson *et al.*, 2007). Therefore given the lack of presence in *C. jejuni* and the unusual GC content, the functional importance of CfhAABD in iron uptake and the identity of the cognate ATP-binding component require further characterisations.

Many *C. jejuni* strains contain a highly conserved *cj1658-cj1663* locus which the NCTC 11168 homologue encodes proteins functioning in ferri-rhodotorulic acid utilisation (Miller *et al.*, 2009). The CM permease coding gene *cj1658* is located upstream from *cj1659* which the gene product P19 is a PBP (Janvier *et al.*, 1998) and possesses both ferric iron- and copper-binding capacities (Chan *et al.*, 2010). Although the involvement of P19 in copper uptake is not fully characterised, neither NCTC 11168 *cj1658* nor *p19* mutants are able to utilise ferric-rhodotorulic acid to support cellular growth (Stintzi *et al.*, 2008). Furthermore, an 81-176 *p19* mutant survives poorly in iron restricted conditions when compared with the wild-type strain, which suggests that P19 is able to acquire iron from other sources and the *p19* mutant cannot be fully compensated by other *C. jejuni* iron transporters (Chen *et al.*, 2010). The *cj1660-cj1663* locus encodes a putative ABC permease complex and putative CM proteins and no dedicated ferri-rhodotorulic acid OM receptor has been identified to date (Miller *et al.*, 2009).

1.4.1.3 Iron acquisition from host iron-containing compounds

C. jejuni was once considered incapable of obtaining iron from host ferri-glycoproteins (Pickett *et al.*, 1992), however the function of a putative OM receptor Cj0178 and a PBP-dependent transport system consisting of a PBP Cj0175c, a CM permease Cj0174c and an ATP-binding protein Cj0173c have been linked with the utilisation of iron-bound human transferrin, lactoferrin, and avian ovotransferrin in NCTC 11168 (Miller *et al.*, 2008). NCTC 11168 *cj0178* is divergently transcribed from the *cj0173c-cj0175c* locus which forms an operon with *cj0176c*, though no *cj0178* homologue has been identified from the genomes of 81-176 and 81116 (Hofreuter *et al.*, 2006; Pearson *et al.*, 2007; Miller *et al.*, 2008). Unlike the TbpA and LbpA systems in *Neisseria* spp, Cj0178 is a multispecific OM receptor for both transferrin and lactoferrin as mutation of *cj0178* showed reduced growth in the presence of ferri-lactoferrin and reduced ability to bind and acquire iron from ferri-transferrin (Miller *et al.*, 2008). However the ability to acquire iron from ferri-lactoferrin in the *cj0178* mutant is only partially abrogated and together with a small growth defect seen for the *cj0174c* mutant with ferri-transferrin suggests that *C. jejuni* may deploy alternative ferri-glycoprotein uptake systems (Miller *et al.*, 2008; Gilbreath *et al.*, 2010). In addition, the *cj0178* mutant also resulted in reduced colonisation potential in both the chick cecum and rabbit ileal loop models which demonstrates the importance of Cj0178 and ferri-glycoprotein-mediated iron acquisition *in vivo* (Palyada *et al.*, 2004; Stintzi *et al.*, 2005).

Under iron-restricted conditions, many *C. jejuni* strains are able to acquire iron from

haem, haemoglobin, haem-haemopexin and haemoglobin-haptoglobin and an OM receptor ChuA has been identified and associated with haem utilisation in 81-176 and NCTC 11168 (Pickett *et al.*, 1992; Ridley *et al.*, 2006). NCTC 11168 *chuA* is the leading gene of a four gene operon that also encodes a PBP ChuD, a CM permease ChuB and an ATP-binding protein ChuC, and this operon is divergently transcribed from *chuZ* the gene product of which functions as a haem oxygenase (Ridley *et al.*, 2006). Cellular growth in the presence of haem or haemoglobin as a sole iron source is compromised in both the *chuA* and *chuZ* mutants whereas ChuBCD appear to be unessential and partially redundant in haem utilisation (Ridley *et al.*, 2006). Although the expression of NCTC 11168 *chuA* and *chuB* are elevated in the chick cecum model (Woodall *et al.*, 2005), preliminary data has suggested that the 81-178 *chuA* is not required for optimal chick colonisation (Haigh *et al.*, 2010). Other putative proteins associated with haem utilisation include Cj0177 and Cj0178 which both bind haem *in vitro* (Chan *et al.*, 2006), and also CfrA which displays haemolytic activity in an *E. coli* background (Park and Richardson, 1995). However haem utilisation is not affected by the *cj0178* mutant (Miller *et al.*, 2008) and the *cfrA* mutant (R. Haigh, personal communication) and further investigation is required to establish conclusive roles for Cj0177 in haem uptake.

1.4.1.4 *TonB* and iron storage proteins

A search of the NCTC 11168 genome reveals the presence of three *tonB* homologues, in which both *tonB1* and *tonB2* are transcriptionally coupled with their cognate *exbB* and

exbD pairs and are located near the coding regions of ferri-glycoprotein and haem transporters respectively. *tonB3* on the other hand is not adjacent to *exbB/D3* and instead it is divergently transcribed from *cfrA* (Parkhill *et al.*, 2000). The ability for NCTC 11168 to utilise ferri-enterobactin is dependent on TonB3 whereas ChuA can only be energised by either TonB1 or TonB2, and these observations indicate some degree of functional specificity among the three TonB proteins in *C. jejuni* (Stintzi *et al.*, 2008). Unlike NCTC 11168, many strains like 81-178 and 81116 for instance only possess the *tonB2* homologue (Hofreuter *et al.*, 2006; Pearson *et al.*, 2007) and the 81-178 TonB is required to achieve optimal chick colonisation (Haigh *et al.*, 2010). Likewise, only one *tonB3* homologue has been identified so far in *C. coli* and the gene product is essential for the utilisation of haem, ferri-enterobactin and ferrichrome as iron sources (Guerry *et al.*, 1997).

Intracellular iron acquired through various iron uptake systems in *C. jejuni* is generally stored in Cft, a ferritin-like protein that shares a high degree of similarity with *H. pylori* Pfr (Wai *et al.*, 1996). The iron-containing Cft provides an intracellular iron source during iron deprivation as the growth of a *cft* mutant is inhibited under iron restricted conditions. A *cft* mutant also shows increased susceptibility to oxidative damage which indicates an additional role of Cft in oxidative stress response (Wai *et al.*, 1996). 81-176 produces an additional iron-binding protein Dps which lacks the DNA-binding ability seen with the *E. coli* Dps. 81-176 *dps* is constitutively expressed and the *dps* mutant is more sensitive to hydrogen peroxide which suggests a primary role for Dps in cellular

defence against iron-induced oxidative stress (Ishikawa *et al.*, 2003).

1.4.2 *C. jejuni* Fur homologues and their function in gene regulation

C. jejuni possess two Fur homologues: the Fur_{Cj} protein which regulates the expression of iron metabolism genes (Wooldridge *et al.*, 1994; van Vliet *et al.*, 1998) and PerR_{Cj} which functions in oxidative stress defence (van Vliet *et al.*, 1999). Recent transcriptomic and proteomic analysis of Fur_{Cj} and PerR_{Cj} reveal the functional role of Fur_{Cj} and PerR_{Cj} as global transcriptional regulators and their importance of coordinating iron homeostasis and oxidative stress responses in *C. jejuni* colonisation and survival (Palyada *et al.*, 2004; 2009; Holmes *et al.*, 2005). In addition, the *C. jejuni* zinc uptake system coding locus *znuABC* is not regulated by Fur_{Cj} or PerR_{Cj} (Davis *et al.*, 2009) potentially indicating the presence of a putative Zur homologue or a novel member of the Fur family in *C. jejuni*.

1.4.2.1 Fur_{Cj} and fur_{Cj} regulation

The *fur_{Cj}* gene was originally identified by reporter assays in 81116 (Wooldridge *et al.*, 1994) and independently by direct sequencing upstream of the ATCC 43431 *lysS* gene (Chan *et al.*, 1995). The 17.9 kDa Fur_{Cj} displays 40% identity to Fur_{Ec}, particularly at the C-terminal domain (van Vliet *et al.*, 2002), and shows sequence homology with orthologues from other bacterial species (Wooldridge *et al.*, 1994; Chan *et al.*, 1995). Despite the sequence similarity between Fur_{Cj} and Fur_{Ec}, Fur_{Cj} is only able to partially repress a Fur_{Ec}-regulated promoter in a *fur_{Ec}* mutant and it is not recognised by Fur_{Ec}

antiserum, which together indicates that Fur_{Cj} differs significantly from Fur_{Ec} and further structural and functional characterisation of Fur_{Cj} are required (Wooldridge *et al.*, 1994). The *fur*_{Cj} mutant grows poorly under both iron-restricted and repleted conditions when compared with the wild-type strain, though some of this growth defect may be attributed to altered transcription of the downstream *lysS* and *glyA* genes (van Vliet *et al.*, 1998). The *fur*_{Cj} mutant is more resistant to hydrogen peroxide, but more sensitive to cumene hydroperoxide and menadione when compared with the wild-type, suggesting the role of Fur_{Cj} in oxidative stress defence (Palyada *et al.*, 2009). *fur*_{Cj} mutation also affects chick colonisation which indicates the importance of Fur_{Cj} regulation *in vivo* and the role of Fur_{Cj} in *C. jejuni* virulence (Palyada *et al.*, 2004; 2009).

The genomic organisation of *fur*_{Cj} is rather unusual compared to *fur*_{Ec} and *fur*_{Hp} as it is located in an operon which also contains the downstream housekeeping genes *lysS* and *glyA* and upstream genes *gatC* and *Cj0399*. *fur*_{Cj} also does not have its own promoter and it is likely to be co-transcribed as a multicistronic mRNA by two distal promoters located upstream of *gatC* and *Cj0399* respectively. These promoters are not iron regulated, which suggests the absence of iron-responsive autoregulation of *fur*_{Cj} (van Vliet *et al.*, 2000). This iron and Fur-independent regulation of *fur* has also been observed for *P. aeruginosa* (Ochsner *et al.*, 1999) and the unique promoter configuration of *fur*_{Cj} would allow *C. jejuni* to regulate Fur_{Cj} in response to unknown environmental stimuli other than just iron (van Vliet *et al.*, 2000).

1.4.2.2 Iron and Fur_{Cj}-mediated gene regulation in *C. jejuni*

In order to understand iron homeostasis and the role of Fur_{Cj} in iron regulation, comparative analysis of protein expression profiles of the NCTC 11168 wild-type and a *fur_{Cj}* mutant in response to iron availability were initially carried out to identify members of the iron and Fur_{Cj} regulon (van Vliet *et al.*, 1998). As expected, derepressed expression of several iron transport proteins including CfrA, CeuE, P19, Cj0178, ChuA and ChuD were observed under iron-restricted conditions in the wild-type strain and in the *fur_{Cj}* mutant demonstrating the classic role of Fur_{Cj} as a repressor in controlling iron homeostasis. By contrast, oxidative stress defence proteins KatA and AhpC, which function as a catalase and an alkyl hydroperoxide reductase respectively (Grant and Park, 1995; Baillon *et al.*, 1999) were still iron-repressed in the *fur_{Cj}* mutant, suggesting the involvement of Fur_{Cj}-independent iron regulation (van Vliet *et al.*, 1998).

In a more comprehensive global transcriptomic analysis of NCTC 11168 in response to iron, expressions of 208 genes were significantly altered between iron-limited and iron-rich growth conditions during steady state. In addition, 460 genes, representing 27% of the *C. jejuni* genome, were differently transcribed within 15 minutes of iron supplementation illustrating a global adaption in *C. jejuni* to increased iron (Palyada *et al.*, 2004). Genes encoding proteins involved in iron acquisition and storage systems including *cfrA*, *ceuC*, *p19*, *cj1658*, *cj1661-1664*, *cj0173c-0175c*, *chuABCD*, *chuZ*, *tonB1*, *tonB3*, *exbB1*, *exbB2*, *exbD1*, *exbD2* and *cft* were up-regulated in iron limited

conditions. Iron-repressed transcription was also observed for components of the oxidative stress response system such as *perR_{Cj}*, *kata*, *ahpC*, *sodB* and *tpx*, which encodes a thiol peroxidase. By contrast, genes induced after the addition of iron, such as ferredoxin coding gene *fdxA* and oxidoreductase coding genes *oorABCD*, are mostly associated with energy metabolism, and not surprisingly, these genes encode enzymes that require iron for their function (Palyada *et al.*, 2004). When the transcriptome profiles of wild-type cells grew at steady state under iron-limitation and iron-rich conditions were compared with the *fur_{Cj}* mutant, 53 genes were found to be *Fur_{Cj}* regulated and in particular, 29 of these *Fur_{Cj}* regulated genes have their expression directly repressed by iron and *Fur_{Cj}*. Indeed, 17 iron-repressed iron acquisition genes reported in this study were directly repressed by *Fur_{Cj}*, once again illustrating the primary regulatory role of *Fur_{Cj}* in iron homeostasis (Palyada *et al.*, 2004).

In another independent transcriptomic and also proteomic investigation of the NCTC 11168 iron and *Fur_{Cj}* regulon, the transcription of 147 genes were altered with respect to iron availability and the expression of 43 iron-regulated genes were also altered in the *fur_{Cj}* mutant compared to the wild-type in iron-rich conditions (Holmes *et al.*, 2005). Many iron-repressed genes identified previously by Palyada *et al.* (2004), especially genes associated with iron acquisition and oxidative stress defence were consistently observed in this study with the addition of *tonB2*, *cj0444* and *cj0178*, where *cj0178* was also repressed by *Fur_{Cj}* (Holmes *et al.*, 2004). Interestingly, unlike other iron acquisition genes, iron and *Fur_{Cj}*-dependent regulation was not detected for *feoB* in both studies

(Palyada *et al.*, 2004; Holmes *et al.*, 2005). Many genes associated with general cellular physiology were identified as iron-responsive in Palyada *et al.*'s study (2004) but not by Holmes *et al.* (2005) and in fact, only 65 iron-responsive genes were reported in both studies. The discrepancies between these two studies are likely reflected by the different growth media used which would alter, to a certain degree, the cellular physiology and consequently alter the transcriptome in response to iron availability (Stintzi *et al.*, 2008). The temperature variations between the two studies are also likely to influence the experimental outcomes as the expression of approximately 20% of the NCTC 11168 genome is responsive to temperature elevation from 37 °C to 42 °C (Stintzi *et al.*, 2003).

Despite slight variations in experimental design and outcomes, both studies provide a genome wide picture of *C. jejuni* responses to iron availability and the regulatory role of Fur_{Cj} not only in controlling iron acquisition genes, but also the function of Fur_{Cj} as a global regulator (Palyada *et al.*, 2004; Holmes *et al.*, 2005). Additionally in both studies, several members of the Fur_{Cj} regulon were non-classically regulated by Fur_{Cj} such as *fdxA*, several flagellum biosynthesis genes (Palyada *et al.*, 2004) and *fumC* (Holmes *et al.*, 2005). *fumC* codes for a fumarase, a key enzyme of the TCA cycle (Guest and Roberts, 1983) and the expression of *fumC* was found to be iron-induced and Fur_{Cj}-activated (Holmes *et al.*, 2005). As transcriptomic analysis cannot distinguish between a direct and indirect effect of Fur_{Cj} on gene expression, the exact involvement of Fur_{Cj} in *fumC* regulation and indeed for all other non-classically Fur_{Cj} regulated genes in *C. jejuni* are currently unknown.

In a recent transcriptional analysis of the 81-176 *dsb* genes which have a role in intramolecular disulfide bridge formation, *apo-Fur_{Cj}* repression was demonstrated for the *dsbA2* promoter (Grabowska *et al.*, 2011). Prior to Grabowska *et al.*'s investigation (2011), *apo-Fur* repression has been exclusively demonstrated in *H. pylori* (Delany *et al.*, 2001; Ernst *et al.*, 2005), and this type of regulation was believed to be unconserved across bacterial species (Miles *et al.*, 2010a). *Fur_{Hp}* possesses an N-terminal extension which is proposed to stabilise the active DNA-binding domain in the absence of a metal cofactor (Dian *et al.*, 2011) and a similar extension has also been observed in *Fur_{Cj}* by sequence analysis (Carpenter *et al.*, 2010). However, *fur_{Cj}* when presented *in trans* was unable to complement *apo-Fur_{Hp}* regulation in a *H. pylori fur_{Hp}* mutant (Miles *et al.*, 2010a) indicating subtle structural and sequence differences between both proteins in their *apo* forms and their corresponding binding sites respectively.

1.4.2.3 Characterisation of the *Fur_{Cj}* box

The *Fur_{Cj}* box was first described in two *fur_{Cj}* characterisation studies where several putative *Fur_{Cj}*-binding sites resembling the *E. coli* consensus sequence were identified closely upstream of the *fur_{Cj}* gene (Wooldridge *et al.*, 1994; Chan *et al.*, 1995). The 81116 *Fur_{Cj}* was demonstrated to partially recognise the consensus *Fur_{Ec}* box (Wooldridge *et al.*, 1994) and purified ATCC 43431 *Fur_{Cj}* was able to bind to the four *Fur_{Cj}* box-like sequences associated with the *fur_{Cj}* gene (Chan *et al.*, 1995), both results therefore indicated that *Fur_{Cj}* potentially deploys a similar recognition sequence when

compared with *E. coli* (van Vliet *et al.*, 2002). However these Fur_{Cj} box-like sites were later demonstrated to be functionally irrelevant as Fur_{Cj} does not have its own promoter (van Vliet *et al.*, 2000). Fur_{Cj} also shows a degree of variation to Fur_{Ec} in the N-terminal DNA recognition and binding domain (van Vliet *et al.*, 2002), which suggests that the Fur recognition sequence may have diverged between *C. jejuni* and *E. coli* (Wooldridge *et al.*, 1994).

The initial search for the Fur_{Cj} binding site failed to identify any good matches in the genome when the *E. coli* three consecutive hexamer model (Escobar *et al.*, 1999) was applied, however further refined searches with six NAT (N represents any nucleotide) in the promoter region of iron acquisition genes, including *chuA*, *cfrA*, *p19*, *feoB*, *ceuB*, *cj0177*, *cfhuA* and *exbB* have enabled the verification of this trimer repeat as the putative Fur_{Cj} recognition site (van Vliet *et al.*, 2002). In a more comprehensive transcriptomic analysis of the Fur_{Cj} regulon, a 19 bp consensus sequence was derived from the promoter regions of 16 iron and Fur_{Cj}-regulated operons by computational analysis (Palyada *et al.*, 2004). This Fur_{Cj} binding site however poorly matches the *E. coli* consensus sequence and does not resemble any known Fur-recognition motifs (Table 1.2).

Direct Fur_{Cj} binding with various affinities have been observed for several *C. jejuni* promoters, including the *cfrA* and *ceuB* promoters and the *p19* operon promoter (Holmes *et al.*, 2005, Berg, 2007), the *chuA* and *ahpC* promoters (Li, 2005), the

chuA-chuZ intergenic region (Ridley *et al.*, 2006), the *cj0176c* and *cj777* promoters (Miller *et al.*, 2008), and the *tonB3-cfrA* intergenic region (Shearer *et al.*, 2009). Nevertheless, the putative Fur_{Cj} box proposed by Palyada *et al.* (2004) has not been verified with detailed mutational and DNase I footprinting analysis.

1.4.2.4 PerR_{Cj} and oxidative stress response

As a microaerophilic bacterium, *C. jejuni* requires protection against reactive oxygen species generated during aerobic metabolism, iron acquisition and by the host immune system. Several oxidative stress response proteins have been characterised in *C. jejuni*, including SodB which catalyses the dismutation of superoxide radicals into hydrogen peroxide and oxygen (Pesci *et al.*, 1994), KatA which converts hydrogen peroxide into water and oxygen (Grant and Park, 1995) and AhpC which converts alkyl peroxide into alcohol (Baillon *et al.*, 1999). A *sodB* mutant shows impaired ability to survive hydrogen peroxide, cumene hydroperoxide and menadione whereas *katA* and *ahpC* mutants are more sensitive to hydrogen peroxide and cumene hydroperoxide respectively (Palyada *et al.*, 2009). Furthermore, both *sodB* and *katA* mutants are unable to colonise the chick cecum and the colonisation ability of an *ahpC* mutant is also significantly reduced when compared to the wild-type (Palyada *et al.*, 2009). These observations indicate the direct role of SodB, KatA and AhpC in oxidative stress responses as well as in *C. jejuni* pathogenesis. Other less well characterised oxidative stress defence proteins in *C. jejuni*, include the thioredoxin reductase TrxB, which is predicted to function in AhpC recycling (Stintzi *et al.*, 2008), and FdxA, which in its

absence significantly reduces aerotolerance of *C. jejuni* (van Vliet *et al.*, 2001).

Regulation of oxidative stress response genes in many Gram-negative bacteria is usually mediated by SoxRS and OxyR (Imlay, 2008), both regulators however are absent from the *C. jejuni* genome and instead they are functionally substituted by PerR_{Cj} (van Vliet *et al.*, 1999; Palyada *et al.*, 2009). The 15.9 kDa PerR_{Cj} shares 32% and 37% identity with PerR_{Bs} and Fur_{Cj} respectively and contains a conserved HTH domain and two metal-binding domains. Unlike *furCj*, *perR_{Cj}* has its own promoter and is transcribed as a monocistronic mRNA (van Vliet *et al.*, 1999). A protein profiling analysis of the *perR_{Cj}* mutant shows derepressed expression of both KatA and AhpC in levels much higher when compared with the wild-type and in addition, the iron-responsive repression of KatA is only fully abolished in the *perR_{Cj} furCj* double mutant indicating co-regulation of *kata* by PerR_{Cj} and Fur_{Cj} (van Vliet *et al.*, 1999). A *perR_{Cj}* mutant exhibits reduced motility but is more resistant to hydrogen peroxide, cumene hydroperoxide and menadione (van Vliet *et al.*, 1999; Palyada *et al.*, 2009). The *perR_{Cj}* mutant also shows attenuated colonisation of the chick cecum and the colonisation ability is abolished in the *perR_{Cj} furCj* double mutant demonstrating the importance of oxidative stress regulation by PerR_{Cj} *in vivo* (Palyada *et al.*, 2009). Putative PerR_{Cj} boxes have been identified for the *kata* and *ahpC* promoters, however due to the lack of experimental support and the potential overlap between the PerR_{Cj} and Fur_{Cj} boxes, the PerR_{Cj} box remains poorly characterised (van Vliet *et al.*, 2002).

In a recent transcriptome comparison between wild-type and a *perR_{Cj}* mutant strain in response to iron availability and exposure of hydrogen peroxide, cumene hydroperoxide and menadione, 104 genes were identified to belong to the PerR_{Cj} regulon. Those PerR_{Cj} regulated genes found were associated with a variety of biological functions ranging from oxidative stress defence, iron acquisition and flagellar and fatty acid biosynthesis illustrating the regulatory role of PerR_{Cj} beyond its classic function in controlling oxidative stress response genes (Palyada *et al.*, 2009). Within 82 iron- and PerR_{Cj}-repressed genes identified in this study, the transcript levels of oxidative stress genes such as *katA* and *ahpC* and iron storage genes *cft* and *dps* were increased in response to one of the three oxidants, whereas the expression of 11 flagellar biosynthesis genes were found to be nonresponsive to oxidant exposures. In addition, many previously identified Fur_{Cj}-regulated iron acquisition genes (Palyada *et al.*, 2004; Holmes *et al.*, 2005) were also PerR_{Cj} repressed and down-regulated in response to iron-limitation and oxidant exposure indicating a tight link between iron homeostasis and oxidative stress (Palyada *et al.*, 2009). The regulatory potential of PerR_{Cj} as a transcriptional activator was also observed in this study with or without the presence of iron. The level of *sodB* transcript for instance was PerR_{Cj}-activated under the conditions of iron restriction, whereas the expression of *perR_{Cj}* itself was auto-activated by PerR_{Cj} in the presence of iron (Palyada *et al.*, 2009). However like in the case of Fur_{Cj}, the exact mechanism of direct or indirect transcriptional activation by PerR_{Cj} is currently unknown.

1.5 Research aims

Recognition of the Fur box by the Fur protein and the subsequent protein-DNA interaction are key steps in Fur-mediated gene regulation (Carpenter *et al.*, 2009b). Despite recent advances in the understanding of the global regulatory role of Fur_{Cj} in controlling iron homeostasis and other cellular processes (Palyada *et al.*, 2004; Holmes *et al.*, 2005), the mechanism of Fur_{Cj}-Fur_{Cj} box interaction and the Fur_{Cj} box itself (van Vliet *et al.*, 2002; Palyada *et al.*, 2004) are poorly studied when compared with other bacteria such as *E. coli* and are proposed to be different from *E. coli* as seen by the Fur and Fur box sequence variations between the two bacteria (Wooldridge *et al.*, 1998; Palyada *et al.*, 2004). The primary aim of this research was therefore to determine the functionally important bases in the Fur_{Cj} box that are essential for Fur_{Cj}-Fur_{Cj} box interaction by mutational analysis of Fur_{Cj} boxes from differently Fur_{Cj}-regulated promoters. The outcome of such an investigation will allow a better understanding of the basis of sequence-specific recognition of the Fur_{Cj} box by Fur_{Cj} and provide a model of Fur_{Cj}-Fur_{Cj} box interaction as well as an experimental verification of the proposed Fur_{Cj} box consensus sequence.

In addition, although Fur has long been considered as a transcriptional repressor, transcriptional activation by Fur or by a Fur-regulated sRNA intermediate(s) have been characterised in many bacteria (Carpenter *et al.*, 2009b). Iron-induced and Fur_{Cj}-activated genes such as *fumC* have also been identified in *C. jejuni* (Holmes *et al.*, 2005), however without the detailed characterisation of Fur_{Cj}-regulated sRNA

intermediate or evidence of direct binding of Fur_{Cj} to the *fumC* promoter (*pfumC*, Li, 2005), the involvement of Fur_{Cj} in iron-induced regulation of *fumC* is unclear. The second research aim was therefore to verify the iron- and Fur_{Cj}-responsive regulation of *fumC* and to determine any additional regulators or stimuli that are potentially involved, either directly or indirectly, in controlling *fumC* expression. The research outcome will reveal any additional regulatory potential of Fur_{Cj} and the functional interplay between Fur_{Cj} and other regulators in iron-responsive gene regulation in *C. jejuni*.

Chapter 2: Material and methods

2.1 Microbial analysis

2.1.1 Bacterial growth media, antibiotics and supplements

All media were purchased from Oxoid and sterilised before use in an Omega™ (Prestige Medical) autoclave at 121 °C, under 1.5 bar pressure for 15 minutes. Luria-Bertani (LB) broth was prepared with 1% (weight/volume, w/v) tryptone, 0.5% (w/v) yeast extract and 1% (w/v) NaCl. LB agar was prepared by the addition of 1.5% (w/v) agar to LB broth. Mueller-Hinton (MH) broth was prepared with 30% (w/v) beef dehydrated infusion, 1.75% (w/v) casein hydrolysate and 0.15% (w/v) starch. MH agar was prepared by the addition of 1.7% (w/v) agar to MH broth.

All chemicals were purchased from Fisher Scientific and all reagents were dissolved in distilled water (dH₂O) unless specified otherwise. Antibiotics and supplements were added to media for selective and supportive microbial growth and their concentrations were: 100 µg/ml ampicillin (Amp) sodium salt (Melford), 20 µg/ml chloramphenicol (Cm, Sigma-Aldrich, dissolved in 100% ethanol), 50 µg/ml kanamycin (Kan) monosulphate (Melford), 5 µg/ml trimethoprim (Tri, Sigma-Aldrich, dissolved in 50% ethanol), 10 µg/ml vancomycin (Van, Duchefa Biochemie), 6% (volume/volume, v/v) pre-warmed defibrinated house blood (Oxoid), 20 µM deferoxamine mesylate salt (Desferal, Sigma-Aldrich), 40 µM iron (II) sulphate heptahydrate (FeSO₄, Sigma-Aldrich), 4 mM malic acid (Malate, Sigma-Aldrich), 0.2 mM IPTG (Melford) and 40 µg/ml 5-bromo-4-chloro-3-indoyl-β-D-galactoside [X-gal (Melford), dissolved

in dimethylformamide (DMF)]. Antibiotics and supplements were filter sterilised with a Plastipak™ syringe (BD) and an Acrodisc® 2.5 mm syringe filter (Pall) and stored at 4 °C. Antibiotics and supplements were added to room temperature broth before microbial inoculation. Molten agar was cooled to 55 °C before supplementation with antibiotics and supplements and poured into Petri dishes (Sterilin) prior to storage at 4 °C for up to a month.

2.1.2 Bacterial strains used

Strain name	Description	Source/Reference
<i>E. coli</i>		
DH5α™	F ⁻ φ80 <i>lacZ</i> Δ <i>M15</i> Δ(<i>lacZYA-argF</i>)U169 <i>recA1 endA1 hsdR17</i> (e _k ⁻ m _k ⁺) <i>phoA supE44 thi-1 gyrA96 relA1 λ⁻</i>	Invitrogen
Rosetta™ (DE3) pLysS	F ⁻ <i>ompT hsdS_B</i> (r _B ⁻ m _B ⁻) <i>gal dcm</i> (DE3) pLysSRARE (Cm ^R)	Novagen
Top10	F ⁻ <i>mcrA</i> Δ(<i>mrr-hsdRMS-mcrBC</i>) φ80 <i>lacZ</i> Δ <i>M15</i> Δ <i>lacX74 recA1 araD139</i> Δ(<i>ara-leu</i>)7697 <i>galU galK rpsL</i> (Str ^R) <i>endA1 nupG</i>	Invitrogen
XL1-Blue	<i>recA1 endA1 gyrA96 thi-1 hsdR17 supE44 relA1 lac</i> [F ⁻ <i>proAB lacI^f</i> Δ <i>M15</i> Tn10 (Tet ^R)]	Stratagene
<i>C. jejuni</i>		
NCTC 11168	Wild-type clinical isolate	National Collection of Type Culture, Colindale, London
480 (NCTC 12744)	Clinical isolate for maintaining shuttle vector pMW10	King <i>et al.</i> , 1991
81-176	Clinical isolate	Korlath <i>et al.</i> , 1985
81116 (NCTC 11828)	Clinical isolate	Manning <i>et al.</i> , 2001
AB3	NCTC 11168 Δ <i>racR::aphA-3</i> (Kan ^R)	A. M. Brás
AV17	NCTC 11168 Δ <i>fur::aphA-3</i> (Kan ^R)	van Vliet <i>et al.</i> , 1998
AV41	NCTC 11168 Δ <i>fur::cat</i> (Cm ^R)	van Vliet <i>et al.</i> , 1998
AV63	NCTC 11168 Δ <i>perR::aphA-3</i> (Kan ^R)	van Vliet <i>et al.</i> , 1999
AV67	NCTC 11168 Δ <i>fur::aphA-3</i> (Kan ^R) Δ <i>perR::cat</i> (Cm ^R)	van Vliet <i>et al.</i> , 1999
RR1	480 Δ <i>fur::aphA-3</i> (Kan ^R)	This study
RR2	NCTC 11168 Δ <i>fumC::aphA-3</i> (Kan ^R)	This study

Table 2.1: Bacterial stains used in this study.

2.1.3 Bacterial growth conditions

E. coli strains were cultured aerobically at 37 °C in LB media for 16 hours (overnight). A liquid culture was set up in a 5 ml volume in a 30 ml universal tube (Sterilin) and incubated with shaking on a G10 Gyrotory[®] shaker (New Brunswick Scientific) at 200 revolutions per minute (rpm), whereas for plate culture, cells were spread or streaked onto an agar plate. LB media were supplemented with appropriate antibiotics for selection of a desired recombinant plasmids and LB agar was also supplemented with IPTG and X-gal for blue/white screening.

C. jejuni strains were cultured at 42 °C in MH media in a variable atmosphere incubator (VAIN, Don Whitely Scientific Limited), which maintains an atmosphere of 84% nitrogen, 10% carbon dioxide and 6% oxygen. Each liquid culture was set up in a 5 ml volume in a 15 ml centrifuge tube (Corning) with a loosened cap and incubated with shaking on an Orbit 300 (Labnet) shaker at 50 rpm for up to 16 hours. To achieve large scale liquid growth, 50 ml cultures were set up in 250 ml Cellstar[®] cell culture flasks (Greiner Bio-One) and incubated with shaking at 70 rpm. For plate culture, cells were spread on agar plates with a Eurotubo[®] collection swab (Beltalab) and incubated for up to a week. MH media were supplemented with Van and Tri to reduce the chance of contamination and other appropriate antibiotics for mutant selection. Media supplemented with FeSO₄ or Desferal were used to achieve high or low iron growth conditions respectively and malate was supplemented to promote growth of RR2. MH

agar supplemented with defibrinated horse blood was used to recover poorly growing mutants.

2.1.4 Strain maintenance and recovery

For long-term storage, *E. coli* overnight liquid cultures or *C. jejuni* harvested from plate cultures using MH broth were mixed with an equal amount of 25% (v/v) glycerol in a 1.5 ml screw cap tube (Sarstedt) and stored at -80 °C. For *E. coli* short-term storage, liquid and plate cultures were stored at 4 °C for up to a month. For *C. jejuni*, short-term storage was not possible and strains were maintained by sub-culture onto fresh media and incubated for up to a week.

E. coli strains were recovered from glycerol stocks by streaking onto LB agar plates and single colonies obtained were used for subsequent liquid inoculations. *C. jejuni* strains were recovered from glycerol stocks by swabbing onto MH agar plates and incubating for 2 days prior to sub-culture onto fresh plates and incubating for further 2 days. The cells were harvested and used for subsequent liquid inoculations or assays.

2.1.5 Preparation of electrocompetent *E. coli*

LB broth (200 ml) was inoculated with 2 ml of overnight *E. coli* liquid culture and was incubated at 37 °C with shaking until the optical density at 600 nm (OD₆₀₀) reached 0.5. The OD was measured in an Ultrospec 10 cell density spectrometer (Amersham Bioscience) using 1.5 ml semi-micro disposable cuvettes (Kartell). The cells were

chilled on ice for 30 minutes and pelleted by centrifugation at 3220 x g at 4°C for 15 minutes in a centrifuge 5810 R (Eppendorf). The cell pellet was then washed with 200 ml of ice-cold dH₂O followed by subsequent washes with 100 ml (once) and 50 ml (twice) of ice-cold dH₂O. The cell pellet was resuspended in 2 ml of ice-cold 10% (v/v) glycerol and aliquoted into 40 µl volumes in ice-cold microcentrifuge tubes (Eppendorf). The aliquots were flash frozen on dry ice and stored at -80 °C.

2.1.6 Preparation of electrocompetent *C. jejuni*

C. jejuni plate cultures were harvested with 10 ml of ice-cold *Campylobacter* electroporation buffer [CEB, 272 mM sucrose, 15% (v/v) glycerol and autoclaved] and centrifuged at 3220 x g at 4 °C for 20 minutes. The cell pellet was then washed twice with 10 ml of ice-cold CEB and resuspended in 1 ml of ice-cold CEB prior to aliquoting into 50 µl volumes in ice-cold microcentrifuge tubes. The aliquots were flash frozen on dry ice and stored at -80 °C.

2.1.7 *C. jejuni* growth assay

C. jejuni plate cultures were harvested and used to inoculate 5 ml of MH broth containing appropriate antibiotics to an OD₆₀₀ of 0.1. The culture was incubated overnight and was then used to inoculate three 5 ml volumes of MH broth (triplicate samplings) containing appropriate antibiotics and 40 µM FeSO₄ or 20 µM Desferal to an OD₆₀₀ of 0.025. The cultures were incubated and the OD₆₀₀ of each culture was measured every 5 hours for up to a total of 30 hours.

2.2 DNA analysis

2.2.1 *Extraction and purification of C. jejuni chromosomal DNA*

C. jejuni plate cultures were harvested with 10 ml of MH broth and centrifuged at 3220 x g for 20 minutes. The cells were lysed in 600 µl of buffer 1 [40 mM tris-acetate (TA) pH 7.8, 20 mM sodium acetate, 1 mM ethylenediamine tetraacetic acid (EDTA) and 1% (w/v) sodium dodecyl sulphate (SDS)] and neutralised with the addition of 200 µl of 5 M NaCl. The cell lysate was centrifuged at 15700 x g for 5 minutes in a centrifuge 5415 D (Eppendorf) and the supernatant was thoroughly mixed with 600 µl of chloroform/iso-amyl alcohol (24:1 v/v) in a fresh microcentrifuge tube by inverting the tube 100 times. The mixture was centrifuged at 15700 x g for 1 minute and the aqueous layer containing the DNA was transferred to a fresh microcentrifuge tube. The chloroform/iso-amyl alcohol extraction step was repeated at least twice. The aqueous layer was then transferred to a microcentrifuge tube containing 1 ml of 100% ethanol and thoroughly mixed to allow precipitation of the chromosomal DNA. The precipitated DNA was transferred to a microcentrifuge tube containing 800 µl of 70% (v/v) ethanol and pelleted at 15700 x g for 2 minutes. The ethanol was removed by aspiration and the DNA was hydrated in 200 µl of dH₂O at 4 °C overnight.

2.2.2 *C. jejuni natural transformation*

C. jejuni natural transformation was carried out using a biphasic system (Wang and Taylor, 1990). *C. jejuni* plate cultures were harvested with MH broth and the cell

concentration was adjusted to an OD₆₀₀ of 0.5 with MH broth. 0.5 ml of the cell suspension was added to a 15 ml centrifuge tube containing 1 ml of solidified MH agar and incubated for 5 hours. 1 to 5 µg of *C. jejuni* chromosomal DNA was then mixed with the cell culture and incubated for 4 hours prior to plating onto MH agar containing appropriate antibiotics and incubated for up to a week.

2.2.3 Extraction and purification of plasmid DNA

Plasmid DNA from 5 ml of *E. coli* or *C. jejuni* overnight cultures were extracted and purified using the E.Z.N.A.[®] plasmid mini kit I (Omega Bio-Tek) in accordance with the manufacturer's instructions. *E. coli*-derived plasmids were routinely eluted in 50 µl of dH₂O and 30 µl for *C. jejuni*-derived plasmids and were stored at -20 °C.

2.2.4 Plasmids used

Plasmid name	Description	Source/Reference
p23E5	<i>C. jejuni</i> 129108 <i>pmetK</i> cloned into the <i>Bgl</i> II site of pMW10 (Kan ^R)	Wösten <i>et al.</i> , 1998
pAV32	<i>C. coli</i> <i>aphA-3</i> cloned into the <i>Bcl</i> I site of <i>fur</i> in pAV25 (Kan ^R)	van Vliet <i>et al.</i> , 1998
pAV35	<i>C. coli</i> <i>cat</i> cloned into pBluescript (Amp ^R Cm ^R)	van Vliet <i>et al.</i> , 1998
pAV80	<i>cat</i> cloned into the <i>Bgl</i> II site of <i>fur</i> in pAV57 (Cm ^R)	van Vliet <i>et al.</i> , 1998
pGEMCWH01	NCTC 11168 <i>cj0752</i> with internal multi-cloning sites (MCSs) cloned into pGEM [®] -T (Amp ^R)	Elvers <i>et al.</i> , 2005
pGEM [®] -T Easy	General cloning vector (Amp ^R)	Promega
pJDR13	NCTC 11168 <i>chuA</i> promoter (<i>pchuA</i> , genome position 1540370-1540988) cloned into the <i>Bam</i> HI site of pMW10 (Kan ^R)	Ridley <i>et al.</i> , 2006
pJMck1	NCTC 11168 <i>fur</i> cloned into the <i>Bsa</i> I site of pASK-IBA7 (Amp ^R)	Holmes <i>et al.</i> , 2005
pJMck6	NCTC 11168 <i>pchuA</i> (genome position 1540722-1540995) cloned into the <i>Eco</i> RI site of pUC19 (Amp ^R)	J. McNicholl-Kennedy

pJMCK30	<i>C. coli apha-3</i> cloned into pUC19 (Amp ^R Kan ^R)	van Vliet <i>et al.</i> , 1998
pLEICES-01	Protein expression vector containing N-His ₆ tag (Amp ^R)	Protex, University of Leicester
pMW10	<i>E. coli-C. jejuni</i> shuttle <i>lacZ</i> reporter vector (Kan ^R)	Wösten <i>et al.</i> , 1998
pRRE	<i>ermC'</i> cloned into pRR [(Karlyshev and Wren, 2005), Amp ^R Ery ^R]	O. Bridle
pUC19	General cloning vector (Amp ^R)	New England Biolabs
pYL1	NCTC 11168 <i>pfumC</i> (genome position 1297511-1297743) cloned between <i>Bam</i> HI and <i>Eco</i> RI sites of pCR [®] 2.1-TOPO [®] (Amp ^R Kan ^R)	Li, 2005
pRR1	pJMCK6 containing the 10 th base mutation of the <i>chuA</i> Fur box (Amp ^R)	This study
pRR2	pJMCK6 containing the 13 th base mutation of the <i>chuA</i> Fur box (Amp ^R)	This study
pRR3	pJMCK6 containing the 19 th base mutation of the <i>chuA</i> Fur box (Amp ^R)	This study
pRR4	pJMCK6 containing 10 th and 13 th base mutations of the <i>chuA</i> Fur box (Amp ^R)	This study
pRR5	pJMCK6 containing 10 th and 19 th base mutations of the <i>chuA</i> Fur box (Amp ^R)	This study
pRR6	pJMCK6 containing 13 th and 19 th base mutations of the <i>chuA</i> Fur box (Amp ^R)	This study
pRR7	pJMCK6 containing 10 th 13 th and 19 th base mutations of the <i>chuA</i> Fur box (Amp ^R)	This study
pRR8	pYL1 containing the 10 th base mutation of the <i>fumC</i> Fur box (Amp ^R Kan ^R)	This study
pRR9	pYL1 containing the 13 th base mutation of the <i>fumC</i> Fur box (Amp ^R Kan ^R)	This study
pRR10	pYL1 containing the 19 th base mutation of the <i>fumC</i> Fur box (Amp ^R Kan ^R)	This study
pRR11	pYL1 containing 10 th and 13 th base mutations of the <i>fumC</i> Fur box (Amp ^R Kan ^R)	This study
pRR12	pYL1 containing 10 th and 19 th base mutations of the <i>fumC</i> Fur box (Amp ^R Kan ^R)	This study
pRR13	pYL1 containing 13 th and 19 th base mutations of the <i>fumC</i> Fur box (Amp ^R Kan ^R)	This study
pRR14	pYL1 containing 10 th and 13 th and 19 th base mutations of the <i>fumC</i> Fur box (Amp ^R Kan ^R)	This study
pRR15	<i>pchuA</i> amplified from pJMCK6 cloned between <i>Bam</i> HI and <i>Xba</i> I sites of pMW10 (Kan ^R)	This study
pRR16	<i>pchuA</i> from amplified pRR1 cloned between <i>Bam</i> HI and <i>Xba</i> I sites of pMW10 (Kan ^R)	This study
pRR17	<i>pchuA</i> amplified from pRR2 cloned between <i>Bam</i> HI and <i>Xba</i> I sites of pMW10 (Kan ^R)	This study

pRR18	<i>pchuA</i> amplified from pRR3 cloned between <i>Bam</i> HI and <i>Xba</i> I sites of pMW10 (Kan ^R)	This study
pRR19	<i>pchuA</i> amplified from pRR4 cloned between <i>Bam</i> HI and <i>Xba</i> I sites of pMW10 (Kan ^R)	This study
pRR20	<i>pchuA</i> amplified from pRR5 cloned between <i>Bam</i> HI and <i>Xba</i> I sites of pMW10 (Kan ^R)	This study
pRR21	<i>pchuA</i> amplified from pRR6 cloned between <i>Bam</i> HI and <i>Xba</i> I sites of pMW10 (Kan ^R)	This study
pRR22	<i>pchuA</i> amplified from pRR7 cloned between <i>Bam</i> HI and <i>Xba</i> I sites of pMW10 (Kan ^R)	This study
pRR23	<i>pfumC</i> amplified from pYL1 cloned between <i>Bam</i> HI and <i>Xba</i> I sites of pMW10 (Kan ^R)	This study
pRR24	<i>pfumC</i> amplified from pRR8 cloned between <i>Bam</i> HI and <i>Xba</i> I sites of pMW10 (Kan ^R)	This study
pRR25	<i>pfumC</i> amplified from pRR9 cloned between <i>Bam</i> HI and <i>Xba</i> I sites of pMW10 (Kan ^R)	This study
pRR26	<i>pfumC</i> amplified from pRR10 cloned between <i>Bam</i> HI and <i>Xba</i> I sites of pMW10 (Kan ^R)	This study
pRR27	<i>pfumC</i> amplified from pRR11 cloned between <i>Bam</i> HI and <i>Xba</i> I sites of pMW10 (Kan ^R)	This study
pRR28	<i>pfumC</i> amplified from pRR12 cloned between <i>Bam</i> HI and <i>Xba</i> I sites of pMW10 (Kan ^R)	This study
pRR29	<i>pfumC</i> amplified from pRR13 cloned between <i>Bam</i> HI and <i>Xba</i> I sites of pMW10 (Kan ^R)	This study
pRR30	<i>pfumC</i> amplified from pRR14 cloned between <i>Bam</i> HI and <i>Xba</i> I sites of pMW10 (Kan ^R)	This study
pRR31	<i>pchuA</i> from pJMCK6 extended by 61 bp upstream and cloned between <i>Bam</i> HI and <i>Xba</i> I sites of pMW10 (Kan ^R)	This study
pRR32	<i>pchuA</i> from pRR1 extended by 61 bp upstream and cloned between <i>Bam</i> HI and <i>Xba</i> I sites of pMW10 (Kan ^R)	This study
pRR33	<i>pchuA</i> from pRR2 extended by 61 bp upstream and cloned between <i>Bam</i> HI and <i>Xba</i> I sites of pMW10 (Kan ^R)	This study
pRR34	<i>pchuA</i> from pRR3 extended by 61 bp upstream and cloned between <i>Bam</i> HI and <i>Xba</i> I sites of pMW10 (Kan ^R)	This study
pRR35	<i>pchuA</i> from pRR4 extended by 61 bp upstream and cloned between <i>Bam</i> HI and <i>Xba</i> I sites of pMW10 (Kan ^R)	This study
pRR36	<i>pchuA</i> from pRR5 extended by 61 bp upstream and cloned between <i>Bam</i> HI and <i>Xba</i> I sites of pMW10 (Kan ^R)	This study

pRR37	<i>pchuA</i> from pRR6 extended by 61 bp upstream and cloned between <i>Bam</i> HI and <i>Xba</i> I sites of pMW10 (Kan ^R)	This study
pRR38	<i>pchuA</i> from pRR7 extended by 61 bp upstream and cloned between <i>Bam</i> HI and <i>Xba</i> I sites of pMW10 (Kan ^R)	This study
pRR39	PolyG-tailed NCTC 11168 <i>chuA</i> cDNA cloned between <i>Bam</i> HI and <i>Xba</i> I sites of pUC19 (Amp ^R)	This study
pRR40	PolyG-tailed NCTC 11168 <i>waaC</i> cDNA cloned between <i>Bam</i> HI and <i>Xba</i> I sites of pUC19 (Amp ^R)	This study
pRR41	<i>cat</i> and partial <i>fur</i> amplified from pAV80 and cloned between <i>Sal</i> I and <i>Bam</i> HI sites of pUC19 (Amp ^R Cm ^R)	This study
pRR42	<i>pfumC</i> from pYL1 extended by 217 bp upstream and cloned between <i>Bam</i> HI and <i>Xba</i> I sites of pMW10 (Kan ^R)	This study
pRR43	5' oligonucleotide tagged NCTC 11168 <i>chuA</i> cDNA TA cloned into pGEM [®] -T Easy (Amp ^R)	This study
pRR44	5' oligonucleotide tagged NCTC 11168 <i>fumC</i> cDNA 1 TA cloned into pGEM [®] -T Easy (Amp ^R)	This study
pRR45	5' oligonucleotide tagged NCTC 11168 <i>fumC</i> cDNA 2 TA cloned into pGEM [®] -T Easy (Amp ^R)	This study
pRR46	NCTC 11168 <i>racR</i> (genome position 1191788-1192459) cloned into pLEICES-01 by recombination (Amp ^R)	This study (by Protex, University of Leicester)
pRR47	NCTC 11168 <i>pchuA</i> (genome position 1540661-1540995) cloned between <i>Bam</i> HI and <i>Xba</i> I sites of pUC19 (Amp ^R)	This study
pRR48	pRR47 containing the 1 st base A to C mutation of the <i>chuA</i> Fur box (Amp ^R)	This study
pRR49	335 bp <i>pchuA</i> amplified from pRR48 cloned between <i>Bam</i> HI and <i>Xba</i> I sites of pMW10 (Kan ^R)	This study
pRR50	274 bp <i>pchuA</i> amplified from pRR48 cloned between <i>Bam</i> HI and <i>Xba</i> I sites of pMW10 (Kan ^R)	This study
pRR51	NCTC 11168 <i>fumC</i> and flank regions (genome position 1295731-1298155) cloned between <i>Bam</i> HI and <i>Xba</i> I sites of pUC19 (Amp ^R)	This study
pRR52	1067 bp internal deletion of <i>fumC</i> in pRR51 by insertion of <i>aphA-3</i> into the <i>Bgl</i> III site created by inverse PCR (Amp ^R Kan ^R)	This study
pRR53	NCTC 11168 <i>racS</i> histidine kinases domain (<i>racS</i> -HK genome position 1192948-1193691) cloned into pLEICES-01 by recombination (Amp ^R)	This study (by Protex, University of Leicester)
pRR54	pRR47 containing the 1 st base A to T mutation of	This study (by T.

	the <i>chuA</i> Fur box (Amp ^R)	Caudle)
pRR55	335 bp <i>pchuA</i> amplified from pRR54 cloned between <i>Bam</i> HI and <i>Xba</i> I sites of pMW10 (Kan ^R)	This study (by T. Caudle)
pRR56	274 bp <i>pchuA</i> amplified from pRR54 cloned between <i>Bam</i> HI and <i>Xba</i> I sites of pMW10 (Kan ^R)	This study (by T. Caudle)
pRR57	pRR47 containing the 7 th base mutation of the <i>chuA</i> Fur box (Amp ^R)	This study (by T. Caudle)
pRR58	335 bp <i>pchuA</i> amplified from pRR57 cloned between <i>Bam</i> HI and <i>Xba</i> I sites of pMW10 (Kan ^R)	This study (by T. Caudle)
pRR59	274 bp <i>pchuA</i> amplified from pRR57 cloned between <i>Bam</i> HI and <i>Xba</i> I sites of pMW10 (Kan ^R)	This study (by T. Caudle)
pRR60	pRR47 containing 1 st and 7 th base mutations of the <i>chuA</i> Fur box (Amp ^R)	This study (by T. Caudle)
pRR61	335 bp <i>pchuA</i> amplified from pRR60 cloned between <i>Bam</i> HI and <i>Xba</i> I sites of pMW10 (Kan ^R)	This study (by T. Caudle)
pRR62	274 bp <i>pchuA</i> amplified from pRR60 cloned between <i>Bam</i> HI and <i>Xba</i> I sites of pMW10 (Kan ^R)	This study (by T. Caudle)
pRR63	pRR47 containing 1 st , 7 th , 13 th and 19 th base mutations of the <i>chuA</i> Fur box (Amp ^R)	This study (by T. Caudle)
pRR64	335 bp <i>pchuA</i> amplified from pRR63 cloned between <i>Bam</i> HI and <i>Xba</i> I sites of pMW10 (Kan ^R)	This study (by T. Caudle)
pRR65	274 bp <i>pchuA</i> amplified from pRR63 cloned between <i>Bam</i> HI and <i>Xba</i> I sites of pMW10 (Kan ^R)	This study (by T. Caudle)
pRR66	NCTC 11168 <i>fumC</i> and flank regions (genome position 1296244-1297960) cloned into the <i>Kpn</i> I site of pGEMCWH01 (Amp ^R)	This study
pRR67	<i>cat</i> cloned into the <i>Bam</i> HI site of pRR66 (Amp ^R Cm ^R)	This study

Table 2.2: Plasmids used in this study. All pRR plasmids were maintained in *E. coli* Top 10 with the exception of pRR46 and pRR53 which were maintained in *E. coli* RosettaTM(DE3) pLysS. All pMW10 based plasmids were also maintained in *C. jejuni* 480. pJMCK1 was maintained in *E. coli* XL1-Blue and all other plasmids were maintained in *E. coli* DH5TM.

2.2.5 Nucleic acid quantification

DNA and RNA concentrations were quantified by Nanodrop® ND-1000 spectrophotometer (Thermo Scientific) which converts 260 nm absorbance into ng/μl.

2.2.6 Transformation of electrocompetent *E. coli*

Plasmid DNA (0.5 µg) purified from a bacterial culture (2.2.3) or a whole ligation reaction (2.2.17) was routinely introduced into *E. coli* by electroporation. Plasmid DNA was dialysed against dH₂O for 30 minutes on a 0.025 µm MFTM membrane filter (Millipore) prior to electroporation to remove any traces of salt. Desalted DNA was then mixed with 40 µl of thawed electrocompetent *E. coli* cells (2.1.7) in a pre-cooled 2 mm electroporation cuvette (Cell Projects) and a pulse of 2.5 kV was applied through the cuvette using a Gene PulserTM (Bio-Rad) electroporator set at 200 Ω and 125 µFD. The cells were recovered by the addition of 1 ml of LB broth and incubated for an hour. The cells were then plated onto LB agar plates with appropriate antibiotic selection, 0.2 mM IPTG and 40 µg/ml X-gal and incubated overnight.

2.2.7 Transformation of electrocompetent *C. jejuni*

Desalted plasmid DNA (5 µg) was electroporated into 50 µl of electrocompetent *C. jejuni* cells (2.1.8) in the same manner as for *E. coli* (2.2.6). The cells were recovered by the addition of 100 µl of MH broth and incubated on MH agar overnight. The cells were then sub-cultured onto MH agar plates with appropriate antibiotic selection and supplements, and incubated for up to a week.

2.2.8 DNA purification by ethanol precipitation

DNA was mixed thoroughly with 0.1 volumes of 3 M sodium acetate, 1 µl of glycogen (Roche) and 2 volumes of 100% ethanol and incubated at -80 °C or in an ethanol/dry ice

bath for 30 minutes. The DNA was pelleted at 15700 x g for 30 minutes and was washed twice with 70% (v/v) ethanol. The ethanol was removed by aspiration and the DNA was hydrated in an appropriate amount of dH₂O.

2.2.9 DNA purification by phenol/chloroform extraction

Equal amounts of DNA sample and phenol/chloroform/iso-amyl alcohol (25:24:1) were mixed thoroughly in a Phase Lock Gel[™] tube (Eppendorf) by shaking vigorously for 30 seconds. The mixture was centrifuged at 15700 x g for 15 minutes and the aqueous layer was transferred to a fresh microcentrifuge tube prior to purification by ethanol precipitation (2.2.8). For DNA samples contaminated with small amounts of protein, chloroform/iso-amyl alcohol (24:1) was used instead of phenol/chloroform/iso-amyl alcohol.

2.2.10 Agarose gel electrophoresis

DNA samples were visually analysed by electrophoresis on 1% (w/v) agarose gels which were prepared by dissolving Seakem[®] LE agarose (Lonza) in 1x tris-acetate-EDTA (TAE, 40 mM TA and 1 mM EDTA, pH 7.8) at 55 °C. Ethidium bromide (0.5 µg/ml) was added to pre-cooled molten agarose and the agarose was poured into a casting tray. DNA samples were mixed with 6x DNA loading buffer [50x TAE pH 7.8, 15% (v/v) glycerol and 0.3% (w/v) Orange G (Sigma-Aldrich)] and were loaded into the wells on the gel (formed using appropriate size combs) along with 5 µl of DNA size markers [λ DNA *Hind*III-digest/ Φ X174 DNA *Hae*III-digest (2.5:1, New

England Biolabs), 75 mM NaCl and 30% (v/v) 6x DNA loading buffer]. The gel was run at 110 V in 1x TAE for an appropriate amount of time and visualised in a GeneGenius bio imaging system (Syngene).

2.2.11 DNA purification from agarose gel

DNA samples excised from an agarose gel on a Chromato-Vue[®] transilluminator (UVP) were purified using the Zymoclean[™] gel DNA recovery kit (Zymo Research) in accordance with the manufacturer's instructions. DNA samples were routinely eluted in 15 µl of dH₂O.

2.2.12 Standard polymerase chain reaction (PCR)

Standard PCR was used to amplify a specific DNA fragment or to screen for the presence of a specific gene or plasmid. A full list of reagents and cycle conditions used are listed in Table 2.3 and 2.4 respectively. In general, PCR was routinely carried out in 20 µl or 50 µl reaction volumes in a 0.2 ml Thermo-Tube (Thermo Scientific) and consisted of high fidelity Phusion[®] DNA polymerase (Finnzymes) and 5x Phusion[®] HF buffer (Finnzymes) for cloning purpose. KAPA Taq (KAPA Biosystems) DNA polymerase and 10x high fidelity buffer (Eppendorf) were used for other purposes. 10 mM of pre-mixed deoxynucleotide triphosphates [dNTPs, from 100 mM dATP, dTTP, dGTP and dCTP stocks (Promega)] as well as an appropriate primer set (2.2.11) and a template such as linear, plasmid or chromosomal DNA were also included. DNA extracted from bacterial colonies were also used as DNA templates and in each case, a

Reaction types Reagents (μ l)	20 μ l Taq PCR with		20 μ l Phusion [®] PCR with		50 μ l Phusion [®] PCR with		
	DNA extracted from a colony	Chromosomal DNA	Plasmid or linear DNA	Chromosomal DNA	Plasmid or linear DNA	Chromosomal DNA	Plasmid or linear DNA
Buffer	2	2	2	4	4	10	10
dNTPs	0.4	0.4	0.4	0.4	0.4	1	1
Forward primer	2	1	1	1	1	12.5	12.5
Reverse primer	2	1	1	1	1	12.5	12.5
DNA polymerase	0.25	0.25	0.25	0.2	0.2	0.5	0.5
Template	2	2	0.25	1	1	2	1
dH ₂ O	11.35	13.35	15.1	12.4	12.4	11.5	12.5

Table 2.3: Reagents used in various types and volumes of PCR. Primers used in all the reactions were diluted to 2 pmol with the exception of primers used in 20 μ l Phusion[®] PCR. They were diluted to 10 pmol in order to fit into the 20 μ l reaction volume. Plasmids and linear DNA fragments used in Taq PCR were diluted to 1 μ g/ μ l whereas DNA used in Phusion[®] PCR was diluted to 10 μ g/ μ l. The concentration of chromosomal DNA was not usually measured.

Cycle name	Initial denaturation	Denaturation	Annealing	Extension	Final extension
Number of cycles	1		30		1
Cycle temperature and time for Taq PCR	94 °C 2 minutes	94 °C 30 seconds	45-65 °C 30 seconds	72 °C 1 minute per 1 kb product	72 °C 5 minutes
Cycle temperature and time for Phusion [®] PCR	98 °C 30 seconds	98 °C 10 seconds	45-65 °C 10 seconds	72 °C 1 minute per 1 kb product	72 °C 5 minutes

Table 2.4: Cycle conditions used in various types of PCR. The appropriate annealing temperature for each set of primers was determined by gradient PCR. Gradient PCR was carried out in the same manner as a standard PCR, except the annealing temperature was set to 55 °C and the gradient G value was set to 10 °C. In this way, 12 temperatures ranged from 45 to 65 °C were applied simultaneously. For inverse PCR, the standard PCR principle and conditions were applied except overlapping primers facing outward from each other were used.

single colony was boiled in 20 µl of dH₂O at 96 °C for 5 minutes and centrifuged at 15700 x g for 2 minutes prior to using the supernatant in PCR reactions. The amplification step was performed in a GS1 (G-Strom) thermal cycler with an initial denaturation step followed by 30 cycles of denaturation, annealing and extension and finished with a final extension step.

2.2.13 Primers used

Primer Name	Primer Sequence 5'-3'	Primary Target DNA
Site-directed mutagenesis and cloning of <i>chuA</i> and <i>fumC</i> Fur boxes		
<i>chuA10F</i>	GAAATTATCATTATTTATTTT ATTTAAG	pJMCK6
<i>chuA10R</i>	TGATAATTTCTATCATAATAA TTTAG	pJMCK6
<i>chuA13F</i>	TAATTTATCATTATTTATTTTA TTTAAG	pJMCK6
<i>chuA13R</i>	TGATAAATTATATCATAATAA TTTAG	pJMCK6
<i>chuA19F</i>	TAAATTATCTTTATTTATTTTA TTTAAG	pJMCK6
<i>chuA19R</i>	AGATAATTTATATCATAATAA TTTAG	pJMCK6
<i>chuA10-13F</i>	GAATTTATCATTATTTATTTT ATTTAAG	pJMCK6
<i>chuA10-13R</i>	TGATAAATTCTATCATAATAA TTTAG	pJMCK6
<i>chuA10-19F</i>	GAAATTATCTTTATTTATTTT ATTTAAG	pJMCK6
<i>chuA10-19R</i>	AGATAATTTCTATCATAATAA TTTAG	pJMCK6
<i>chuA13-19F</i>	TAATTTATCTTTATTTATTTTA TTTAAG	pJMCK6
<i>chuA13-19R</i>	AGATAAATTATATCATAATAA TTTAG	pJMCK6
<i>chuA10-13-19F</i>	GAATTTATCTTTATTTATTTTA TTTAAG	pJMCK6
<i>chuA10-13-19R</i>	AGATAAATTCTATCATAATAA TTTAG	pJMCK6

<i>chuA1CF</i>	CTTATGATATAAATTATCATT ATTTATTTTATTTAAG	pRR47
<i>chuA1CR</i>	ATAATTTATATCATAAGAATT TAGAAATAAATTTATC	pRR47
<i>chuA1TF</i>	TTTATGATATAAATTATCATT ATTTATTTTATTTAAG	pRR47
<i>chuA1TR</i>	ATAATTTATATCATAAAAATT TAGAAATAAATTTATC	pRR47
<i>chuA7TF</i>	ATTATGTTATAAATTATCATT ATTTATTTTATTTAAG	pRR47
<i>chuA7TR</i>	ATAATTTATAACATAATAATT TAGAAATAAATTTATC	pRR47
<i>chuA1-7TF</i>	TTTATGTTATAAATTATCATT ATTTATTTTATTTAAG	pRR47
<i>chuA1-7TR</i>	ATAATTTATAACATAAAAATT TAGAAATAAATTTATC	pRR47
<i>chuA1-7-13-19TF</i>	TTTTATGTTATAATTTATCTTT ATTTATTTTATTTAAGG	pRR47
<i>chuA1-7-13-19TR</i>	AGATAAATTATAACATAAAA ATTTAGAAATAAATTTATC	pRR47
<i>chuA5(BamHI)</i>	ATGC GGATCC CTAGATTAAG TTAATAAAGG	pJMcK6, pRR1-7, 48, 54, 57, 60, 63
<i>chuA3(XbaI)</i>	ATGC TCTAGA ATTTTGTAGA TCTTTGCC	pJMcK6, pRR1-7, 48, 54, 57, 60, 63
<i>chuAFUSION5'</i>	CTAGATTAAGTTAATAAAGG	pJMcK6, pRR1-7
<i>chuANEW5'(BamHI)</i>	ATGC GGATCC CAATTATCAA ATTA AAAAGC	NCTC 11168 genome position 1540661-1540680, pRR54, 57, 60, 63
<i>chuAFUSION3'</i>	CCTTTATTA ACTTAATCTAG	NCTC 11168 genome position 1540722-1540741
<i>fumC10F</i>	TTATTTATTTTTTTAGCTTATA ATAAATA	pYL1
<i>fumC10R</i>	AAATAAATAATTTCAAAAAC GTTTTCTAC	pYL1
<i>fumC13F</i>	GTAATTATTTTTTTAGCTTAT AATAAATA	pYL1
<i>fumC13R</i>	AAATAACTTTCAAAAAC GTTTTCTAC	pYL1
<i>fumC19F</i>	GTATTTATTTTTTAGCTTATA ATAAATA	pYL1
<i>fumC19R</i>	TAATAAATACTTTCAAAAAC GTTTTCTAC	pYL1
<i>fumC10-13F</i>	TTAATTATTTTTTTAGCTTAT AATAAATA	pYL1

<i>fumC</i> 10-13R	AAATAATTAATTTCAAAAAC GTTTTCTAC	pYL1
<i>fumC</i> 10-19F	TTATTTATTATTTTAGCTTATA ATAAATA	pYL1
<i>fumC</i> 10-19R	TAATAAATAATTTCAAAAAC GTTTTCTAC	pYL1
<i>fumC</i> 13-19F	GTAATTATTATTTTAGCTTAT AATAAATA	pYL1
<i>fumC</i> 13-19R	TAATAATTACTTTCAAAAAC GTTTTCTAC	pYL1
<i>fumC</i> 10-13-19F	TTAATTATTATTTTAGCTTATA ATAAATA	pYL1
<i>fumC</i> 10-13-19R	TAATAATTAATTTCAAAAAC GTTTTCTAC	pYL1
<i>fumC</i> 5(<i>Bam</i> HI)	ATGC GGATCC CTCATAATGC CTATGAATTGC	pYL1, pRR8-14
<i>fumC</i> 3(<i>Xba</i> I)	ATGC TCTAGA CCTTTGGCAT TTTCTACAACC	pYL1, pRR8-14
<i>fumC</i> FUSION5'	CTCATAATGCCTATGAATTG C	pYL1
<i>fumC</i> NEW5'(<i>Bam</i> HI)	CTAAA GGATCC GAGCAAGA TGATTATCAAGC	NCTC 11168 genome position 1297941-1297960
<i>fumC</i> FUSION3'	GCAATTCATAGGCATTATGA G	NCTC 11168 genome position 1297723-1297743
Primer extension and rapid amplification of cDNA ends (RACE)		
<i>chuA</i> PE+FAM (fluorescein amidite)	[6FAM]GATCTTTGCCTTCTAT GCTGATTACATTGC	NCTC 11168 genome position 1540958-1540987
<i>chuA</i> 3'(<i>Xba</i> I) short	GATT TCTAGA CATTAAATT AGTTATTAGC	NCTC 11168 genome position 1540854-1540873
<i>chuA</i> RT	CCTTGTCCACGCATATC	NCTC 11168 genome position 1541077-1541093
<i>chuA</i> nested	GATCTTTGCCTTCTATGC	NCTC 11168 genome position 1540970-1540987
<i>fumC</i> PE+FAM	[6FAM]CAAGTTTGCCAAGTT TGTTATTGACCAAAG	NCTC 11168 genome position 1297443-1297472
<i>fumC</i> RT	GAACCTGTTTGCCAATC	NCTC 11168 genome position 1297346-1297363
<i>fumC</i> nested	GCCAAGTTTGTTATTGACC	NCTC 11168 genome position 1297450-1287468
<i>waaC</i> PE+FAM	[6FAM]GGGCAGGGCATAGA GTTTGTATTATAAAGG	NCTC 11168 genome position 1066943-1066972
<i>waaC</i> 3'(<i>Xba</i> I)	ATGC TCTAGA TAGAGTTTGT TTATTAAAGG	NCTC 11168 genome position 1066943-1066963
<i>Bam</i> HI + poly(C)	ATGC GGATCC CCCCCCCCCC	Poly(G) tailed cDNA

5'-adapter-specific DNA oligonucleotide B6	GCGCGAATTCCTGTAGA	RNA oligonucleotide A3 (Wagner and Vogel, 2009)
<i>fur</i> mutagenesis		
PxhCATF	TACCTGCAGAACTCGAGTG CTCGGCGGTGTTCC	pAV80
<i>fur3'</i> BamHI	GTTCGGATCCAATCAAGGCT TGCTGTC	pAV80
DNase I footprinting		
<i>chuAR</i> +DIG (digoxygenin)	[DIG]ATGC GAATTC ATTTTGT AGATCTTTGCC	NCTC 11168 genome position 1540978-1540995
<i>chuA3'</i> label	GCTTTATTGATTCTTGTGC	pRR15-22
<i>chuA3'</i> label long	CTATGCTGATTACATTGCG	pRR15-22
<i>fumCR</i> +DIG	[DIG] GAATTC CCTTTGGCAT TTTCTCACAACC	NCTC 11168 genome position 1297512-1297533
<i>fumC3'</i> label	CACCCATGGTATCATGTTC	pRR23-30
<i>fumC3'</i> label long	GGCATTCTCACAACCG	pRR23-30
pMW105' non-label	GGCGCTTCATAGAGTAATTC	pRR15-22, 22-30
Probe amplification for northern blot		
<i>chuA</i> NB F	AGATATGCGTGGACAAGG	NCTC 11168 genome position 1541076-1541093
<i>chuA</i> NB R	CAGGGCGATTGATTTGTG	NCTC 11168 genome position 1541621-1541638
<i>fumC</i> NB F	CGTTGCGGTTGAGCAAGTA GAG	NCTC 11168 genome position 1297168-1297189
<i>fumC</i> NB R	CTTGGGCCTGAAGCTAACCA TC	NCTC 11168 genome position 1296731-1296752
<i>chuZ5'</i>	TTGCATGAGTGCAAAGAG	NCTC 11168 genome position 1540375-1540392
<i>chuZ3'</i>	CCTACATGTGCAACATTTCC	NCTC 11168 genome position 1539898-1539917
<i>racRF</i>	GTGGGTATTCAAGGCTATG	NCTC 11168 genome position 1191905-1191923
<i>racRR</i>	CGACTTACAAGCTGTTCTC	NCTC 11168 genome position 1192302-1192320
RacR and RacS expression and purification		
N-ter <i>racR</i>	TACTTCCAATCCATGATTAAT GTGTTGATGATAGA	NCTC 11168 genome position 1191788-1191810
C-ter <i>racR</i>	TATCCACCTTTACTGTTCATCC TATCAGTTTATATCCT	NCTC 11168 genome position 1192438-1192459
N-ter <i>racS</i>	TACTTCCAATCCATGAGAAG ACAAGTTGCCGAAGT	NCTC 11168 genome position 1192948-1192967
C-ter <i>racS</i>	TATCCACCTTTACTGTTCATTT TTCTTTATCTCCAAAGA	NCTC 11168 genome position 1193669-1193688

<i>aspA</i> gel shift		
<i>aspAF</i>	GTAATTTCTTCCATATTATCC C	81116 genome position 102283-102304
<i>aspAR</i>	GCCAAAGCTCTAACAAAGC G	81116 genome position 102696-102715
<i>fumC</i> mutagenesis and complementation		
<i>fumCF</i>	ATGC GGATCC TCAGCCCAG CTTGGTGTAAC	NCTC 11168 genome position 1298136-1298155
<i>fumCR</i>	ATGC TCTAGA TTTAAGCGAG GTGGGTAATG	NCTC 11168 genome position 1295731-1295750
<i>fumCinvF</i>	ATGC AGATCT ACGCTGCTAA AGTAGCC	pRR51
<i>fumCinvR</i>	ATGC AGATCT TGCCAAGTTT GTTATTGACC	pRR51
<i>fumCC5(KpnI)</i>	CTAAA GGTACC GAGCAAGA TGATTATCAAGC	NCTC 11168 genome position 1297941-1297960
<i>fumCC3(KpnI)</i>	GTTT GGTACC CTAGGCTTTT GGGCCTATC	NCTC 11168 genome position 1296244-1296262
Sequencing and screening		
M13F	GTTGTA AACGACGGCCAG TG	pUC19 based plasmid
M13R	GGAAACAGCTATGACCATGA TTAC	pUC19 based plasmid
SKanR	GGTTATTGTCCTGGGTTTCA AGCATTAG	<i>aphA-3</i> (kanamycin resistance cassette)
STM invKan-F	CTGGGGATCAAGCCTGATTG	<i>aphA-3</i> (kanamycin resistance cassette)
<i>cat3'</i>	ATATCACGCAATTA ACTTGG	<i>cat</i> (chloramphenicol resistance cassette)
<i>catR_KpnI</i>	GG GGTACC GAATTCAGCTG CGCCCTTTAG	<i>cat</i> (chloramphenicol resistance cassette)
<i>catInvF</i>	GGAATGTCCGCAAAGCCTA ATCC	<i>cat</i> (chloramphenicol resistance cassette)
<i>catInvR</i>	GCGGTCCTGAACTCTTCATG TC	<i>cat</i> (chloramphenicol resistance cassette)
<i>furF</i>	GATCGTATTGGTGGCTTTATA TTTGG	NCTC 11168 genome position 364984-365009
<i>furR</i>	CAACAGCATTGACACTTTCA TCTC	NCTC 11168 genome position 365871-365894
<i>furR long</i>	CCTCATCGCTACGTCTTG	NCTC 11168 genome position 366885-366902
Cj81-176 <i>fur5'</i>	GCTACTCCGCAAAGACTATG	81-176 genome position 368349-368368
Cj81-176 <i>Fur3'</i>	CAGATGATTGACGAGATTGC	81-176 genome position

		368659-368678
Cj81-176 <i>fur5'</i> long	GGTTATGGACAAGGTGTGG C	81-176 genome position 367893-367874
Cj81-176 <i>fur3'</i> long	CCCTAAAAGAGTGCAATCA G	81-176 genome position 268800-368819
<i>racR5'</i>	GGACACTAGAATGATTAATG	NCTC 11168 genome position 1191778-1191797
<i>racR3'</i>	CATCCTATCAGTTTATATCC	NCTC 11168 genome position 1192439-1192458
<i>fumC</i> flank F	GTAGTAGAGCAGCCAATTG AAG	NCTC 11168 genome position 1295666-1295687
<i>fumC</i> flank R	GGAACAGAACTTGTTATCTA TC	NCTC 11168 genome position 1298179-1298200
<i>cj0752upF</i>	GGAATAATCAAGCCTACAA AATC	pGEMCWH01, pRR66-67
<i>cj0752downR</i>	GTTTTGCTTGTATATTGTGGA TTGAC	pGEMCWH01, pRR66-67

Table 2.5: Primers used in this study. All primers were designed based on the genetic information obtained from CampyDB website (<http://xbase.bham.ac.uk/campydb/>) or commercial plasmid providers using Clone Manager Professional 9 (Scientific and Educational Software). Primers were purchased from Sigma-Aldrich and were diluted to 100 pmol with either dH₂O or for primers used in RNA analysis, diethyl pyrocarbonate (DEPC, Melford) treated H₂O [0.1% (v/v) DEPC resuspended in H₂O, allowed to evaporate overnight and autoclaved] prior to storage at -20 °C. Restriction sites incorporated into primers are boxed.

2.2.14 PCR product purification

PCR products (as well as other DNA fragments) were purified using the E.Z.N.A.[®] cycle pure kit I (Omega Bio-Tek) in accordance with the manufacturer's instructions. PCR products were routinely eluted into 30 µl of dH₂O. This kit was also used to concentrate DNA samples into smaller volumes.

2.2.15 Automated DNA sequencing

DNA sequence was determined using the BigDye[®] terminator v3.1 cycle sequencing kit (Applied Biosystems) in accordance with the manufacturer's instructions. The

sequencing reaction was terminated with 0.1 volumes of 2.2% (w/v) SDS at 98 °C for 5 minutes and purified using a Performa[®] DTR gel filtration cartridge (EdgeBio) in accordance with the manufacturer's instructions. The sequencing reaction was processed using a 3730 DNA analyser (Applied Biosystems) by the Protein nucleic acid chemistry laboratory (PNAAC, University of Leicester) and analysed using Chromas v1.45 (Technelysium Pty Ltd) and Clone Manager Professional 9.

2.2.16 Restriction of DNA

Restriction enzymes were routinely used to allow insertion of DNA fragments into plasmids during the process of constructing recombinant plasmids (cloning). 500 ng of DNA was digested in a 50 µl reaction at 37 °C for 2 hours and the reaction was purified (terminated) by the E.Z.N.A.[®] cycle pure kit I in accordance with the manufacturer's instructions. Restriction enzymes and cognate digestion buffers (New England Biolabs) were used in accordance with the manufacturer's instructions.

2.2.17 Ligation of DNA

Ligation reactions were carried out to join DNA fragments and linearised plasmids with compatible ends in a reaction consisting of 1 µl of 400 U/µl T4 DNA ligase (New England Biolabs), 10x buffer (New England Biolabs) and 1 µl of 10 mM adenosine 5'-triphosphat disodium salt. A 3:1 molecular ratio of insert to vector DNA was usually used and the total reaction volume was kept to a minimum in order to increase ligation efficiency. The reaction was incubated at 16 °C overnight and was purified by dialysis

(2.2.6).

2.2.18 Standard mutagenesis and complementation

Standard mutagenesis was used to create a *C. jejuni* mutant strain with a specific gene deletion in the genome. A desired gene along with 400 bp flanking DNA on each side of this gene was amplified from the wild-type *C. jejuni* genome using Phusion[®] DNA polymerase and cloned into pUC19. The majority portion of this gene was deleted by inverse PCR (Table 2.4) and replaced with a desired antibiotic resistance gene in the same orientation as the gene. The finishing construct was finally electoporated into a desired *C. jejuni* strain (2.1.7) and the wild-type copy of this gene in the genome was replaced by the mutated copy by recombination. As well as plasmid based mutagenesis, chromosomal DNA of a *C. jejuni* strain carrying a desired mutation was naturally transformed (2.2.2) into another *C. jejuni* wild-type strain and the wild-type copy of the target gene in the recipient strain was replaced by the mutated donor copy by recombination.

Complementation was used to reverse the effect of mutagenesis by inserting a wild-type copy of the gene into the *cj0752* of the mutant genome (Elvers *et al.*, 2005). The mutagenesis principal was applied in complementation except pGEMCWH01 was used instead of pUC19.

2.2.19 Site-directed mutagenesis

Site-directed mutagenesis adapted from the QuickChange[®] site-directed mutagenesis kit (Stratagene) was used to create specific single base mutations. A DNA fragment containing the target base was cloned into a cloning vector (pUC19 or pCR2.1-TOPO) and the construct was then used as the template in a 50 µl inverse PCR (Table 2.4) with Phusion[®] DNA polymerase and a pair of complementary primers containing the desired mutations (Table 2.5). 25 µl of the reaction was digested with *DpnI* (2.2.16) to remove the wild-type methylated template and the intact synthesised DNA containing the desired mutation was electroporated into *E. coli* Top10 (2.1.6). The synthesised DNA was finally circularised in *E. coli* Top10 and the resulting vector was screened by sequencing (2.2.15).

2.2.20 *β*-galactosidase assay

β-galactosidase assay was used to detect specific promoter activities in a pMW10 transcriptional *lacZ* fusion system (Wösten *et al.*, 1998) and the *β*-galactosidase activity was measured by the conversion of 2-nitrophenyl-*β*-D-galactopyranoside (ONPG, Melford) to nitrophenol (Miller, 1972). *C. jejuni* strain 480 harbouring a desired promoter construct was cultured on a MH agar plate with appropriate antibiotics for 2 days and was sub-cultured onto a MH agar plate with appropriate antibiotics and 40 µM FeSO₄ or 20 µM Desferal for 2 more days. The cells were harvested and used to inoculate three 5 ml cultures in MH broth (triplicate samplings) with appropriate antibiotics and 40 µM FeSO₄ or 20 µM Desferal to an OD₆₀₀ of 0.1. The cells were incubated for 5 hours and cooled on ice for 20 minutes prior to centrifugation at 15700

x g for 20 minutes. The cells were resuspended in 1 ml of phosphate buffered saline (PBS, Oxoid, 1 PBS tablet dissolved in 100 ml of dH₂O and autoclaved) and the OD₆₀₀ was measured prior to transfer of 0.05 ml of the cell suspension to a fresh microcentrifuge tube. The cell suspension was mixed with 450 µl of buffer Z [60 mM Na₂HPO₄·2H₂O, 40 mM NaH₂PO₄·2H₂O, 10 mM KCl, 1 mM MgSO₄·7H₂O and 0.39% (v/v) β-mercaptoethanol (Sigma-Aldrich)], 8 µl of 0.1% (w/v) SDS and 15 µl of chloroform and vortexed for 30 seconds. The reaction was incubated at 28 °C for 5 minutes and incubated for a further hour in the presence of 250 µl of 4 mg/ml ONPG prior to termination of the reaction by the addition of 250 µl of 1M Na₂CO₃. The β-galactosidase activity was measured at OD₄₂₀ in an Ultrospec 200 UV/visible spectrophotometer (Pharmacia Biotech) and converted to Miller units using the equation: Miller units = 1000 x OD₄₂₀ / t x v x OD₆₀₀ where t is the 60 minutes incubation time and v is the starting 0.05 ml cell volume.

2.2.21 Polyacrylamide gel electrophoresis (PAGE)

Polyacrylamide gels were used instead of agarose gel to achieve better separation and visualisation of smaller or similar sizes DNA fragments. A Mini-Protean[®] II electrophoresis cell (Bio-Rad) was used to run small gels and all the components were set up in accordance with the manufacturer's instructions. An 8% (v/v) polyacrylamide gel mix was prepared with 4.1 ml of dH₂O, 0.3 ml of 10x tris-boric acid (TB, 0.89 M tris and 0.89 M boric acid, pH 8), 1.6 ml of Ultra Pure ProtoGel[®] [National Diagnostics, 30% (w/v) acrylamide:0.8% (w/v) bis-acrylamide (37.5:1)], 100 µl of 10% (w/v)

ammonium persulphate (APS, Melford) and 5 μl of N,N,N',N'-tetramethylethylene diamine (TMEDA, Sigma-Aldrich). The gel mix was loaded into a gel casting assembly and allowed to set. The gel was pre-run in 0.5x TB at 40 V for 15 minutes and DNA samples were electrophoresed through the gel at 80 V for an appropriate amount of time.

2.2.22 Transfer DNA from polyacrylamide gel onto membrane (Southern blot)

DIG-labelled DNA samples separated by PAGE (2.2.21) were routinely transferred onto a 0.45 micron Magna™ nylon transfer membrane (GE Healthcare). Following PAGE, each component of the Trans-Blot™ cell (Bio-Rad) blotting cassette was soaked in 0.5x TB and the cassette was set up as follows: negative side of the cassette, sponge, 2 pieces of 3 mm Chr chromatography paper (Whatman), the gel, the membrane, 2 pieces of 3 mm paper, sponge and the positive side of the cassette. The gel was blotted in 0.5x TB at 40 V for an hour and fixed onto the membrane in an ultraviolet crosslinker (Amersham Bioscience) at $70 \times 10^3 \mu\text{J}/\text{cm}^2$.

2.2.23 Detection of DNA by anti-DIG-antibodies

DIG-labelled DNA samples were blotted onto a nylon transfer membrane (2.2.22) and were detected by interaction with anti-DIG-antibody. The membrane was rinsed in 20 ml of washing solution [0.3% (v/v) Tween® 20 (Sigma-Aldrich) resuspended in maleic acid buffer (0.1 M maleic acid and 0.15 M NaCl, pH 7.5 and autoclaved)] and blocked in 100 ml of blocking solution [1% (w/v) blocking reagent (Roche) dissolved in maleic

acid buffer and autoclaved] for 30 minutes. The membrane was incubated with 20 ml of antibody solution [0.005% (v/v) anti-DIG-alkaline phosphatase antibody (Roche) resuspended in blocking solution] for 30 minutes and washed twice with 100 ml of washing solution for 15 minutes. The membrane was then incubated with 20 ml of detection solution (0.1 M tris and 0.1 M NaCl, pH 9.5 and autoclaved) for 5 minutes and incubated with 1 ml of disodium 3-(4-methoxy Spiro{1,2-dioxetane-3,2'-(5'-chloro)tricyclo[3.3.1.1^{3,7}]decan}-4-yl) phenyl phosphate (CSPD) working solution [1% (v/v) CSPD resuspended in detection solution] at 37 °C in a hybridisation bag (Roche) for 10 minutes. The membrane was placed into a fresh hybridisation bag and exposed to a Super RX Fuji medical X-ray film (Fujifilm) for an hour prior to developing in a Compact x4 automatic X-ray film processor (Xograph).

2.2.24 Electrophoretic mobility shift assay

EMSA was used to analyse specific protein-DNA interactions (Garner and Revzin, 1986). The desired DNA fragment containing the putative protein interaction site was amplified by PCR (2.2.12) and extracted from agarose gel (2.2.11). 3.85 pmol of DNA was DIG-labelled in a 20 µl reaction in accordance with the DIG gel shift kit, 2nd generation (Roche) instructions and the volume of the reaction was brought up to 25 µl with dH₂O (instead of EDTA) to give a final labelled DNA concentration of 155 fmol/µl. The EMSA reaction was carried out in a total volume of 20 µl which consisted of 1 µl of 1.55 fmol labelled DNA, an appropriate amount of recombinant protein (2.4.1 and 2.4.2), 4 µl of 5x binding buffer (20 mM bis-tris, pH 7.6), 2 µl of 20 mM dithiothreitol

(DTT), 2 μ l of 1 mg/ml bovine serum albumin (BSA), 2 μ l of 1 mM MnSO₄ and 2 μ l of 3 mg/ml UltraPure™ salmon sperm DNA solution (Invitrogen). The reaction was incubated at room temperature for 10 minutes and then mixed with 5 μ l of 5x loading buffer [10x TB and 60% (v/v) glycerol]. The sample was run on a polyacrylamide gel (2.2.21) for 2 hours, blotted onto nylon membrane (2.2.22) and DNA detected by anti-DIG-antibody (2.2.23).

2.2.25 Sequencing PAGE

The Sequi-Gen® GT nucleic acid electrophoresis cell (Bio-Rad) was used to run large sequencing gels and all the components were set up in accordance with the manufacturer's instructions. 60 ml of 6% (v/v) polyacrylamide gel was prepared using Pur1te select (Ondeo) purified H₂O, 30 g of urea, 7.2 ml of Long Ranger® 50% gel solution (Lonza), 3 ml of 20x glycerol tolerant gel (GTG) buffer (USB), 60 μ l of 25% (w/v) APS and 60 μ l of TMEDA. The gel mix was injected into a gel casting assembly, of which one side of the inner glass plate was pre-treated with Gel Slick® solution (Cambrex), and the gel was allowed to set overnight. The gel was pre-run in 1x GTG buffer at 90 W for 30 minutes and DNA samples denatured at 100 °C for 10 minutes were loaded using a shark's tooth comb (Bio-Rad) and then separated on the gel at 50 W until the dye front reached the end of the gel. The gel was then transferred onto 3 mm paper and vacuum dried in a Model 583 gel dryer (Bio-Rad) for 2 hours. The gel was wrapped in Saran™ film (DOW) and exposed to an X-ray film at -80 °C for 2 days.

2.2.26 Manual DNA sequencing

Manual sequencing reaction (Sanger *et al.*, 1977) was used in DNase I footprinting (2.2.27) and primer extension (2.3.6) to generate a DNA reference sequence for comparison. The sequencing primer was 5' labelled with EasyTides[®] ATP γ -³²P (PerkinElmer) and OptiKinase[™] (USB) in accordance with the manufacturer's instructions. The radio-labelled primer was then used to sequence a DNA fragment using the thermo sequenase cycle sequencing kit (USB) in accordance with the manufacturer's instructions. 1.5 μ l of each sequencing sample was denatured at 100 °C for 10 minutes and analysed by sequencing PAGE (2.2.25).

2.2.27 DNase I footprinting assay

DNase I footprinting assay was used to identify the location of protein-DNA interactions (Galas and Schmitz, 1978) and the method used was adapted from Fuangthong and Helmann (2003). DNA template was amplified in a 20 μ l PCR reaction (2.2.12) with 1 μ l of 2 pmol forward primer and 1 μ l of radio-labelled reverse primer. 5 μ l of the PCR product was then used in a 20 μ l reaction containing an appropriated amount of recombinant protein (2.4.1 and 2.4.2), 4 μ l of 5x binding buffer, 2 μ l of 20 mM DTT, 2 μ l of 1 mg/ml BSA, 2 μ l of 1 mM MnSO₄ and 2 μ l of 3 mg/ml UltraPure[™] salmon sperm DNA solution. The reaction was incubated at room temperature for 10 minutes and mixed with 2 μ l of RQ1 RNase-free DNase 10x reaction buffer (Promega) and 10 μ l of CaCl₂/MgCl₂ solution (5 mM CaCl₂ and 10 mM MgCl₂). The reaction was digested with 1 μ l of 0.025 U/ μ l RQ1 RNase-free DNase (Promega) at 37 °C for 80

seconds and terminated with 1 μ l of RQI DNase stop solution (Promega) at 65 °C for 10 minutes. The reaction was ethanol precipitated (2.2.8) and hydrated in 6 μ l of dH₂O and 4 μ l of stop solution (USB). 2.5 μ l of DNase I footprinting sample along with sequencing samples (2.2.26) were denatured at 100 °C for 10 minutes and analysed by sequencing PAGE (2.2.25).

2.3 RNA analysis

2.3.1 Extraction and purification of *C. jejuni* total RNA

For RNA analysis, screw cap tubes, Biosphere[®] filter tips (Sarstedt) and solutions made from DEPC H₂O were used to avoid RNase contamination. *C. jejuni* strains were cultured on MH agar plates with appropriate selection for 2 days and were sub-cultured onto MH agar plates with selection for 2 more days. The cells were harvested and used to inoculate 50 ml of MH broth in a cell culture flask with appropriate antibiotics to an OD₆₀₀ of 0.1. The culture was incubated overnight and harvested. The cells were then used to inoculate 50 ml of MH broth in a cell culture flask with appropriate selection and 40 μ M FeSO₄ or 20 μ M Desferal to an OD₆₀₀ of 0.1 and incubated for 10 hours. The cells were harvested and resuspended in 1 ml of RNAlater[®] tissue collection: RNA stabilisation solution (Applied Biosystems). *C. jejuni* total RNA was extracted and purified using the total RNA purification kit (Norgen Biotek Corporation) in accordance with the manufacturer's instructions. DNA contamination was removed using the TURBO DNA-free[™] kit (Applied Biosystems) in accordance with the manufacturer's instructions and RNA samples were stored at -80 °C.

2.3.2 Formaldehyde agarose gel electrophoresis

For RNA virtualisation, formaldehyde agarose gels adapted from the protocol in the RNeasy[®] mini kit (Qiagen) handbook were used. 1.8 g of agarose was first heat dissolved in 130.5 ml of DEPC H₂O and mixed with 3 µl of 10 mg/ml ethidium bromide, 4.5 ml of 37% formaldehyde solution (Sigma-Aldrich) and 15 ml of 10x 3-(N-morpholino) propanesulfonic acid (MOPS, 0.2 M MOPS pH 7, 50 mM sodium acetate and 1 mM EDTA) in a 50 ml centrifuge tube (Corning) prior to pouring into an ethanol cleaned casting tray. Each RNA sample was mixed with 5x RNA loading buffer [0.16% (v/v) saturated aqueous bromophenol blue solution, 4 mM EDTA pH 8, 2.7 % (v/v) formaldehyde, 20% (v/v) glycerol, 30.8 % (v/v) deionised formamide and 4x formaldehyde agarose gel buffer (80 mM MOPS, 12.5 mM sodium acetate and 2.5 mM EDTA, pH 7)] and the mixture as well as 10 µl of RNA size markers [40% (v/v) RNA markers 0.5-9 kbp (Lonza) and 40% (v/v) 5x RNA loading buffer] were denatured at 65 °C for 10 minutes. The sample and markers were cooled on ice for 5 minutes and loaded onto the gel prior to run at 120 V in 1x MOPS for an appropriate amount of time.

2.3.3 Transfer RNA from agarose gel onto membrane (northern blot)

RNA samples separated in a formaldehyde agarose gel (2.3.2) were routinely transferred onto a nylon transfer membrane by capillary action created in a saline sodium citrate (SSC) solution gradient. Following formaldehyde agarose gel electrophoresis, the blotting assembly was set up as follows: a 3 mm paper wick soaked in 20x SSC (3 M

NaCl and 300 mM tri-sodium citrate, pH 7) and rested in a tray filled with 20x SSC, the gel, the membrane soaked in 2x SSC, 2 pieces of 3 mm paper soaked in 2x SSC, stack of paper towels and a weight. The gel was blotted overnight and fixed onto the membrane at $70 \times 10^3 \mu\text{J}/\text{cm}^2$.

2.3.4 RNA detection by RNA-DNA hybridisation

RNA samples blotted onto a nylon transfer membrane (2.3.3) were detected by RNA hybridisation with radio-labelled DNA. A membrane containing fixed RNA samples was first prehybridised for 3 hours in a hybridisation oven (Hybaid) at 65 °C in a hybridisation bottle (Hybaid) one third filled with Church Gilberts buffer [0.5 M $\text{Na}_2\text{HPO}_4/\text{NaH}_2\text{PO}_4$ pH 7.4, 1 mM EDTA and 7% (w/v) SDS]. 30 ng of DNA fragment complementary to the target RNA (DNA probe) was denatured at 100 °C for 5 minutes and labelled in a 27.5 μl reaction with 5 μl of 5x oligolabelling buffer [250 mM tris pH 8, 25 mM MgCl_2 , 5 mM β -mercaptoethanol, 2 mM dATP, 2 mM dTTP, 2 mM dGTP, 1 M 4-(2-hydroxyethyl)-1-piperazineethanesulfonic acid pH 6.6 and 1 mg/ml hexadeoxyribo nucleotides], 1 μl of 10 mg/ml BSA, 1 μl of 5 U/ μl DNA polymerase I large (Klenow) fragment (New England Biolabs) and 2.5 μl of 10 μCi of EasyTides[®] CTP α -³²P (PerkinElmer) at 37 °C for 2 hours. The labeled probe was purified with an illustra NICK[™] column in accordance with the manufacturer's instructions and denatured at 100 °C for 10 minutes. The labelled probe was then cooled on ice for 10 minutes and allowed to hybridise with the membrane at 65 °C overnight. The membrane was rinsed with washing solution [2x SSC and 0.1% (w/v) SDS] and washed three times

for 30 minutes and once for an hour with washing solution. The membrane was wrapped in Saran[™] film and exposed to an X-ray film at -80 °C for an appropriate amount of time. Radio-labelled probe was finally stripped away from the membrane with multiple 15-minute 0.1% (w/v) SDS washes at 65 °C in a hybridisation oven/shaker S1 2OH (Stuart Scientific) and the membrane was then re-probed with a radio-labelled control probe. All probes used in this study were approximately 400 bp PCR products amplified from the middle section of desired genes using gene-specific primers (Table 2.5).

2.3.5 Complementary DNA (cDNA) synthesis by reverse transcriptase (RT)

cDNA template was synthesised from total *C. jejuni* RNA by RT and used in primer extension (2.3.6) and RACE (2.3.7). 6 µg of total RNA was adjusted to a volume of 10 µl with DEPC H₂O and denatured at 65 °C for 5 minutes prior to cooling on ice. 4 µl of 5x cDNA synthesis buffer (Invitrogen), 2 µl of 10 mM dNTPs, 1 µl of 0.1 M DTT, 0.5 µl of 20 U/µl RNasin[®] ribonuclease inhibitor (Promega), 1 µl of 15 U/µl ThermoScript[™] RT (Invitrogen), 1 µl of 2 pmol gene specific primer and 0.5 µl of DEPC H₂O were added to the RNA sample and the reaction was incubated (in a thermal cycler) at 65 °C for 5 minutes followed by 20 minutes each of incubation at 55 °C, 60 °C and 65 °C, ending with a 5-minute denaturation at 85 °C. Total RNA template was removed from the cDNA product with 1 µl of 5 U/µl RNase H (New England Biolabs) at 37 °C for 20 minutes.

2.3.6 *Primer extension*

Primer extension was carried out to identify the transcriptional start site (+1 site) of *C. jejuni* genes and the method was adopted from Lloyd *et al.* (2005). cDNA template was synthesised (2.3.5) using 1 µl of 2 pmol FAM-labelled primer and ethanol precipitated (2.2.8). The FAM-labelled cDNA pellet was resuspended in 9.5 µl of deionised formamide (Amresco) and 0.5 µl of Gene Scan™ 500 LIZ™ size standard (Applied Biosystems). The sample was processed using a DNA analyser by PNACL and the exact length of the FAM-labelled cDNA was determined using Peak Scanner™ software v0.1 (Applied Biosystems). The +1 site was deduced using the exact cDNA length and the position where the FAM-labelled primer binds.

Alternatively, 1.5 µl of radio-labelled primer was used to synthesise radio-labelled cDNA (2.3.5) and DNA sequencing samples (2.2.26) and the +1 site was deduced following cDNA and sequencing samples separation by sequencing PAGE (2.2.25).

2.3.7 *RACE*

RACE was also performed to identify the +1 site of *C. jejuni* gene. The method described by Gerhart *et al.* (2009) was used and this method was originally adapted from Bensing *et al.* (1996). 6 µg of total RNA was adjusted to 43.75 µl with DEPC H₂O and mixed with 5 µl of 10x tobacco acid pyrophosphatase (TAP) digestion buffer (Epicentre Biotechnologies), 0.25 µl of 20 U/µl ribonuclease inhibitor and 1 µl of 10 U/µl TAP (Epicentre Biotechnologies) prior to incubation at 37 °C for 30 minutes. The

reaction was then mixed with 1 μl of 500 pmol RNA oligonucleotide A3 (5'AUAUGCGCGAAUCCUGUAGAACGAACACUAGAAGAAA) and 100 μl of DEPC H₂O and purified by phenol/chloroform extraction (2.2.9) prior to resuspension in 14 μl of DEPC H₂O. The sample was denatured at 90 °C for 5 minutes and allowed to cool on ice for 5 minutes. 2 μl of 10x RNA ligation buffer (New England Biolabs), 2 μl of dimethyl sulfoxide, 1.8 μl of 20 U/ μl T4 RNA ligase 1 (New England Biolabs) and 0.2 μl of 20 U/ μl ribonuclease inhibitor were mixed with the sample and the ligation reaction was incubated at 16 °C overnight. 1 μl of 2 pmol gene specific primer was added to the ligation reaction and the volume was adjusted to 150 μl with DEPC H₂O. The sample was purified by phenol/chloroform extraction and resuspended in 20 μl of DEPC H₂O. 10 μl of the RNA sample was then used in a RT reaction (2.3.5) to generate cDNA template (N.B. gene specific primer was added to each RNA sample before phenol/chloroform extraction rather than in the RT reaction). 2 μl of cDNA was used as the template in a PCR reaction with 25 μl of HotStarTaq master mix (Qiagen), 1 μl of 25 pmol 5'-adapter-specific DNA oligonucleotide B6, 1 μl of 25 pmol gene specific nested primer and 21 μl of dH₂O. The PCR reaction was performed with an initial denaturation cycle of 95 °C of 15 minutes, followed by 30 cycles of 40 seconds denaturation at 95 °C, annealing at 58 °C and extension at 72°C and ended with a 10 minutes final extension at 72 °C. The PCR products were analysed by agarose gel electrophoresis (2.2.10) and the desired product was purified from the gel (2.2.11) and eluted in 25 μl of dH₂O. The product was finally TA cloned into pGEM[®]-T Easy and the +1 site was deduced by sequence analysis (2.2.15).

Alternatively, 13 μ l of purified cDNA (2.3.5) was used in a G tailing reaction with 2 μ l of 10 mM dGTP, 5 μ l of 5x terminal transferase buffer (Roche) and 4 μ l of 25 mM CoCl₂ (Roche). The reaction was denatured at 94 °C for 3 minutes and incubated at 37 °C for 30 minutes with the addition of 1 μ l of 40 U/ μ l terminal transferase (Roche). The reaction was terminated at 70 °C for 10 minutes and purified (2.2.14). PolyG-tailed cDNA was then used in a PCR reaction (see above paragraph) with polyG-tail specific primer and gene specific nested primer. The product was finally cloned into pUC19 and the +1 site was deduced by sequence analysis (2.2.15).

2.4 Protein analysis

2.4.1 Expression and purification of recombinant Fur_{Cj}

pASK-IBA7 (IBA) harbouring NCTC 11168 *fur_{Cj}* (pJMCK1) had been previously constructed (Holmes *et al.* 2005), which allowed the expression and purification of N-terminal Strep-tagged Fur_{Cj} induced by anhydrotetracycline (AHT). 200 ml of LB broth supplemented with Amp was inoculated with 2 ml of overnight liquid DH5 α TM culture carrying pJMCK1 and incubated at 37 °C with shaking until the OD₆₀₀ reached 0.5. The culture was induced with 20 μ l of 2 mg/ml AHT (dissolved in DMF) and incubated for 3 more hours at 37 °C. The cells were harvested at 3220 x g at 4 °C for 15 minutes and resuspended in 2 ml of buffer W (100 mM tris pH 8 and 150 mM NaCl) and 10 μ l of 100 mg/ml lysozyme prior to incubation at 37 °C for 2 hours. One complete mini EDTA-free protease inhibitor cocktail tablet (Roche) was added to the cell

suspension and the cells were lysed at 4 °C by 10 rounds of 30 seconds sonication in a MSE sonicator (MSE Scientific Instruments) set at 6 amplitude microns and low power. Cell debris was removed by centrifugation at 3220 x g at 4 °C for 20 minutes and the protein suspension was passed through a syringe to remove any remaining cell debris. The Fur_{Cj} protein was purified using a 5 ml gravity flow Strep-Tactin® Sepharose® column (IBA) in accordance with the manufacturer's instructions with the exception that EDTA was not included in buffer E (100 mM tris pH 8, 150 mM NaCl and 2.5 mM desthiobiotin) and buffer R (1 mM hydroxyl-azophenyl-benzoic acid resuspended in buffer W).

2.4.2 Expression and purification of recombinant *C. jejuni* RacR and RacS-HK

NCTC 11168 *racR* and *racR*-HK which only encodes the histidine kinase domain of RacS predicted by Prosite <http://www.expasy.ch/prosite> (ExpASy proteomics server, Swiss Institute of Bioinformatics) were cloned into pLEICES-01 (pRR46 and pRR53 respectively) to enable the expression and purification of N-terminal His₆-tagged RacR and RacS-HK induced by IPTG. 200 ml of LB broth supplemented with Amp and Cm was inoculated with 2 ml of overnight liquid *E. coli* Rosetta culture carrying either pRR46 or pRR53 and incubated at 37 °C with shaking until an OD₆₀₀ of 0.5 was reached. The culture was induced with 0.8 mM IPTG and incubated for 3 more hours at 37 °C. The cells were harvested at 3220 x g at 4 °C for 15 minutes and resuspended in 10 ml of binding buffer (50 mM tris, 500 mM NaCl and 80 mM imidazole, pH 7.4). One protease inhibitor tablet was added to the cell suspension and the cells were lysed by sonication

(2.4.1). RacR and RacS-HK proteins were both purified using 5 ml His Trap™ FF crude (GE Healthcare) columns in accordance with the manufacturer's instructions with the exception that tris was used instead of sodium phosphate in the binding buffer and the elution buffer (50 mM tris, 500 mM NaCl and 500 mM imidazole, pH 7.4).

2.4.3 Protein buffer exchange

RacR and RacS-HK were buffer exchanged to buffer B [(van Mourik *et al.*, 2009), 50 mM tris pH 7.6, 200 mM KCl, 10 mM MgCl₂, 0.1 mM EDTA, 1 mM DTT and 10% (v/v) glycerol] using Zeba™ desalt spin columns (Thermo Scientific) in accordance with the manufacturer's instructions.

2.4.4 Protein concentration

Fur_{Cj} was concentrated using a 10 K Microcon® centrifugal filters (Millipore) in accordance with the manufacturer's instructions and protein aliquots were stored at -20 °C. RacR and RacS-HK were concentrated using 10 K Amicon® Ultra-15 centrifugal filters (Millipore) in accordance with the manufacturer's instructions and stored at 4 °C.

2.4.5 SDS-PAGE

SDS-PAGE carried out in a Mini-Protean® II electrophoresis cell was used to separate protein samples and all the components were set up in accordance with the manufacturer's instructions. A 12% (v/v) resolving gel mix was prepared with 3.35 ml of dH₂O, 2.5 ml of resolving gel buffer (1.5 M tris pH 8.8), 0.1 ml of 10% (v/v) SDS, 4

ml of Ultra Pure ProtoGel[®], 50 µl of 10% (w/v) APS and 5 µl of TMEDA. The gel mix was loaded into a gel casting assembly and overlaid with 1 ml of iso-butanol. When the gel was set, the iso-butanol was washed away and the resolving gel layer was overlaid with a 4% (v/v) stacking gel mix consisting of 2.38 ml of dH₂O, 1 ml of stacking gel buffer (0.5 M tris pH 6.8), 0.62 ml of Ultra Pure ProtoGel[®], 40 µl of 10% (w/v) APS and 4 µl of TMEDA. Protein samples were mixed with an equal amount of 2x SDS-PAGE sample buffer [0.15 M tris pH 6.8, 1.2% (w/v) SDS, 30% (v/v) glycerol, 15% (v/v) β-mercaptoethanol and 0.0018% (w/v) bromophenol blue] and denatured at 100 °C for 10 minutes. Once the gel was set, protein samples and 5 µl of PageRuler[™] prestained protein ladder (Fermentas) were loaded and run at 70 V in the stacking gel layer and at 110V in the resolving gel layer in 1x SDS-PAGE running buffer [1% (w/v) SDS, 25 mM tris and 192 mM glycine] until the dye front reached the end of the gel.

2.4.6 SDS-PAGE gel visualisation and drying

For protein visualisation, SDS-PAGE gel containing protein samples (2.4.5) were stained overnight in coomassie blue staining solution [45% (v/v) methanol, 10% (v/v) acetic acid and 0.25% (w/v) coomassie brilliant blue R-250 (Thermo Scientific)] and destained with 4 rounds of 30-minute washes with coomassie blue destaining solution [45% (v/v) methanol and 10% (v/v) acetic acid]. For long term storage, destained gels were washed with water for 30 minutes and incubated with gel drying buffer [10% (v/v) glycerol and 20% (v/v) ethanol] for 30 minutes. The gel was then sealed in between two sheets of DryEase mini cellophane (Invitrogen) and allowed to air dry for 2 days.

2.4.7 Transfer protein from SDS-PAGE gel onto membrane (western blot)

Protein samples separated by SDS-PAGE (2.4.5) were routinely transferred onto Hybond™-C extra supported nitrocellulose membrane (Amersham Biosciences) to allow further protein detection. Following SDS-PAGE, each component of the OmniPAGE mini electroblotter (Geneflow) blotting cassette was soaked in ice-cold transfer buffer [0.037% (w/v) SDS, 47.9 mM tris and 38.6 mM glycine] and the cassette was set up in the following order: negative side of the cassette, sponge, 3 pieces of 3 mm paper, the gel, the membrane, 3 pieces of 3 mm paper, sponge and the positive side of the cassette. The gel was blotted in ice-cold transfer buffer at 150 mA for an hour.

2.4.8 Detection of protein by anti-His-antibody

His₆-tagged protein samples blotted onto nitrocellulose membrane (2.4.7) were detected by anti-His-antibody. The membrane was rinsed in PBST [0.5% (v/v) Tween® 20 resuspended in PBS] and blocked in 50 ml of blocking solution [7% (w/v) skimmed milk powder (Oxoid)] for an hour. The membrane was incubated with 20 ml of antibody solution [0.005% (v/v) anti-polyHis-peroxidase antibody (Sigma- Aldrich) resuspended in blocking solution] for an hour and washed with three times for 5 minutes, twice for 15 minutes and finally three times for 5 minutes with 20 ml of PBST. The membrane was then incubated with 4 ml of equilibrated (5 minutes at room temperature) detection solution [50% (v/v) EZ-ECL solution A and 50% (v/v) EZ-ECL solution B (Biological

industries)] for 2 minutes and wrapped in Saran™ film prior to exposure to X-ray film for 30 seconds.

2.4.9 Protein identification

Protein samples from a destained SDS-PAGE gel (2.4.6) were identified by peptide mass fingerprinting and the entire identification process was conducted by PNACL. In brief, the protein sample was excised from the gel and digested with trypsin. The sample was then analysed by MALDI-ToF mass spectrometry using a 4000 Q TRAP® LC/MS/MS system (Applied Biosystems) and the MASCOT peptide mass fingerprint searching tool http://www.matrixscience.com/cgi/search_form.pl?FORMVER=2&SEARCH=PMF (Mascot search, Matrix Science) was used to determine the protein identity.

2.4.10 Protein quantification

The concentration of purified recombinant protein was estimated by Bradford assay (Bradford, 1976). A series of BSA protein standards and recombinant protein dilutions were prepared in 100 µl volumes in 0.15 M NaCl. The protein mixtures were mixed with 900 µl of Bradford reagent (Sigma-Aldrich) and their OD₅₉₅ was measured. The absorbance value of each standard was plotted against protein concentration to construct a standard curve from which the concentration of recombinant protein was determined.

2.4.11 Phosphorylation assay

Phosphorylation assay was used to detect the autophosphorylation of RacS-HK and the phosphate transfer from RacS-HK to RacR (van Mourik *et al.*, 2009). 30 μl of RacS-HK was mixed with 1 μl of 10 μCi ATP γ - ^{32}P and incubated at room temperature for 15 minutes. 2 μl of the RacS-HK mixture was transferred into a screw cap tube containing 3 μl of dH_2O and 5 μl of 2x SDS-PAGE sample buffer and incubated on ice to inactive the reaction. 18 μl of RacR was then added to the RacS-HK mixture and 5 μl of the RacS-HK/RacR mixture was transferred into a screw cap tube containing 5 μl of 2x SDS-PAGE sample buffer after 15 seconds, 30 seconds, 1 minute, 2 minutes, 4 minutes, 8 minutes and 16 minutes. All the samples were denatured at 100 $^{\circ}\text{C}$ for 10 minutes and analysed by SDS-PAGE (2.4.5). The gel was then transferred onto 3 mm paper and vacuum dried for 30 minutes prior to wrapping in SaranTM film and exposed to X-ray film at -80 $^{\circ}\text{C}$ for a day.

2.4.12 Fumarase activity assay

The fumarase activity assay was used to detect the level of translation of *C. jejuni fumC* mRNA in wild-type and mutant backgrounds under different iron conditions. Fumarase activity was measured by the conversion of L-malate to fumarate (Kanmarke and Hill, 1964) and whole cell extract was used instead of the pure protein (Hassett *et al.*, 1997). *C. jejuni* cells cultured under different iron conditions (2.3.1) were harvested and resuspended in 5 ml of 50 mM sodium phosphate pH 7.3 (0.5 M Na_2HPO_4 and 0.5 M $\text{Na}_2\text{H}_2\text{PO}_4$, pH 7.3). Whole cell extracts were obtained by sonication (2.4.1) and diluted to an OD_{280} of 0.5 with 50 mM sodium phosphate pH 7.3. 200 μl of each cell extract

was mixed with 800 μ l of malate solution (50 mM L-malate and 50 mM sodium phosphate, pH 7.3) and the change of OD₂₈₀ was measured every 10 seconds at 25 °C for a minute. The fumarase activity (U/mg) was calculated by the equation: Specific activity = units of activity per ml x 0.51 / OD₂₈₀. 0.51 is the extinction coefficient for crystalline fumarase at OD₂₈₀ and units of activity per ml is defined as the initial rate of change in OD per 10 seconds at 25 °C times a thousand (Kanarke and Hill, 1964).

2.5 Bioinformatics

Based on the Fur_{Cj} box consensus sequence proposed by Palyada *et al.* (2004), the *chuA* and *fumC* Fur_{Cj} box sequences were predicted using the CampyDB pattern search tool <http://campy.bham.ac.uk/pattern/index.cgi?help=pattern&frame=> (xBASE, N.B. this site is no longer available). The criteria used for this prediction were set as the following: genome to search: *C jejuni* NCTC 11168; pattern: [at][ta][ta][tag]tga[ta]a[at][tag][ta][ag][atg]ta[ta][tca]a (square brackets indicate base redundancy, i.e. [at] means a or t); restricted to regions within: 200 bp upstream of a gene start; report matches within intergenic regions only and allow up to 3 mismatched bases.

The sequence of *H. pylori* 26695 *fumC* was obtained from NCBI website (<http://www.ncbi.nlm.nih.gov>) and was compared with the sequence of *C. jejuni* NCTC 11168 *fumC* using ALIGN Query <http://xylian.igh.cnrs.fr/bin/align-guess.cgi> (Genestream Search).

Other bioinformatics software and searching tools used were CampyDB website (Table 2.5), Clone Manager Professional 9 (Table 2.5), Chromas v1.45 (2.2.15), Peak Scanner[™] software v0.1 (2.3.6), Prosite (2.4.2) and Mascot (2.4.9).

Chapter 3: Site-directed mutagenesis of the *chuA* and *fumC* Fur boxes

3.1 Introduction

In order to characterise the sequence specificity of binding to the Fur_{Cj} box by Fur_{Cj} and to verify the proposed Fur_{Cj} box sequence, candidate Fur_{Cj} box sequences from two differently Fur_{Cj}-regulated promoters were required for subsequent comparative mutational analyses in conjunction with an EMSA based experimental design.

With a 100-fold increase in the level of transcription under iron-limiting conditions in a wild-type background and a non-iron-responsiveness in a *furCj* mutant background, the *C. jejuni* NCTC 11168 haem OM receptor gene *chuA* has been extensively characterised as an example of a classically iron- and Fur-repressed genes (van Vliet *et al.*, 1998; Palyada *et al.*, 2004; Holmes *et al.*, 2005; Ridley *et al.*, 2006). A computational searching of the *chuA* promoter region for the consensus Fur_{Cj} box sequence proposed by Palyada *et al.* (2004) revealed a perfect matched sequence (Table 3.1) and the *chuA* promoter region containing this Fur_{Cj} box sequence has been shown by EMSA to bind Fur_{Cj} with a high affinity (Li, 2005; Ridley *et al.*, 2006). Based on these previous observations, the *chuA* Fur_{Cj} box was therefore chosen as the first candidate sequence for this study.

Detailed transcriptomic and proteomic analysis of the Fur_{Cj} regulon have revealed many genes that are positively regulated by Fur_{Cj} and iron (Palyada *et al.*, 2004; Holmes *et al.*, 2005). The *C. jejuni* fumarate hydratase gene *fumC* (see chapter 4 for a more detailed

description) is such an example in that its transcription decreased 2.4-fold under iron-limited conditions in a wild-type background and in a *fur_{Cj}* mutant background (Holmes *et al.*, 2005). A computational analysis of the *fumC* promoter region revealed a Fur_{Cj} box-like sequence that contains three mismatches at the 10th, 13th, and 19th base positions when compared with the putative Fur_{Cj} box sequence (and the *chuA* Fur_{Cj} box, Table 3.1) and direct Fur_{Cj} binding in this region was not detected (Li, 2005) indicating the iron-responsive regulation of *fumC* is indirectly mediated by Fur_{Cj}. The variation between the *fumC* Fur_{Cj} box-like sequence (referring to as the *fumC* Fur_{Cj} box from this point onward) sequence and the *chuA* Fur_{Cj} box at these positions is likely to be a key determinant for the previous observed contrasting iron regulation and Fur_{Cj}-Fur_{Cj} box binding affinity between *chuA* and *fumC* and the *fumC* Fur_{Cj} box was therefore chosen as a reverse control of the *chuA* Fur_{Cj} box.

3.2 Aims

Previous experimental and computational evidence strongly demonstrated that *C. jejuni* NCTC 11168 *chuA* and *fumC* are differently Fur_{Cj}-regulated and their Fur_{Cj} box sequences varied only at the 10th, 13th and 19th positions with respect to the consensus Fur_{Cj} box sequence. It was hypothesised that by making *chuA* Fur_{Cj} box *fumC*-like and vice versa at these three base positions (Table 3.2), both mutated promoters would exhibit altered iron- and Fur_{Cj}-regulation and affinity to Fur_{Cj} binding similar to their opposite wild-type counterparts thus illustrating the importance of these three bases (positions) of the consensus Fur_{Cj} box sequence in Fur_{Cj}-DNA interaction and

base position	wt Fur _{Cj} box		mutated <i>chuA</i> and <i>fumC</i> Fur _{Cj} boxes						
	<i>chuA</i>	<i>fumC</i>	10	13	19	10/13	10/19	13/19	10/13/19
10 th	T	G	T↔G			T↔G	T↔G		T↔G
13 th	A	T		A↔T		A↔T		A↔T	A↔T
19 th	A	T			A↔T		A↔T	A↔T	A↔T

Table 3.2: Illustration of the mutational change at the 10th, 13th and 19th positions of the *chuA* and *fumC* putative Fur_{Cj} boxes. Mutants were named based on the position/s of mutational change/s. ↔ indicates base change at a particular position, i.e. for *chuA* 10/19 mutant, T and A at 10th and 19th positions of the *chuA* wild-type (wt) Fur_{Cj} box were changed to G and T respectively and vice versa for the *fumC* 10/19 mutant.

Fur_{Cj}-responsive gene regulation. By using site directed mutagenesis at the 10th, 13th and 19th positions of the *chuA* and *fumC* Fur_{Cj} boxes, we were initially aiming to determine how *chuA* and *fumC* are differentially regulated by Fur_{Cj} in terms of Fur_{Cj} box sequence variation by assessing the changes in the affinity of Fur_{Cj} binding to the mutated Fur_{Cj} boxes by EMSA; analysing the changes in promoter activity of mutated *chuA* and *fumC* promoters using *lacZ* reporter gene assay in a wild type or a *furCj* mutant background; and determining the changes in the location of Fur_{Cj}-Fur_{Cj} box interaction by DNase I footprinting method (outlined in Figure 3.1).

3.3 results

3.3.1 Site-directed mutagenesis

In order to verify the proposed theory of Fur_{Cj} box sequence variation-mediated differential Fur_{Cj} regulations between *chuA* and *fumC*, the 10th, 13th and 19th positions of each Fur_{Cj} box were mutated by site-directed mutagenesis (2.2.19). The mutation scheme was designed to swap the wild-type consensus matched bases at the 10th, 13th and 19th positions of the *chuA* Fur_{Cj} box with the wild-type mismatches in the *fumC* Fur_{Cj} box and vice versa. In other words, it was designed to make *chuA* Fur_{Cj} box *fumC*-like and *fumC* Fur_{Cj} box *chuA*-like at these three base positions (Table 3.2).

An inverse PCR-based mutagenesis approach exploiting the different methylation status between the wild-type PCR template and mutated products was applied in this study (Zheng *et al.*, 2004). A 274 bp fragment containing part of the *chuZ-chuA* intergenic

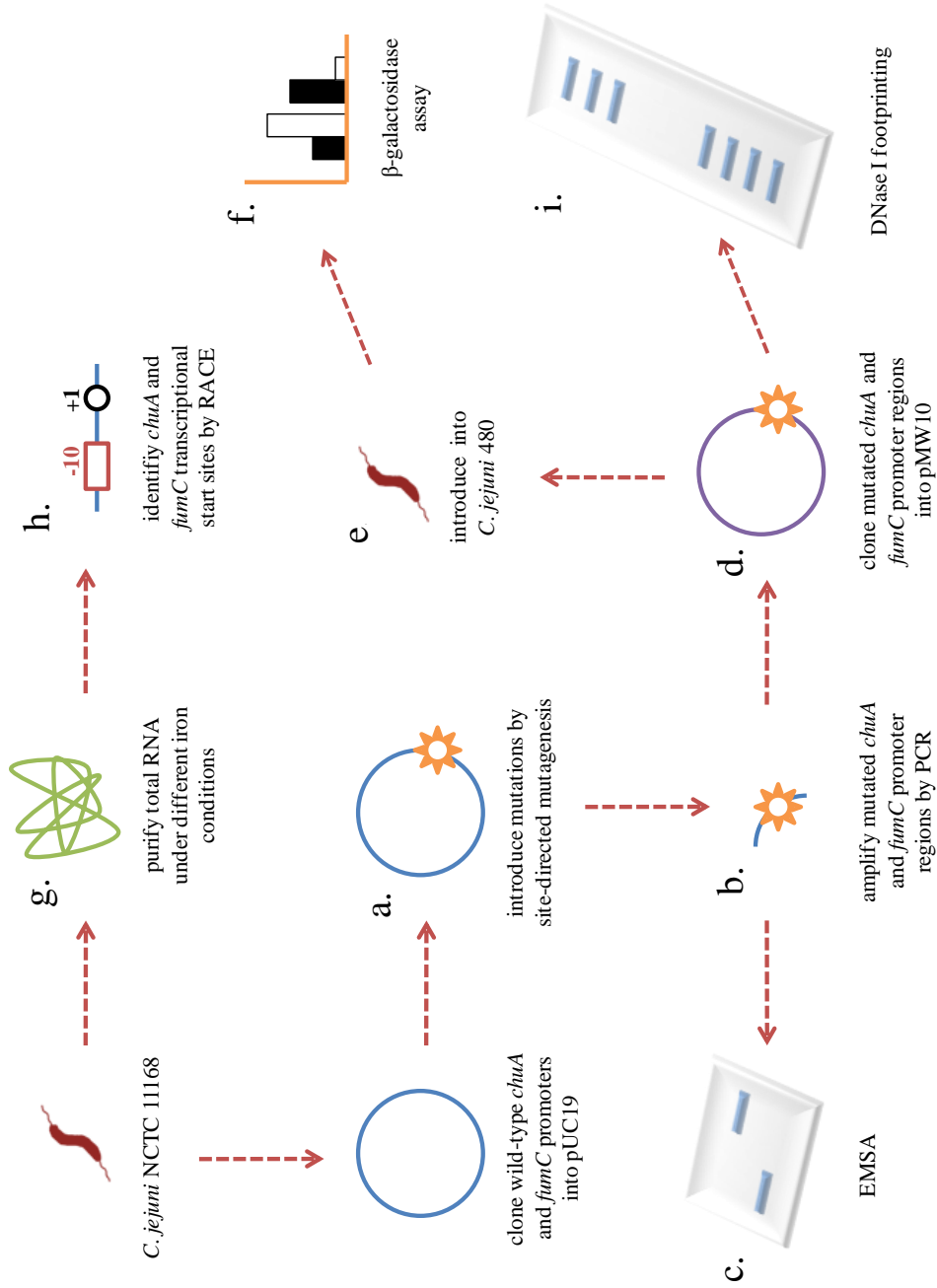


Figure 3.1: A brief outline of the stages carried out in the characterisation of the putative Fur_{Cj}-binding site using *chuA* and *fumC* Fur_{Cj} boxes as models. The actual order of each stage carried out is alphabetically listed in the figure.

region and part of the *chuA* gene and a 233 bp fragment containing the *cj365c-fumC* intergenic region and parts of the *cj1365c* and *fumC* genes (Figure 3.2) were previously cloned into pUC19 and pCR 2.1-TOPO respectively to form pJMCK6 and pYL1 (Li, 2005) and were used as templates for the inverse PCR. 5' overlapping complementary inverse primers harbouring desired mutation(s) were used in a standard inverse PCR fashion with proof reading Phusion DNA polymerase to ensure high fidelity and the nicked circular products containing mutational change(s) were selected by the removal of methylated template using *DpnI*. Once introduced into *E. coli* Top10 strain by electroporation, the nicks on the mutated recombinant plasmids are repaired and the putative mutants were verified by sequencing. 14 mutated recombinant plasmids named pRR1-14 were successfully obtained and each construct is essentially a pJMCK6 or pYL1 variant containing mutational change(s) in the cloned *chuA* or *fumC* Fur_{Cj} boxes respectively. The combination of mutational change(s) for each Fur_{Cj} box are listed in Table 3.3 and with sufficient *DpnI* digestion, this inverse PCR-based site-directed mutagenesis method was shown in this study as a simple and efficient tool to create mutational changes in the AT rich *C. jejuni* promoter regions.

3.3.2 Purification of the recombinant Fur_{Cj} protein

The *fur_{Cj}* gene was previously cloned into the pASK-IBA7 expression vector (pJMCK1) and the Strep-tagged recombinant Fur_{Cj} was expressed in *E. coli* XL1-Blue host cells and purified by affinity chromatography (2.4.1, Holmes *et al.*, 2005). Two bands of 17.5 kDa and 18.6 kDa in size were typically observed for the Fur_{Cj} protein when analysed

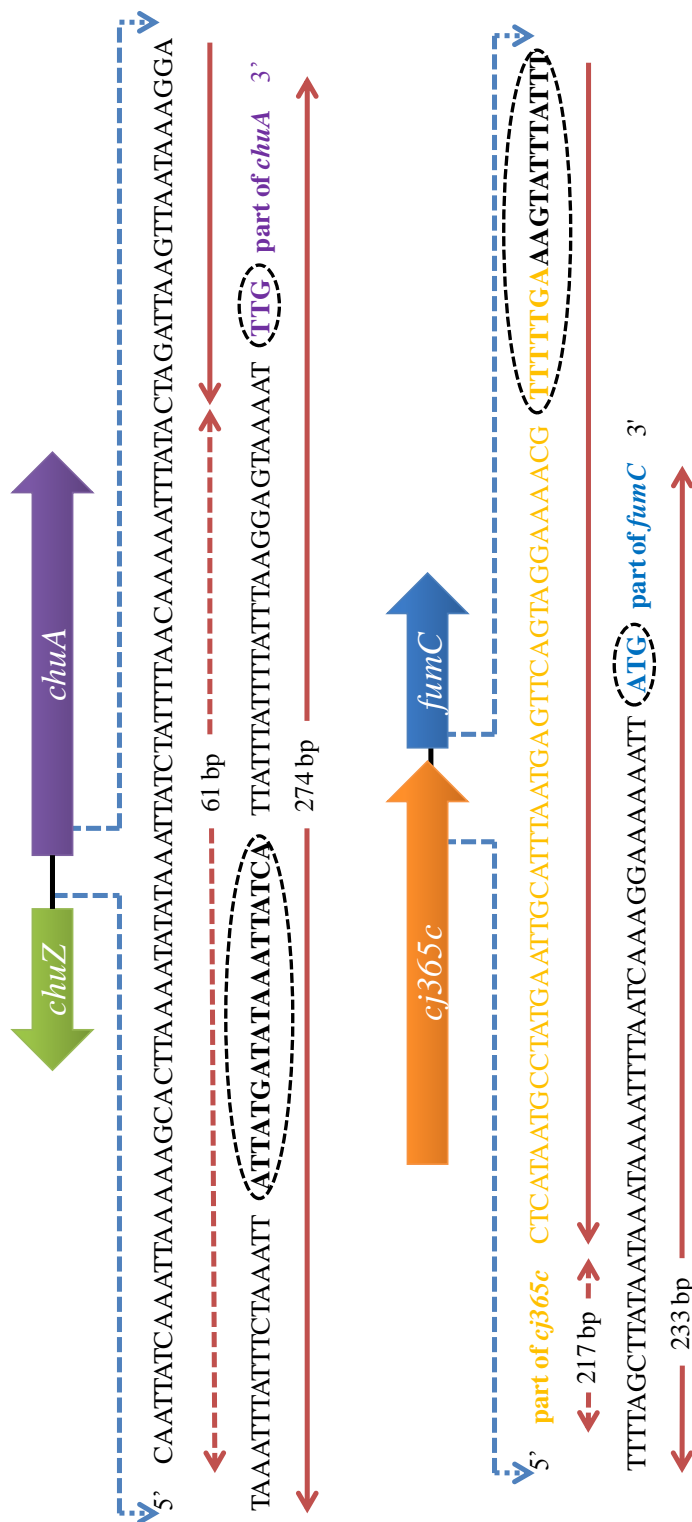


Figure 3.2: The *C. jejuni* NCTC 11168 *chuA* and *fumC* promoter regions under investigation. *chuA* is co-transcribed with *chuBCD* (not shown) as a operon in the opposite direction downstream from *chuZ* whereas *fumC* is located upstream from *cj365c* which encodes a secreted serine protease. For easy visualisation, *fumC* and *cj365c* are drawn in the opposite orientation to their natural genomic positions. The putative Fur_{Cj} box and the start codon for each gene are circled and DNA sequences are coloured corresponding to the colour of each gene. The regions underlined were originally included in the pJMCK6 and pYL1 constructs whereas regions under dash lines were extended in this study.

Mutant name	Construct name	Sequence alignment	Mutant name	Construct name	Sequence alignment
<i>chuA</i> 10	pRR1	attatgatatcaaaattatca attatgatatcaaaattatca	<i>fumC</i> 10	pRR8	tttttggaaaattattttttt tttttggaaaattattttttt
<i>chuA</i> 13	pRR2	attatgatatcaaaattatca attatgatatcaaaattatca	<i>fumC</i> 13	pRR9	tttttggaaaattattttttt tttttggaaaattattttttt
<i>chuA</i> 19	pRR3	attatgatatcaaaattatca attatgatatcaaaattatca	<i>fumC</i> 19	pRR10	tttttggaaaattattttttt tttttggaaaattattttttt
<i>chuA</i> 10/13	pRR4	attatgatatcaaaattatca attatgatatcaaaattatca	<i>fumC</i> 10/13	pRR11	tttttggaaaattattttttt tttttggaaaattattttttt
<i>chuA</i> 10/19	pRR5	attatgatatcaaaattatca attatgatatcaaaattatca	<i>fumC</i> 10/19	pRR12	tttttggaaaattattttttt tttttggaaaattattttttt
<i>chuA</i> 13/19	pRR6	attatgatatcaaaattatca attatgatatcaaaattatca	<i>fumC</i> 13/19	pRR13	tttttggaaaattattttttt tttttggaaaattattttttt
<i>chuA</i> 10/13/19	pRR7	attatgatatcaaaattatca attatgatatcaaaattatca	<i>fumC</i> 10/13/19	pRR14	tttttggaaaattattttttt tttttggaaaattattttttt

Table 3.3: Partial sequence alignments between wild-type (top stand) and mutated Fur_{*C_j*} boxes (bottom stand) preformed using Clone Manager software. Base changes in respect to the wild-type Fur_{*C_j*} box are highlighted in red.

by SDS-PAGE (Figure 3.3). They were the untagged and tagged version of the protein respectively as confirmed by previous western blotting experiments using anti-Strep-tag antibodies and N-terminal protein sequencing (Li, 2005). Because the Strep-tag was dissociated from a large proportion of the recombinant Fur_{Cj} protein, further tag removal was not carried out.

3.3.3 EMSA

chuA and *fumC* promoter regions containing the wild-type Fur_{Cj} boxes were first amplified from pJMCK6 and pYL1 respectively using their original cloning primers (Table 2.5) and the DIG-labelled PCR products were then subjected to EMSA (2.2.24) with purified Fur_{Cj} to confirm previous observations. The Fur_{Cj} concentration range used previously (Li, 2005; Holmes *et al.*, 2005; Ridley *et al.*, 2006) was first tested with the wild-type *chuA* Fur_{Cj} box, however high affinity Fur_{Cj} binding was not observed (results not shown). The actual Fur_{Cj} protein sample used in these studies was also tested and similar results were obtained which indicated that an error had occurred when the Fur_{Cj} concentration used in these studies was originally calculated. A new range of Fur_{Cj} concentration was determined and applied for wild-type *chuA* and *fumC* Fur_{Cj} boxes. As shown in Figure 3.4, high affinity Fur_{Cj} binding was observed for wild-type *chuA* Fur_{Cj} box with as little as 25 nM Fur_{Cj} and two distinct shift species were observed. The bottom species indicated the binding of a Fur_{Cj} dimer and binding of two dimers was represented by the upper shift species. When the Fur_{Cj} concentration was increased, majority of the labelled DNA was bound with Fur_{Cj} and predominately in the form of



Figure 3.3: A SDS-PAGE analysis of the purified recombinant Fur_{Cj}. Lane 1 and 10: ProSieve® color protein markers (Lonza); lane 2: pre-column sample; lane 3: flow-through sample; lane 4: mid-wash sample; lanes 4-9 and 11-15: elution samples 1-10 respectively.

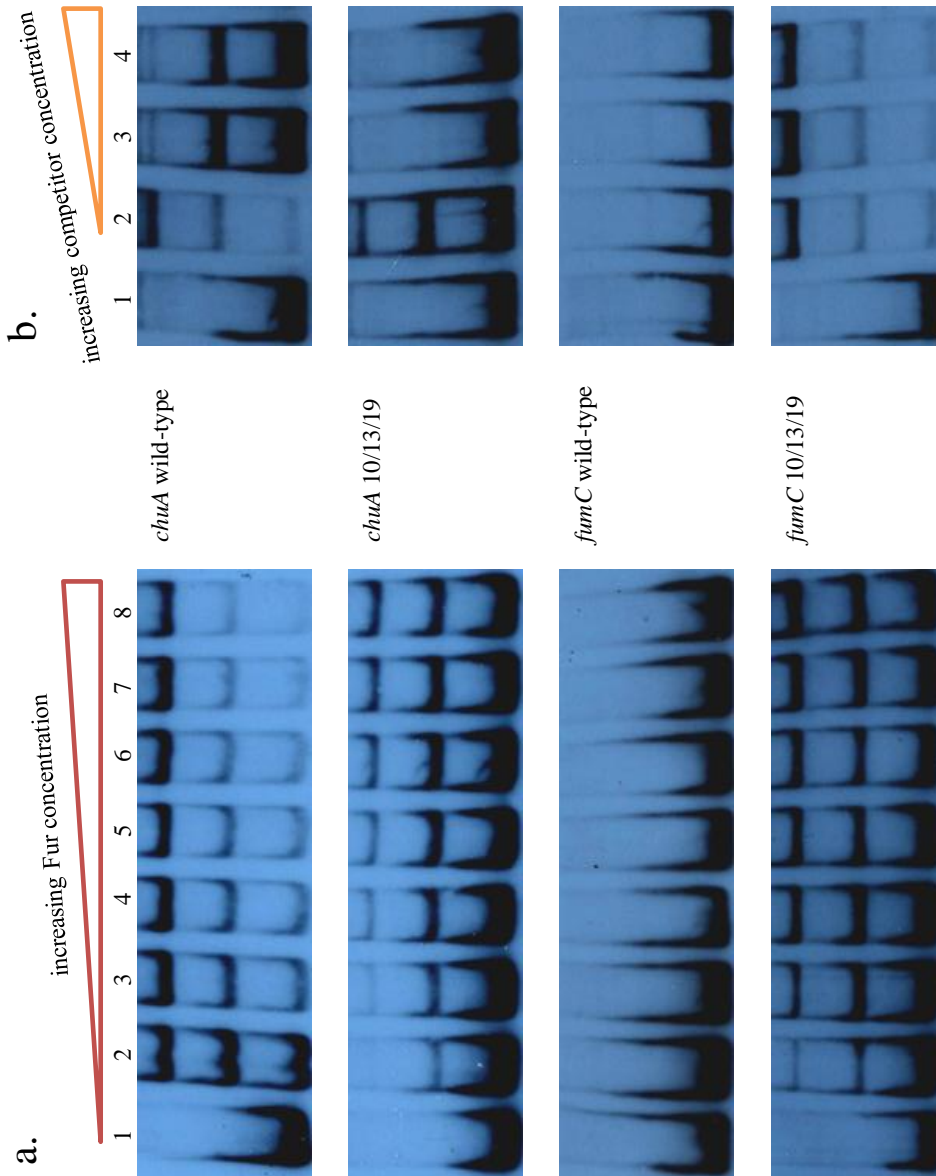


Figure 3.4: Standard (a) and competitive (b) EMSA of 1.55 fmol DIG-labelled *chuA* and *fumC* promoter regions containing the wild-type and triple mutated Fur_{Cj} boxes with the purified Fur_{Cj} protein. For standard EMSA, lanes 1-8: labelled DNA with 0 nM, 25 nM, 50 nM, 75 nM, 100 nM, 125 nM, 150 nM and 175 nM Fur_{Cj} respectively. For competitive EMSA, lanes 1-2: labelled DNA with 0 nM and 175 nM Fur_{Cj} respectively; lanes 3-4: labelled DNA with 175 nM Fur_{Cj} respectively; lanes 3-4: labelled DNA with 175 nM Fur_{Cj} and 1500x and 2000x unlabelled competitor respectively. Unlabelled *chuA* and *fumC* wild-type promoter regions were used as competitors for *chuA* and *fumC* (both wild-type and triple mutant) competitive EMSA respectively.

two Fur_{Cj} dimers. For the *fumC* Fur_{Cj} box, no Fur_{Cj} binding was detected even at 175 nM Fur_{Cj}. Despite differences in Fur_{Cj} concentration ranges used in this study and previous studies, the shift patterns observed for the wild type *chuA* and *fumC* Fur_{Cj} boxes were consistent with previous observations indicating the purified Fur_{Cj} protein in this study was functional.

To test the effects of mutational changes in the affinity of Fur_{Cj} binding, *chuA* and *fumC* Fur_{Cj} boxes containing triple mutational changes were first analysed as they were predicted to give the most dramatic changes in Fur_{Cj} binding (Figure 3.4). For *chuA*10/13/19, although two shift species were still detectable, most of the Fur_{Cj}-DNA complex was in the single dimer state and a large amount of unbound DNA was observed which indicated a significant decrease in the ability for at least one Fur_{Cj} dimer to recognise and bind to this mutated Fur box. Two shift species were also demonstrated for *fumC*10/13/19 with as little as 25 nM Fur_{Cj} and these species were not observed for the wild-type *fumC* Fur_{Cj} box. The shift pattern obtained for *fumC*10/13/19 was comparable with *chuA*10/13/19, however in this case, these two shift species were created with the substitution of three mismatches in the *fumC* Fur_{Cj} box thus the ability for Fur_{Cj} to recognise and bind to the Fur_{Cj} box with a relatively high affinity was partially restored.

To verify the results obtained, competitive EMSAs were performed for *chuA* and *fumC* wild-type Fur_{Cj} boxes and triple mutants with 1500 and 2000 times corresponding

unlabelled wild-type promoter region as competitors (Figure 3.4). For *chuA*, specific Fur_{Cj} binding was reduced for both the wild-type and mutant as most of the Fur_{Cj} protein was competed away by the unlabelled DNA. The opposite effect was observed for *fumC* where the shift pattern was unchanged for the wild-type and mutant as *fumC* wild-type Fur_{Cj} box does not bind Fur_{Cj}. A much higher affinity of Fur_{Cj} binding was observed for *fumC*10/13/19 with 175 nM Fur_{Cj}, however this high level of Fur_{Cj} binding was not observed when standard EMSA was performed therefore was likely to be caused by cross contamination. The results obtained from competitive EMSAs again demonstrated the different specificity of Fur_{Cj} binding between *chuA* and *fumC* promoters and verified the shift patterns observed for standard EMSAs were caused solely by the interaction between labelled promoter regions and *C. jejuni* Fur_{Cj}.

To determine the importance of each individual base at the 10th, 13th and 19th positions of the Fur_{Cj} box, EMSA was subsequently conducted for all the *chuA* and *fumC* single and double mutants. For *chuA* mutants, there was a clear correlation between the unbound DNA profiles and mutational positions in the *chuA* Fur_{Cj} box. An increase in the intensity of the unbound DNA in the presence of 175 nM Fur_{Cj} was observed for all the *chuA* mutants and most notably with the *chuA*10/19 and *chuA*13/19 (Figure 3.5), which indicated a decrease in the affinity of Fur_{Cj} binding.

For *fumC* mutants, no shift species was observed for *fumC*10 (Figure 3.6). A weak higher shift species representing a double Fur_{Cj} dimers-DNA complex was detected for

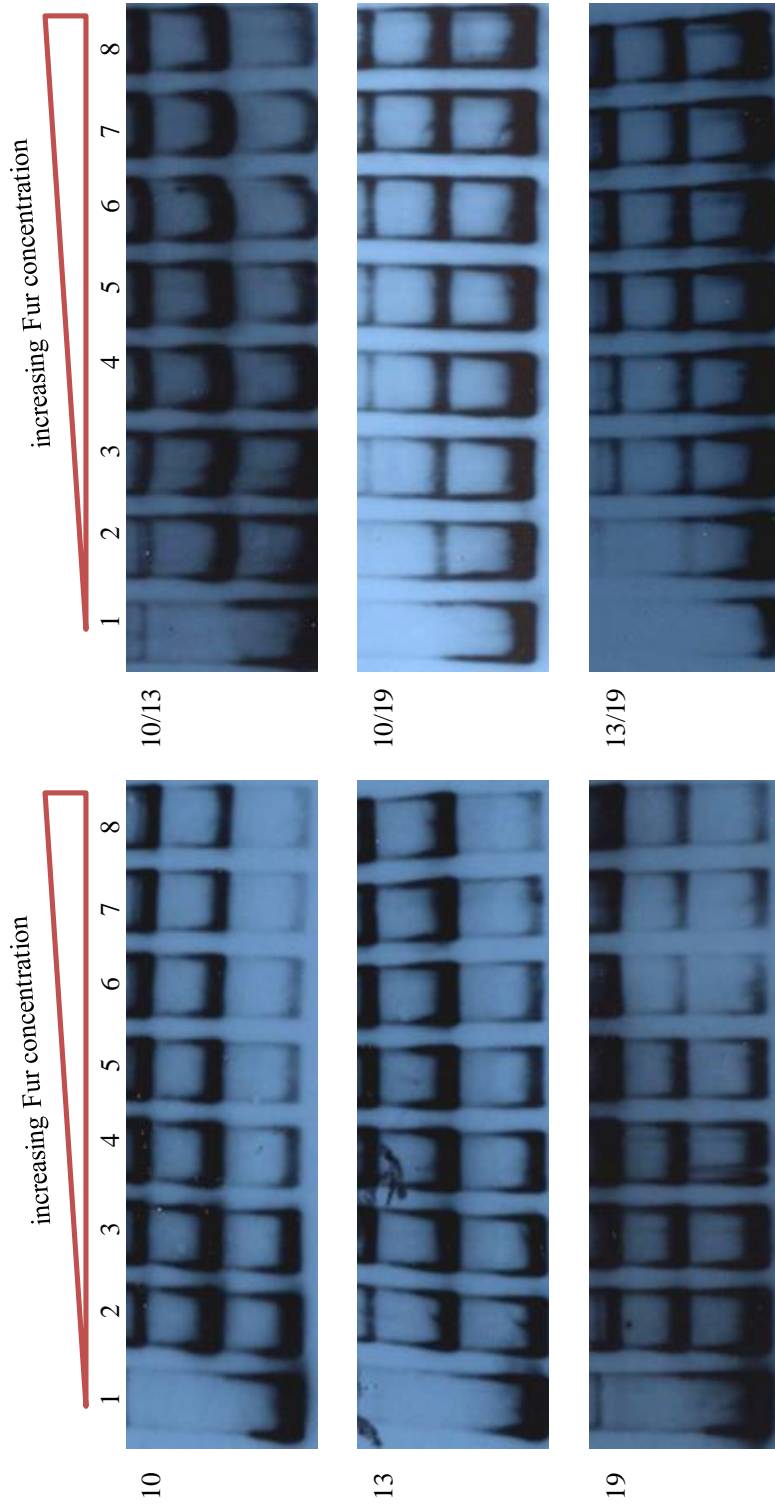


Figure 3.5: Standard EMSA of 1.55 fmol labelled *chuA* promoter regions containing mutated *Fur_{Cj}* boxes with the purified *Fur_{Cj}* protein.
Lanes 1-8: labelled DNA with 0 nM, 25 nM, 50 nM, 75 nM, 100 nM, 125 nM, 150 nM and 175 nM *Fur_{Cj}* respectively.

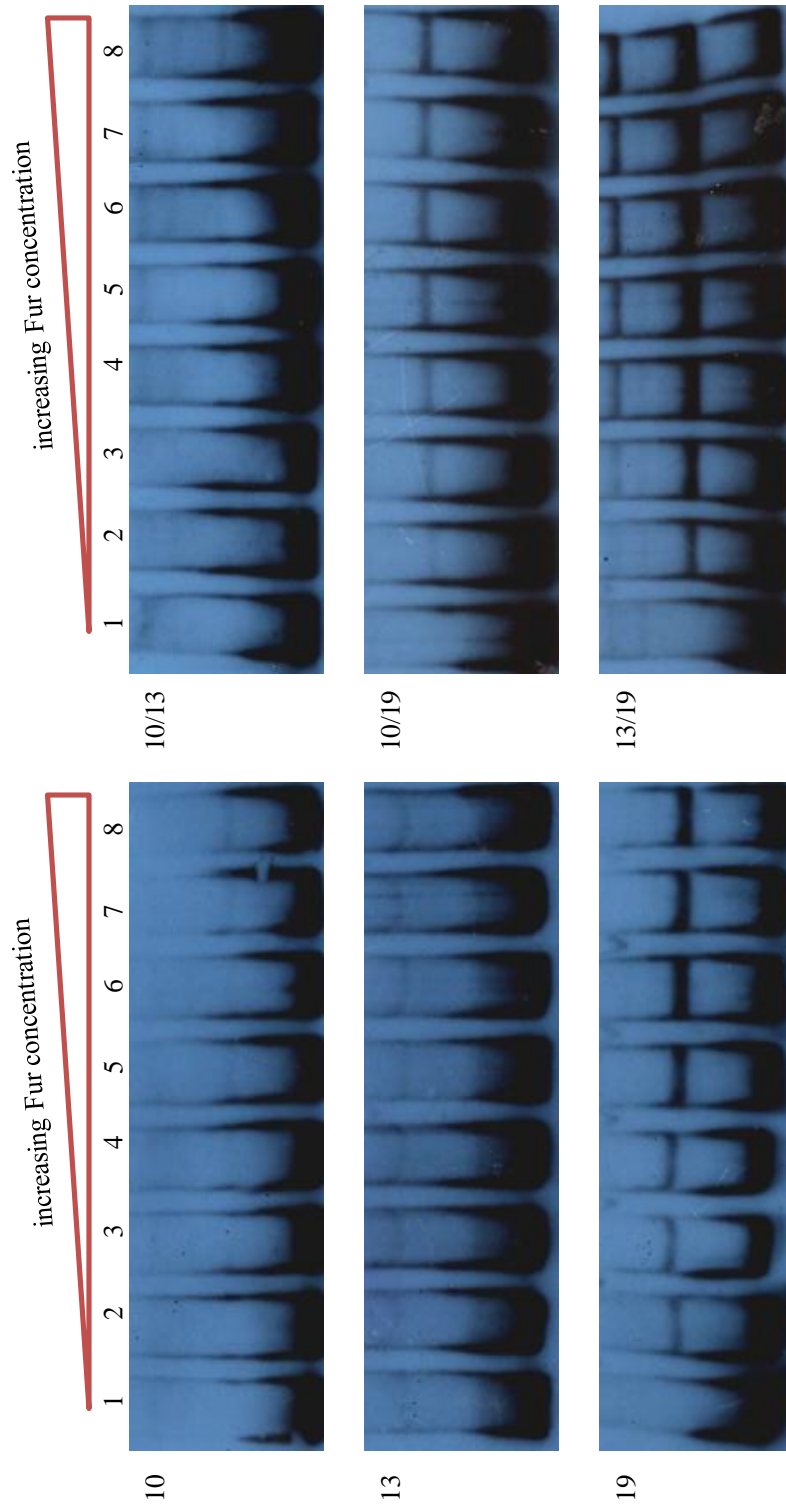


Figure 3.6: Standard EMSA of 1.55 fmol labelled *fumC* promoter regions containing mutated *Fur_{Cj}* boxes with the purified *Fur_{Cj}* protein.
Lanes 1-8: labelled DNA with 0 nM, 25 nM, 50 nM, 75 nM, 100 nM, 125 nM, 150 nM and 175 nM *Fur_{Cj}* respectively.

fumC13 while a lower shift species was observed for *fumC19* that demonstrated the forming of single Fur_{Cj} dimer-DNA complexes. The reason for this higher shift species formation (but not the lower species) seen with *fumC13* was unclear, however it was likely that although high affinity binding of Fur_{Cj} single dimer was not achieved, the mutational change at position 13 of the Fur_{Cj} box has led to a conformational change of the DNA such that allowed the formation of a weak DNA-double Fur_{Cj} dimers complex. Both DNA binding patterns observed for *fumC13* and *fumC19* were also consistently observed in the *fumC* double mutants and the intensities of these two shift species were significantly increased for *fumC13/19*. These findings have collectively indicated that mutations introduced into the *chuA* and *fumC* Fur_{Cj} boxes, in particular the 13th and 19th positions, strongly affect Fur_{Cj} binding whereas the 10th position may play a subsidiary role.

3.3.4 β -galactosidase assay

To corroborate the *in vitro* interactions observed between *chuA* and *fumC* promoters and Fur_{Cj}, β -galactosidase assays were performed to verify the functional relevance of these interactions *in vivo* and to investigate the effects in promoter activities due to mutational changes in the *chuA* and *fumC* promoter regions. The goal was to amplify the wild type and mutant *chuA* and *fumC* promoters and clone into the multi-copy shuttle vector pMW10 (Wösten *et al.*, 1998) for subsequent screening in a *C. jejuni* background under high and low iron conditions. pMW10 is a 10 kb shuttle vector contains *ori* of both *C. jejuni* and *E. coli* and a MCS situated upstream of a promoterless *lacZ* gene (Wösten *et*

al., 1998). *C. jejuni* NCTC 11168 could not be used as a host strain as it cannot be successfully transformed by plasmids, therefore *C. jejuni* 480, a strain readily accept plasmids, was used instead and this system has been successfully used in several occasions to study specific promoter activities in *C. jejuni* (van Vliet *et al.*, 2000; Ridley *et al.*, 2006; Miller *et al.*, 2008). It should be noted that although using a difference *C. jejuni* strain was not ideal, it was essential to investigate Fur_{Cj} regulation in a *C. jejuni* background as previous studies indicated that when presented in an *E. coli* background, the AT-rich *C. jejuni* sequence interact non-specifically with Fur_{Ec} (Rock, 2003).

The original cloning primers for *chuA* and *fumC* wild-type promoters were not compatible with pMW10, cloning primers with 5' *Bam*HI and *Xba*I restriction sites were therefore designed and used to allow directional cloning of the promoter region into pMW10. All the wild-type and mutated promoter regions were cloned into pMW10 in this manner and the resulting constructs pRR14-30 were transformed into *C. jejuni* 480.

β-galactosidase assays (2.2.20) were first carried out with the *chuA* wild-type promoter construct (pRR15) along with several controls under high iron (40 μM FeSO₄) and low iron (20 μM Desferal) conditions. The promoter region of housekeeping gene *metK* cloned into pMW10 (p23E5) and pMW10 without insert were used as non-iron-regulated positive and negative controls respectively. The *chuA* wild-type promoter previously cloned into pMW10 (pJDR13) that contains the *chuZ-chuA*

intergenic region (Table 2.2) was used as an iron-regulated comparative positive control. Promoter activities previously observed for all the controls (Ridley *et al.*, 2006) were consistently observed though no promoter activity was determined for the *chuA* wild-type promoter cloned in this study (Figure 3.7). The entire pRR15 construct was later sequenced and no mutations or deletions were found, which led to the conclusion that the length of the original *chuA* promoter region cloned in pJMCK6 (Figure 3.2) and subsequently cloned in pRR15 was not sufficient to allow the promoter to function correctly.

As all the mutated promoter regions had already been cloned into pMW10, therefore instead of remaking all the mutants, each wild-type and mutated *chuA* promoter regions were PCR amplified and fused using fusion PCR with a 61 bp fragment amplified directly upstream of the *chuA* promoter region originally cloned (Figure 3.2). The extended *chuA* promoters were re-cloned back into pMW10 (pRR31-38) and promoter activities were tested along with controls (Figure 3.8).

Iron-induced gene repression was observed for the *chuA* wild-type promoter under high iron conditions and the promoter was de-repressed when the iron concentration was reduced, therefore indicating the iron responsive regulation of the *chuA* promoter was restored with the extended promoter region. Mutational change at the 10th position of the *chuA* Fur_{Cj} box did not alter the level of gene expression when compared to the wild-type, however three- to four-fold de-repression was observed under high iron

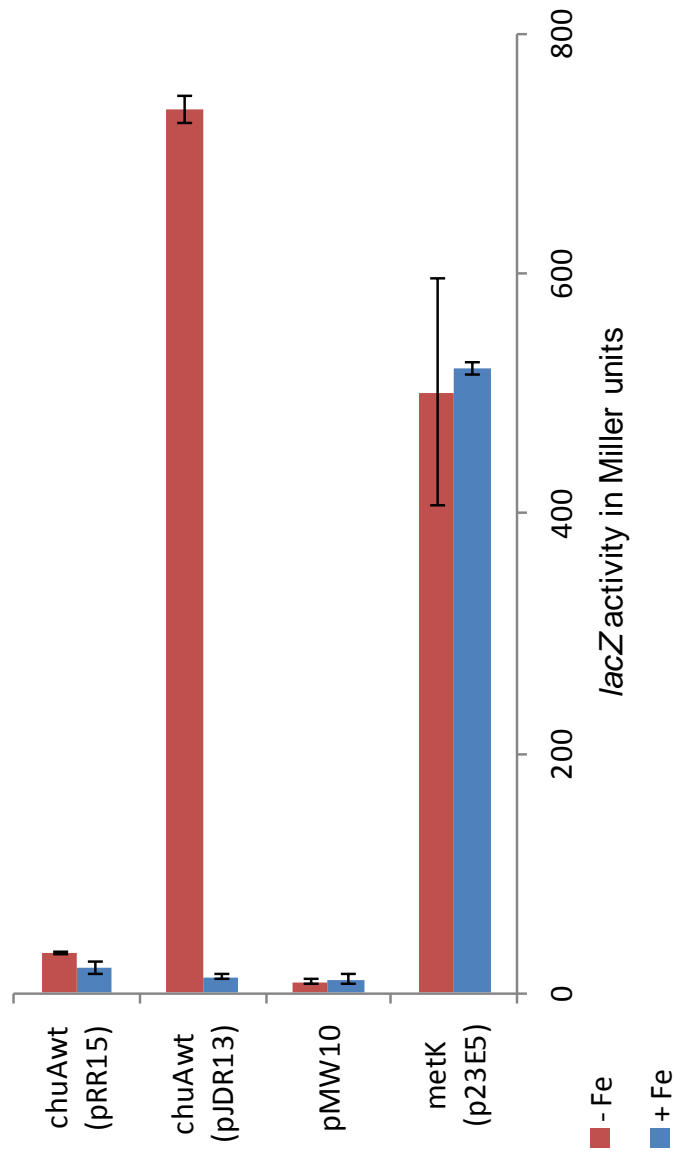


Figure 3.7: β -galactosidase assay of the *chuA* wild-type promoter region with controls under high iron (40 μ M FeSO₄) and low iron (20 μ M Desferal) conditions. Data presented are the means of triplicate sampling from two independent experiments with the standard error.

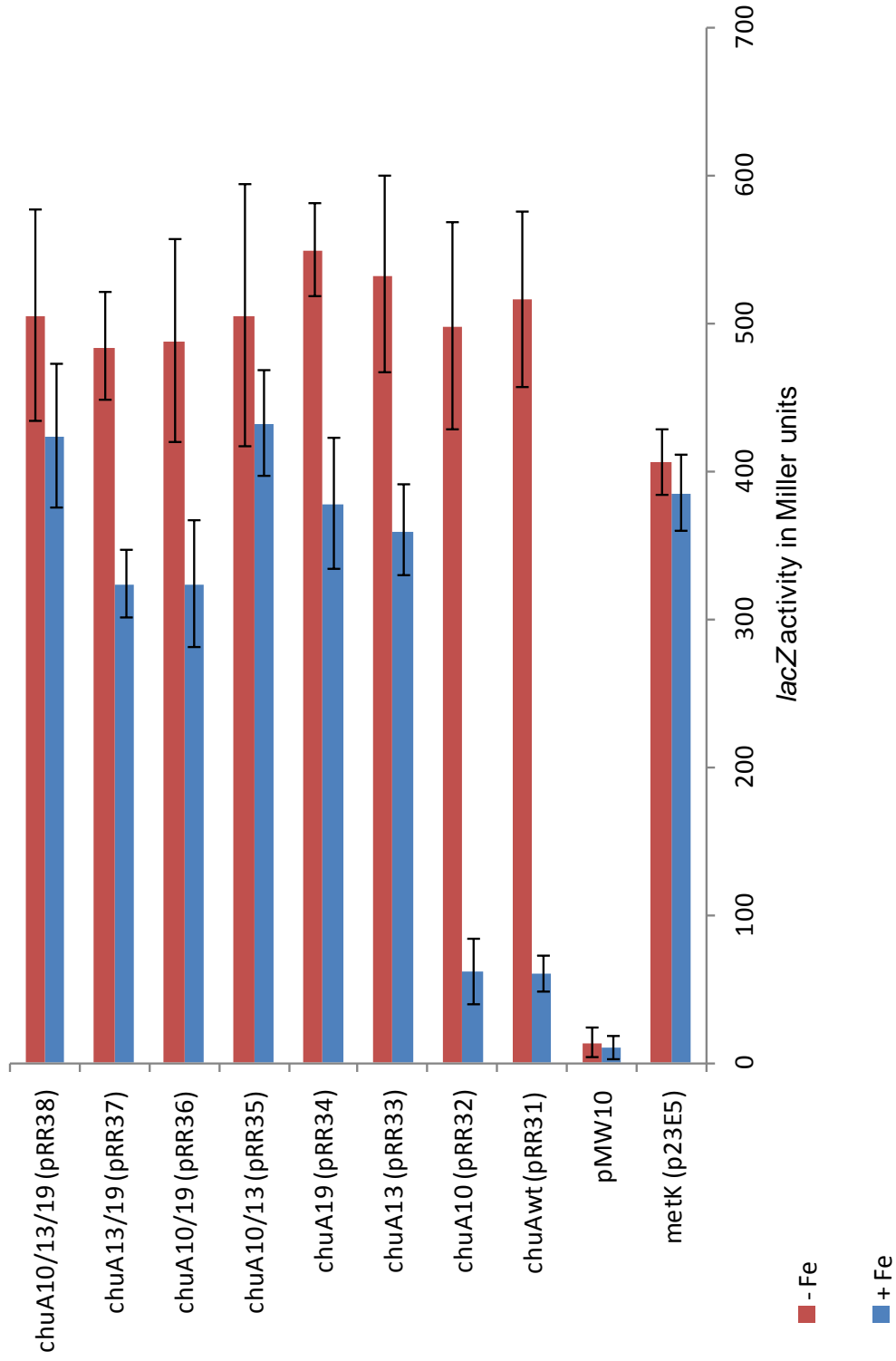


Figure 3.8: β -galactosidase assay of the *chuA* wild-type and mutated promoter regions with controls under high iron ($40 \mu\text{M FeSO}_4$) and low iron ($20 \mu\text{M Desferal}$) conditions. Data presented are the means of triplicate sampling from two independent experiments with the standard error.

conditions for mutants containing 13th and/or 19th base changes which indicated a decrease in the ability of Fur_{Cj} to interact with the mutated Fur_{Cj} box and hence has allowed these promoters to be partially transcribed by the RNA polymerase. These results have demonstrated the importance of the 13th and 19th bases of the Fur_{Cj} box in Fur_{Cj}-Fur_{Cj} box interaction and this finding was consistent with the EMSA results (Figures 3.4 and 3.5).

In addition, although similar levels of Fur_{Cj}-repression were detected for *chuA* wild-type and *chuA10* under iron-rich conditions, clear differences in the level of derepression were observed between mutants with and without the 10th base mutation (i.e. *chuA13* was different from *chuA10/13* and *chuA13/19* was different from *chuA10/13/19*). These differences were possibly non-statistical variations caused by inaccuracies of the β -galactosidase assays, but most likely, they were reflected by the important but unessential role of the 10th position of the Fur_{Cj} box in facilitating or stabilising the Fur_{Cj}-Fur_{Cj} box interaction.

When β -galactosidase assays were carried out for the wild-type and mutated *fumC* promoters under the same experimental conditions (Figure 3.9), unexpected results were observed. Although promoter activities were observed for *fumC* wild-type promoter under both iron conditions, the iron-dependent gene regulation identified previously (Holmes *et al.*, 2005) was not reproduced for the wild-type *fumC* promoter. This non-iron-responsive gene regulation was further observed for *fumC10*, *fumC19* and

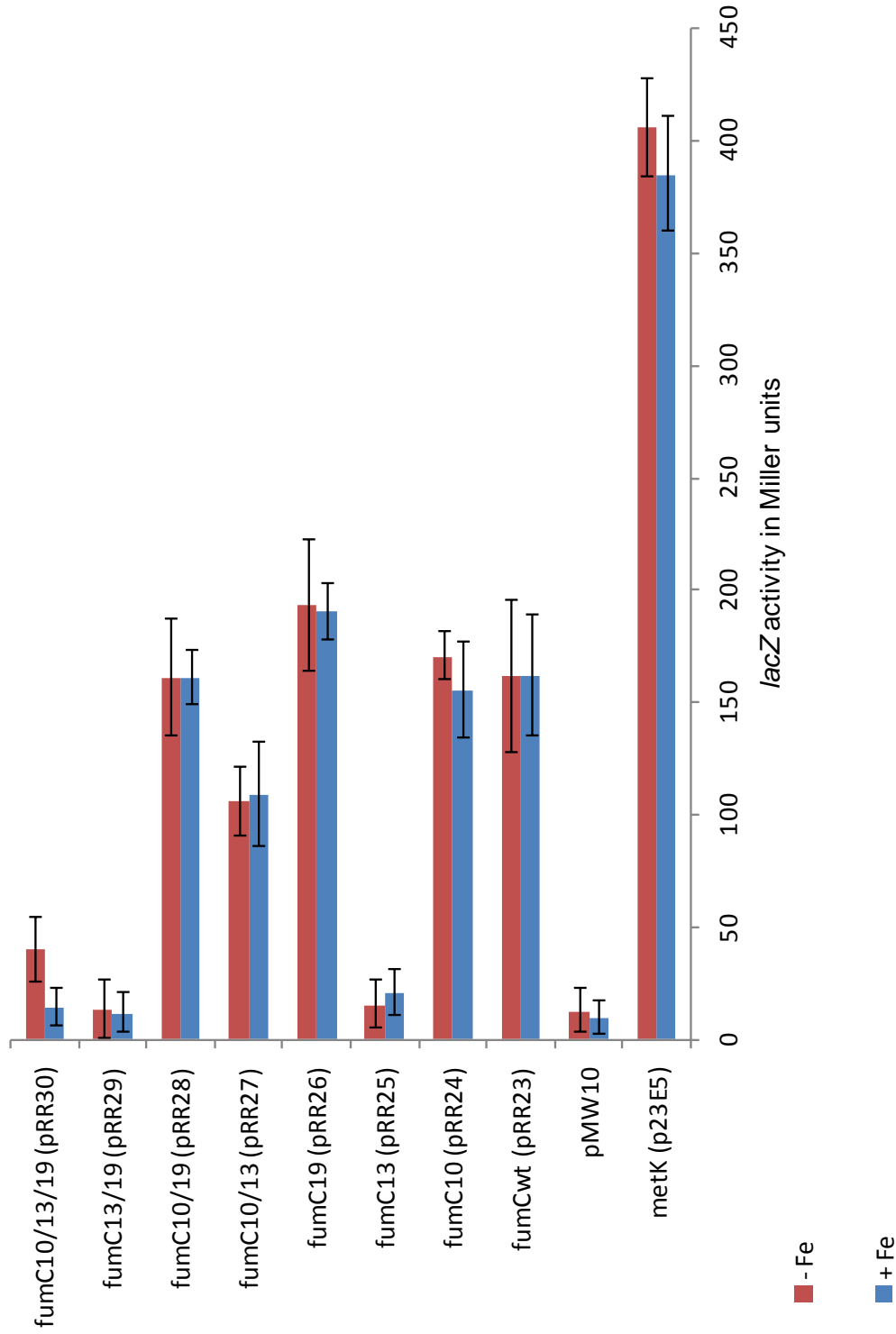


Figure 3.9: β -galactosidase assay of the *fumC* wild-type and mutated promoter regions with controls under high iron (40 μ M FeSO_4) and low iron (20 μ M Desferal) conditions. Data presented are the means of triplicate sampling from two independent experiments with the standard error.

*fumC*_{10/19} which indicated that although Fur_{C_j}-binding was demonstrated for mutated *fumC* Fur_{C_j} boxes *in vitro* (Figure 3.6), these Fur_{C_j}-Fur_{C_j} box interactions were physiologically insignificant to alter the expression of *fumC* *in vivo*. The promoter activates for mutants containing the 13th base change (*fumC*₁₃, *fumC*_{13/19} and *fumC*_{10/13/19}) were severely reduced comparing to *fumC* wild-type, which indicated that the *fumC* Fur_{C_j} box is overlapping with the recognition site of one of the importance transcription regulatory element hence the promoter activity was disrupted when the 13th base was mutated. Interestingly the expression of *fumC*_{10/13} was only partially affected by the 13th base mutation. In this case, the detrimental effect of the 13th base mutation was potentially compensated by the G to T change at the 10th position of the *fumC* Fur_{C_j} box as T is a more favourable base generally found in the -10 and -35 regions of a bacterial promoter.

The non-iron responsive gene regulation observed for *fumC* wild-type promoter was possibly caused by the inadequate promoter length cloned into pYL1. As in the case of *chuA*, fusion PCR was used to extend the *fumC* promoter region by 217 bp upstream (217 bp was used for the convenience of primer design) and both the original and extended (pRR42) versions were tested in β-galactosidase assays (Figure 3.10). Iron induced activation was observed for both promoters, though the differences in promoter activity between high and low iron were marginal and no obverse difference was noticeable between the two versions of the *fumC* promoter. Iron responsive regulation of *fumC* may also have been mediated by growth phase as cells were routinely cultured to

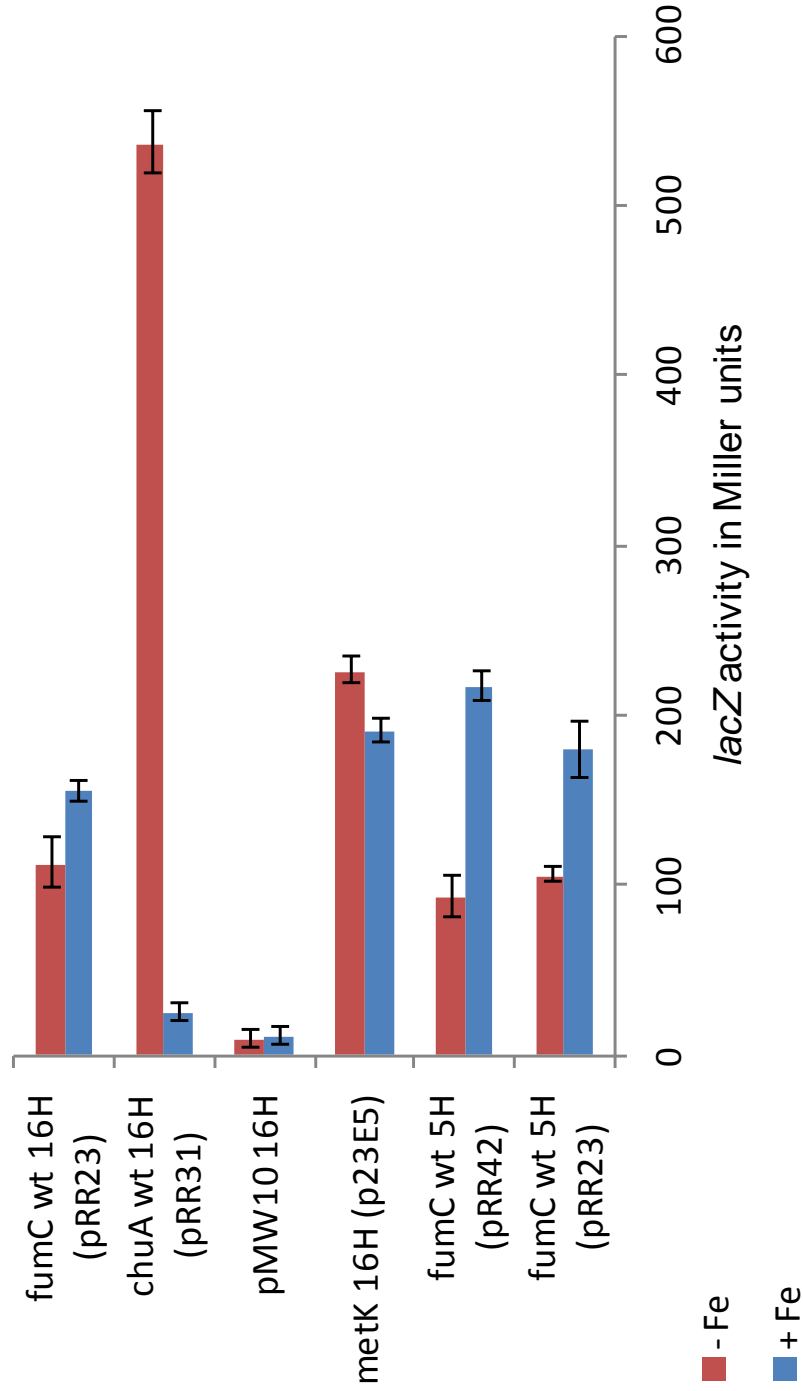


Figure 3.10: β -galactosidase assay of the original (pRR23) and extended (pRR42) *fumC* wild-type promoter regions with controls under high iron (40 μ M FeSO₄) and low iron (20 μ M Desferal) conditions for different amount of time i.e. 5 and 16 hours. Data presented are the means of triplicate sampling from two independent experiments with the standard error.

late lag - early exponential phase in high and low iron conditions for β -galactosidase assay whereas the cells used in Holmes's study were grown to mid - late exponential phase (Holmes *et al.*, 2005). 16 hours incubation time was subsequently used prior to β -galactosidase assays of the *fumC* wild-type promoter and controls and a similar level of iron responsive gene regulation was observed when compared with the standard 5 hours incubation (Figure 3.10). Although this minor difference in *fumC* promoter activity between high and low iron was consistent with the 2.4-fold decrease in transcription level under iron-limited conditions previously observed (Holmes *et al.*, 2005), however promoter activity fluctuations were commonly observed for non-iron regulated *metK* due to inaccuracies of the assay, therefore the genuine iron responsive regulation of *fumC* could not be solely substantiated by β -galactosidase assays of the wild-type promoter and controls.

3.3.5 Construction of the *C. jejuni* 480 *fur_{Cj}* mutant

To verify the minor iron responsive regulation observed for *fumC* promoter by β -galactosidase assays, one of the strategies applied was to construct a *C. jejuni* 480 *fur_{Cj}* mutant where any Fur_{Cj}-dependent iron regulation would be abolished. By using β -galactosidase assays in different Fur_{Cj} backgrounds, iron-mediated differential gene regulation of *fumC* would be determined by a direct comparison of the promoter activity profiles.

A *C. jejuni* 480 *fur_{Cj}* mutant strain has been previously constructed by Grabowska *et al.*

(2011) where *C. jejuni* 81-176 *fur_{Cj}* mutant was first created by electroporation of pAV80 (Figure 3.11) into the wild-type 81-176 strain and the genomic DNA extracted from the resulting mutant was then naturally transformed into the wild-type 480 strain to facilitate homologous recombination between the wild-type 480 *fur_{Cj}* and the 81-176 mutated *fur_{Cj}* (Grabowska *et al.*, 2011). pAV80 is a mutational construct harbouring a Cm resistance cassette inserted into the 5' of the NCTC 11168 *fur_{Cj}* in a forward direction and was previously used to create a NCTC 11168 *fur_{Cj}* mutant (AV41, van Vliet *et al.*, 1998). As pMW10 based constructs used for β -galactosidase assays were Kan resistance, therefore a Cm resistance 480 *fur_{Cj}* knockout would be an ideal strain to analyse the iron responsive regulation of *fumC*. However in order to avoid any *C. jejuni* 480 strain differences, the 81-176 *fur_{Cj}* mutant genomic DNA purified by Grabowska *et al.* (2011) was obtained and was used in an attempt to create a 480 *fur_{Cj}* mutant strain that would allow valid comparisons with the wild-type 480 strain using β -galactosidase assays.

The 81-176 *fur_{Cj}* mutant genomic DNA and the wild-type counterpart were first PCR analysed to confirm the presence of a Cm resistance cassette. A 1798 bp fragment containing the *fur_{Cj}* gene with the cassette was expected to be obtained using Cj81-176 *fur5'* and 3' long primers and the Cj81-176 *fur5'* long and *catinvR* primer set was expected to confirm the orientation of the cassette (Figure 3.11). When analysed by gel electrophoresis, a 946 bp band representing the wild-type *fur_{Cj}* was observed for 81-176 *fur_{Cj}* mutant and no product was detected using Cj81-176 *fur5'* long and *catinvR*

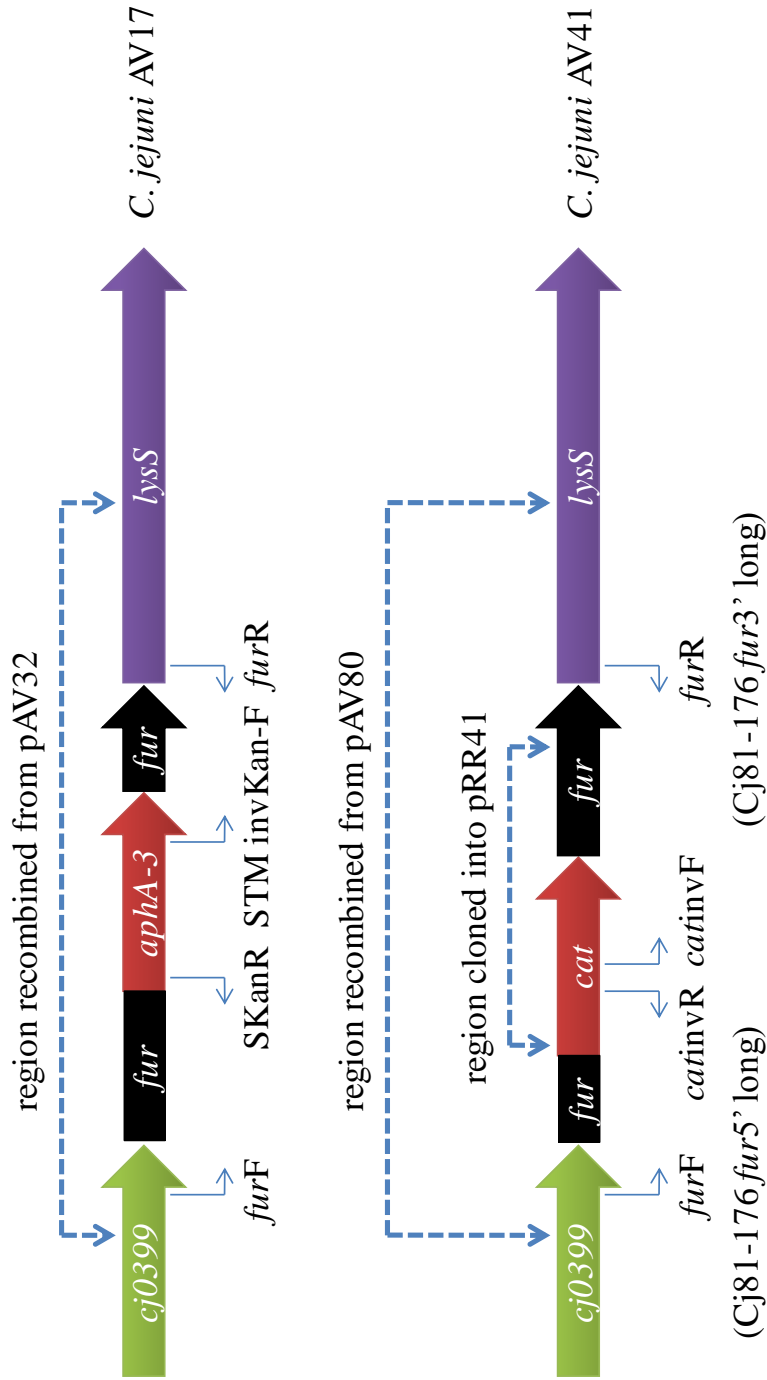


Figure 3.11: The mutated *fur* genes and flanking regions of NCTC 11168 *fur* mutant strains AV17 and AV41. The corresponding regions recombined from the original mutational constructs pAV32 and pAV80 and the fragment cloned into pRR41 are indicated by dashed lines. Primers used for screening *fur* mutants and their binding sites and directions are indicated by arrows. Cj81-176 *fur*5' long and Cj81-176 *fur*3' long primers were used for *C. jejuni* 81-176 strain and their binding sites and directions on 81-176 are equivalent to *fur*F and *fur*R respectively on NTCT 11168.

primers (Figure 3.12). When a pair of Cm resistance cassette specific primers was used, a 322 bp fragment confirming the present of the cassette was observed which indicated that either the genomic DNA was amplified from the wrong strain or homologous recombination has occurred elsewhere in the 81-176 genome.

As further communication regarding to 81-176 *fur_{Cj}* mutant was not established, the two steps method was repeated and further simplified by introducing NCTC 11168 mutated *fur_{Cj}* gene (in the forms of mutational constructs or genomic DNA) straight into 480 as the 480 *fur_{Cj}* and flanking regions (300 bp on each side of the gene) shares 94% identity to the NCTC 11168 *fur_{Cj}* when compared by sequencing (result not shown). In order to explore the possibility of single recombination event, mutational construct pRR41 was also created that contained part of the Cm resistance cassette and part of the NCTC 11168 *fur_{Cj}* gene amplified from pAV80.

No colonies were obtained when pAV80, pRR41 and AV41 genomic DNA were introduced straight into 480 whereas for 81-176, the non-homologous recombination determined in Figure 3.12 was consistently observed for both DNA samples (Table 3.4). The mechanism of this Cm resistance cassette-associated non-homologous recombination in 81-176 was not clear and it was likely that either the 81-176 strain used by Grabowska *et al.* (2011) was different from the 81-176 strain used for this study or the 480 *fur_{Cj}* mutant they have created was incorrect. Although it's not an ideal host for pMW10 based β -galactosidase assays, the possibility to create a Kan resistance 480

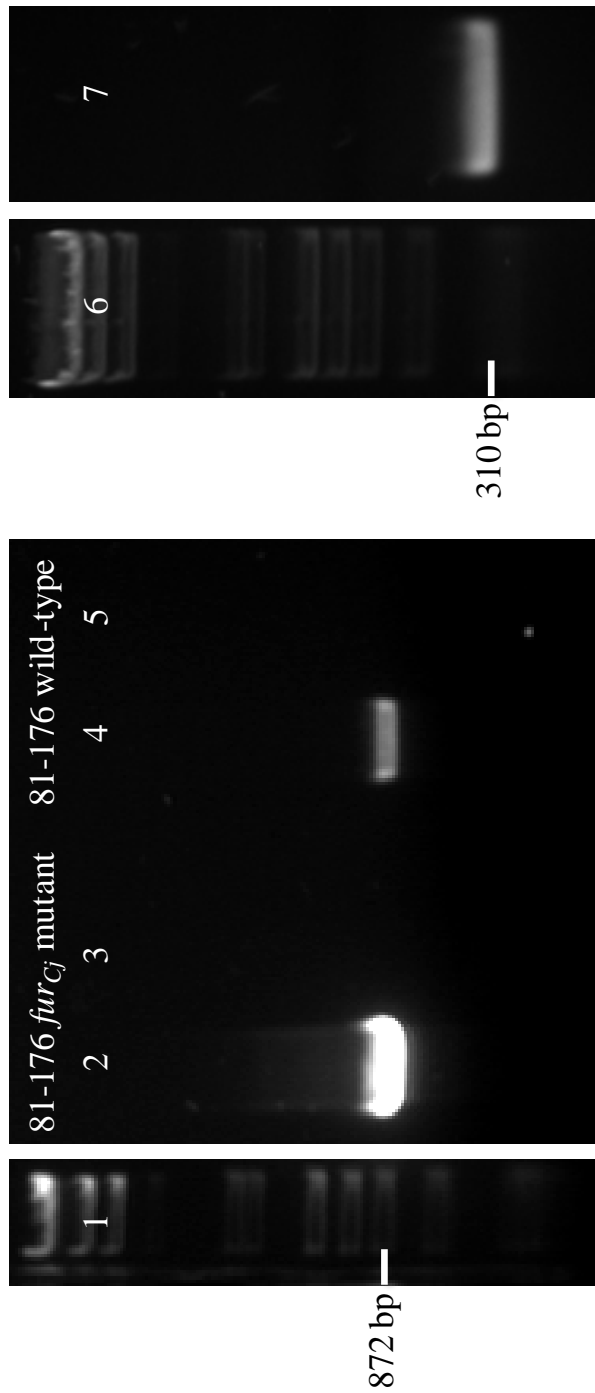


Figure 3.12: Verification of the 81-176 *fur_{Cj}* mutant by PCR. Lanes 1 and 6: λ/Φ DNA size marker; lanes 2 and 4: PCR amplification using Cj81-176 *fur5'* and 3' long primers; lanes 3 and 5: PCR amplification using Cj81-176 *fur5'* long and *catInvR* primers; lane 7: PCR amplification using *catInvF* and *catR_KpnI* primers.

DNA used	recipient strain	outcomes
pAV80	<i>C. jejuni</i> 480	no transformants
AV41 genomic DNA	<i>C. jejuni</i> 480	no transformants
pAV80	<i>C. jejuni</i> 81-176	non-homologous recombinants
AV41 genomic DNA	<i>C. jejuni</i> 81-176	non-homologous recombinants
pAV32	<i>C. jejuni</i> 480	<i>furCj</i> merodiploid
AV17 genomic DNA	<i>C. jejuni</i> 480	<i>furCj</i> mutant
pAV32	<i>C. jejuni</i> 81-176	non-specific breakthroughs
AV17 genomic DNA	<i>C. jejuni</i> 81-176	non-specific breakthroughs
pRR41	<i>C. jejuni</i> 480	no transformants

Table 3.4: Summary of the approaches used to create the *C. jejuni* 480 *furCj* mutant strain. pAV80, pAV32 and pRR41 were introduced into the recipient strains by electroporation whereas AV41 and AV17 genomic DNA were naturally transformed.

fur_{Cj} mutant strain was also explored using pAV32 and AV17 genomic DNA (Figure 3.11). When both DNA samples were separately introduced into 480, and resulting clones screened by PCR using *fur_{Cj}* flanking primers (*furF* and *furR*), two bands indicating the mutated (2414 bp) and wild-type *fur_{Cj}* (911 bp) were detected in each clones. The presence of *fur_{Cj}* merodiploid clones was initially predicted to be caused by cross-contaminations between *fur_{Cj}* mutants and wild-type breakthroughs and the screened colonies were therefore re-streaked and re-screened by PCR.

As shown in Figure 3.13, for 480 *fur_{Cj}* mutant created using AV17 genomic DNA, only the 2414 bp band representing the mutated *fur_{Cj}* gene was detected. A band of 996 bp confirming the presence of the Kan resistance cassette in the *fur_{Cj}* gene was also obtained using *furF* and cassette specific primer SkanR which together confirming the identity of a pure 480 *fur* knockout clone. This *fur_{Cj}* mutant strain was named RR1. For the 480 *fur_{Cj}* mutant created using pAV32, the merodiploid state of *fur_{Cj}* remained and further investigation was not followed. When AV17 genomic DNA and pAV32 was separately introduced into 81-176, clones containing only wild-type *fur_{Cj}* were obtained. There were likely to be non-specific breakthroughs and the presence of the Kan resistance cassettes elsewhere in the genome was not investigated.

As pMW10 and RR1 are both resistant to Kan, the level of antibiotic resistances was tested as the wild-type 480 strain containing the multi-copy pMW10 was predicted to be more resistant to high Kan concentrations than the single copy resistance cassette on the



Figure 3.13: Verification of the 480 *furC_j* mutant by PCR. Lane 1: λ/Φ DNA size marker; lanes 2 and 4: PCR amplification using *furF* and *furR* primers; lanes 3 and 5: PCR amplification using *furF* and SKanR primers.

chromosome of RR1. 8- and 9-fold diluted wild-type 480 cells carrying pMW10 and RR1 cells were plated onto plate agars with increasing Kan concentrations and colonies formed were counted and compared. At a concentration of 4 mg/ml Kan, which was 80 times more concentrated than the level routinely used for Kan resistance selections, a selection against RR1 was achieved whereas colonies for pMW10 harbouring strain were able to form on agar containing up to 7 mg/ml Kan.

When pRR31 (*chuA* wild-type), p23E5 (*metK*) and pMW10 were electroporated into RR1 and plated onto agar containing 4 mg/ml Kan, large amount of breakthroughs were formed. The cultures were further selected with 7 mg/ml Kan and colonies formed were verified by PCR using pMW10 backbone- and Kan resistance cassette-specific primers. Only RR1 strain carrying pMW10 was successfully selected and further screening of RR1 strain harbouring pRR31 or p23E5 failed to identify any positive clones. When all the pRR31 and p23E5 transformants were washed off from their plates and used as templates for PCR verifications (plate PCR), the presence of positive clones were identified amongst the clone populations, through the proportion was very low as indicated by the faint bands (Figure 3.14). Higher Kan concentrations were not tested due to the poor solubility of concentrated Kan in dH₂O and plate hybridisation technique for clone screening was considered unpractical due to the relative large number of mutants used in this study.

The difficulties associated with maintaining pRR31 or p23E5 in RR1 were likely caused

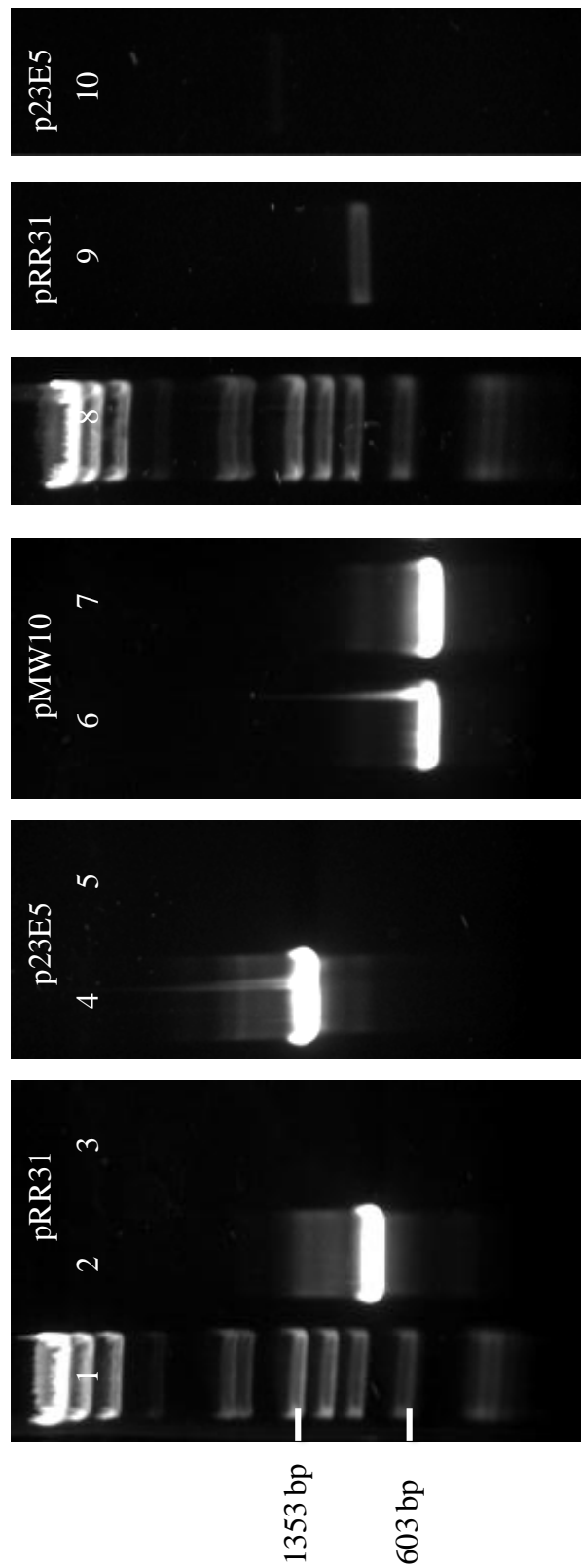


Figure 3.14: Verification of the RR1 transformants by PCR using M13F and SKanR primers. Lanes 1 and 8: λ/Φ DNA size marker; lanes 2, 4 and 6: PCR amplification using 480 strain harbouring pRR31, p23E5 and pMW10 respectively; lanes 3, 5 and 6: PCR amplification using RR1 strain potentially harbouring pRR31, p23E5 and pMW10 respectively; lanes 9 and 10: plate PCR from re-streaked RR1 transformants potentially harbouring pRR31 and p23E5 respectively.

by the constant expression of pRR31 and p23E5' *lacZ* genes which put pressures on the already weakened RR1 strain due to the lack of a functional *fur_{Cj}* gene. pMW10 by contrast was readily maintained in RR1 due to the lack of a promoter upstream of the *lacZ* gene. To backup this theory, pRR15 which contains an incomplete *chuA* promoter was electroporated into RR1 and positive clones were identified on 7 mg/ml Kan agar (results not shown) conferring that the 480 *fur_{Cj}* mutant was not a suitable host to study Fur_{Cj}-responsive gene regulation using multi-copy plasmids system and a single copy system (i.e. single chromosomal *lacZ* reporter system) would be more appropriate.

3.3.6 Verification of *fumC* iron regulation by northern blot

The second approach used to verify the *fumC* iron responsive regulation was to purify the NCTC 11168 total RNA from cells cultured under high and low iron conditions and subsequently subject to northern blot analysis. In order to allow direct comparisons with the results obtained by β -galactosidase assays, cells were cultured as described in 2.2.20 with the exception that a 16-hour liquid culture incubation under high (40 μ M FeSO₄) and low (20 μ M Desferal) iron conditions was used to obtain sufficient amount of cells for total RNA purification. The total RNA purified from NCTC 11168 wild-type and *fur_{Cj}* mutant (AV17) cultured under different iron conditions were separated by electrophoresis and hybridised with labelled *fumC*-specific probe and *16S*-specific probe as a loading control (Figure 3.15). An approximate 1.4 kb single transcript slightly longer than the *fumC* gene was observed which indicated that *fumC* has its own promoter. *fumC* was expressed in both iron conditions though the level of expression

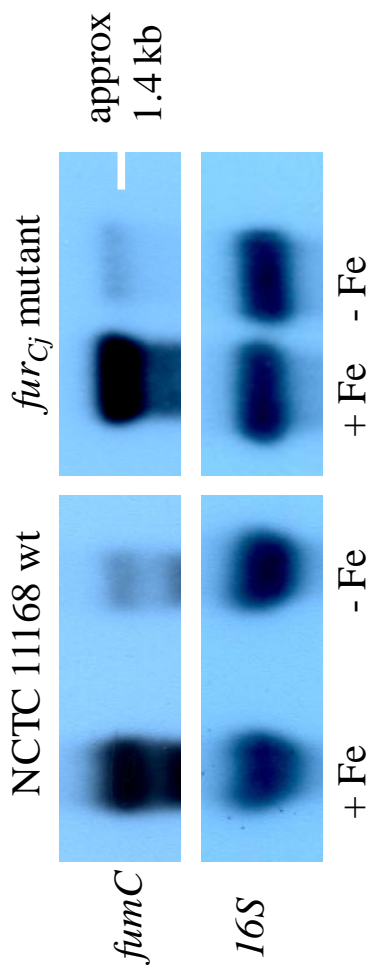


Figure 3.15: Northern blot analysis of the iron- and Fur_{Cj}-responsive regulation of *fumC*.

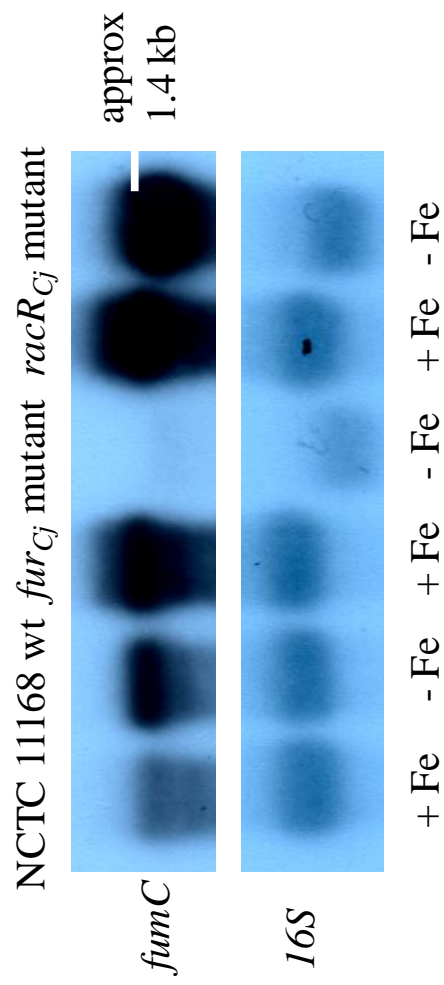


Figure 3.16: Northern blot analysis of the iron-, Fur_{Cj}- and RacR_{Cj}-responsive regulation of *fumC*.

was significantly increased under high iron conditions and was consistent with data obtained from β -galactosidase assays. However this iron induced transcriptional activation was not mediated by Fur_{Cj} as an identical transcriptional profile was observed for the *furCj* mutant strain and this result was in contradiction with previous observations (Holmes *et al.*, 2005).

The northern experiment shown in Figure 3.15 was repeated with the addition of RNA purified from a NCTC 11168 *perR_{Cj}* knockout strain (AV63) to explore the possibility of PerR_{Cj}-mediated iron regulation of *fumC*, iron-induced transcriptional activation for *fumC* was observed though independently from Fur_{Cj} and PerR_{Cj} (results not shown). The same set of RNA used was re-hybridised with labelled *chuA*-specific probe as a quality control for the RNA samples and expected iron- and Fur_{Cj}-mediated gene regulation were observed for *chuA* indicating that in this experimental setup (i.e. the growth conditions used to culture cells prior to RNA purification), *C. jejuni fumC* is not regulated, or at least directly regulated by Fur_{Cj} and the iron-responsive regulation of *fumC* is likely to be mediated by other unknown regulator/s.

A recent investigation of oxygen responsive metabolic gene regulation was conducted by van Mourik *et al.* (2009) in which *fumC* was demonstrated to be repressed by the two component regulator, RacR, under oxygen limited conditions in *C. jejuni* 81116. Regulation of gene expression in response to oxygen concentration is essential due to oxygen-mediated oxidative stress and oxidative stress is also intimately linked with iron

availability in *C. jejuni* (Palyada *et al.*, 2009). As van Mourik *et al.*'s study was mainly focused on the global effect of the RacR/RacS TCS in 81116 but not specifically on the regulatory effect of RacR on *fumC* expression, the involvement of NCTC 11168 RacR in the iron-responsive regulation of *fumC* was therefore assessed.

NCTC 11168 wild-type, *fur_{Cj}* mutant and a previously constructed *racR* mutant (AB3, A. Brás, unpublished data) were cultured under conditions mimicking the conditions described by Holmes *et al.* (2005, 2.3.1) to allow accurate determination of gene expression mediated by iron and also to verify the *Fur_{Cj}*-dependent *fumC* regulation previously observed. Total RNA were purified from each sample and were subjected to northern blot analysis as shown in Figure 3.16. Unexpectedly, the expression of *fumC* was found to be slightly repressed by iron and this finding was in contrast with results previously observed with β -galactosidase assays and northern blot analysis. Despite the slight loading error of RNA purified from *fur_{Cj}* mutant under low iron conditions, the *fumC* transcriptional profiles in *fur_{Cj}* mutant background was consistent with the data shown in Figure 3.15. However as a consistent transcriptional profile of *fumC* was not observed in Figure 3.15 and Figure 3.16, the involvement of *Fur_{Cj}* in *fumC* regulation (if any) and the mechanism could not be substantiated. The same set of strains cultured for 5 hours in high and low iron liquid media (like for β -galactosidase assay) were also analysed, though the same transcriptional profiles were observed which indicated that the differences in iron- and *Fur_{Cj}*-mediated *fumC* regulation was caused by the variations in the initial plate culturing stage between β -galactosidase assay and Holmes'

study and *fumC* regulation is growth condition dependent.

A derepression of *fumC* was observed under high iron conditions in the *racR* mutant background, which indicated NCTC 11168 *fumC* is repressed by RacR under iron replete conditions. A much higher level of transcription was observed for *fumC* under both iron conditions in a *racR* mutant background and under high iron conditions in the *fur_{Cj}* mutant background, and a potential longer secondary transcript of *fumC* was also observed under high iron conditions in the *racR* mutant background. As contradictory results were obtained for iron- and Fur_{Cj}-mediated *fumC* regulation and the involvements of oxygen and PerR were not determined, a detailed characterisation of *fumC* regulation by Fur_{Cj}, RacR and PerR_{Cj} in response to iron and oxygen was performed and is described in chapter 4.

3.3.7 Identification of the transcriptional start site

As promoter activity was not determined from the *chuA* promoter originally cloned in pJMCK6 and contradictory iron-responsive regulations were observed for *fumC*, transcriptional start sites for both *chuA* and *fumC* promoters were identified. Several approaches were investigated in this study including primer extension, RACE and RNA ligation RACE methods (Figure 3.17), and primer extension was initially chosen due to its simplicity (i.e. no cloning involved) over the RACE methods.

Total RNA purified from NCTC 11168 wild-type cultured under low iron conditions

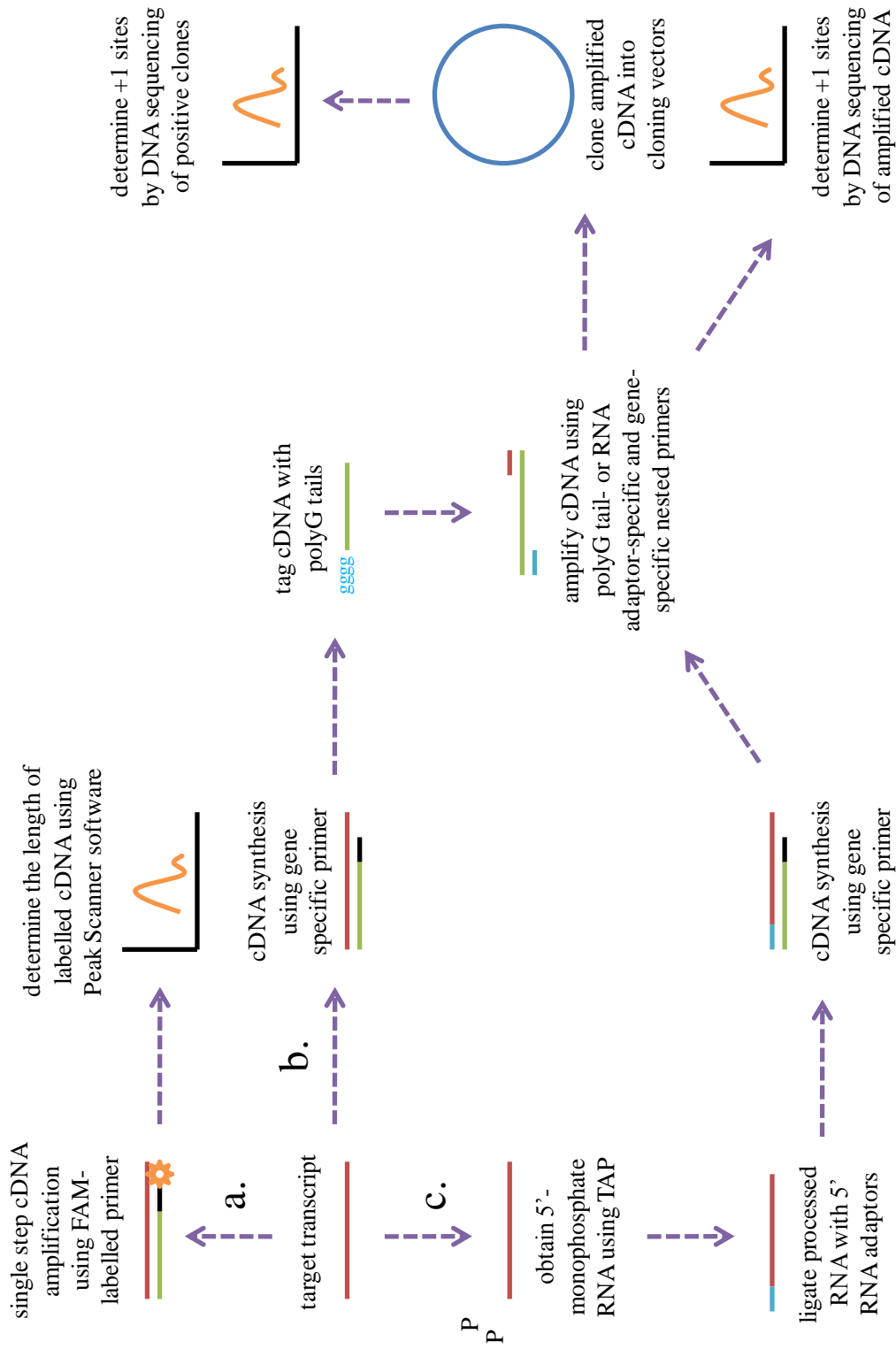


Figure 3.17: Illustration of different approaches used to identify the transcriptional start sites for *chuA* and *fumC*. a. fluorescent primer extension; b. RACE; c. RNA ligation RACE (see text for more detailed descriptions).

was used as a template for *chuA* cDNA synthesis whereas total RNA purified from a *racR* mutant cultured under high iron conditions was used for *fumC* cDNA synthesis as the maximal level of *fumC* transcription was detected. In addition, two *fumC* transcripts with different lengths were also observed in the *racR* mutant background (Figure 3.16) indicating that the *fumC* transcript repressed by RacR is transcribed from an alternative +1 site to the one used for the Fur_{Cj} regulated *fumC* transcript and using total RNA purified from a *racR* mutant would allow the identification of these two +1 sites. The +1 site for the non-iron responsive lipopolysaccharic heptosyltransferase coding *waaC* gene was used as a positive control (Phongsisay and Fry, 2007) and total RNA purified from NCTC 11168 wild-type cultured under normal conditions was used for *waaC* cDNA synthesis.

A fluorescent approach (2.3.6) that had advantages over the conventional radioactive primer extension method in speed and safety was initially applied in which the +1 site could be deduced by determining the length of a FAM-labelled cDNA primer extension product using the Peak Scanner software (Lloyd *et al.*, 2005). *waaC*, *fumC* and *chuA* cDNA were synthesised with corresponding FAM-labelled primers and the labelled cDNA products were concentrated by ethanol precipitation and resuspended with formamide and size markers prior to analysis in a DNA sequencer (Figure 3.17.a). The length of each cDNA product represented by a peak in Peak Scanner software was measured by comparison with the size markers and the +1 site was then deduced from the primer annealing site using the measured cDNA length. No peaks were initially

detected for both samples and the *waaC* control and it was likely to be caused by RNA degradation or low concentration of labelled primer. These possibilities were subsequently eliminated as PCR products with the correct sizes were amplified by reverse transcriptase PCR using the same RNA samples and primer concentration. Ethanol precipitation and formamide rehydration steps were also verified using FAM-labelled PCR product and samples with correct sizes were observed with the detectable level as low as 5 ng of DNA. Both verification steps indicated that the proportion of target transcripts from the total RNA purified was too low, therefore although the concentration of the resulting cDNA product was sufficient enough to allow downstream PCR amplification, it was below the detection level by the DNA sequencer. Several cDNA enrichment steps were subsequently included during the cDNA synthesis step with additional enzyme and dNTPs and although cDNA fragments with stronger signals were detected, they were non-specific cDNA products as fragments of the same size were obtained for *chuA*, *fumC* and *waaC*.

Due to the low cDNA concentration encountered with the primer extension approach, RACE (2.3.7) was used instead to allow amplification of the cDNA by PCR. *chuA*, *fumC* and *waaC* cDNA were amplified with standard primers and tagged with a polyG tail using terminal transferase and dGTPs. The tagged cDNA was then amplified using polyG tail- and nested gene-specific primers and the PCR products were cloned into pUC19. The +1 site for each gene was then determined either by direct sequencing of the PCR products or the final constructs (Figure 3.17.b). Sequencing results were not

obtained from direct sequencing of the DNA products and *fumC* DNA could not be cloned into pUC19 despite several attempts. *chuA* and *waaC* cDNA cloned into pUC19 were sequenced and only one putative site was determined for *chuA* though this site was 4 bp downstream from the start codon. As the control *waaC* +1 was not determined, the validity of the site determined for *chuA* could not be substantiated and the *chuA* cDNA amplified and cloned was likely to be a truncated version caused by RNA secondary structure. An additional RNA denaturation step was applied prior to cDNA synthesis but no +1 site was determined for any of the genes.

The last approach investigated was RNA ligation RACE (2.3.7) in which the primary 5'-triphosphate transcripts from the total RNA sample were hydrolysed with TAP and the resulting 5'-monophosphate transcripts were then ligated with RNA adaptors and used as templates for cDNA synthesis. The cDNA samples were amplified using RNA adaptor- and nested gene-specific primers and the PCR products were cloned and the +1 sites were determined as described by standard RACE (Figure 3.17.c.). The RNA ligation RACE has many advantages over the standard RACE as it allows a selection and enrichment of the primary transcripts from processed RNA and the RNA adaptor is more specific than the less defined homo nucleotide adaptor that allows more accurate identification of +1 site by sequencing (Gerhart *et al.*, 2009). *chuA* and *fumC* cDNA were synthesised from the TAP treated and untreated RNA samples and were compared by electrophoresis (Figure 3.18). Enriched *chuA* cDNA product was observed for TAP treated RNA when compared with untreated RNA and two bands containing enriched

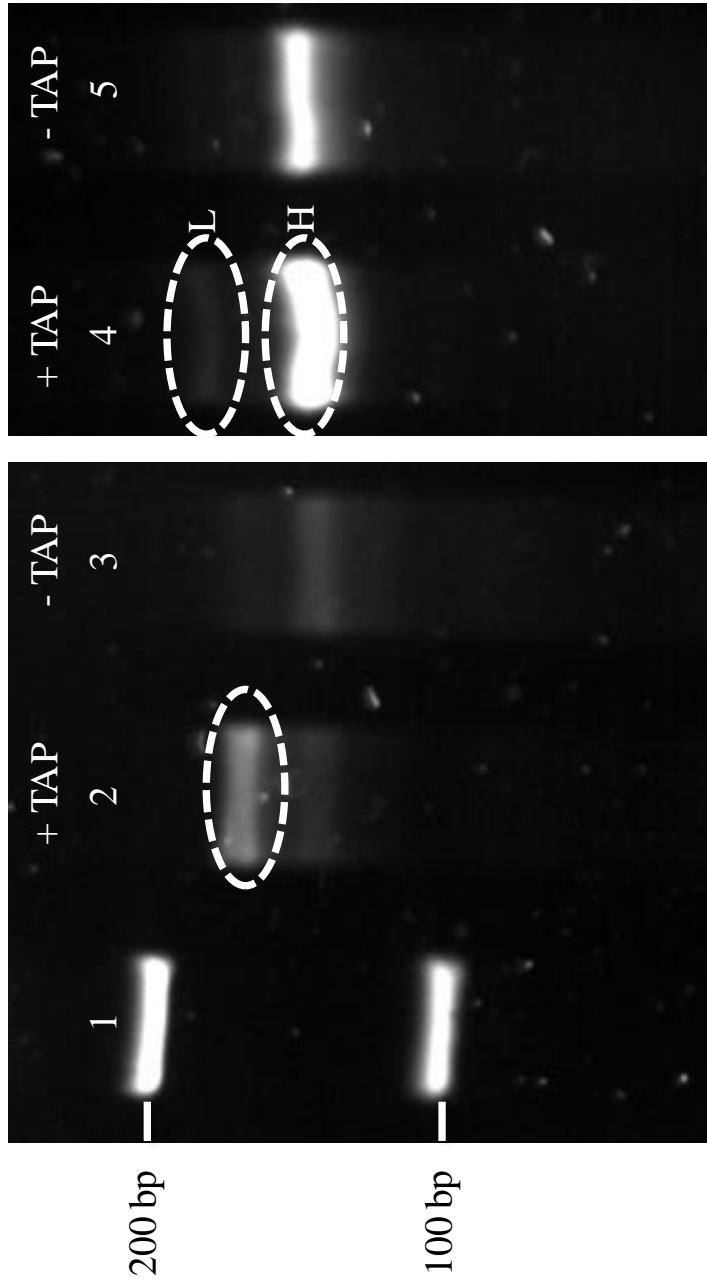


Figure 3.18: Comparison of *chuA* and *fumC* cDNA synthesised from the TAP treated and untreated RNA. Lane: 100 bp log ladder (New England Biolabs); lanes 2 and 3: *chuA* cDNA; lanes 4 and 5: *fumC* cDNA. Bands containing the enriched cDNA are circled and two bands circled for *fumC* are termed L and H intensity.

fumC cDNA (L and H) were detected which indicated the presence of two transcripts with difference lengths and hence two potential corresponding +1 sites.

The enriched cDNA samples for *chuA*, *fumC* L band and *fumC* H band were extracted from the gel and used as templates for cDNA amplification. The PCR products were then cloned into pGEM-t easy and the +1 sites were determined by sequencing. A +1 site 51 bp upstream of the *chuA* start codon and a +1 site 25 bp upstream of the *fumC* start codon were identified from direct PCR product sequencing and the -10 region for each promoter were subsequently mapped (Figure 3.19). The +1 site identified for *fumC* was in agreement with previously 454 RNA sequencing data (A. van Vliet, unpublished data), however the same +1 site was determined for PCR products amplified using cDNA extracted from both the L and H bands which indicated that both cDNA samples were not completely separated during electrophoresis. The distance between the *chuA* +1 site and -10 region was not ideal but the +1 site was acceptable when compared with the 454 RNA sequencing data and was within the optimal range for a *C. jejuni* 5' un-translated region (UTR, A. van Vliet, personal communication). The predicted -35 region for the *fumC* promoter overlaps with the 11th to 16th bases of the *fumC* Fur_{Cj} box which indicated that the decreased promoter activities observed for mutated *fumC* Fur_{Cj} boxes containing the 13th base change (Figure 3.9) were caused by the disruption of the *fumC* -35 region. Likewise the predicted *chuA* -10 region was located just downstream from the 5' boundary of the *chuA* promoter originally cloned in pJMCK6 (Figure 3.11) therefore the absence of promoter activity observed for the original construct (Figure

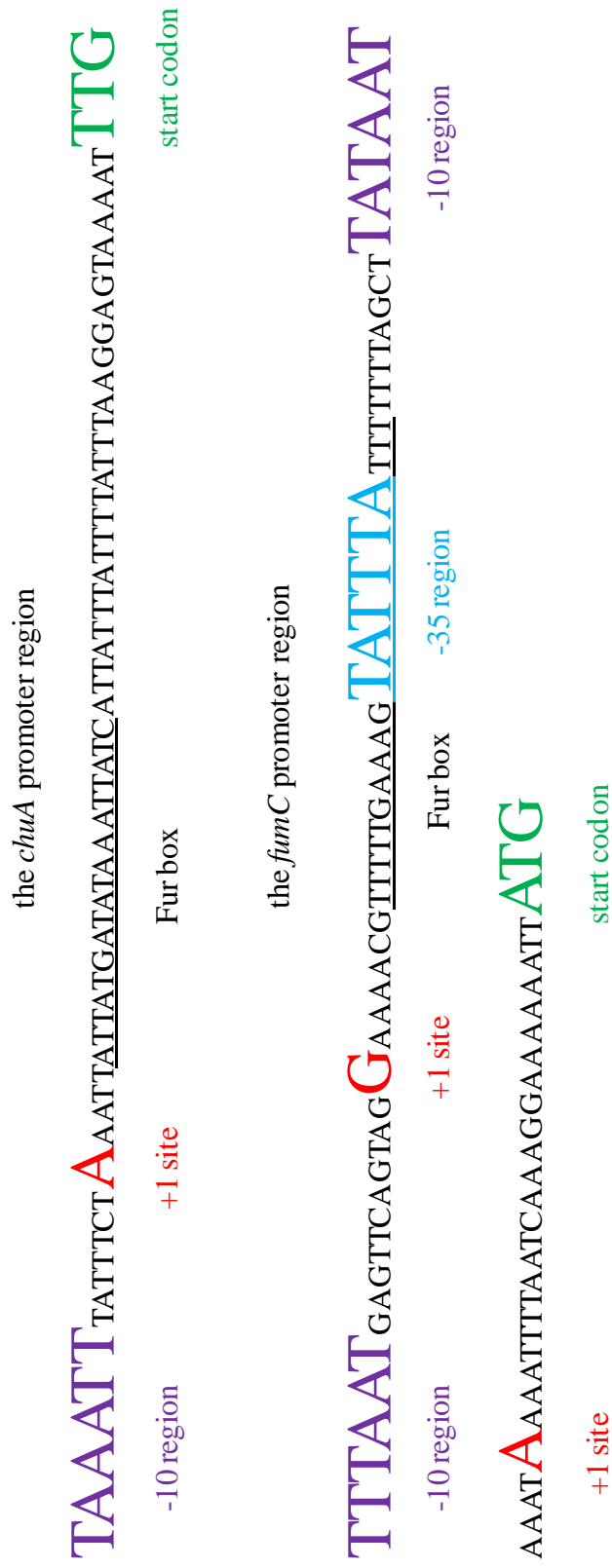


Figure 3.19: Organisation of the *chuA* and *fumC* promoter regions. The +1 site for *chuA* is located 4 bp upstream from the *chuA* Fur_{Cj} box while the *fumC* Fur_{Cj} box overlaps the *fumC* -35 region. The -35 region, the -10 region, the +1 site and the start codon are coloured in blue, purple, red and green respectively whereas the Fur_{Cj} box is underlined.

3.7) was caused by the absence of a functional -35 region.

When constructs containing *chuA* and *fumC* PCR products were sequenced, a second +1 site located 69 bp upstream from the *fumC* start codon was identified for PCR products amplified from the L band. The longer transcript transcribed from this second +1 site was only detected in RNA samples purified from a *racR* mutant cultured under high iron conditions and the level of this longer transcript was much less than the primary transcript detected by northern blot and cDNA synthesis (indicated by the H band) suggesting that the mRNA transcribed from this +1 site was likely to be a weaker secondary transcript repressed only by RacR. Two faults “+1 sites” were also detected for *chuA* as both sites were located downstream from the start codon, therefore they were likely to be caused by truncated cDNA products due to RNA secondary structures. RNA ligation RACE was repeated for *chuA* and the +1 site determined was in agreement with the results originally determined by direct PCR sequencing.

3.3.8 DNase I footprinting assay

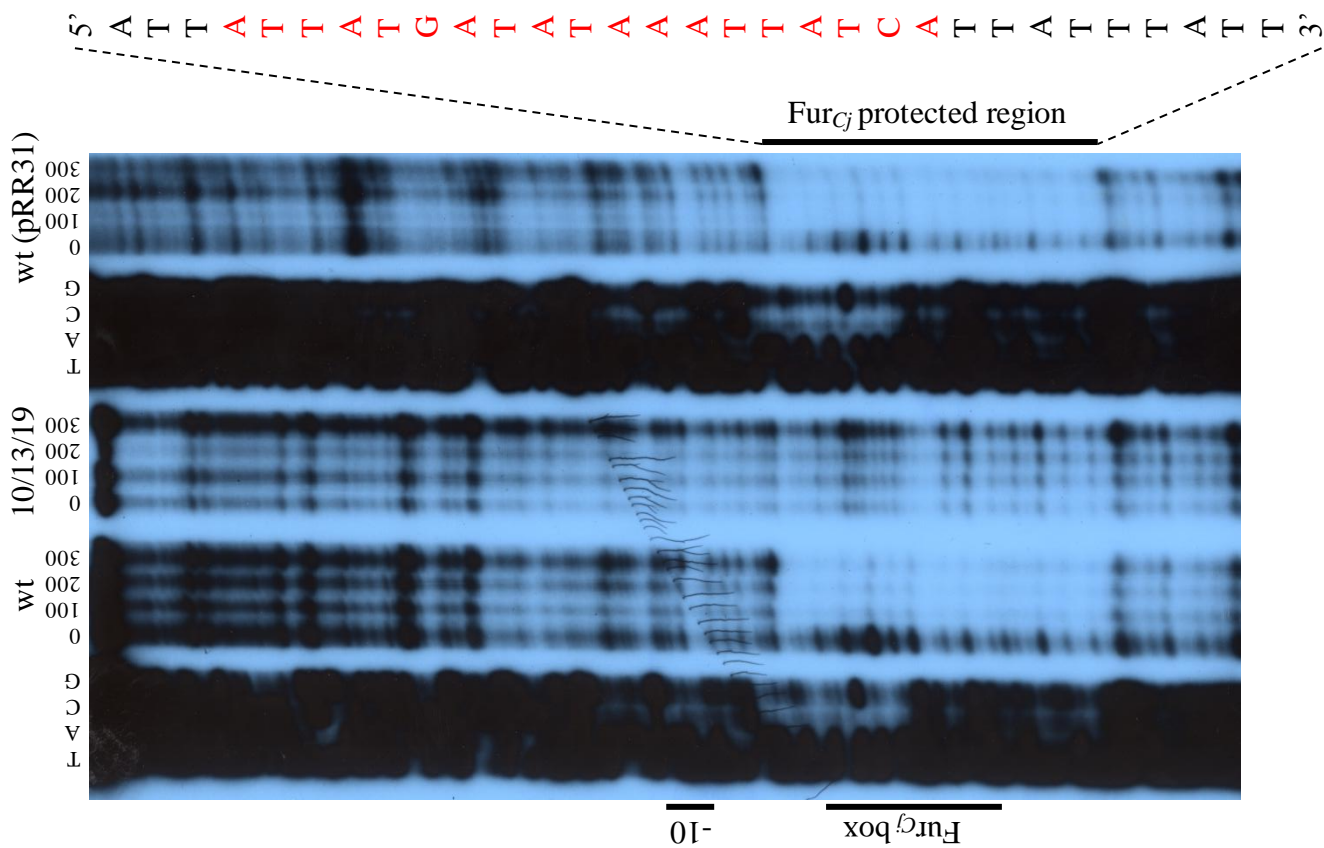
To determinate the location of Fur_{Cj} binding site on the *chuA* and *fumC* promoters and to verify the proposed Fur_{Cj} box sequence, DNase I footprinting assays were performed for the wild-type and mutated *chuA* and *fumC* promoter regions. A DIG-based DNase I footprinting technique was previously used to identify the Fur_{Hp} binding site for *H. pylori sodB* gene though a sequencing ladder was not included in this investigation thus the relative position of the Fur_{Hp} box could not be determined (Ernst *et al.*, 2005). A

possibility of generating a DIG-based sequencing ladder was therefore initially explored and although various sequencing reactions and PAGE conditions were tested, a ladder with clear separation and resolution was not achieved and the more conventional radioactive alternative was therefore used. The method described by Fuangthong and Helmann (2003) was used for this investigation and various buffer concentrations and experimental conditions were optimised (2.2.27).

The *chuA* wild-type promoter (the unextended version without promoter activity) and the *chuA*_{10/13/19} promoter cloned into pMW10 (pRR15 and pRR22 respectively) were first used as templates to amplify DNA fragments for subsequent manual sequencing and DNase I footprint assays. The primers used for these amplifications were designed so that the Fur_{Cj} box was positioned in the centre of each amplicon that contained part of pMW10 and part of the *chuA* promoter thus allowing a better separation and resolution on the PAGE gel. However to avoid overlooking any additional Fur_{Cj} binding or polymerisation sites further upstream from the *chuA* Fur_{Cj} box, the extended *chuA* wild-type promoter (pRR31) containing the *chuA* and *chuZ* intregenic region up to the *chuZ* Fur_{Cj} box was also tested.

A 31 bp Fur_{Cj} protected region was detected for the *chuA* wild-type promoter (Figure 3.20) resulting from the binding of two Fur_{Cj} dimers, and this mechanism of Fur_{Cj}-Fur_{Cj} box interaction was in agreement with the two shift species observed by EMSAs. The Fur_{Cj} protected region was positioned 2 bp downstream from the +1 site and the

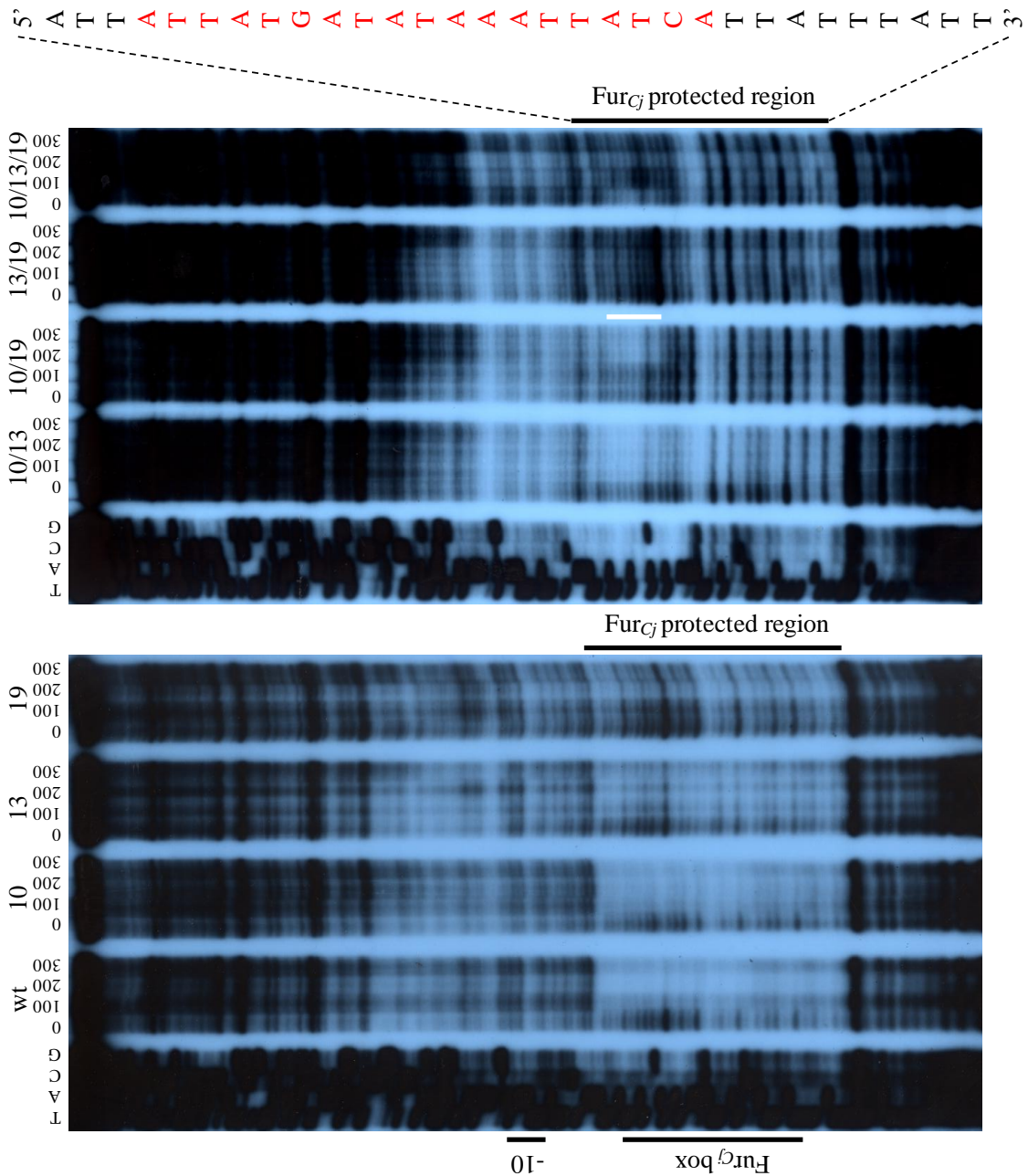
Figure 3.20: DNase I footprinting assays for *chuA* wild-type and *chuA10/13/19* promoters along with corresponding sequencing ladders. *Fur_{Cj}* concentration used ranged from 0 to 300 nM. Regions representing the -10 region and the *Fur_{Cj}* box and the *Fur_{Cj}* protected region are indicated by black lines on the left and right sides of the film respectively. The DNA sequence for the *Fur_{Cj}* protected region is indicated on the left hand side of the figure with the putative *Fur_{Cj}* box highlighted in red.



predicted *chuA* Fur_{Cj} box was completely overlapped by this region. These observations provided direct physical evidence that the iron induced *chuA* repression is mediated by the direct binding of the Fur_{Cj} protein to the *chuA* Fur_{Cj} box located in the promoter region. Such binding will prevent the functional interaction between the RNA pol and the -10 region or prevent the RNA pol from transcribing the DNA template. The Fur_{Cj} protected region was completely abolished for *chuA10/13/19* as a direct result from the mutational changes in the Fur_{Cj} box which have led to a dramatic decrease in the affinity of Fur_{Cj} binding, an observation in agreement with the corresponding EMSA data (Figure 3.4). No secondary Fur_{Cj} binding or polymerisation sites were detected for the extended *chuA* promoter which indicated that the binding of two Fur_{Cj} dimers is sufficient to block the transcription of *chuA* and the only Fur_{Cj} binding site is associated with the predicted Fur_{Cj} box.

Based on the DNase I footprinting data obtained with the unextended wild-type *chuA* promoter, DNase I footprinting assays were subsequently performed for all the unextended *chuA* mutant promoters cloned into pMW10 (pRR16-22) and are shown in Figure 3.21. The 31 bp Fur_{Cj} protected region was consistently observed for the wild-type and *chuA10* promoters and a less defined but identifiable protected region was obtained with *chuA13* and *chuA19* promoters. Smaller protected regions were observed for the *chuA10/13* and *chuA10/19* promoters. The latter case clearly demonstrated that a high affinity Fur_{Cj} binding was not achieved at the 3' end of the *chuA* Fur_{Cj} box containing the 13th or 19th mutational changes and this smaller protected

Figure 3.21: DNase I footprinting assays for *chuA* wild-type and mutated promoters along with corresponding sequencing ladders. *Fur_{Cj}* concentration used ranged from 0 to 300 nM. Regions representing the -10 region and the *Fur_{Cj}* box and the *Fur_{Cj}* protected region are indicated by black lines on the left and right sides of the film respectively. A smaller protected region seen with *chuA*10/19 is indicated by a white line. The DNA sequence for the *Fur_{Cj}* protected region is indicated on the left hand side of the figure with the putative *Fur_{Cj}* box highlighted in red.



region may reflect the binding of a single dimer. No Fur_{Cj} protected region was observed for *chuA*13/19 and *chuA*10/13/19 promoters and the DNase I footprinting results for *chuA* wild-type and mutated promoters collectively demonstrated the importance of the 13th and 19th positions of the Fur_{Cj} box in Fur_{Cj}-Fur_{Cj} box interaction and in maintaining the integrity of the Fur_{Cj}-Fur_{Cj} box complex and this observation was also consistently observed by EMSAs and β-galactosidase assays.

For the *fumC* wild-type promoter, no Fur_{Cj} protected region was observed (Figure 3.22). This was expected as EMSA data (Figure 3.4) indicated that Fur_{Cj} protein does not bind to the *fumC* promoter region. A 31 bp Fur_{Cj} protected region was identified for the *fumC*10/13/19 promoter immediately upstream from the -10 region and the mutated Fur_{Cj} box was again completely overlapped by this region. When DNase I footprinting assays were carried out for all the *fumC* mutant promoters (Figure 3.23), a poorly defined Fur_{Cj} protected region was only observed for the *fumC*19, *fumC*13/19 and *fumC*10/13/19 promoters with a high Fur_{Cj} concentration. The clear defined Fur_{Cj} protected region demonstrated for the *fumC*10/13/19 promoter (Figure 3.22) was not reproduced and the Fur_{Cj} binding activities for *fumC*10 and *fumC*13 Fur_{Cj} boxes detected by EMSA were also not observed. The intensity of the DNase I footprinting samples for the *fumC* wild-type promoter was very low, and this was likely to be caused by the degradation of pRR23 which was used to amplify this promoter. Several experimental repeats were performed though clearer results were not obtained possibility due to Fur_{Cj} degradation. The protected regions obtained the *fumC*19,

Figure 3.22: DNase I footprinting assays for *fumC* wild-type and *fumC*10/13/19 promoters along with corresponding sequencing ladders. *Fur_{Cj}* concentration used ranged from 0 to 300 nM. Regions representing the -10 region and the *Fur_{Cj}* box and the *Fur_{Cj}* protected region are indicated by black lines on the left and right sides of the film respectively. The DNA sequence for the *Fur_{Cj}* protected region is indicated on the left hand side of the figure with the putative *Fur_{Cj}* box highlighted in red. N.B. DNase I footprinting samples for both promoters with 100 nM *Fur_{Cj}* were loaded the wrong way around due to human error.

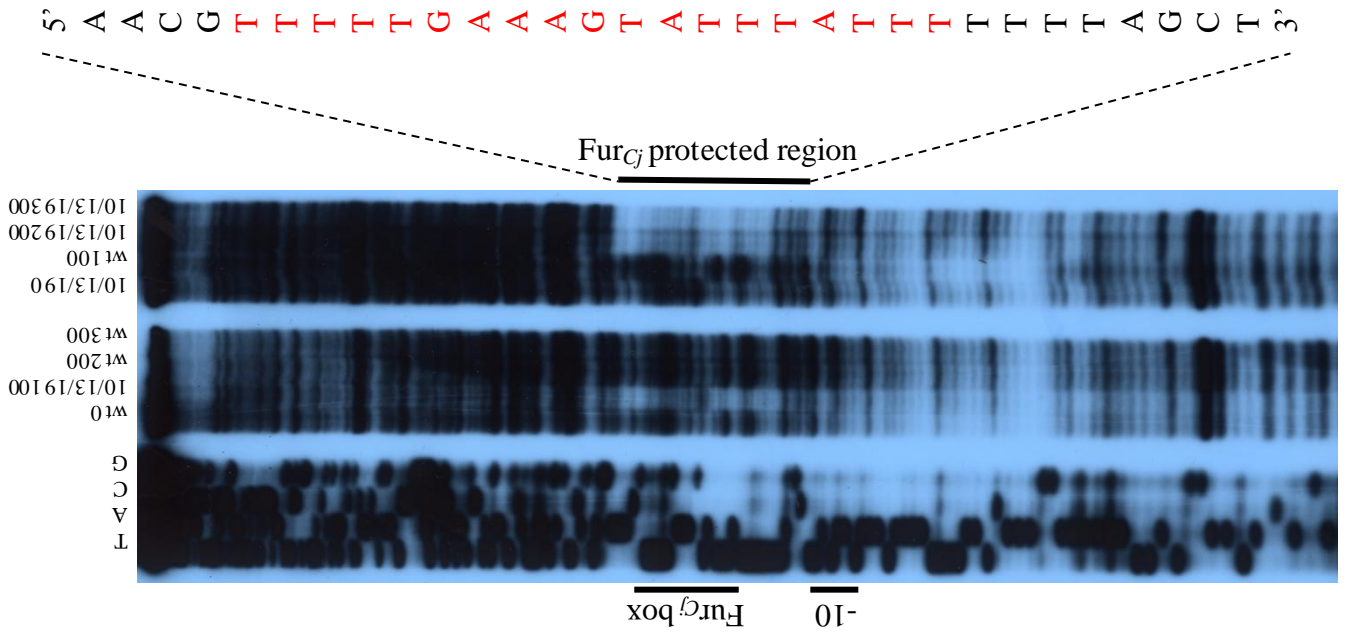
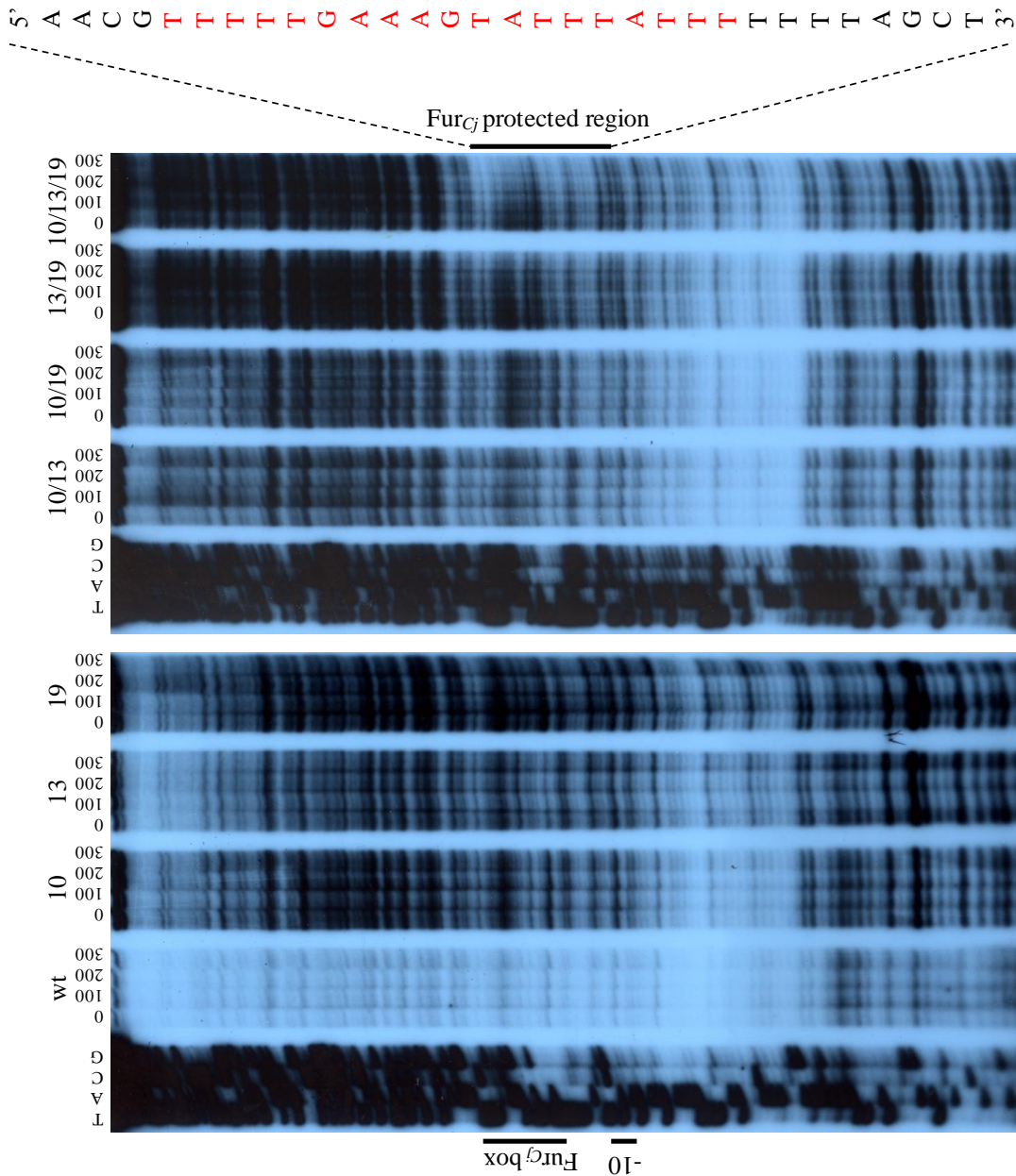


Figure 3.23: DNase I footprinting assays for *fumC* wild-type and mutated promoters along with corresponding sequencing ladders. *Fur_{Cj}* concentration used ranged from 0 to 300 nM. Regions representing the -10 region and the *Fur_{Cj}* box and the *Fur_{Cj}* protected region are indicated by black lines on the left and right sides of the film respectively. The DNA sequence for the *Fur_{Cj}* protected region is indicated on the left hand side of the figure with the putative *Fur_{Cj}* box highlighted in red.



*fumC*_{13/19} and *fumC*_{10/13/19} promoters nevertheless demonstrated the crucial roles of the 13th and 19th positions of the Fur_{Cj} box and these observations were consistent with the increased affinity of Fur_{Cj} binding toward the mutated *fumC* Fur_{Cj} box observed with EMSAs.

3.3.9 Further characterisation of the Fur_{Cj} box

Although the importance of the 13th and 19th positions of the Fur_{Cj} box were clearly demonstrated in this study, however mutation of these positions only enables the investigation of the 3' end of the Fur_{Cj} box. The 1st and 7th positions of the Fur_{Cj} box were subsequently analysed as they are in symmetry with the 13th and 19th bases and also contain the base adenine. To keep a consistency in the mutational schemes, A to T mutational changes were applied to these two bases (1T and 7), and as T is also an option for the 1st base of the consensus sequence, an A to C mutational change was also applied (1C). The extended wild-type *chuA* promoter region was cloned into pUC19 (pRR47) and was used as template for mutagenesis. Promoters containing the mutational changes were then cloned into pMW10 and were used as templates for EMSAs and for β -galactosidase assays. Mutagenesis, EMSAs and β -galactosidase assays described in this section were carried out by T. Caudle under supervision.

No shift pattern variations were observed for *chuA*_{1T} when compared with the wild-type (Figure 3.24), however for *chuA*_{1C}, *chuA*₇ and *chuA*_{1T/7} mutants, the concentration of upper shift species representing the binding of two Fur_{Cj} dimers was

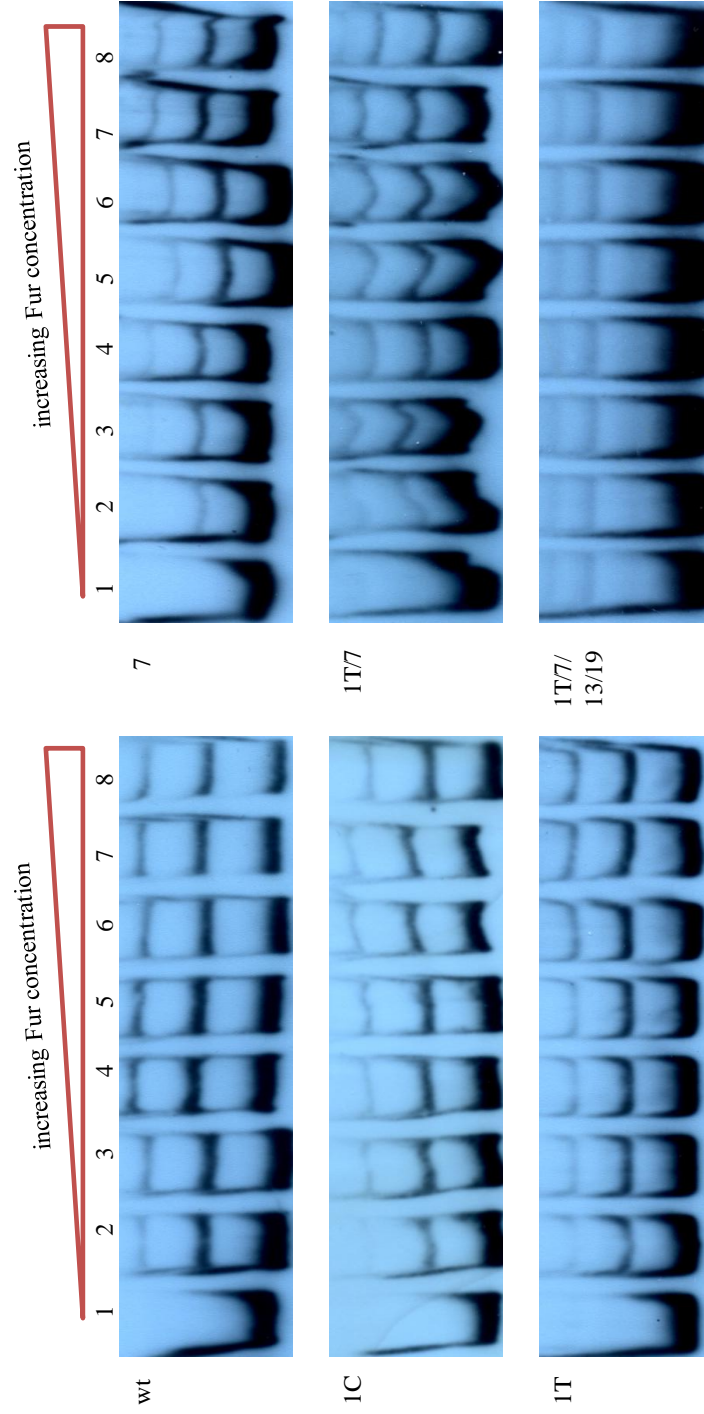


Figure 3.24: Standard EMSA of 1.55 fmol labelled *chuA* promoter regions containing the wild-type and mutated Fur_{CJ} boxes with the purified Fur_{CJ} protein. Lanes 1-8: labelled DNA with 0 nM, 25 nM, 50 nM, 75 nM, 100 nM, 125 nM, 150 nM and 175 nM Fur_{CJ} respectively.

decreased and was only observed when the Fur_{Cj} concentration was increased to 50 - 75 nM. When EMSA was performed for *chuA1T/7/13/19*, the ability for Fur_{Cj} to bind the Fur_{Cj} box was completely abolished indicating the functional importance of these four positions in the Fur_{Cj} box. When compared with the EMSAs data shown in Figure 3.4, the affinity of Fur_{Cj} binding to the wild-type *chuA* Fur_{Cj} box was decreased indicating potential Fur_{Cj} degradation or person to person variation. However due to the comparative nature of this test and the clear observation of two shift species, further Fur_{Cj} purification was not performed.

When the promoter activity for each mutant was tested by β -galactosidase assays (Figure 3.25), various levels of derepression were observed for *chuA1C*, *chuA7*, *chuA1T/7* and *chuA1T/7/13/19* which indicated a decrease in the affinity of Fur_{Cj} binding and also in agreement with the EMSA results. When compared with the wild-type promoter under high iron conditions, the level of repression for *chuA1T* mutant was higher than the wild-type which indicated that at this position of the Fur_{Cj} box, T is more favourable for Fur_{Cj} than A. However, a higher level of derepression was observed under high iron conditions for *chuA1T/7* when compared with *chuA7*. In addition, although the ability for Fur_{Cj} to interact with the *chuA1T/7/13/19* Fur_{Cj} box was completely abolished (Figure 3.24), the *chuA1T/7/13/19* promoter was only partially derepressed under high iron conditions (Figure 3.25). These observations were likely to be caused by inaccuracies of the β -galactosidase assays

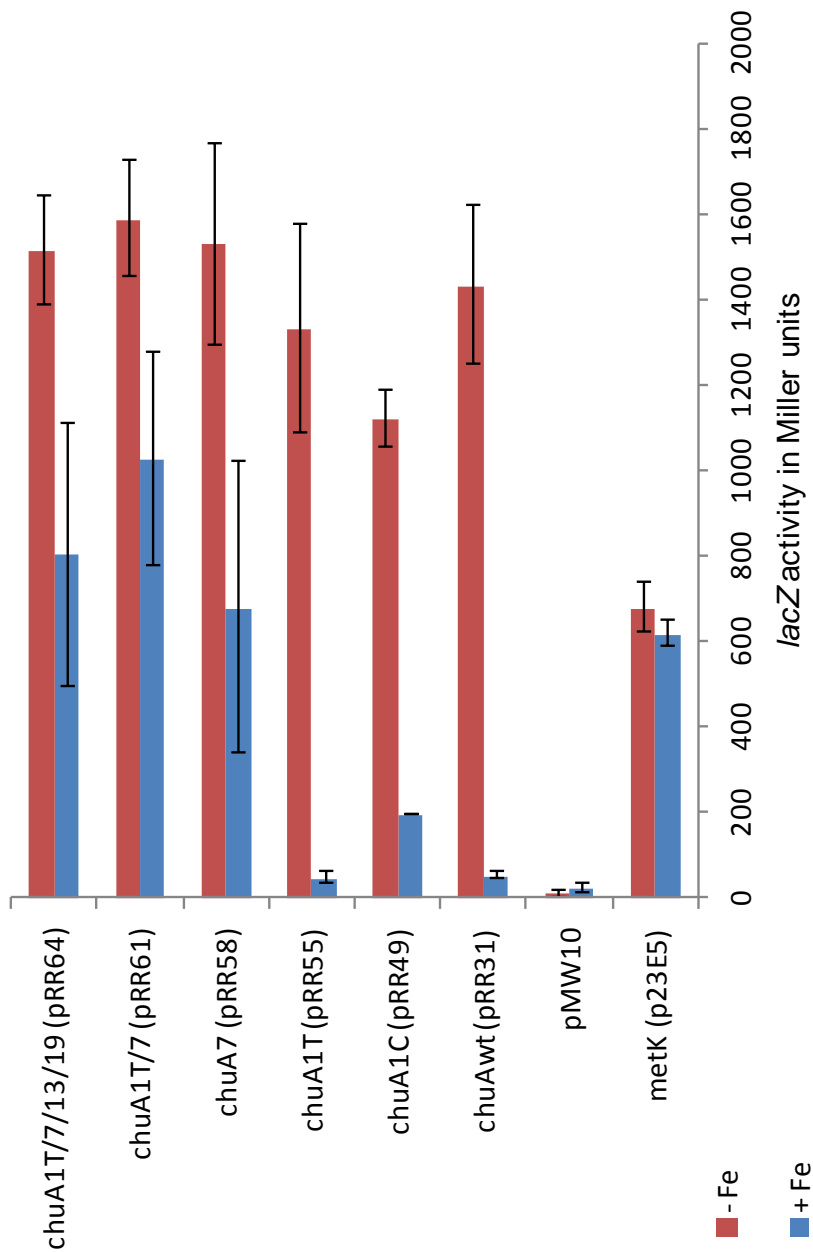


Figure 3.25: β -galactosidase assay of the *chuA* wild-type and mutated promoter regions with controls under high iron ($40 \mu\text{M FeSO}_4$) and low iron ($20 \mu\text{M Desferal}$) conditions. Data presented are the means of triplicate sampling from two independent experiments with the standard error.

3.4 Discussions

The Fur protein has been extensively characterised in many bacteria as a global regulator that controls an array of genes ranging from iron acquisition to enzyme metabolism, however the model of Fur-Fur box interaction has been controversial which led to several interpretations of the functional Fur binding site (Lee and Helmann, 2007). The transcriptional response of *C. jejuni* genes to iron availability and Fur_{Cj} is also pleiotropic (Palyada *et al.*, 2004; Holmes *et al.*, 2005) and although *in vitro* binding of Fur_{Cj} to the promoter region of several members of the Fur_{Cj} regulon involved in iron acquisition have been previously demonstrated (Holmes *et al.*, 2005; Li, 2005; Ridley *et al.*, 2006; Berg, 2007; Miller *et al.*, 2008; Shearer *et al.*, 2009), the mechanism and the location of Fur_{Cj} binding were not defined. An early characterisation of the promoter region of Fur_{Cj}-regulated genes indicated that the Fur_{Cj} binding site does not correspond well with the defined Fur_{Ec} box (van Vliet *et al.*, 2002), a fact also reflected by the recent proposed Fur_{Cj} box consensus sequence (Palyada *et al.*, 2004), which together suggested potential variation in the mechanism of DNA recognition and Fur-DNA interaction between Fur_{Cj} and Fur_{Ec}. In this investigation, the 19 bp Fur_{Cj} box was verified using the *chuA* and *fumC* promoter regions and functionally important bases were determined, which revealed an unconserved mechanism of Fur_{Cj} box recognition by Fur_{Cj}.

3.4.1 Fur_{Cj}-Fur_{Cj} box interaction

Detailed EMSA and Ferguson analysis of natural and synthetic DNA hexamers and

heptamers with Fur_{Ec} and Fur_{Bs} have determined two shift species which represented the forming of a DNA-Fur complex with either single or double Fur dimers and the binding of two Fur dimers on each side of the DNA template was associated with the 19 bp Fur box (Lavrrar and McIntosh, 2003; Baichoo and Helmann, 2002). When the wild-type *chuA* promoter region was analysed by EMSA, two distinct shift species were observed at a low Fur_{Cj} concentration and the concentration of the upper shift species was significantly increased at a higher Fur_{Cj} concentration. The same two species were also observed with *fumC*_{10/13/19}, and these findings indicated that in the functional state, two Fur_{Cj} dimers recognise and cooperatively bind to the Fur_{Cj} box and the binding of one dimer observed by EMSAs is likely to be the intermediate state rather than the functional state.

Further characterisation of the *chuA* promoter region by DNase I footprinting assay has revealed a 31 bp Fur_{Cj} protected region that is typical of the size observed for *E. coli* (de Lorenzo *et al.*, 1987). Fur_{Pa} is approximately 15.2 kDa in size (Vasil, 2007) which is expected to protect 20 bp of DNA in a DNase I footprinting assay (Pohl *et al.*, 2003). As Fur_{Cj} is approximately 17.5 kDa in size, therefore the formation of a typical 31 bp protected region indicated that the binding of the two Fur_{Cj} dimers are likely associated with opposite sides of the DNA molecule. Fur_{Cj} polymerisation was not detected when the extended *chuA* promoter was analysed indicated the binding of two Fur_{Cj} dimers is sufficient to repress the transcription of *chuA*.

Two shift species were also observed when the iron-regulated *p19* operon promoter and *cj0176c* and *cj0177* promoters were analysed by EMSA (Berg, 2007; Miller *et al.*, 2008) which suggested that potentially in *C. jejuni*, Fur_{Cj}-dependent transcriptional repression is mediated by the binding of only two Fur_{Cj} dimers to the Fur_{Cj} box. Fur_{Cj} polymerisation was reported when the *chuA-chuZ* intergenic region was investigated where four shift species were observed (Ridley *et al.*, 2006). However as the *chuA* and *chuZ* Fur_{Cj} boxes were both within the intergenic region, the multiple shift species were likely to be the various stages of Fur_{Cj} binding to the two Fur_{Cj} boxes rather than Fur_{Cj} polymerisation along the DNA template. Only one shift species was observed when the *cfrA* and *ceuB* promoters and the *p19* operon promoter were investigated (Holmes *et al.*, 2005), and this was potentially caused by the different amount of the Fur_{Cj} protein used rather than any functional difference in Fur_{Cj} binding between these promoter regions. The relatively small Fur_{Cj} concentration used by Holmes *et al.* (2005) was not reproduced in this and Berg's (2007) studies even when the original protein sample was used suggesting a possible miscalculation of the Fur_{Cj} concentration in Holmes *et al.*'s study.

3.4.2 The location of Fur_{Cj} binding

When DNase I footprinting assays were carried out for the wild-type *chuA* promoter region, a 31 bp protected region that completely overlaps the consensus Fur_{Cj} box sequence was observed (Figure 3.20). When the consensus matching Fur_{Cj} binding sequence was introduced into the *fumC* promoter (i.e. *fumC10/13/19*), a Fur_{Cj} protection

region with the same size was also detected that overlapped the mutated Fur_{Cj} box-like sequence. These observations indicated the validity of the proposed Fur_{Cj} box sequence and this sequence was sufficient to induce Fur_{Cj} binding to functional unrelated DNA sequence (i.e. *fumC* Fur_{Cj}-box like sequence). However due to the limitation of the DNase I footprinting assay, whether the proposed 19 bp sequence is or only contains part of the Fur recognition site cannot be easily established. As this is the only verification of the Fur_{Cj} binding site to date, further detailed DNase I footprinting analyses of other defined Fur_{Cj}-repressed promoters are required to allow direct comparisons of experimentally conferred Fur_{Cj} protected regions.

To identify the location of Fur_{Cj} binding with respect to the promoter elements, +1 site for *chuA* and *fumC* transcripts were mapped. Initial difficulties such as the low level of target transcripts and RNA secondary structure were encountered with both fluorescent primer extension and conventional RACE methodologies and the +1 site for each gene was eventually identified using RNA ligation RACE which offers high specificity and accuracy. The mapped promoter region of each gene with identified Fur_{Cj} protected regions are summarised in Figure 3.26.

The *chuA* transcript contains a 51 bp 5' UTR and the Fur_{Cj} box is located just 4 bp downstream from the +1 site. This finding combined with the Fur_{Cj} protected region identified by DNase I footprint assay demonstrated the iron-repressed regulation of *chuA* is mediated by the direct binding of Fur_{Cj} to the UTR downstream of the *chuA*

promoter region and this Fur_{Cj}-DNA interaction thus prevents the RNA pol from further transcribing the downstream *chuA* gene. Two *fumC* +1 sites were identified in a *racR* mutant background suggesting *fumC* is under the control of more than one regulator. RacR as well as Fur_{Cj} are likely to play important role in the regulation of *fumC* and this is characterised in chapter 4. The mapping of the promoter region of both genes has also provided a physical explanation of the abnormal promoter activities encountered for both genes as the -35 region was missed out from the original *chuA* promoter clone whereas the *fumC* -35 region was disrupted by the mutation introduced to the 13th position of the *fumC* Fur_{Cj}-box like region. As the *C. jejuni* genome is very AT-rich and especially in the promoter regions, therefore detailed promoter mapping should always be applied in future promoter or gene regulation studies.

3.4.3 Functional important bases of the Fur_{Cj} box

The *chuA* Fur_{Cj} box is a perfect match to the proposed Fur_{Cj} box and it has a high affinity of Fur_{Cj} binding and a strong functional repression *in vivo*. The Fur_{Cj}-box like sequence for *fumC* on the other hand does not bind Fur_{Cj} and this is likely caused by the three mismatches at the 10th, 13th and 19th positions of this Fur_{Cj}-box like sequence when compared to the 19 bp consensus sequence. This Fur_{Cj} box sequence variation was predicted to play an important role in the contrasting Fur_{Cj} and iron regulation between *chuA* and *fumC*. When the mutated *chuA* and *fumC* promoter regions were compared by a combination of EMSA, β -galactosidase and DNase I footprinting assays, a dramatic decrease in the ability of Fur_{Cj} to recognise and bind to the mutated Fur_{Cj} box was

observed for *chuA*, in particular with mutants containing 13th and/or 19th base changes. When these bases were introduced into the *fumC* Fur_{Cj}-box like sequence, the ability to bind Fur_{Cj} was partially restored which supported the functional importance of these two bases. Further characterisation of the 5' end of the *chuA* Fur_{Cj} box also indicated the functional importance of the adenine at the 1st and 7th positions of the Fur_{Cj} box as the Fur_{Cj}-DNA interaction was completely abolished for *chuA*1T/7/13/19 (Figure 3.24).

Based on missing T contact studies of the hexamer model described by Escolar *et al.* (1998), the AT motif of the GATAAT hexamer was predicted to be an essential recognition element in direct contact with Fur_{Ec} as the Fur_{Ec}-DNA interaction was abolished or impaired when the thymine at the 3rd and 6th and -2nd and -5th (corresponding to the second and fifth adenines on the top strand) were substituted with uracil (Escolar *et al.*, 1998). Using UV crosslinking and mass spectrometry, Tyr55 of the Fur_{Ec} protein and the thymines at the 15th and 16th position of the Fur_{Ec} box were demonstrated to be involved in binding and the TT motif is also presented in the *P. aeruginosa* and *B. subtilis* Fur boxes (Tiss *et al.*, 2005). Furthermore, mutational studies of the Fur_{Bs}, PerR_{Bs} and Zur_{Bs} boxes have also demonstrated that the 5th and 6th bases of the heptamer model are important for the discrimination of their target site by Fur_{Bs}, PerR_{Bs} and Zur_{Bs} as small changes in these sites were sufficient to alter binding preferences amongst the three proteins (Fuangthong and Helmann, 2003). When a five base AT-rich region of the Fur_{Ec} binding site in the *E. coli* *fepDGC-entS* promoter region was substituted with a GC-rich sequence, the ability of Fur_{Ec} binding was inhibited.

However when the important AT bases were introduced into the Fur_{Ec} box to enhance Fur_{Ec} binding, dramatic improvements in the affinity of Fur_{Ec} bind to this sequence were not observed which have led to the suggestion that although certain bases in the Fur box may play a more important role than others in determining Fur binding affinity, the overall architecture of the binding site is more critical in determining how well Fur recognises the Fur box (Lavrrar *et al.*, 2002).

As each study has its own interpretation of the Fur box, a consensus model of base-dependent sequence recognition by Fur and subsequent protein-DNA interaction could not be easily determined, therefore it's difficult to conclude the functional importance of the adenine at the 1st, 7th, 13th and 19th bases of the Fur_{Cj} box by correlating with previous observations in other organisms. When EMSAs were carried out for *chuA13* and *chuA19* (Figure 3.5), although the concentration of unbound DNA was slightly increased at a higher Fur_{Cj} concentration, two shift species were clearly observed with as little as 25 nM Fur_{Cj}. On the other hand, the higher shift species was only clearly observed for *chuA1C* and *chuA7* at a Fur_{Cj} concentration between 50-75 nM therefore potentially suggesting that adenine at the 13th and 19th positions may play important roles in stabilising the Fur_{Cj}-Fur_{Cj} box complex or maintaining the important overall binding site architecture that allows high affinity Fur_{Cj} binding. The 1st and 7th bases on the other hand are likely to play roles in initial Fur_{Cj} recognition. In addition, because the Fur_{Cj} protected region determined for *chuA* has suggested that Fur_{Cj} binds to the Fur_{Cj} box on both sides of the DNA, therefore some mutational effects observed for

the adenine bases may be caused by the indirect alteration of the four thymine bases on the bottom stand of the Fur_{Cj} box and as the precise model of Fur_{Cj} box recognition by Fur_{Cj} was not determined, the potential importance of these bases could not be substantiated. In order to understand the precise mechanism of Fur_{Cj}-Fur_{Cj} box interaction, it would require the determination of a Fur_{Cj}-DNA complex crystal structure, however such study has not yet been performed for any of the Fur orthologues.

3.4.4 Interpretation of the Fur_{Cj} box

Since the identification of the 19 bp Fur_{Ec} box consensus sequence (de Lorenzo *et al.*, 1987), the interpretation of a functional pattern of the Fur box has been the centre of attention rather than the consensus sequence itself. However it should be noted that an exact match to the consensus sequence has not been identified in *E. coli* to date, 14 to 15 bp matches out of the 19 bp are rather more typical and as little as 11 bp matches has been observed for the *tonB* Fur_{Ec} box (Newman and Shapiro, 1999). Therefore considering Fur_{Cj} only shares 40% identity with Fur_{Ec}, it's not all too surprising that the putative Fur_{Cj} box proposed by van Vliet *et al.* (2002) and Palyada *et al.* (2004) matched poorly with the Fur_{Ec} box.

The NAT trimer motif used to identify a Fur_{Cj} binding site for *C. jejuni* (van Vliet *et al.*, 2002) has also been previously used to successfully determine Fur_{Hp} binding site for the closely related *H. pylori* (A. van Vliet, unpublished data). A consensus sequence of AATAATNNTNA has also been proposed as the Fur_{Hp} binding site using a

bioinformatic approach though further experimental analysis of the proposed site were not conducted (Merrell *et al.*, 2003). This divergence in Fur box sequence between the closely related *C. jejuni* and *H. pylori* and *E. coli* is also extended to bacteria from other taxonomic groups. The Fur_{Bj} binding site of *B. japonicum* for example contains three direct hexamer repeats (Friedman and O'Brain, 2003) whereas a consensus of WTGAAAATNATTTTCAW (W represents A or T) was observed for members of the δ -proteobacteria group (Rodionov *et al.*, 2004). Although bioinformatic tools have been generally used to determine the functional Fur binding site that resembles the Fur_{Ec} box, most of the experimental studies with detailed DNase I footprinting analysis were only limited to *E. coli*, *B. subtilis* and *P. aeruginosa*, therefore the Fur-DNA recognition mechanism described for these organisms may not represent all the bacteria.

The Fur_{Cj} box is such an example that although the mechanism of Fur_{Cj}-DNA interaction determined in this study closely resembles of that described for *E. coli* and *B. subtilis*, none of the Fur box interpretations proposed fits well with this sequence. A similar mutational study was carried out for the *C. jejuni p19* operon Fur_{Cj} box where several bases were altered in order to determine bases that are functionally important in Fur_{Cj}-Fur_{Cj} box interaction (Berg, 2007). When the 1st, 5th, 6th, 7th, 9th, and 16th base positions that contained the match bases were mutated and analysed by EMSAs, no significant decreases in the affinity of Fur_{Cj} binding were determined. Surprisingly when the 19th base that contains a mismatch thymine was mutated to adenine to resemble the consensus sequence, a decrease in the ability of Fur_{Cj} to bind the *p19*

operon Fur_{Cj} box was observed that was in contrast to this current investigation (Berg, 2007). As DNase I footprinting assays were not performed in Berg's study, the result variations in particular at the 1st, 7th and 19th positions of the Fur_{Cj} box were likely due to the inaccurate prediction of the *p19* operon Fur_{Cj} box. However both investigations have indicated that most of the bases in the *C. jejuni* Fur_{Cj} box may not play important roles in direct Fur_{Cj}-Fur_{Cj} box interaction and rather is the AT-rich Fur_{Cj} box sequence that maintains the overall architecture of the Fur_{Cj} binding site that allows the Fur_{Cj} protein to bind the target site with various affinities. In another words, the proposed 19 bp sequence might not be the consensus Fur_{Cj} box sequence *per se*, but rather allows the promoter region to form an overall architecture that is in favour of high affinity Fur_{Cj} binding. Further DNase I footprinting analysis of defined Fur_{Cj} regulated promoters are needed to support this hypothesis and to refine or redefine the consensus Fur_{Cj} box sequence.

The importance of individual bases in the Fur_{Cj} box also should not be overlooked as important bases are likely required for Fur_{Cj} to discriminate the true Fur_{Cj} regulatory site from the overall AT-rich genome. When the *chuA10/19* was analysed with DNase I footprinting assay, a much smaller Fur_{Cj} protected region of ATTATGA was observed (Figure 3.21). This region is probably too small to be caused by the binding of one Fur_{Cj} dimer, but this sequence is likely to play an important role in Fur_{Cj} recognition. Interestingly this region is enclosed by the 1st and 7th adenine that are also determined to play critical roles in Fur_{Cj}-DNA recognition, therefore the region enclosed by the 13th

and 19th adenine may also be an important Fur_{Cj} binding site perhaps for the second Fur_{Cj} dimer that binds the bottom strand of the Fur_{Cj} box. Further investigation of the exact role of each important adenine and the region enclosed by them are needed by mutational studies on the refined *C. jejuni* Fur_{Cj} box.

In addition, although a clear correlation between the *in vitro* Fur_{Cj} binding and the *in vivo* transcriptional Fur_{Cj}-repression was observed for the *chuA* wild-type promoter. The altered affinity of Fur_{Cj} binding determined *in vitro* for each mutated promoter may not be accurately reflected or even physiological relevant *in vivo*. For example, although Fur_{Cj}-binding (despite a relative low affinity compared to *chuA*) has been clearly observed for *fumC*_{10/19} by EMSAs and DNase I footprinting assays (Figures 3.6 and 3.23), its expressions was not affected under high iron conditions in β-galactosidase assays. The ability for Fur_{Cj} to bind the *chuA*_{1T/7/13/19} promoter was complete abolished (Figure 3.24), however its expression was only partially derepressed under iron-rich conditions. These result discrepancies were largely due to the drawbacks of the multi-copy plasmid reporter system used in this study. The large pMW10 copy number meant that *in vivo*, the Fur_{Cj} binding site cloned into each plasmid was essentially diluting the intercellular Fur_{Cj} level, thus the expression of the promoter on each plasmid was not reflected accurately by the overall outcome. Furthermore although the sequences of the NCTC 11168 *fur*_{Cj} and the 480 *fur*_{Cj} are almost identical, both Fur_{Cj} proteins may not behave in an identical manner. As the 480 *fur*_{Cj} mutant constructed (RR1) was also concluded not suitable for expression studies of strong Fur_{Cj}-regulated

promoters (such as *chuA*), single copy chromosomal reporter systems in the NCTC 11168 wild-type and *furCj* mutant backgrounds are therefore more appropriate and accurate, and should be applied for future studies of *C. jejuni* gene regulation.

Chapter 4: The iron- and oxygen-responsive regulation of *fumC*

4.1 Introduction

4.1.1 Regulation of fumarase genes in *E. coli*

Fumarase is a key component of the TCA cycle that catalyses the interconversion of fumarate to L-malate and it also participates in the reductive conversion of oxaloacetate to succinate during anaerobic growth. *E. coli* contains three fumarase genes, *fumA* (Guest and Roberts, 1983), *fumB* and *fumC* (Guest *et al.*, 1985), which encode biochemically distinct enzymes. *fumA* and *fumB* share a high degree of homology and both express class I fumarase that form thermolabile dimers. *fumC* is transcribed from its own and upstream *fumA* promoters (Park and Gunsalus, 1995), however it does not show any homology with either *fumA* and *fumB* and the gene product is a class II fumarase that forms thermostable tetramers (Woods *et al.*, 1988). Both FumA and FumB are iron-dependent hydrolases whereas FumC does not require iron for its function (Ueda *et al.*, 1991). The expression of each fumarase gene has been demonstrated to respond to an array of environmental stimuli such as oxygen, iron and carbon sources in a hierarchical fashion and is controlled in overlapping regulatory networks by several global regulators.

The oxygen responsive regulation of fumarase genes is mediated by the global oxygen limitation and oxidative stress regulators Fnr, ArcA and SoxS proteins (Park and Gunsalus, 1995; Tseng, 1997). FumA is the major fumarase under microaerophilic conditions as FumA activity peaks between 1-2% oxygen, but is constitutively

synthesised at a basal level under anaerobic conditions; the partial repression of *fumA* during anaerobic growth is mediated by ArcA (Park and Gunsalus, 1995; Tseng *et al.*, 2001). FumB activity is predominantly detected during anaerobic growth where the *fumB* gene is positively regulated by both the ArcA and Fnr proteins (Tseng, 1997; Tseng *et al.*, 2001). FumB acts as an alternative fumarase for FumA under anaerobic conditions as it has a higher affinity for L-malate than for fumarate which allows it to mediate the conversion of L-malate to fumarate during anaerobic respiration (Woods and Guest, 1988). FumC activity remains at a basal level under anaerobic and microaerophilic conditions and this partial repression is facilitated by the interaction of ArcA with both the *fumA* and *fumC* promoters and also by Fnr through the *fumA* promoter (Park and Gunsalus, 1995; Tseng *et al.*, 2001). Under high oxygen concentrations where iron-dependent FumA and FumB are inactivated due to oxidative stress, *fumC* is activated by SoxS to allow an elevation of FumC activity that maintains the TCA cycle flux (Park and Gunsalus, 1995; Tseng *et al.*, 2001). In addition, *fumC* is also directly activated by Rob, a transcriptional regulator functionally related to SoxS and the multiple antibiotic resistance regulator MarA (Ariza *et al.*, 1995; Jair *et al.*, 1996).

The expression of *fumA* and *fumB* that encode iron-dependent fumarases is activated by iron and Fur_{Ec} (Park and Gunsalus, 1995; Tseng, 1997). Although the mechanism of *fumB* activation by Fur_{Ec} is unclear, the positive regulation of *fumA* by Fur_{Ec} is mediated by the intermediate sRNA RhyB (Massé and Gottesman, 2002). The iron-independent

fumarase gene *fumC* is induced under iron limitation and oxidative stress conditions and the activation of the *fumC* promoter is mediated by SoxS (Park and Gunsalus, 1995). Interestingly in a *hemA* mutant strain which is defective in haem synthesis, the expression of all the fumarase genes is down regulated though the regulatory mechanism is unclear (Park and Gunsalus, 1995; Tseng, 1997).

The expression of *fumA* and *fumC* is also affected by the available carbon substrates as the expression of both genes is repressed when glucose is used as the sole carbon source (Park and Gunsalus, 1995) and FumA and FumC activity is elevated when acetate is used instead of glucose (Tseng *et al.*, 2001). The catabolite regulation of *fumA* and *fumC* occurs primarily from the *fumA* promoter (Park and Gunsalus, 1995) and involves Cap-cAMP complexes as Cap binding sites have been proposed within the *fumA* promoter region (Woods and Guest, 1988). Cap-cAMP complexes are also involved in the lower growth rate induction of *fumA* and *fumC* as the growth rate-dependent fumarase activity is abolished in a *cya* mutant strain which lacks the ability to synthesise cAMP, however this growth rate-dependent catabolite control of both genes is independent from carbon source utilisation (Tseng *et al.*, 2001).

The expression of both *fumA* and *fumC* is also affected by the cell growth phase where an increase expression of *fumC* through different growth phases is correlated with the growth phase-dependent expression of the global regulator gene *rpoS* and RpoS is predicated to play more significant role than SoxR in the regulation of *fumC* when cells

enter stationary growth phase (Rahman *et al.*, 2008). DNA superhelicity has also been reported to affect *fumB* expression as *fumB* is negatively regulated in a *topA* mutant strain that contains highly negatively supercoiled DNA (Tseng, 1997).

4.1.2 *fumC* regulation and the function of FumC in other bacteria

P. aeruginosa possesses at least two fumarase genes and the level of fumarase activity is greater in mucoid bacteria than nonmucoid cells (Hassett *et al.*, 1997b). The *fumC* gene is located in a four-gene operon that also contains the *sodA* gene which encodes a manganese-cofactored superoxide dismutase that protects the cell under oxidative stress (Hassett *et al.*, 1997a). *fumC* is co-transcribed with *sodA* and the operon is negatively regulated by iron and Fur_{Pa}. Two overlapping Fur_{Pa} boxes were identified upstream from the first gene in the operon and interaction with both *P. aeruginosa* and *E. coli* Fur has been demonstrated within this region (Polack *et al.*, 1996; Hassett *et al.*, 1997a; Ochsner *et al.*, 2002). The production of alginate, a viscous exopolysaccharide, is greatly reduced in a *fumC* mutant strain, which indicates the importance of FumC in *P. aeruginosa* pathogenicity as the production of alginate leads to the deterioration of the condition of cystic fibrosis patients (Hassett *et al.*, 1997b). In *Pseudomonas fluorescens*, the enzymatic activity of FumA is severely inhibited by the toxicities of aluminium and gallium while FumC displays an increase in expression and activity under these metal induced stress conditions (Chenier *et al.*, 2008).

In *V. cholerae*, *fumC* as well as *sodA* is repressed by iron and Fur_{Vc} and the putative

Fur_{vc} box sequence has been identified for both genes (Mey *et al.*, 2005). sRNA IG-524 is encoded in the opposite strand of the *H. pylori fumC* gene and is proposed to participate in *fumC* regulation in a sequence complementary manner (Xiao, *et al.*, 2009). A significant reduction in virulence for mice was demonstrated in a *fumC* defective strain of *L. monocytogenes* and the ability for the mutant to grow in cultured mouse phagocytes is abolished (Gahan and Hill, 2000). Phylogenetic analysis of the *N. meningitides fumC* indicates that it belongs to a unique cluster that is separated from those of other genera (Goh *et al.*, 2005) and a virulent clone of *N. meningitides* serotype 2a carrying a mutation in the *fumC* gene was responsible for the outbreak and spreading of meningococcal group C disease in Canada during the late 1980s (Ashton *et al.*, 1991). Both *fumA* and *fumC* genes in *Brucella abortus* are functionally redundant and the FumC protein co-localises at the old pole of *B. abortus* with an essential cytoplasmic histidine kinase PdhS (Mignolet *et al.*, 2010).

4.1.3 Regulation of *fumC* in *C. jejuni*

The *C. jejuni cj1364* gene has been identified through genome analysis as a homologue to *fumC* of *E. coli* and *H. pylori*. Fumarase activity in *C. jejuni* is not affected by oxygen concentration and cell age, and as no gene orthologous to *fumA* and *fumC* are identified, FumC is proposed to be the only fumarase in *C. jejuni* (Smith *et al.*, 1999). Transcriptomic analysis of the *C. jejuni* NCTC 11168 Fur_{Cj} regulon indicated that unlike *P. aeruginosa* and *V. cholerae*, *C. jejuni fumC* is positively regulated by iron and Fur_{Cj} (Holmes *et al.*, 2005) and although a Fur_{Cj} box-like sequence was identified upstream of

the gene, the *fumC* promoter does not bind Fur_{Cj} and therefore if it's Fur_{Cj}-responsive this is likely to be indirect.

The transcriptional regulation of *fumC* by iron and Fur_{Cj} was investigated using β -galactosidase and northern blot assays as part of this study to characterise the *C. jejuni* Fur box_{Cj}. Under the growth conditions routinely used for *C. jejuni* based β -galactosidase assays (2.2.20), which involve the setting up of *C. jejuni* cultures on high or low iron MHA plates prior to inoculating into MHB supplemented with 40 μ M FeSO₄ or 20 μ M Desferal respectively and incubated for 16 hours, the expression of *fumC* at a basal level was detected under iron limited conditions and the level of transcription was significantly elevated in the presence of additional iron but independent of Fur_{Cj} (Figure 3.10 and 3.15). A *C. jejuni* 480 *furCj* mutant was also constructed in order to verify the iron and Fur_{Cj} responsive regulation of *fumC*, though the *furCj* mutant was determined as an unsuitable host for the pMW10-based reporter system due to the constant expression of the *lacZ* gene and a high antibiotic concentration required for maintaining the reporter construct.

During the course of this study, a microarray based investigation of the *C. jejuni* strain 81116 has been published which demonstrated that the expression of several energy metabolism genes are altered by the RacR-RacS TCS in response to oxygen (van Mourik *et al.*, 2009). The response regulator RacR has been previously demonstrated in 81116 to affect the cell growth in a temperature-dependent manner and the inactivation

of *racR* has led to a reduced ability for the bacteria to colonise the alimentary tract in chickens (Brás *et al.*, 1999), which is presumably caused by the inability for the mutant to alter its energy metabolism in response to the low oxygen environment encountered in the chicken gut (van Mourik *et al.*, 2009). The expression of 81116 *fumC* as well as other metabolic genes such as the aspartase gene *aspA* was up regulated in the RacR mutant under oxygen limited conditions and a direct binding of the purified RacR protein in the presence of RacS-HK and ATP was demonstrated for the *aspA* promoter (van Mourik *et al.*, 2009). In *E. coli*, *fumC* and *aspA* genes share a high degree of homology and their gene products are also structurally related and are predicated to use analogous chemical mechanisms to fulfil their biological functions (Woods *et al.*, 1986).

The involvement of Fur_{Cj} and RacR in the iron responsive regulation of NCTC 11168 *fumC* was reevaluated by northern blot assays using growth conditions described by Holmes *et al.* (2005, 2.3.1), which involve the setting up of *C. jejuni* cultures on plain MHA plates prior to inoculating into MHB supplemented with 40 µM FeSO₄ or 20 µM Desferal respectively and incubated for 10 hours. Under these conditions, *fumC* was unexpectedly repressed by iron and the repression was mediated by RacR. The repression of *fumC* by iron was also facilitated by Fur_{Cj} and PerR_{Cj} though the exact mechanism was unclear (Figure 3.16).

4.2 Aims

Like *E. coli*, the *fumC* regulatory system in *C. jejuni* is complex and involves

overlapping regulatory networks that respond to changes in environmental iron and oxygen concentrations. However the preliminary data illustrated in chapter 3 suggested that unlike in *E. coli* where iron and oxygen responsive regulation is mediated by separate global regulators, RacR and Fur_{Cj} and possibly PerR_{Cj} are likely to play important roles in the co-regulation of *C. jejuni fumC* in response to both stimuli. To confirm this hypothesis, the first aim was therefore to comprehensively re-examine the expression of NCTC 11168 *fumC* in response to iron and oxygen concentrations and the co-involvement of Fur_{Cj}, RacR and PerR_{Cj} in this regulatory network using northern blot analyses. In addition, although the preliminary data from this investigation and previous microarray study (van Mourik *et al.*, 2009) indicated that the expression of *fumC* in both NCTC 11168 and 81116 is negatively regulated by RacR, the exact mechanism of RacR regulation is unknown. Thus the second aim was to investigate the *in vitro* interaction between the purified recombinant RacR and the *fumC* promoter by EMSAs and DNase I footprinting analyses. Lastly, unlike *E. coli*, which possesses three fumarases, the *C. jejuni fumC* gene product was predicated to be the only functional fumarase in *C. jejuni* (Smith *et al.*, 1999). To test this prediction, the last aim was to construct a NCTC 11168 *fumC* mutant and to determine the functional importance of *fumC* by investigating the impact of this gene deletion on the mutant's *in vitro* growth and cellular fumarase activities.

4.3 Results

4.3.1 Iron-responsive regulation of 81116 racR

Using 2-D gel electrophoresis, previous work (Brás *et al.*, 1999) compared the expression of 81116 RacR under different iron conditions and found that RacR does not respond to changes in iron levels. However as the expression of *fumC* is repressed by RacR and potentially by iron, the expression of 81116 *racR* in response to changing iron concentrations was first examined by northern blot analysis in order to reveal a clear picture of this regulatory process.

In other experiments, *C. jejuni* liquid cultures were routinely cultured in 5 ml volumes in 15 ml centrifuge tubes and incubated under 50 rpm agitation. However due to the large volume of cells required to extract a sufficient amount of total RNA for the northern blot analysis, multiple culture tubes were required for each sample; this was determined to be both inaccurate and impractical. To achieve the maximum cell recovery while ensuring that all samples have reached to the same growth phase, *C. jejuni* liquid cultures were scaled up and grown in 250 ml tissue culture flasks with gas permeable caps. A growth level difference between using the tubes and flasks was observed though this variation was corrected with 70 rpm agitation (results not shown) and the total RNA purified from cells grown in tissue culture flasks were used for all the northern blot assays described in this chapter.

Total RNA purified from wild-type 81116 cultured under high iron (40 μM FeSO_4) and low iron (20 μM Desferal) conditions were analysed by northern blot analysis (Figure 4.1) using 81116 *racR*- and *16S*-specific probes (2.3.4). A transcript of approximately

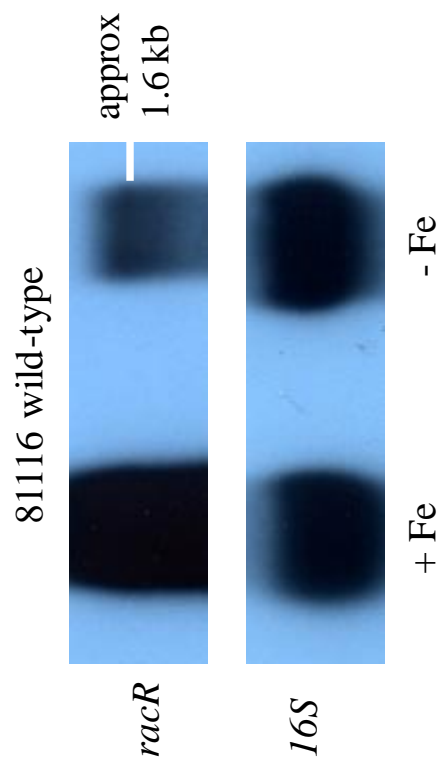


Figure 4.1: Northern blot analysis of the iron-responsive regulation of 81116 *racR*. Total RNA samples were purified from 81116 wild-type strain cultured under high iron (40 μM FeSO_4) and low iron (20 μM Desferal) conditions and were hybridised with 81116 *racR*- and NCTC 11168 *16S*-specific probes.

1.6 kb was detected indicating 81116 *racR* and *racS* are co-transcribed. A dramatic increase in the level of *racR/racS* transcript was observed under high iron conditions which demonstrated that although the cellular 81116 RacR levels are iron independent, the transcription of *racR* and indeed *racS* is iron-induced.

4.3.2 Iron- and oxygen-responsive gene regulation

To comprehensively characterise the iron- and oxygen-responsive regulation of NCTC 11168 *fumC* and *racR* and the involvement of Fur_{Cj}, PerR_{Cj} and RacR, total RNA purified from NCTC 11168, AV17 (*fur_{Cj}* mutant), AV63 (*perR_{Cj}* mutant) and AB3 (*racR* mutant) cultured under high iron (40 µM FeSO₄) and low iron (20 µM Desferal) conditions under 3%, 7% and 11% oxygen were examined by northern blot analysis using *fumC*- and *racR*-specific probes. The 7% oxygen was routinely used for culturing *C. jejuni* cells in this study, and the 3% and 11% oxygen were chosen to study the effect of changing oxygen concentrations on gene expression while maintaining a viable cell growth. A *fur perR* double mutant strain (AV67) was initially tested, however this strain was not included in the northern blot analyses due to poor growth and RNA recovery rate. All the RNA samples used to determine the expression of *fumC* and *perR* were re-hybridised with *chuA*- and *chuZ*-specific probes respectively as positive controls to demonstrate response to iron.

Under 3% oxygen (Figure 4.2), both *chuA* and *chuZ* were repressed by iron and Fur_{Cj} and the expression profiles of both genes were consistent with the previous

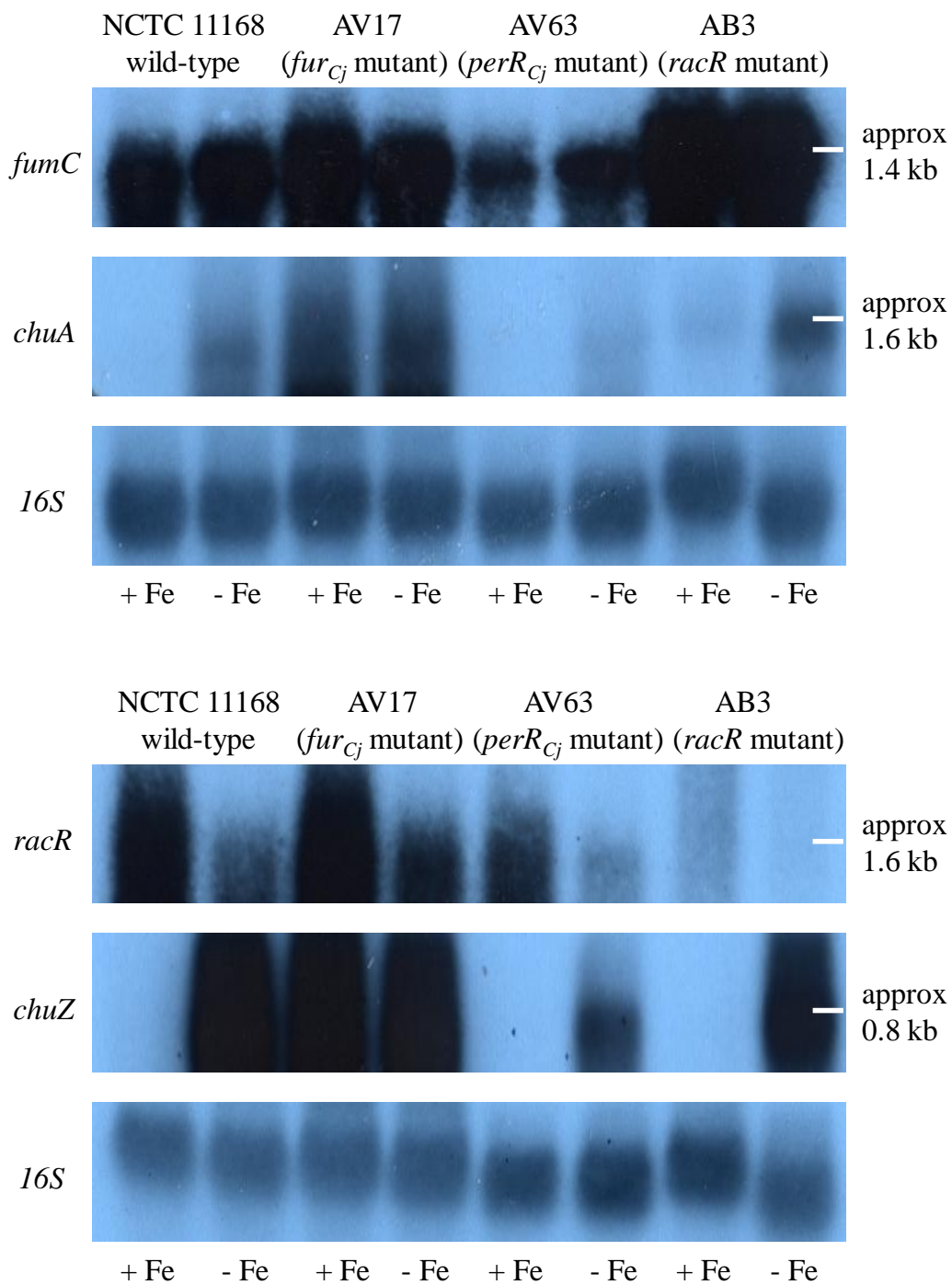


Figure 4.2: Northern blot analysis of the iron-responsive regulation of *fumC*, *racR*, *chuA* and *chuZ* under 3% oxygen. Total RNA samples were purified from NCTC 11168 wild-type, AV17, AV63 and AB3 strains cultured under 3% oxygen under high iron (40 μ M FeSO₄) and low iron (20 μ M Desferal) conditions and were hybridised with *fumC*-, *racR*-, *chuA*-, *chuZ*- and *16S*-specific probes.

characterisation of iron and Fur_{Cj} regulation of *chuA* and *chuZ* (Palyada *et al.*, 2004; Holmes *et al.*, 2005; Ridley *et al.*, 2006). The expression of *chuA* and *chuZ* however were noticeably decreased in AV63 under iron-limited conditions suggesting the potential involvement of PerR_{Cj} in the regulation of both genes. Interestingly, the size of the *chuA* transcript determined was approximately 1.6 kb indicating that *chuA* is primarily transcribed as a monocistronic mRNA rather than a multicistronic RNA which also contains the RNA of downstream *chuBCD* genes. *racR* was induced by iron and this observation was consistent with 81116 *racR*, however this iron-responsive regulation was independent from Fur_{Cj} and PerR_{Cj}. *fumC* was expressed under both iron conditions, though the difference in the level of expression between both conditions was small and could not be substantiated without quantitative analysis. *fumC* was derepressed under high iron conditions in AV17 and AB3, however as *racR* was not regulated by Fur_{Cj} and Fur_{Cj} binding to the *fumC* promoter region was not observed (Figure 3.4), the exact involvement of Fur_{Cj} in the iron-induced *fumC* repression under a low oxygen concentration was unclear.

Under 7% oxygen (Figure 4.3), the expression profiles for *chuA* and *chuZ* showed same patterns with 3% oxygen which indicated that under microaerobic conditions, the expression of *chuA* and *chuZ* was not affected by changing oxygen conditions from 3% to 7%. The Fur_{Cj} and PerR_{Cj}-independent iron responsive regulation of *racR* was also observed though the level of *racR* expression was much lower when compared to that observed with 3% oxygen. The up regulation of *racR* under low oxygen conditions is in

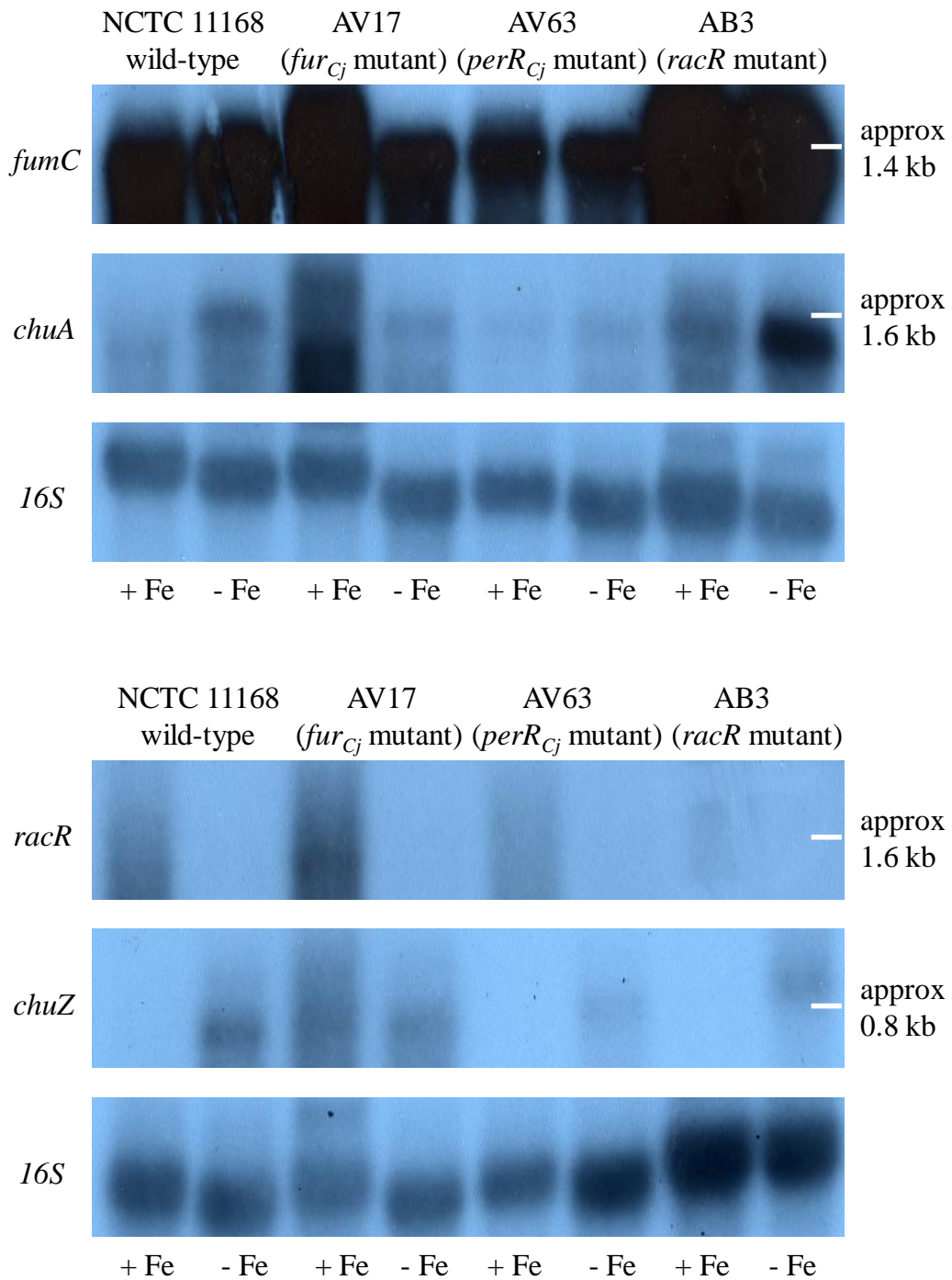


Figure 4.3: Northern blot analysis of the iron-responsive regulation of *fumC*, *racR*, *chuA* and *chuZ* under 7% oxygen. Total RNA samples were purified from NCTC 11168 wild-type, AV17, AV63 and AB3 strains cultured under 3% oxygen under high iron (40 μ M FeSO_4) and low iron (20 μ M Desferal) conditions and were hybridised with *fumC*-, *racR*-, *chuA*-, *chuZ*- and *16S*-specific probes.

agreement with van Mourik *et al.* (2009) and supports the proposal that RacR is an important regulator controlling low oxygen induced adaptive gene expression.

The level of *fumC* expression at 7% oxygen under both iron limited and replete conditions were consistent with 3% oxygen. A derepression of *fumC* was observed in AB3 and a higher level of *fumC* derepression was also detected in AV17 under high iron conditions when compared with the same conditions at 3% oxygen. These observations suggest that Fur_{Cj} plays a more significant role in *fumC* repression under 7% oxygen (an optimal level for cell growth) than RacR, which itself is down regulated. Interestingly, the level of *fumC* transcription was reduced under low iron conditions in both AV17 and the AV63 which suggests that both Fur_{Cj} and PerR_{Cj} also directly or indirectly influence the expression *fumC* under low iron and optimal oxygen conditions. Additionally, the expression profile of *fumC* was consistent with the northern blot analysis using cells cultured in tubes (Figure 3.16) therefore indicated that the expression of at least *fumC*, *racR*, *chuA* and *chuZ* were not altered by using tissue culture flasks under the increased agitation.

Under 11% oxygen (Figure 4.4), the expression profiles of *chuZ* were unaffected by the elevated oxygen concentration, however the iron-responsive regulation of *racR* was completely abolished in AV63. Derepression of *chuA* was also observed under high iron conditions in AV63 and AB3 which suggests that under elevated oxygen and iron concentrations PerR positively regulates the expression of *racR* and the gene product of

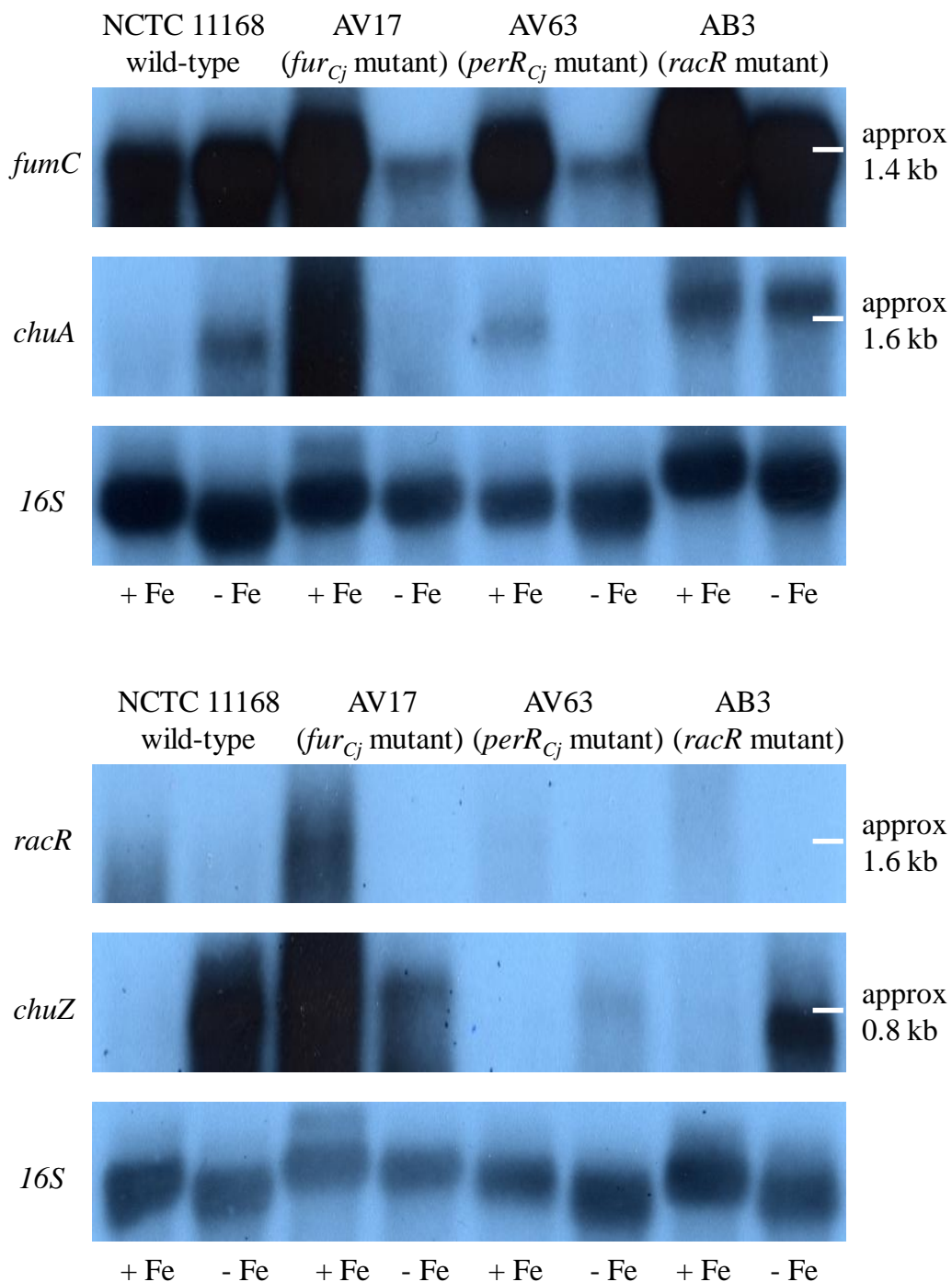


Figure 4.4: Northern blot analysis of the iron-responsive regulation of *fumC*, *racR*, *chuA* and *chuZ* under 11% oxygen. Total RNA samples were purified from NCTC 11168 wild-type, AV17, AV63 and AB3 strains cultured under 3% oxygen under high iron (40 μ M FeSO₄) and low iron (20 μ M Desferal) conditions and were hybridised with *fumC*-, *racR*-, *chuA*-, *chuZ*- and *16S*-specific probes. N.B. Due to the relative shorter half-life of the *chuA* transcripts, the expression of *chuA* under low iron conditions in both AV17 and AV63 were detected in the form of smears on the bottom half of the blot (results not shown).

which acts in turn as a repressor for *chuA*.

The level and patterns of *fumC* expression in the wild-type and AB3 in 11% oxygen were similar to with 3% and 7% oxygen indicating that although *fumC* is differently regulated by several regulators in response to oxygen and potentially iron, the overall level of *fumC* transcript remains constant. An increased level of *fumC* derepression was observed in the AV63 under high iron conditions that presumably was caused by the abolished *racR* expression. A greater decline of *fumC* expression was detected in both AV17 and AV63 under iron limited conditions which further demonstrates that *fumC* is also positively influenced under low iron conditions by Fur_{Cj} and PerR_{Cj}, especially under oxidative stress conditions or indirectly regulated by another regulator.

4.3.3 Expression and purification of recombinant NCTC 11168 RacR and RacS-HK

In order to analysis the interaction between RacR and the *fumC* promoter *in vitro*, His₆-tagged NCTC 11168 RacR and RacS-HK were expressed and purified in *E. coli*. The entire *racR* gene was cloned into an IPTG-induced expression vector. In order to avoid inclusion body formations during the protein purification stage of RacS, only a section of the *racS* gene coding the predicted histidine kinase domain but not the transmembrane sensor domain was cloned (Figure 4.5). The resulting constructs pRR46 and pRR53 were electroporated in the *E. coli* expression strain Rosetta and various parameters in the expression and purification processes for both proteins were optimised. Optimisation of the expression conditions found that 3 hours induction by 0.8 mM

MTKNYSIHT**KLILFVVTFFLVCVLFIVLLKIEGNTYNEEESLKQENLIKNNLLISYENTSGVEIGAYLGNSGFNAIQPNLVKAIRNNGQSL**
FKAGGELCTLSSLKYSNLYFDVQCKDFDGLYEENTSDRVVYNN**LLIGFFSFLLVVFMYFSVLKSL**LEPLK**KLRRQVAEVANGEQPDFLD**
YQEDVGGKIAFEFQKAFKKNQELIQSRQFLRTIMHELKTPIGKGRJISEMIKEDRQKERLJAIFLRMDSLJNEFAKIENLFSKNYNNLHFKPS
RFSTILEEAKHEHLMIDDFNKVVKVDIRYDALINVDMEIFSVILKLNLDNALKYSNNGTCELFCCKECFTIKNPGKPLAEPYHYLEAFTREK
HNQVKGMGLGLYIVSEVCKLHNFDLLYFYDDGKHCFKIFFGDKEK

Figure 4.5: The predicted transmembrane domains (red) and the histidine kinase domain (blue) of NCTC 11168 RacS. Sequence encoding the underlined regions with an added start codon was cloned into the expression vector pLEICES-01 to form pRR53.

IPTG at 37 °C were sufficient to allow expression of both proteins while 80 mM imidazole in the binding (washing) buffer was used in the purification stage to allow the maximum recovery of both proteins with minimum nonspecific protein contaminations (2.4.2).

Single bands were observed when column purified RacR and RacS-HK were analysed by SDS-PAGE (Figure 4.6) and their sizes were consistent with the predicted sizes of tagged RacR (25.6 KDa) and the histidine kinase domain of RacS (28.3 KDa). High levels of protein expression were observed for both proteins during induction trials (results not shown) however the concentration of column purified protein was relative low, particularly with RacR. This was caused by the high imidazole concentration in the column binding buffer used during column purification in order to eliminate co-purification of nonspecific host proteins. A host ribosomal small subunit protein (verified by peptide mass fingerprinting) was co-purified in small quantities with both RacR and RacS-HK. Higher concentrations of imidazole to eliminate the contaminating protein were not used to avoid compromising the protein yield of RacR and RacS-HK.

When both proteins were concentrated and buffer exchanged to buffer B (van Mourik *et al.*, 2009) to allow subsequent analysis in phosphorylation and EMSA assays, the nonspecific host protein was eliminated from both samples presumably due to degradation. The identities of both proteins were verified by peptide mass fingerprinting and western blot analysis; no protein aggregation or degradation was detected for either

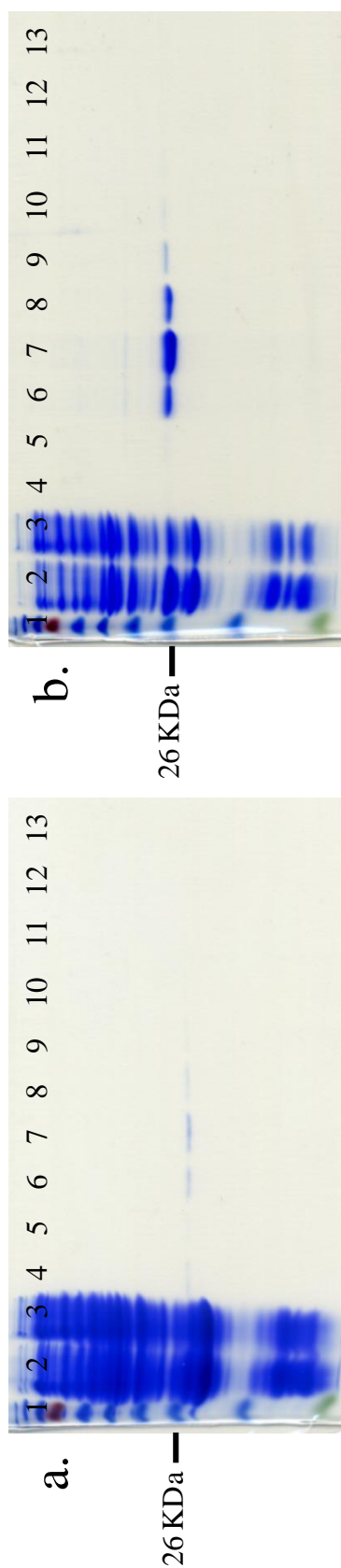


Figure 4.6: SDS-PAGE analysis of the purified recombinant RacR (25.6 KDa, a) and RacS-HK (28.3KDa, b) proteins. Lane 1: PageRuler prestained protein ladder; lane 2: pre-column sample; lane 3: flow-through sample; lane 4: mid-wash sample; lanes 5-13; elution samples 1-9 respectively.

protein (Figure 4.7).

4.3.4 Phosphorylation of *RacR* by *RacS*-HK

Autophosphorylation of 81116 *RacS*-HK and the *in vitro* transfer of phosphate between *RacS*-HK and *RacR* proteins have been previously demonstrated (van Mourik *et al.*, 2009), therefore phosphorylation assays (2.4.11) were performed to verify the functionalities of the newly purified NCTC 11168 *RacR* and *RacS*-HK. *RacR* was added to a *RacS*-HK/ATP γ -³²P solution and aliquots of the mixture were taken at the time indicated in Figure 4.8 and analysed by SDS-PAGE. At time 0 where only *RacS*-HK and ATP γ -³²P were present in the reaction, autophosphorylation of NCTC 11168 *RacS*-HK was detected which indicated the histidine kinase domain predicated was functional. Due to high radioactivity levels and the marginal size difference, *RacR* and *RacS*-HK were not separated very well and a band doublet containing the two proteins was formed between 0.25 and to 4 minutes which demonstrated the phosphorylation of *RacR* by *RacS*-HK. From 8 minutes onward, all the γ -³²P has been transferred onto *RacR* as indicated by the single band (*RacR*) that was smaller in size than *RacS*-HK. The *in vitro* transfer of phosphate between NCTC 11168 *RacR* and *RacS* observed indicates both purified proteins are functional and the NCTC 11168 *RacR* and *RacS* form a true TCS.

4.3.5 Interaction of *RacR* and the *fumC* and *aspA* promoters

To demonstrate the direct repression of the *fumC* promoter region by *RacR*, EMSA and

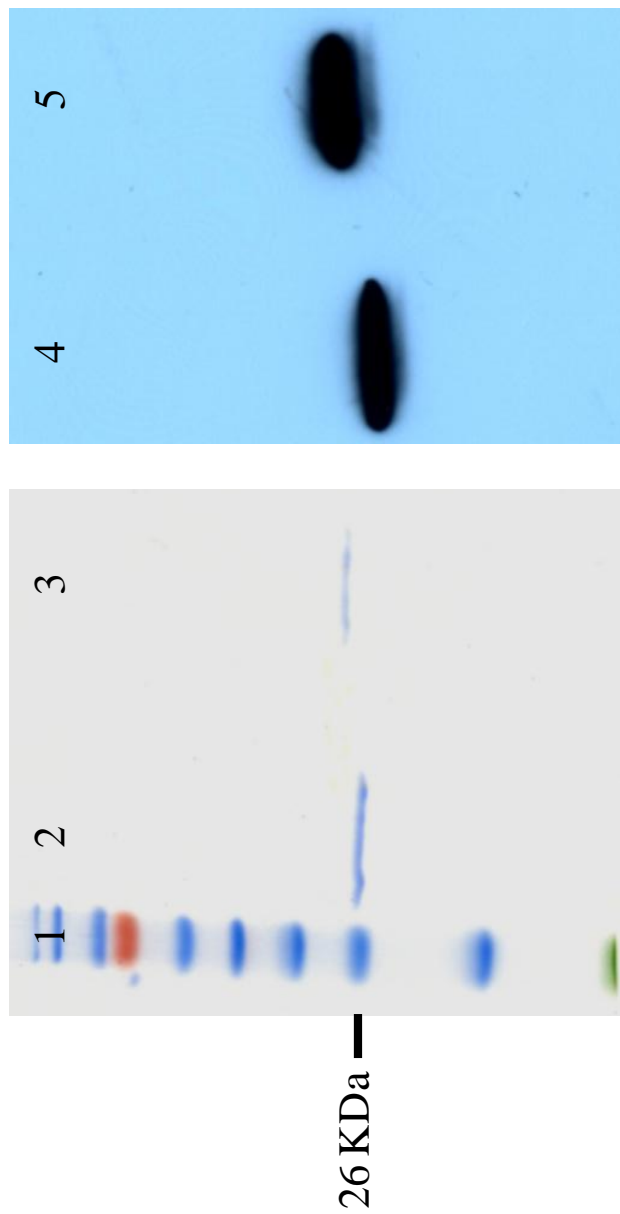


Figure 4.7: SDS-PAGE and western blot analysis of the concentrated recombinant RacR and RacS-HK. Lane 1: PageRuler prestained protein ladder; lanes 2 and 4: RacR; lanes 3 and 5: RacS-HK.

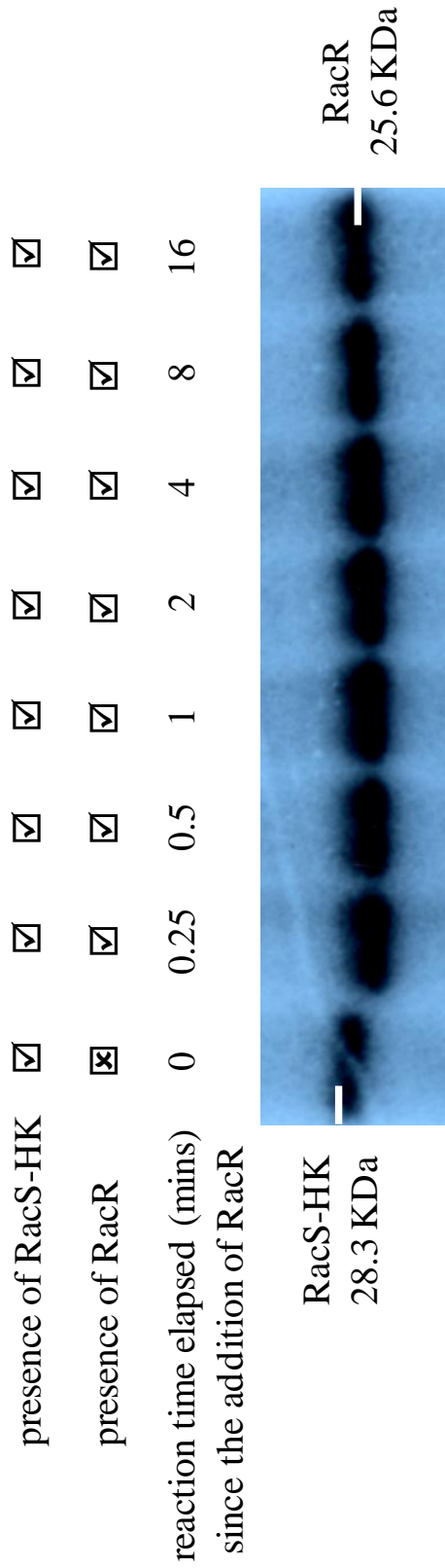


Figure 4.8: *in vitro* phosphorylation of NCTC 11168 RacR and RacS-HK analysed by SDS-PAGE. The presence or absence of RacS-HK/ATP γ -³²P and RacR in each reaction is indicated by or respectively while the time stated for each reaction represents the time elapsed since the addition of RacR to the RacS-HK/ATP γ -³²P mixture.

DNase I footprinting assays were carried out for the NCTC 11168 *fumC* promoter. The 81116 *aspA* promoter has been demonstrated to interact with the phosphorylated 81116 RacR (van Mourik *et al.*, 2009) and was therefore included in this study as a functional control. A DNA fragment containing 149 bp of the 81116 AspA coding region and 284 bp upstream from the start codon was amplified for *aspA* while for *fumC*, the same promoter region used to characterise the Fur_{Cj} box in 3.3.3 was used.

For the *aspA* promoter (Figure 4.9), two shift species were observed with 124 nM RacR in the presence of RacS-HK and ATP which indicated high affinity protein-DNA interactions. The intensity of the shift species was increased with the elevated RacR concentration and at 496 nM RacR, a super shift was detected where all the *aspA* promoter fragments were bound to RacR. The super shift was either caused by an aggregation of protein-DNA complex in the gel well due to the presence of two proteins at high concentration or by the polymerisation of RacR along the DNA molecule. Although NCTC 11168 RacR was used in this study to interact with the 81116 *aspA* promoter, the shift patterns were in full agreement with van Mourik *et al.* (2009).

Interestingly a relatively strong shift was observed with *aspA* promoter and the RacR protein alone. This shift was not detected with DNA and RacS-HK alone and the intensity of this shift was significantly reduced when both RacR and RacS-HK were presented but without ATP. Although the physiological relevance of this interaction is uncertain, it nevertheless suggests that RacR, in its unphosphorylated form, may form

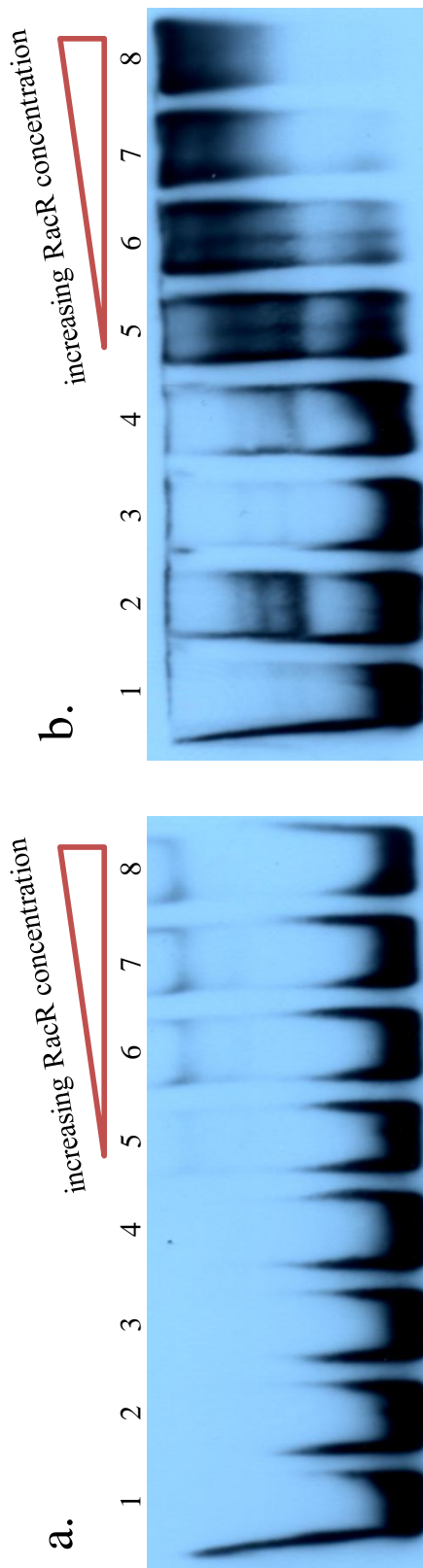


Figure 4.9: Standard EMSA of 1.55 fmol labelled *fumC* (a) and *aspA* (b) promoter regions with purified *C. jejuni* NCTC 11168 RacR, RacS-HK and ATP. Lane 1: labelled DNA; lane 2: labelled DNA with 496 nM RacR; lane 3: labelled DNA with 391 nM RacS-HK; lane 4: labelled DNA with 496 nM RacR and 391 nM RacS-HK; lanes 5-8: labelled DNA with 1 mM ATP, 391 nM RacS-HK and 124 nM, 248 nM, 372 nM and 496 nM RacR respectively.

weak interaction with its target promoter regions and this interaction is negatively influenced by the unphosphorylated RacS protein. The interaction between *aspA* promoter and unphosphorylated RacR and RacS-HK was not investigated by van Mourik *et al.* (2009).

A less intensive shift species was formed for *fumC* with an increasing RacR concentration which demonstrated that the repression of *fumC* by RacR was caused by direct protein-DNA interaction. The affinity of RacR binding was low, a conclusion consistent with the partial repression of *fumC* by RacR detected by northern blot analysis (Figures 4.2-4.4). Nonspecific DNA interaction by unphosphorylated RacR was not observed, presumably due to the low affinity of RacR toward the *fumC* promoter or a different regulatory mechanism involved.

Once the interaction of RacR and the *fumC* and *aspA* promoters was demonstrated by EMSAs, the location of the RacR with respect to the promoter region was subsequently analysed for both genes by DNase I footprinting assays. The highest RacR concentration used for EMSA (496 nM) was used as the starting concentration and due to the large reaction volume, the RacR concentration was also doubled and quadrupled. RacS-HK was kept at 391 nM due to its high phosphorylation activities determined in 4.3.4. However when the *fumC* and *aspA* promoters were analysed, no protected region was observed (Figure 4.10). The starting base of the *aspA* gene is indicated in Figure 4.10 and a protected region is likely to be detected upstream from it while RacR is most

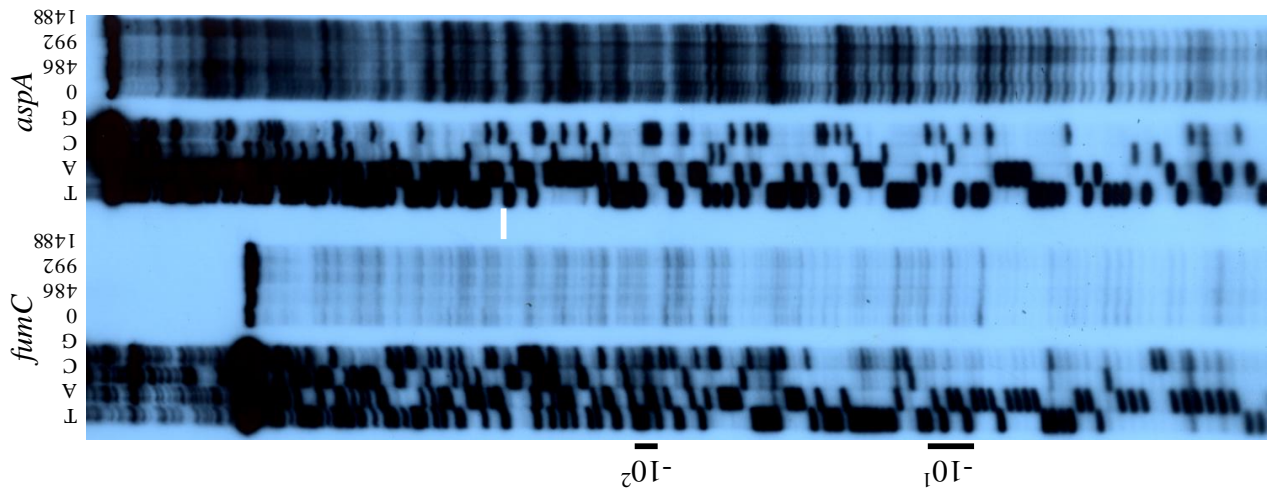


Figure 4.10: DNase I footprinting assays for the *fumC* and *aspA* promoters along with corresponding sequencing ladders. 391 nM RacS-HK and 1 mM ATP were used in each reaction and the RacR concentration ranged from 0 to 1488 nM. Regions representing the two *fumC* -10 regions are indicated by black lines on the left side of the film and the first base of the *aspA* gene indicated by the white line. N.B. no protected region was found.

certainly to interact with *fumC* in the region between or upstream of the two -10 regions.

4.3.6 Construction of the *C. jejuni* NCTC 11168 *fumC* mutant

C. jejuni fumC was previously proposed to encode the only fumarase in the cell (Smith *et al.*, 1999), therefore in order to test this hypothesis and to determine the functional importance of this gene, the NCTC 11168 *fumC* gene was mutated by insertion of an antibiotic resistance cassette (Figure 4.11). The entire *fumC* gene plus 400 bp flanking region on each side were amplified and cloned into pUC19 (pRR51). A 1067 bp internal deletion of *fumC* in pRR51 was carried out by inverse PCR and was ligated with a terminator-less *aphA-3* with its own promoter (a Kan resistance cassette) to form pRR52. pRR52 was then transformed into NCTC 11168 by electroporation. Transformants were recovered on MH agar with selection as well as MH agar supplemented with 6% horse blood or 4 mM malate at pH 7.3 which was previously determined to enhance the wild-type *C. jejuni* growth in liquid cultures (Hinton, 2006; S. Hardy, personal communication). Horse blood and malate were used to provide essential TCA cycle components for the *fumC* mutant thus allowing the recovery of the mutant if *fumC* was the only fumarase coding gene in NCTC 11168. The *fumC* mutant (RR2) was only able to recovery from blood agar and the identity of the mutant was verified by PCR using gene specific primers (*fumCF* and *fumCR*) and *aphA-3* specific inverse primers (SkanR and STM invKan-F).

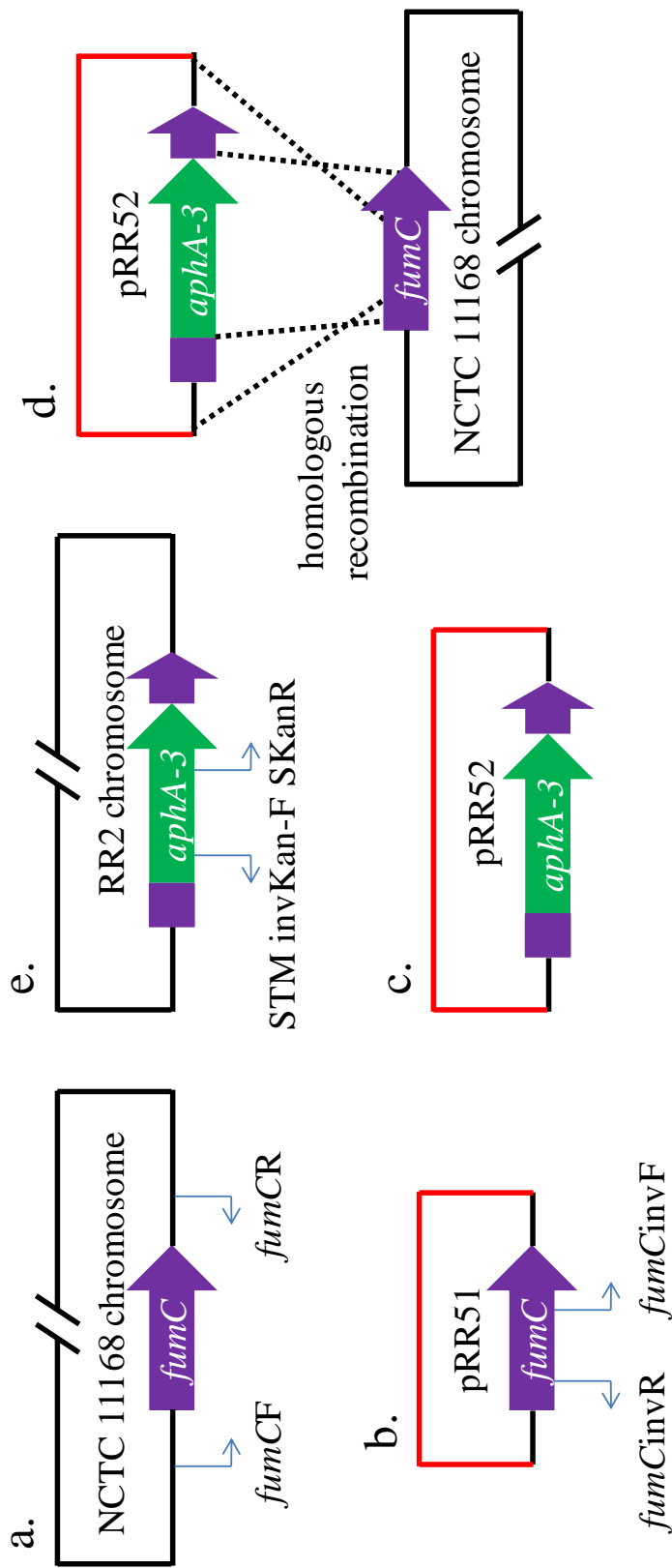


Figure 4.11: Illustration of the mutagenesis strategies used to create a NCTC 11168 *fumC* mutant (RR2). A DNA fragment amplified by *fumCF* and *fumCR* containing the wild-type *fumC* and flanking regions (a) was cloned in to pUC19 to form pRR51 (b). To make an internal deletion of *fumC* in pRR51, an inverse PCR was carried out using *fumCinvR* and *fumCinvF* primers and pRR51 (as the template), and the PCR product was ligated with *aphA-3* (a Kan resistance cassette) to form pRR52 (c). pRR52 was then electroporated in to NCTC 11168 to allow homologous recombination between the flanking regions of *aphA-3* in pRR52 (that contains *C. jejuni* DNA) and their corresponding flanks in the genome of NCTC 11168 wild-type (d). This led to a replacement of the middle section of the wild-type *fumC* gene with *aphA-3* thus creating a *fumC* mutant (RR2, e). Primers used for mutant construction and verification are indicated by blue arrows and genes, plasmids and genomes are not drawn in proportions to their actual sizes.

As shown in Figure 4.12, a single band of 2445 bp in lane 2 containing *fumC* gene and flanking regions was observed for the wild-type whereas a slight larger 2882 bp band in lane 5 was detected for the mutant. Bands with the expected sizes were also observed with the *aphA-3* specific primers which demonstrated that the majority of the *fumC* gene was replaced by the Kan resistance cassette and the cassette was placed in the same orientation as the gene. The *fumC* mutant was also sequenced using a combination of primers indicated in Figure 4.11 and no nonspecific mutations in the 400 bp flanking regions of the mutated *fumC* gene were detected (results not shown).

For constructing a *fumC* complemented strain, the method described by Elvers *et al.* (2005) was applied where the functional copy of the mutated gene was recombined into the mutant strain and inserted into the pseudogene *cj0752*. The *fumC* gene plus approximately 300 bp of flanking regions on each side of the gene were amplified and cloned into the *cj0752* gene in pGEMCWH01 to form pRR66. The *cat* gene (a Cm resistance cassette) was amplified from pAV35 and cloned into pRR66 in the same orientation downstream from the *fumC* gene. The resulting vector pRR67 was verified by sequencing and the construct was electroporated into RR2 prior to recovery on MH agar with selection as well as agar supplemented with blood or malate. No transformants were formed during two transformation attempts and further investigations were not carried out due to time limitations.

4.3.7 The effects of the *fumC* mutant on growth rate and fumarase activities

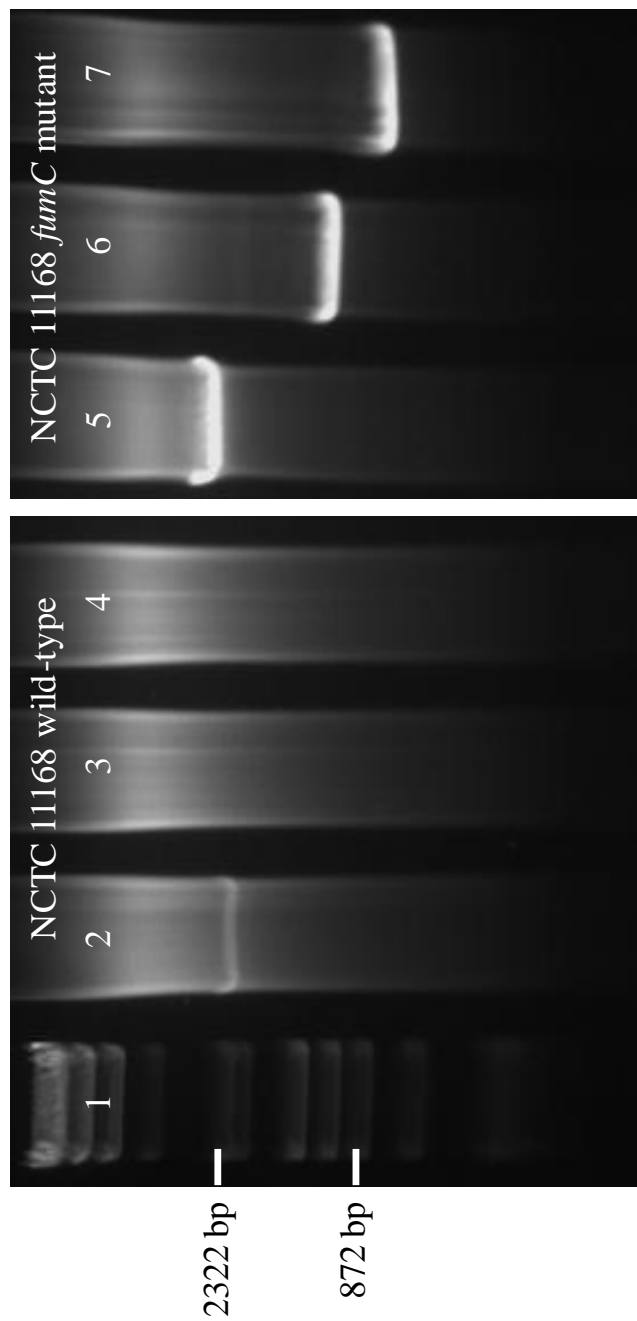


Figure 4.12: Verification of the NCTC 11168 *fumC* mutant (RR2) by PCR. Lane 1: λ/Φ DNA size marker; lanes 2 and 5: PCR amplification using *fumCF* and *fumCR* primers; lanes 3 and 6: PCR amplification using *fumCF* and SKanR primers; lanes 4 and 7: PCR amplification using STM invKan-F and *fumCR*. RR2 and primer positions are shown in Figure 4.11.

The effects of the *fumC* mutation on cell growth were assessed using both plate and liquid cultures. No cell growth was detected when RR2 was plated straight from glycerol stock onto MH agar. The mutant grew poorly on the MH agar plate supplemented with 4 mM malate and a notable increase in cell growth was observed when RR2 was plated onto the blood MH agar. When RR2 grown on blood MH agar was subcultured onto fresh media, marginal cell growth was detected on MH agar. An increase in cell growth compared to cells plated straight from glycerol stocks was also observed on MH agar supplemented with either malate or blood, though the level of growth was notably less when compared with the wild-type.

When the growth rate of the mutant strain was assessed under different iron conditions in MH broth, a significant growth defect was observed in both iron conditions compared with the wild-type strain (Figures 4.13 and 4.14). The reduced growth rate observed for RR2 was consistent in both solid and liquid media and indicated that *C. jejuni fumC* is essential for maintaining active cell growth. When the growth media was supplemented with 4 mM malate, the growth rate of the wild-type cells was improved under both iron conditions. The growth level for the mutant was also approximately doubled though the level and the rate of growth for RR2, especially under high iron conditions were not restored back to the level seen with the wild-type without the malate supplement. When a range of malate concentrations was tested to improve the level of mutant growth, a growth level of RR2 similar to the level shown in Figures 4.13 and 4.14 was observed between 4 to 8 mM malate and a decline in the growth rate for RR2 was detected outside this concentration range (results not shown).

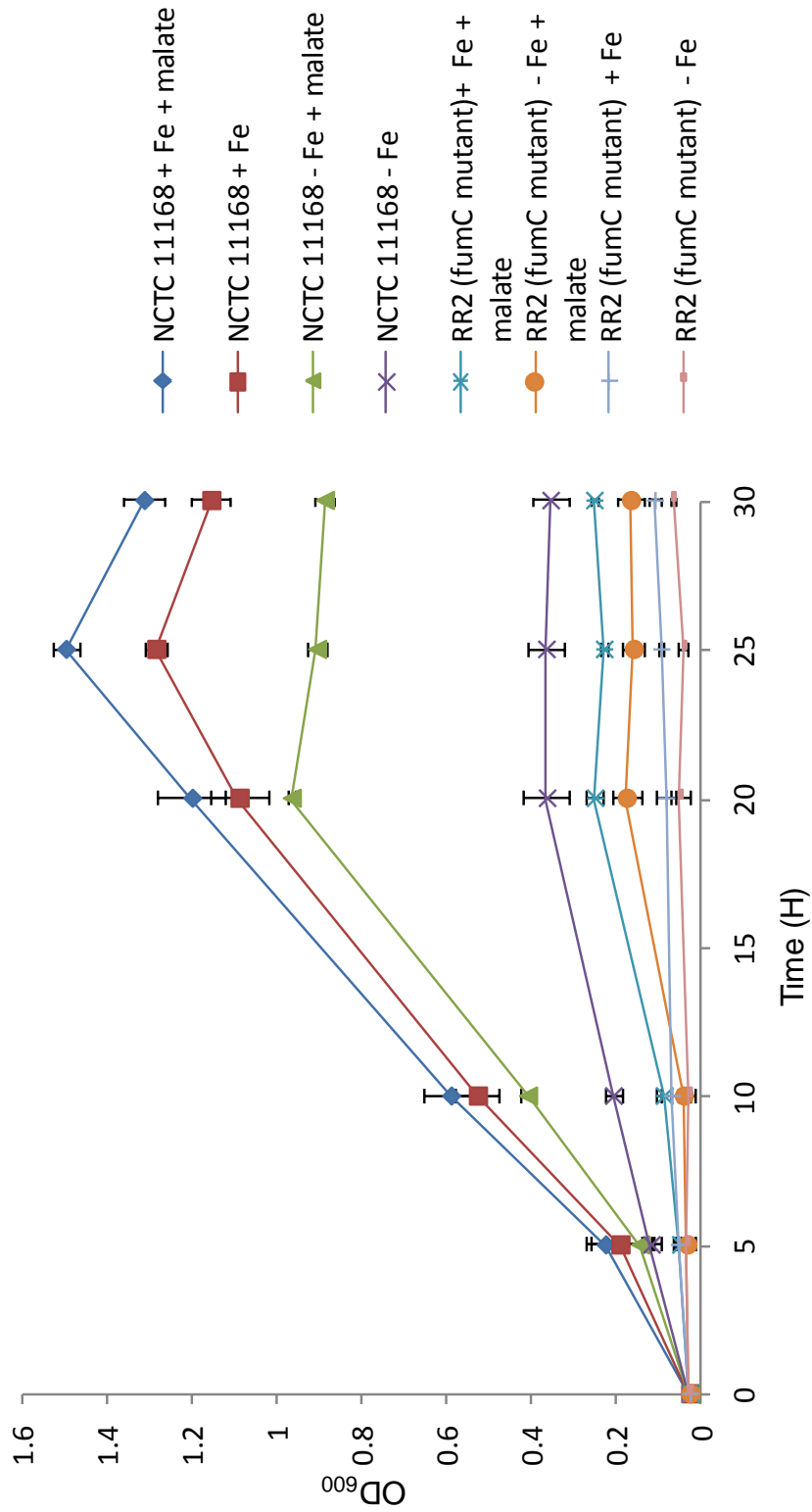


Figure 4.13: Growth assays of the wild-type NCTC 11168 and RR2 (*fumC* mutant). MH broth was used and each assay was supplemented either with 40 μM FeSO_4 (+ Fe) or 20 μM Desferal (-Fe) and with or without 4 mM malate. Data presented are the means of triplicate sampling from two independent experiments with the standard error.

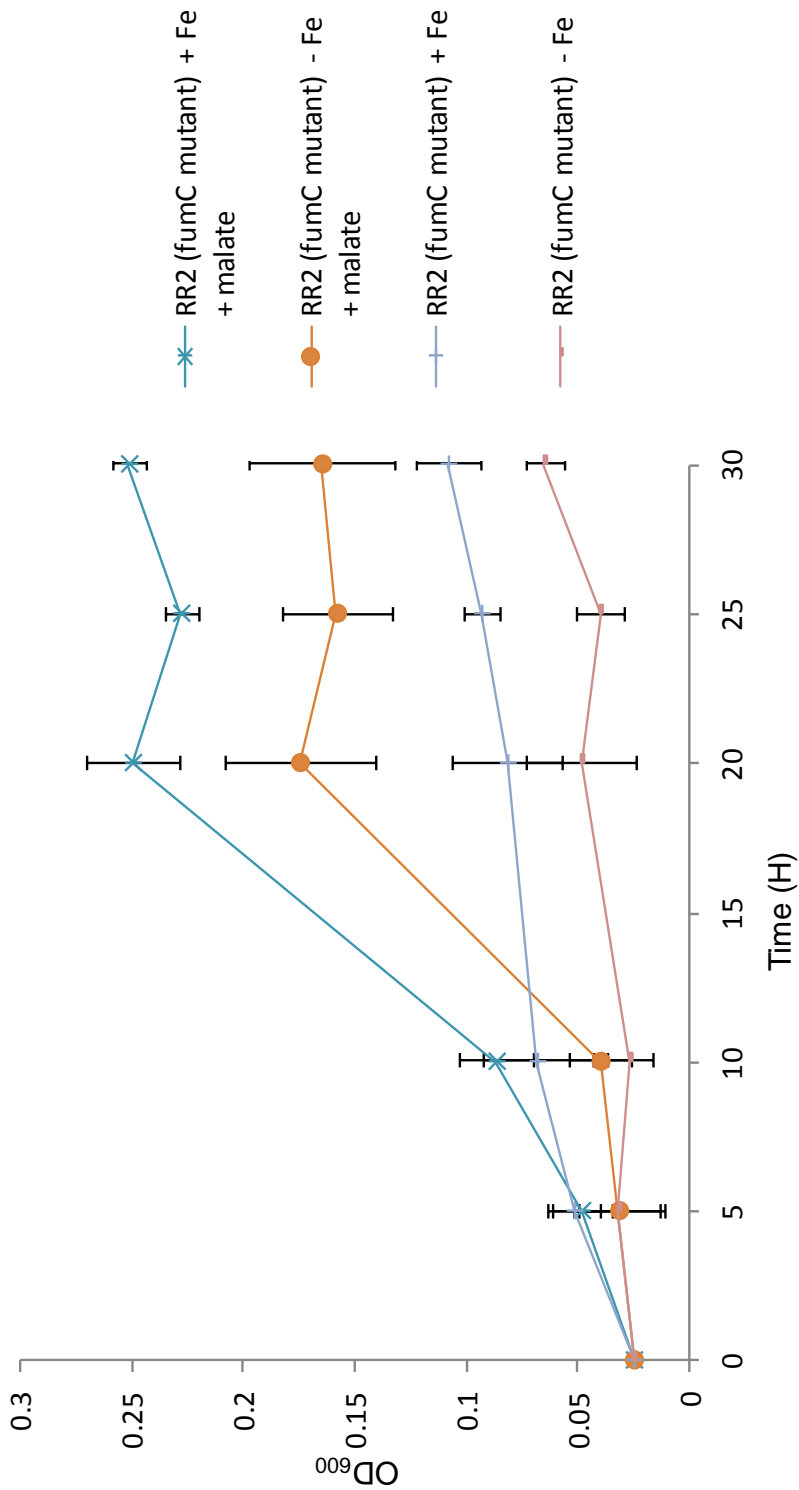


Figure 4.14: Growth assay of RR2 (*fumC* mutant). MH broth was used and each assay was supplemented either with 40 μM FeSO_4 (+ Fe) or 20 μM Desferal (-Fe) and with or without 4 mM malate. Data presented are the means of triplicate sampling from two independent experiments with the standard error. N.B. Data illustrated in this figure are replicates of the RR2 growth assay data in Figure 4.13 and presented with a smaller Y-axis scale to aid visualisation.

The effects of mutational changes and iron on the whole cell fumarase activities were assessed for NCTC 11168 wild-type and RR2 using the method described by Hassett *et al.* (1997). AB3 (*racR* mutant) and AV17 (*fur_{Cj}* mutant) were also included in order to correlate the changing in fumarase activities with the transcriptional regulation of *fumC* by RacR and Fur_{Cj}. The wild-type and mutant cells were cultured in the same growth and iron conditions as used for total RNA purification (2.3.1) with the addition of 4 mM malate. Whole cell extracts were prepared for each sample by sonication and the concentration of each sample was measured and standardised (2.4.12) prior to measuring the conversion of malate to fumarate at 25 °C.

As shown in Figure 4.15, fumarase activity was not detected for RR2 in both iron conditions which strongly indicated that *fumC* is the only fumarase coding gene in the *C. jejuni* genome and therefore plays a critical role in maintaining a functional TCA cycle. Fumarase activities of various levels in response to iron concentrations were detected for the wild-type AB3 and AV17 which illustrated the involvement of both Fur_{Cj} and RacR in the iron responsive regulation of *fumC*. The patterns of FumC expression (measured in the form of fumarase activity) did not match the *fumC* transcriptional profiles demonstrated by northern blot analysis which suggested the involvement of post-transcriptional or translational regulation of *fumC*. However as malate was demonstrated to improve cell growth when supplemented in MH broth, the possibility of malate-induced alterations in gene expression could not be overlooked.

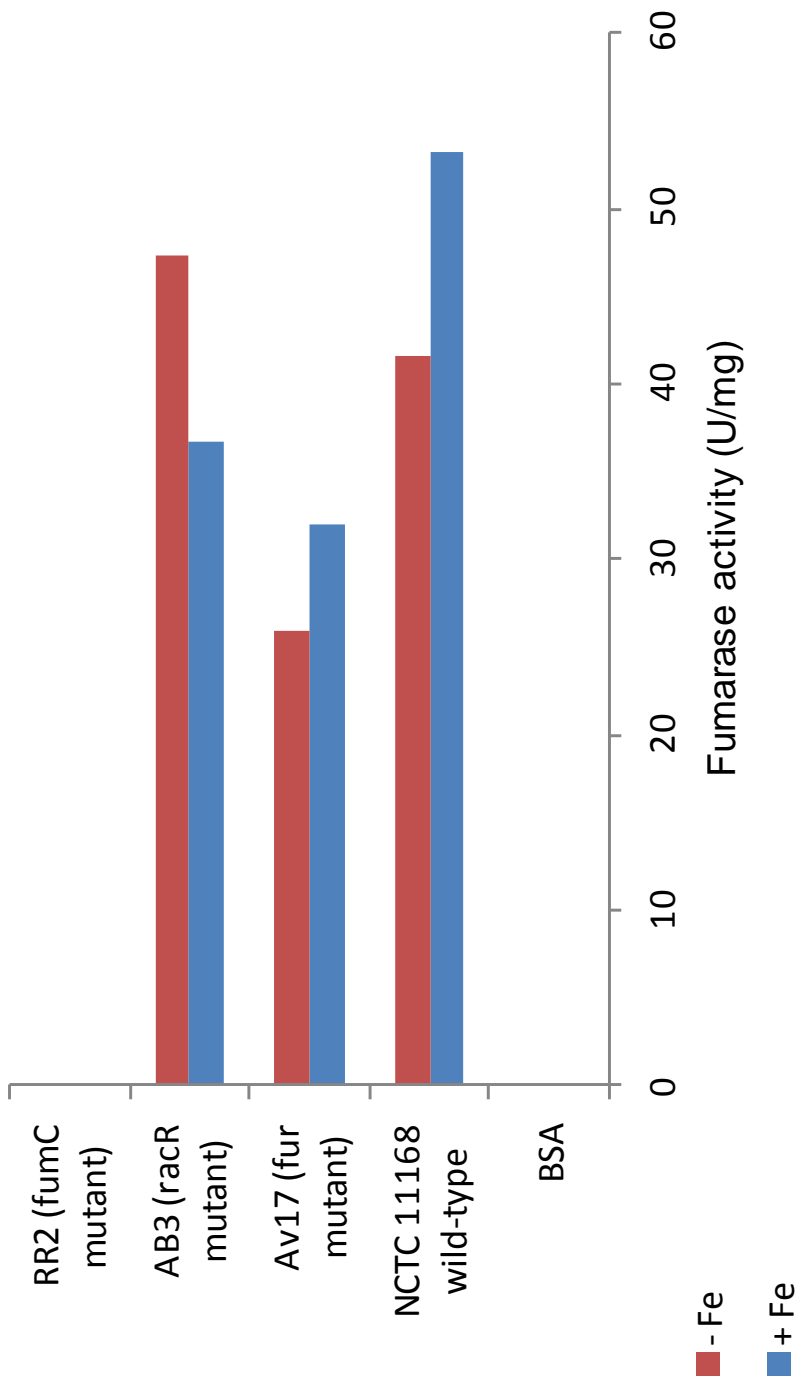


Figure 4.15: Fumarase activity assays of the wild-type NCTC 11168, RR2, AV17 and AB3 under different high iron (40 μ M FeSO_4) and low iron (20 μ M Desferal) conditions along with BSA controls. N.B. Data presented in this figure are from a single preliminary experiment.

4.4 Discussion

The expression of three *E. coli* fumarase genes is controlled in a hierarchical manner by several global regulators that allow *E. coli* to adapt to various environmental conditions by maintaining the TCA cycle flux (Park and Gunsalus, 1995; Tseng *et al.*, 2001). Although *fumC* has been proposed to be the only fumarase coding gene in *C. jejuni* and oxygen-dependent variation of fumarase activity were not observed (Smith *et al.*, 1999), iron and oxygen responsive regulation of *fumC* have been demonstrated recently by microarray analysis where the expression of *fumC* was mediated by the global iron regulator Fur_{Cj} and the RacR-RacS TCS (Holmes *et al.*, 2005; van Mourik *et al.*, 2009). By a combination of mutational analysis and northern blot analysis, the functional importance and transcriptional regulations of *C. jejuni fumC* were revealed in this study. Both NCTC 11168 RacR and RacS-HK were also purified and the interaction of RacR with RacS-HK and RacR regulated promoters were characterised *in vitro*.

4.4.1 NCTC 11168 *fumC* and its functional importance

To determine the functional importance of *C. jejuni fumC* in active cell growth and the role of fumarase in the TCA cycle, a NCTC 11168 *fumC* mutant was constructed and the changes in growth rate and total fumarase activity were assessed in response to iron. The growth of the mutant strain was severely hindered when compared with the wild-type in standard MH broth media under both iron conditions and the mutant failed to grow on standard MH agar plates. This observation clearly demonstrated the impact of the *fumC* gene in maintaining the active cell growth and a functional TCA cycle.

When supplemented with malate, which was determined to enhance cell growth (Hinton, 2006), the growth rate of the mutant strain was expected to restore back to the wild-type level. Although enhanced cell growth was observed for the wild-type and mutant strains under both iron conditions, the growth level for the mutant was still low compared to the wild-type (Figures 4.13 and 4.14) and the growth rate for the *fumC* mutant was not further enhanced with increased malate concentrations.

This growth discrepancy might be caused by the polar effect of the acid membrane antigen gene *amaA* located downstream from the *fumC* gene that is transcribed in the opposite direction. As the *ahpA-3* gene used to construct the *fumC* mutant does not have its own terminator, the expression of the *ahpA-3* might lead to the transcription of the *amaA* from the non-coding strand if the *fumC* terminator is weak. However as the mutant growth rate was influenced by the presence of malate, the growth discrepancy between *fumC* mutant supplement with malate and the wild-type strain is more likely caused by the deletion of the *fumC* gene leading to a disrupted TCA cycle. In addition, as the growth level of the mutant was also increased on MH agar plates supplemented with horse blood, it is likely that other supplements present in the blood are needed to return the mutant growth rate back to the wild-type level. Other possible explanation for this growth difference is the build up of fumarate that negatively affects the cell growth or has a knockback effect on the TCA cycle. As the complemented strain was not constructed due to time limitation, the impact of *fumC* on the cell growth could not be fully evaluated.

When the total fumarase activity was tested for the *fumC* mutant, no fumarase activity was detected (Figure 4.15) which experimentally proved that *fumC* encodes the only fumarase in *C. jejuni* NCTC 11168. The absence of *fumA* and *fumB* in *C. jejuni* is likely reflected by its strictly microaerophilic growth requirement and the abandonment of both genes through evolution allows *C. jejuni* to maintain a small genome while sustaining a functional TCA cycle. By contrast, FumB is essential for *E. coli* during anaerobic respiration and a relative high level of FumA activity has also been detected in *E. coli* under anaerobic conditions despite the expression of *fumA* is down regulated (Tseng *et al.*, 2001).

4.4.2 The iron and oxygen responsive regulation of *fumC* and *racR*

4.4.2.1 Factors affect *fumC* expression

As the only fumarase coding gene in the *C. jejuni* genome, regulation of *fumC* expression was predicted to involve a complicated regulatory network in order to compensate for the absence of *fumA* and *fumB* and to respond to suboptimal growth conditions such as iron limitation or oxidative stress. *fumC* was initially demonstrated to be induced by iron when total RNA used for northern blot analysis were purified from cell grew in conditions routinely used for β -galactosidase assays. The exact mechanism of this positive regulation was unclear as the *fumC* transcriptional profiles were not altered in the *fur_{Cj}* mutant (Figure 3.15) indicating the iron-responsive regulation of *fumC* is mediated by another regulator.

When growth conditions mimicking the conditions used by Holmes *et al.* (2005) were analysed, a potential negative regulation of *fumC* by iron was observed (Figure 3.17) though the involvement of Fur_{Cj} and PerR_{Cj} remained inconclusive. One of the major differences between the two culture conditions was the growth phase variation although no changes in *fumC* regulation between the two phases were detected using northern blot and β -galactosidase assays and this observation was consistent with Smith *et al.*'s observation that fumarase activity is not affected by the age of cultures (Smith *et al.*, 1999). As the levels of internal cellular iron at the start of liquid culture inoculation were also different between the two culturing methods, the variation of *fumC* expression and regulation observed by northern blot analysis is therefore most likely to be caused by the difference in growth rate arising from internal iron availability. In another word, prior to inoculating into MHB supplemented with 20 μ M Desferal, the initial intercellular iron concentration is much higher for *C. jejuni* grown on MHA plates using the Holmes's method (Holmes *et al.*, 2005) than using the β -galactosidase assay method, and this key variation could greatly affect the regulation of *fumC*.

Interestingly the iron responsive regulation of *fumC* was not detected in a separate study of the *C. jejuni* Fur_{Cj} regulon (Palyada *et al.*, 2004) where cells used for RNA purification were grown at 37 °C rather than 42 °C. The different outcomes between these two studies were likely to be caused by this temperature variation that might have had a direct effect on iron responsive regulation of *fumC* or indirect effects on the

growth rate. In fact, a recent comparison of the *C. jejuni* proteome between cells cultured at these two temperatures demonstrated a 2-fold increase in the level of FumC at 37 °C, thus potentially indicating the expression of *fumC* is temperature-dependent. In addition, the minimal essential medium MEM α used by Palyada *et al.* (as suppose to MH used by Holmes *et al.*) may also have direct or indirect effects on the expression of *fumC* (Palyada *et al.*, 2004; Holmes *et al.*, 2005).

The temperature-dependent cell growth of *C. jejuni* has been previously investigated by Brás *et al.* (1999) where the RacR-RacS TCS was characterised. RacR has been recently demonstrated to alter the expression of several metabolism genes including *fumC* although the regulation of *fumC* was mediated by oxygen limitation rather than temperature (van Mourik *et al.*, 2009). The regulation of *fumC* and *racR* in response to iron and oxygen availability and the involvement of Fur_{Cj}, PerR_{Cj} and RacR were comprehensively analysed by northern blot assays in this study and is summarised in Figure 4.16.

4.4.2.2 Regulation of *fumC* expression under high iron conditions

Using the culturing conditions described by Holmes *et al.* (2009), *fumC* is transcribed in both iron conditions and it is repressed by RacR and Fur_{Cj}. The level of *fumC* expression is also marginally decreased in high iron conditions, though the physiological relevance of this transcriptional variation (if any) is unknown and quantitative measurement by densitometry is required to validate this observation. RacR

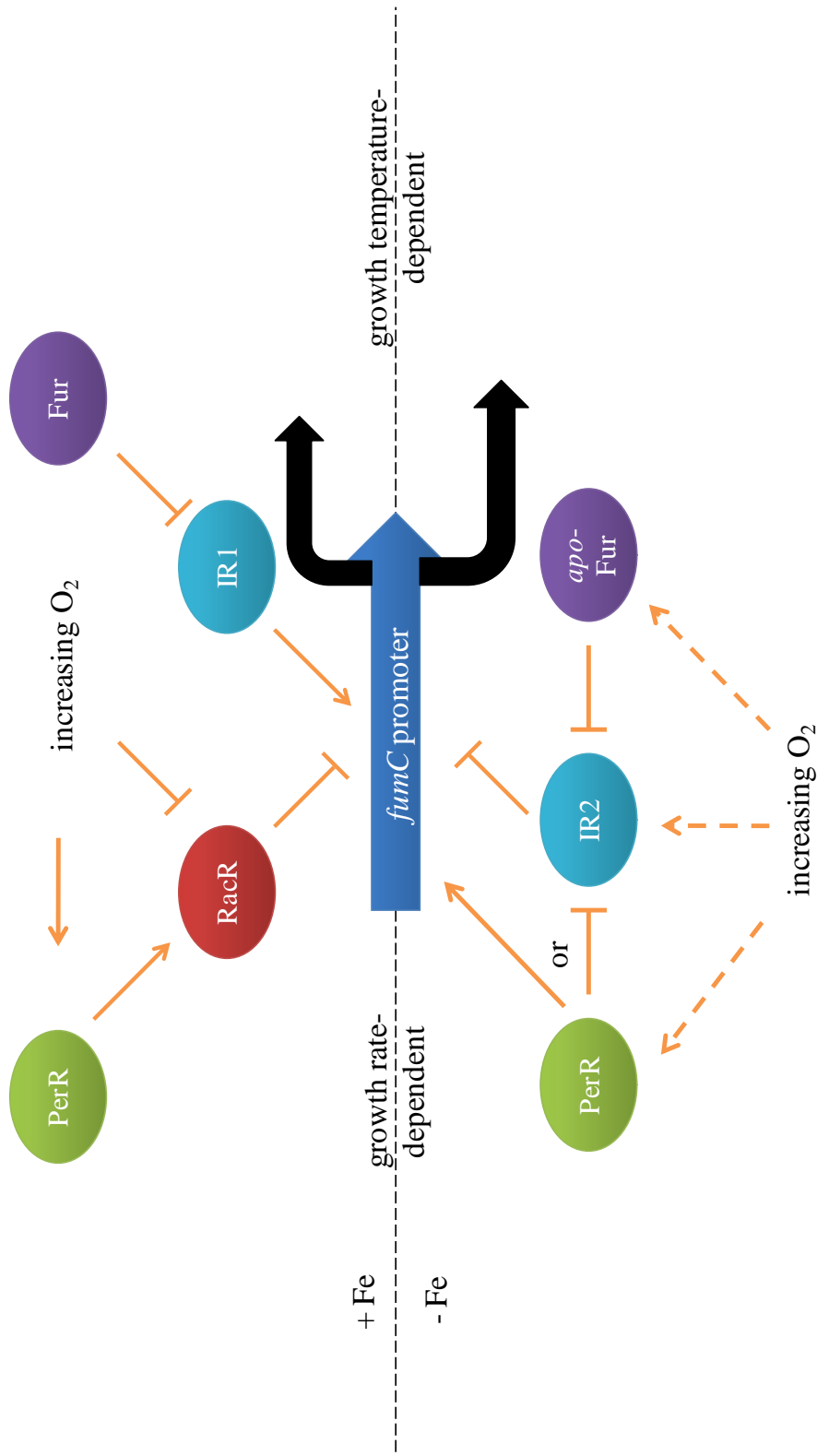


Figure 4.16: Transcriptional regulation of *fumC* by several regulators in response to oxygen and potentially iron availability. Arrow heads represent gene induction whereas gene repression is indicated by flat heads. The effects of oxygen on PerR_{Cj}, apo-Fur_{Cj} and IR2 are uncertain and are indicated by dash arrows. The level of *fumC* expression is represented by the size of black arrows.

is the dominant repressor of *fumC* under low oxygen conditions (3%) where *racR* itself is highly induced by iron and an unknown regulator. Fur_{Cj} plays a less significant role in the repression of *fumC* under this condition and as iron containing Fur_{Cj} does not contact the *fumC* promoter directly, the exact mechanism of *fumC* repression by Fur_{Cj} is unclear. One possible explanation is the repression of *fumC* by Fur_{Cj} using other metal ions such as manganese as the co-factor. Alternatively, *fumC* may be indirectly repressed by Fur_{Cj} through an unknown intermediate regulator (IR1) which itself is negatively regulated by Fur_{Cj} and iron. As *C. jejuni fumC* shares a high degree of identity (76.9%) with the *H. pylori fumC* (Smith *et al.*, 1999), it's highly possible that like in *H. pylori* 26695 (Xiao *et al.*, 2009) the identity of IR1 is a sRNA located on the opposite strand as the *fumC* gene. Sequence alignment of *C. jejuni* NCTC 11168 *fumC* and *H. pylori* 26695 *fumC* (2.5.1) indicated that the two genes shares 68.5% identity and the region that encodes the sRNA in *H. pylori* 26695 shares 64.3% identity with the corresponding region in *C. jejuni* NCTC 11168 *fumC* (data not shown). Therefore further characterisation of this region by northern blot and real time RT-PCR is required to confirm the identity of IR1.

Once the oxygen concentration reaches an optimal level (7%), the expression level of *racR* is reduced which allows Fur_{Cj} to play more significant roles in the repression of *fumC* under high iron conditions. When the oxygen level increases to 11%, the iron-induced activation of *racR* becomes dependent on PerR_{Cj} despite that *perR_{Cj}* itself is normally expressed under iron-limited conditions. However the up regulation of *perR_{Cj}* expression has been previously observed from microarray data where the level of

perR_{Cj} mRNA is elevated in the presence of iron and hydrogen peroxide (Palyada *et al.*, 2009). The induction of *racR* by PerR_{Cj} under oxidative stress conditions presumably allows RacR to resume the dominant role as the *fumC* repressor in order to eliminate the possible derepression of *fumC* caused by the interaction of reactive oxygen species and the iron co-factor of the Fur_{Cj} protein.

The interplay of both RacR and Fur_{Cj} in the regulation of *fumC* is also reflected by the two *fumC* transcripts determined by northern blot analysis (3.16) and during RACE (3.18). One of these transcripts is a longer but weaker transcript detected in a *racR* mutant background under high iron conditions and as *racR* is induced by iron, it's most likely that this weaker (secondary) transcript is repressed solely by RacR. The stronger (primary) *fumC* transcript on the other hand is presumably repressed by RacR when *racR* is high expressed and indirectly by Fur_{Cj} when RacR becomes less dominant such as in 7% oxygen.

4.4.2.3 Regulation of *fumC* expression under low iron conditions

Compared to the repression of *fumC* by RacR and Fur_{Cj} under high iron conditions determined by northern blot analysis, the positive influences of *fumC* expression by PerR_{Cj} and Fur_{Cj} under iron-limited conditions are less clear (Figure 4.16). At 3% oxygen, the expression of *fumC* is derepressed in the absence of RacR and as the oxygen concentration increases to 7%, Fur_{Cj} and PerR_{Cj} also positively influence the expression of *fumC*. The activation of *fumC* by Fur_{Cj} under iron-limited conditions is

particularly puzzling as Fur_{Cj} normally does not function under this condition due to the loss of its iron co-factor. The only possibility is the involvement of *apo-Fur_{Cj}* as a repressor which represses an intermediate repressor (IR2) and in turn allows the expression of *fumC*. Although *apo-Fur_{Hp}* repression has been exclusively studied in *H. pylori* (Delany *et al.*, 2001; Ernst *et al.*, 2005), a recent investigation of the *C. jejuni dsbA2* promoter indicated a direct repression of *dsbA2* by *apo-Fur_{Cj}* *in vitro* and *in vivo* (Grabowska *et al.*, 2011). As this is the only example of *apo-Fur_{Cj}* repression in *C. jejuni* to date, further characterisations of *apo-Fur_{Cj}* repression and its role in the indirect positive regulation of *fumC* are required. In contrast to *fur_{Cj}*, *perR_{Cj}* is induced under low iron conditions therefore whether *PerR_{Cj}* has a direct positive influence on *fumC* expression or through the repression of IR2 or yet another intermediate is unclear.

As the oxygen level reaches 11%, the positive influence of *fumC* expression by Fur_{Cj} and $PerR_{Cj}$ increases as demonstrated by the strong repression of *fumC* under iron limited conditions in AV17 and AV63. As a peroxide sensing regulator, the expression *perR_{Cj}* is induced in the presence of hydrogen peroxide. However as the repressive effect of $PerR_{Cj}$ on the oxidative stress response genes is also released in the presence of hydrogen peroxide, the involvement of oxygen in the positive regulation of *fumC* by $PerR_{Cj}$ cannot be easily determined without the expression profiles of *perR_{Cj}* gene itself and the identity of IR2.

Despite the changing of oxygen concentrations, the overall level and pattern of

iron-responsive regulation of *fumC* is unaffected and this finding is in full agreement with the previous observation that the *C. jejuni* fumarase activity remains constant under different oxygen tensions (Smith *et al.*, 1999). This unaltered expression of *fumC* is expected considering the importance of FumC in maintaining the active cell growth and a functional TCA cycle, however regulation of *fumC* by several global regulators in a complicated overlapping network has therefore evolved in order to compensate for the lack of FumA and FumB and further experiments are required to fully reveal the identity and mechanisms of all the regulators involved in this network.

Although the expression of *fur_{Cj}* and *perR_{Cj}* has been comprehensively characterised (van Vliet *et al.*, 2000; Palyada *et al.*, 2009), different culturing conditions used in these studies and in this current study such as temperature, agitation and oxygen levels making the expression of *fur_{Cj}* and *perR_{Cj}* difficult to predicate and to compare with previous studies. Therefore one critical experiment to further characterise the regulation of *fumC* as well as *racR* by *Fur_{Cj}* and *PerR_{Cj}* is to repeat the northern blot assays with the addition expression profiles of *fur_{Cj}* and *perR_{Cj}*. The addition of a *fur_{Cj}* and *perR_{Cj}* double mutant (AV67) is also important to understand the co-involvement of *Fur_{Cj}* and *PerR_{Cj}* in the regulation of *fumC*, especially under iron-limited conditions. Due to the inability to obtain sufficient amount of AV67 for RNA purification and the inaccuracy of northern blot analysis, real time RT-PCR is more preferable to accurately determine the transcriptional profiles of *fumC* and each of the regulator coding genes.

4.4.2.4 Possible post-transcriptional and translational regulation of *fumC*

The identity of IR2 is difficult to determine which requires the characterisation of other oxidative stress response regulators and one of the possible candidates is the carbon starvation regulator CsrA. CsrA has been identified in *E. coli* as a posttranscriptional regulator (Romeo, 1996) and it plays important roles in *H. pylori* in the regulation of motility, oxidative stress resistance and mouse colonisation (Barnard *et al.*, 2004). CsrA also has significant regulatory roles in *C. jejuni* pathogenesis as it contributes to oxidative stress survival, biofilm formation and host cell invasion (Fields and Thompson, 2008). The expression of over 100 proteins have been demonstrated by proteomic analysis to alter in the *C. jejuni* 81-176 *csrA* mutant (Thompson *et al.*, 2009) and FumC is potentially one of these putative CsrA targets (S. Thompson, personal communication).

The genomic DNA of *C. jejuni* 81-176 *csrA* mutant was obtained, though further investigations were not performed due to time limitations. Further characterisation of *fumC* regulation by CsrA requires the initial construction of NCTC 11168 *csrA* mutant from the 81-176 mutant and subsequently analyse the expression profiles of *fumC* as well as *csrA* in response to iron and oxygen and the possible regulation of *csrA* by Fur_{Cj} and PerR_{Cj}. As CsrA acts as a posttranscriptional regulator, the exact mechanism of *fumC* regulation by CsrA is difficult to determine by northern blot assays alone. EMSA analysis of purified CsrA and *fumC* mRNA is one alternative method to study the interaction between CsrA and the 5' UTR of *fumC* as direct binding of 81-176 CsrA and

C. jejuni RNA have been demonstrated previously (Thompson et al., 2009).

The expression of FumC may also be affected on the translational level as the transcriptional profiles of *fumC* did not match the results of fumarase activity assays. This result discrepancy is potentially caused by the temperature sensitive nature of the fumarase activity assay and a temperature controlled automated spectrometer is more preferable in order to obtain more accurate results. Alternatively, western blot assays can be used to determine the FumC expression profiles although anti-FumC antibodies are required for this method. Regardless of the chosen method, the effects of malate supplementation on the expression of *fumC* and other genes cannot be overlooked and therefore the *fumC* mutant strain (that requires malate supplementation) needs to be excluded from the fumarase activity assays in order to determine the translational regulation of *fumC*.

4.4.3 The interaction of RacR with RacS-HK and RacR regulated promoters

The His₆-tagged NCTC 11168 RacR and the histidine kinase domain of RacS were purified and the *in vitro* transfer of phosphate between the two proteins was observed which demonstrated that RacR and RacS form a TCS. High affinity binding of RacR and the *aspA* promoter was determined in the presence of RacS-HK and ATP and interestingly RacR also interacts with the *aspA* promoter without the presence of ATP and this interaction was partially inhibited by RacS-HK. This observation suggested that RacS plays important roles in preventing interactions between unphosphorylated RacR

and RacR regulated genes and the mechanism involved in this process does not require the transfer of phosphate. As this unphosphorylated RacR-DNA interaction was only observed for the *aspA* promoter, and too faint to be observed for *fumC*, EMSA assays with other RacR regulated genes are required to fully understand this process.

A relatively weak RacR-DNA interaction was determined for the *fumC* promoter and this finding was in agreement with the partial repression of *fumC* by RacR revealed by northern blot analysis. DNase I footprinting assays performed to determine the RacR binding site were unsuccessful despite the strong protein-DNA interactions observed in EMSAs. The result discrepancy between EMSA and DNase I footprinting assays could be explained by a “caging” effect where in EMSA, the protein-DNA complex was stabilised by the non-denaturing polyacrylamide gel, whereas in DNase I footprinting experiments, protein-DNA interaction was weak in solution and the complex could be easily dissociated by DNase I (Fried and Liu, 1994). However due to the high affinity of RacR binding to the *aspA* promoter even without the presence of RacS and ATP, the negative DNase I footprinting results were likely to be caused by incompatibility between the buffers used for phosphorylation, DNA-protein interaction and DNase I footprinting assays. As RacR alone interacts with the *aspA* promoter, a DNase I footprinting assay without the presence of RacS and ATP will be able to eliminate the buffer incompatibilities and further buffer optimisations are required in order to determine the RacR binding site on the *fumC* promoter.

4.4.4 The regulation of *chuA* by *PerR_{Cj}* and *RacR*

When the expression profiles of *chuA* were analysed as a positive control using northern blot assays, a transcript of approximately 1.6 Kb was detected (Figures 4.2-4.4). Although the actual size could not be accurately determined, it nevertheless suggests that *chuA* is predominantly transcribed as a monocistronic mRNA and the downstream *chuBCD* genes may have their own promoter(s).

Additionally, the transcription of *chuA* was also found to be indirectly repressed under high iron conditions and 11% oxygen by *PerR_{Cj}* and this repression was mediated by *RacR* (Figure 4.4). This repression of *chuA* by *PerR_{Cj}* under elevated oxygen levels eliminates the possible derepression of *chuA* by *Fur_{Cj}* due to reactive oxygen species and prevents further uptake of iron under oxidative stress conditions. *chuA* has been previously determined to be repressed by *PerR_{Cj}* though this repression was mediated by hydrogen peroxide in the absence of iron (Palyada *et al.*, 2009). The mechanism of this repression was speculated to be caused by the release of iron from iron-sulphur in the presence of hydrogen peroxide and subsequently led to the repression of *chuA* by *Fur_{Cj}* (Palyada *et al.*, 2009). The expression of *chuA* was also found to be up regulated in the presence of both oxygen and iron and this activation was thought to enhance hydrogen peroxide detoxification by producing haem that is essential for *KatA*'s catalytic activity (Palyada *et al.*, 2009). The culturing temperature and oxygen levels used in this current investigation may explain the results discrepancy between these two studies and the expression of *chuA* as well as *racR* in response to hydrogen peroxide requires further

investigation. Both studies however demonstrated the interconnected link between oxidative stress and iron metabolism and the involvement of oxygen- and iron-responsive regulators in this regulatory network.

Chapter 5: General discussion

Regulation of gene expression in response to environmental or intracellular stimuli is an essential process for the survival of every single living organism and this is particularly so for pathogenic microorganisms. Effectively regulated global and specific regulatory networks allow pathogenic bacteria to survive in the natural environment during transmission, to adapt to the host environment and avoid the host immune response, and to cause disease (Snyder and Champness, 2003). For the foodborne enteric pathogen *C. jejuni*, the co-regulation of iron homeostasis and oxidative stress responses by Fur_{Cj} and its homologue PerR_{Cj} is such an example of global gene regulation. Both transcriptional regulators are vital for *C. jejuni* in *in vivo* survival and colonisation (Palyada *et al.*, 2004; 2009).

Understanding the interaction between Fur_{Cj} and its operator sequence, the Fur_{Cj} box, is essential for revealing the mechanisms of Fur_{Cj} regulation and for identifying Fur_{Cj} regulated genes. The aim of this research was to investigate the base-specific interaction of Fur_{Cj} and the Fur_{Cj} box by a mutagenesis approach using the Fur_{Cj} box of the classically repressed *chuA* promoter and a Fur_{Cj} box-like sequence of the non-classically Fur_{Cj} regulated *fumC* promoter. Additionally, the transcriptional regulation of *fumC* was further investigated to determine the regulatory role of Fur_{Cj} and the interplay between Fur_{Cj} and other regulators in the regulation of *fumC* expression in *C. jejuni*.

5.1 Fur_{Cj}-Fur_{Cj} box interaction

By using a combination of EMSA, β -galactosidase and DNase I footprinting assays, it was demonstrated that in the functional state, two Fur_{Cj} dimers cooperatively recognise and bind to the Fur_{Cj} box. Binding of the two Fur_{Cj} dimers is likely to occur at the opposite face of the Fur_{Cj} box and Fur_{Cj} polymerisation was not observed indicating that the binding of two Fur_{Cj} dimers is sufficient, at least for *chuA*, to mediate transcriptional repression. Although this mechanism of Fur_{Cj}-Fur_{Cj} box interaction is well conserved among many well characterised Fur orthologues, including Fur_{Ec} (Lavrrar *et al.*, 2002), Fur_{Bs} (Baichoo and Helmann, 2002) and Fur_{Pa} (Pohl *et al.*, 2003), the putative Fur_{Cj} box sequence proposed by van Vliet *et al.* (2002) and later by Palyada *et al.* (2004) matched poorly with the 19 bp Fur_{Ec} box consensus sequence (de Lorenzo *et al.*, 1987). The putative Fur_{Cj} box sequence proposed by Palyada *et al.* (2004) was experimentally verified in this study as this sequence was enclosed in the 31 bp Fur_{Cj} protected region of the *chuA* promoter and it was able to promote Fur_{Cj} binding when introduced into a functionally unrelated *fumC* promoter (Table 5.1). This consensus sequence however was only found in 11 out of the 53 Fur_{Cj} regulated genes indentified by Palyada *et al.* (2004) thus further *in vitro* binding studies of other Fur_{Cj} repressed promoters are required to experimentally refine or possibly redefine a consensus Fur_{Cj} box sequence. The experimental design used in this study should also be applied to the newly purified PerR_{Cj} protein (Handley *et al.*, 2010) in order to facilitate the understanding of the Fur_{Cj} regulator family as a whole. However future mutational analyses of the Fur_{Cj} or PerR_{Cj} binding site should always be accompanied by detailed promoter structural studies to avoid any undesired disruption of the functional promoter.

A 7 bp Fur_{Cj} protected region was observed for *chuA10/19* which was likely to be caused by the binding of a single Fur_{Cj} dimer although only one of the Fur_{Cj} monomers was tightly bound, presumably due to the mutations toward the centre and the 3' end of the Fur_{Cj} box. This observation potentially suggests that the Fur_{Cj} box can be interpreted by the (7-1-7)₂ model proposed by Baichoo and Helmann (2002). However no symmetric elements can be observed in the 19 bp consensus sequence indicating that unlike most bacteria, the exact sequence of the Fur_{Cj} box may not play a vital role in Fur_{Cj}-Fur_{Cj} box interaction. Additionally, although mutations of the 1st, 7th, 13th and 19th bases of the *chuA* Fur_{Cj} box introduced in this study as well as mutations of several bases of the *p19* operon promoter introduced in previous work (Breg, 2007) have negative effects on the affinity of Fur_{Cj} binding, the result obtained by these two studies did not correlate well with each other. This result discrepancy also suggests that the overall architecture of a Fur_{Cj} regulated promoter plays a more significant role in Fur_{Cj} box recognition and Fur_{Cj} binding rather than the sequence of the Fur_{Cj} box *per se*. This conclusion is in full agreement with the latest view on the *H. pylori* Fur_{Hp} box (Carpenter *et al.*, 2009). Fur_{Hp} shares 32.6% identity and 52.2% similarity with Fur_{Cj} (Miles *et al.*, 2010a), and as in *C. jejuni*, no strong consensus Fur_{Hp} box sequence is present in the promoter regions of Fur_{Hp} regulated genes (Merrell *et al.*, 2003). Interestingly, although the Fur_{Cj} box does not share any sequence homology with the Fur_{Hp} box, *furCj* when expressed *in trans* was able to complement Fur_{Hp} in the repression of the *amiE* promoter (Miles *et al.*, 2010a), which further indicated that the AT-rich characteristic of both *C. jejuni* and *H. pylori* promoters is a key feature in the

Fur-mediated iron-responsive repression for both bacteria.

In addition to iron-dependent repression, *apo-Fur_{Cj}* has been recently demonstrated to repress the *dsbA2* promoter both *in vitro* and *in vivo* (Grabowska *et al.*, 2011). Although several instances of *apo-Fur_{Hp}* regulation have been investigated in *H. pylori* (Delany *et al.*, 2001; 2002; 2003; Ernst *et al.*, 2005), whether *apo-Fur_{Hp}* functions as a monomer or a dimer is uncertain. The recently resolved *Fur_{Hp}* crystal structure reveals the presence of an N-terminal extension that functions in stabilising the *Fur_{Hp}* structure in the absence of a metal co-factor (Dian *et al.*, 2011). This extension is also present in *Fur_{Cj}* (Miles *et al.*, 2010a) suggesting that both proteins function as dimers in their *apo*-form. EMSAs of the *dsbA2* promoter with *apo-Fur_{Cj}* revealed one shift species whereas multiple species were observed for the *chuZ-chuA* intergenic region with *Fur_{Cj}* (Grabowska *et al.*, 2011), which potentially suggested that a single dimer is the functional state of *apo-Fur_{Cj}* repression. Although the *apo-Fur_{Cj}* operator sequence has not been determined by DNase I footprinting assays, *fur_{Cj}* when expressed *in trans* was not able to complement *apo-Fur_{Hp}* in the repression of the *pfr* promoter, indicating that unlike *Fur*, *apo-Fur* of *C. jejuni* and *H. pylori* recognise their own unique operator sequence.

Although the DNase I footprint assay and EMSA were successfully used in this study to demonstrate the interaction between *Fur_{Cj}* and the *chuA* promoter *in vitro*, those techniques are only suitable for studying individual *Fur_{Cj}*-regulated promoters. In order

to further reveal the global regulatory role of Fur_{Cj} in both the iron-bound and *apo*-form, a comprehensive investigation of Fur_{Cj}-DNA interactions on a genome-wide basis is ultimately required. Such investigation could be achieved by the ChIP-on-chip or the ChIP-Seq techniques, which combine chromatin immunoprecipitation with microarray technology or high-throughput DNA sequencing respectively to allow the study of *in vivo* interactions between proteins and DNA (Ren *et al.*, 2000; Johnson *et al.*, 2007). The outcome of such investigations would allow the identification of genes that are directly regulated by Fur_{Cj} or *apo*-Fur_{Cj} and an alignment of these Fur_{Cj} regulated promoter regions would confirm the presence or the absence of a Fur_{Cj} box and an *apo*-Fur_{Cj} box consensus sequence. The ChIP-on-chip technique could also be used in a Fur_{Cj} mutant background that has been complemented *in trans* by a *fur* orthologue. Such a study would reveal the key differences in the mechanism of DNA recognition and DNA-binding between Fur_{Cj} and other Fur orthologues at a genome-wide level.

Prior to the submission of this dissertation, a ChIP-chip characterisation of Fur_{Cj} was presented in the CHRO 2011 meeting (Butcher and Stintzi, 2011). In this study, approximately 90 genes involved in DNA replication, flagella and surface structure composition, iron acquisition and energy metabolism were identified to be directly Fur_{Cj} regulated (Butcher and Stintzi, 2011). Such observations further illustrated the global regulatory role of Fur_{Cj} and the knowledge acquired from this study would provide a definitive determination of the Fur_{Cj} box and a better understanding of the Fur_{Cj}-Fur_{Cj} box interaction.

5.2 Regulation of *chuA* expression

Although the haem OM receptor *chuA* is perhaps one of the best characterised Fur_{Cj} repressed iron acquisition genes in *C. jejuni* (van Vliet *et al.*, 1998; Ridley *et al.*, 2008), in this study the analysis of *chuA* promoter structure, transcriptional regulation, and interaction with Fur_{Cj} revealed new insights into the regulation of *chuA* expression (Figure 5.1). Under iron-rich conditions in optimal or low oxygen concentrations, Fur_{Cj} binds to the Fur_{Cj}-box in the 5' UTR of *chuA* and prevents the transcription of the downstream coding region by RNA pol. When the extracellular oxygen concentration increases, *chuA* is co-repressed by Fur_{Cj} and RacR. Although EMSA was not carried out for the *chuA* promoter with RacR due to time limitations, northern blot analysis demonstrated that the deletion of either *racR* or *furCj* led to a derepression of *chuA* under high iron conditions. RacR presumably binds to the *chuA* promoter region close to the *chuA* Fur_{Cj} binding site as the expression of the upstream *chuZ* promoter was not affected by RacR. Although *chuA* has been considered to form an operon with the downstream *chuBCD* genes as no intergenic regions are present (Miller *et al.*, 2009), northern blot analysis of *chuA* expression indicates that *chuA* is primarily transcribed as a monocistronic mRNA. As *chuBCD* are also regulated by Fur_{Cj} in response to iron availability (Palyada *et al.*, 2004; Holmes *et al.*, 2005), it is likely that a Fur_{Cj}-regulated promoter is present in the *chuA* coding region that functions in controlling the downstream *chuBCD* genes and this promoter is also potentially regulated by RacR under high oxygen concentrations. To test this hypothesis, northern blot analyses using

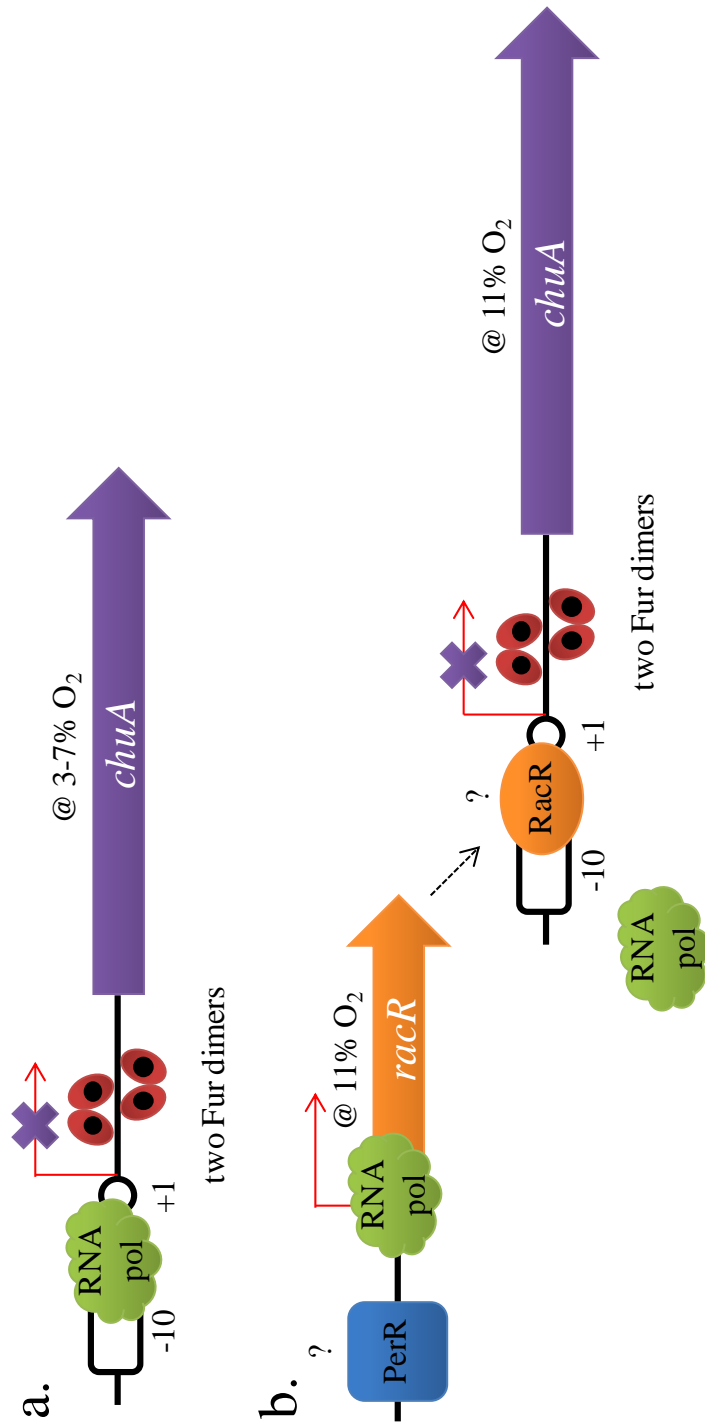


Figure 5.1: Iron-responsive repression of *chuA* at different oxygen concentrations by Fur_{Cj} and RacR. In 3-7% oxygen (a), two Fur_{Cj} dimers bind to the 5' UTR of *chuA* and repress gene expression by preventing RNA pol from transcribing the DNA template. In 11% oxygen (b), PerR_{Cj} activates the expression of *racR*, and then RacR and Fur_{Cj} co-repress the expression of *chuA*. Genes and promoter regions are not drawn in proportion to their sizes and the exact mechanisms of PerR_{Cj} and RacR regulation are unknown.

chuBCD-specific probes would confirm the co-expression of these three genes and their regulation by RacR, and *lacZ* reporter assays using the *chuA* coding region would confirm the presence of a promoter for *chuBCD*.

Interestingly, the regulation of *chuA* expression by RacR is modulated by PerR_{Cj} (Figure 5.1) and although the mechanism of *racR* activation by PerR_{Cj} is unknown, this observation is in agreement of with the recent characterisation of the PerR_{Cj} regulon, which demonstrates that the expression of *chuA* (as well as *chuBCD*) is regulated by PerR_{Cj} and Fur_{Cj} in response to iron and exposure to hydrogen peroxide (Palyada *et al.*, 2009). The outcome of the current study and Palyada *et al.*'s investigation (2009) collectively illustrate an intricate regulatory network of *chuA* expression involving three transcriptional regulators. Under high-rich conditions, Fur_{Cj} represses the expression of *chuA* to prevent further iron uptake. When the extracellular oxygen concentration increases, PerR_{Cj} activates the expression of *racR* which with Fur_{Cj} in turn strengthens the repression of *chuA* to minimise iron-mediated oxidative stress. However, when the cell is exposed to hydrogen peroxide, both PerR_{Cj} and Fur_{Cj} are presumably inactivated due to the oxidation of their ferrous iron co-factor, and this leads to a down regulation of *racR* and subsequent derepression of *chuA*. The expression of *chuA* allows further haem uptake into the cell to enhance hydrogen peroxide detoxification as haem has been shown to exhibit antioxidant properties (Nagababu and Rifkind, 2004) and it is also required for the catalytic activity of the catalase, KatA (Palyada *et al.*, 2009). This derepression of *chuA* to enhance haem uptake, but not for the actual iron content is

further supported in this study and Palyada *et al.*'s investigation (2009) in that the expression of *chuZ* is not affected by the increasing oxidative stress. Additionally, although *chuA* is not required for *C. jejuni* intestinal colonisation (Haigh *et al.*, 2010), the tight regulation of *chuA* by three regulators suggests that it is likely to play other essential roles in pathogenesis such as deep tissue survival (R. Haigh, personal communication). Furthermore, although the expression of other *C. jejuni* iron uptake systems has also been shown to be regulated by Fur_{Cj} and PerR_{Cj} (Palyada *et al.*, 2004; 2009), the exact mechanism of PerR_{Cj} regulation and the possible involvement of RacR in these regulatory networks are currently unknown. Therefore, further transcriptional characterisation of other iron uptake systems in response to iron and oxygen is required to reveal the involvement of any multilevel regulation as seen with *chuA*.

5.3 Regulation of *fumC* expression

The co-involvement of Fur_{Cj}, PerR_{Cj} and RacR in oxygen- and potentially iron-responsive gene regulation has been further demonstrated for the regulation of *fumC*. Encoding the only functional fumarase in *C. jejuni*, *fumC* is essential for supporting active cell growth and maintaining a functional TCA cycle. As illustrated in Figure 4.16, the expression of *fumC* is primarily repressed by RacR, but the transcription level is also potentially regulated by Fur_{Cj}, apo-Fur_{Cj} and PerR_{Cj} through two hypothetical intermediate regulators IR1 and IR2. As well as iron and oxygen levels, the expression of *fumC* is also likely to be dependent on growth rate and growth temperature and evidence of post-transcriptional and translational regulation of *fumC*

have been demonstrated both in a previous study of the CsrA regulon (S. Thompson, personal communication) and using fumarase activity assays in this study. Further transcriptional studies of *fumC* as well as *fur_{Cj}* and *perR_{Cj}* are required to fully appreciate the extent of this complicated regulatory network, but due to technical impracticability and inaccuracy of northern blot analysis, a quantitative method such as reporter assays or real-time PCR would be more appropriate. Although further characterisation of *fumC* expression is required, *fumC* regulation nevertheless serves as a good example to illustrate the necessity for *C. jejuni* to cooperatively regulate essential gene expression by several regulators in response to different environments. This allows *C. jejuni* to efficiently use its rather limited set of regulators to effectively control the expression of this essential TCA cycle enzyme under the sub-optimal conditions usually encountered during transmission and colonisation.

5.4 The RacR-RacS TCS

The response regulator RacR and its cognate sensor RacS form a TCS and, in NCTC 11168, RacR represses the expression of at least *chuA* and *fumC* in response to iron. Recent characterisation of the 81116 RacR regulon indicates that the expression of many metabolism genes is controlled by RacR in response to low oxygen conditions and direct binding of RacR has been demonstrated *in vitro* for five of these RacR regulated promoters including *aspA* (van Mourik *et al.*, 2009). Further investigation of NCTC 11168 RacR and 81116 *aspA* in this project indicated that when RacS senses a decline in the extracellular oxygen concentration, it phosphorylates RacR and allows it

to repress the expression of *aspA* (Figure 5.2). However without an extracellular signal, unphosphorylated RacS physically interacts with RacR and prevents RacR from forming a non-specific interaction with the *aspA* promoter. This mechanism of RacR repression is also likely to be true for *fumC* although the non-specific interaction was too weak to be observed in this study. Due to technical issues, the RacR binding sites on the *aspA* and *fumC* promoters were unable to be determined by DNase I footprinting assays. However comparative DNase I footprinting analyses of phosphorylated and unphosphorylated RacR with the *aspA* promoter would reveal any physiological role of the non-specific interaction of RacR and RacR-regulated promoters. Additionally, as the expression of *racR* is iron- and PerR_{Cj}-induced, the expression of many RacR regulated energy metabolism genes identified by van Mourik *et al.* (2009) are also likely to be indirectly regulated by iron and PerR_{Cj}. Characterisation of the expression of these genes under different oxygen levels would allow further demonstration of the global regulatory role of PerR_{Cj}.

5.5 Final remarks

In conclusion, this study provided a new insight into the Fur_{Cj}-promoter interaction and the inter-regulatory effects of Fur_{Cj}, PerR_{Cj} and RacR in the regulation of *C. jejuni* gene expression in response to iron availability and oxidative stress. This study also provided a novel understanding of the importance of *fumC* in maintaining a functional cellular metabolism and illustrates how *C. jejuni* can effectively utilise its limited set of regulators to control essential gene expression. Ultimately it is hoped that a better

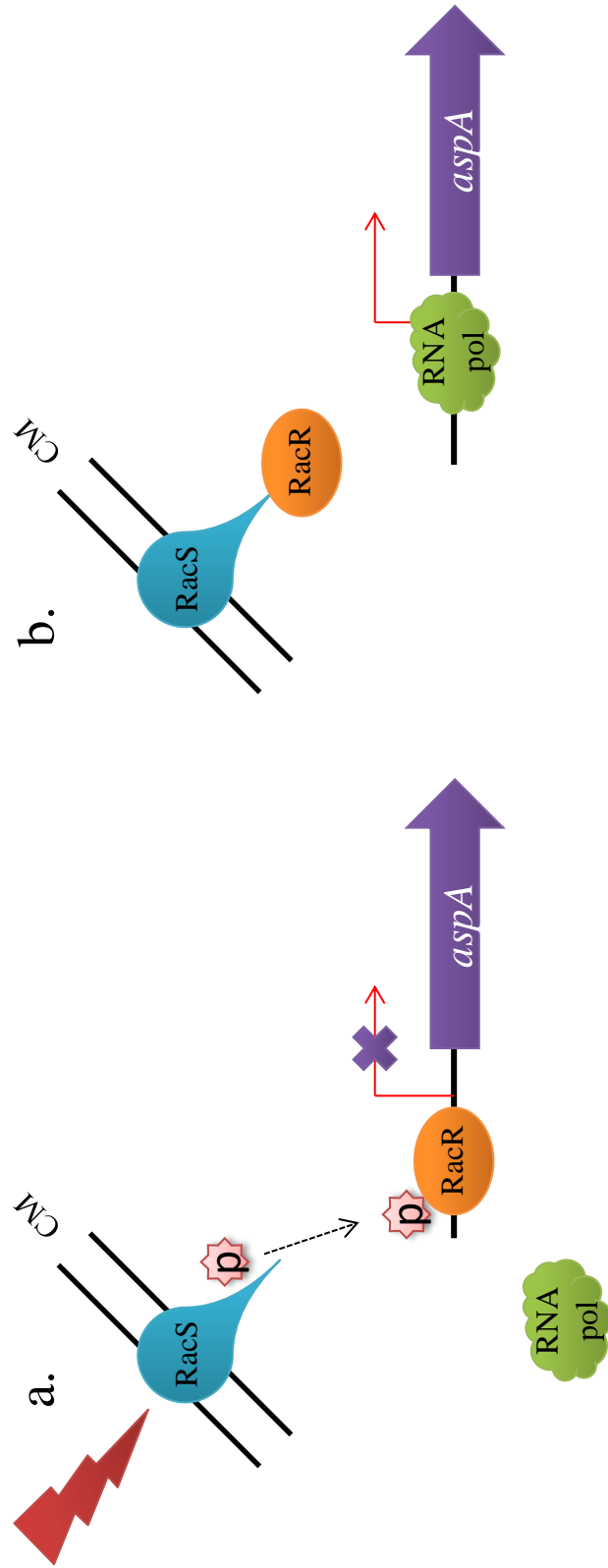


Figure 5.2: Regulation of the *aspA* promoter by the RacR-RacS TCS in response to low oxygen conditions. When RacR senses a decline in the extracellular oxygen concentration (a), it autophosphorylates and transfers the phosphate group to the response regulator RacR. Phosphorylated RacR binds to the promoter of *aspA* to repress expression. In the absence of an extracellular signal (b), unphosphorylated RacS interacts with RacR to inhibit the interaction between unphosphorylated RacR and the *aspA* promoter thus allowing the transcription of *aspA* by RNA pol.

understanding of the role of iron and oxygen as key environmental signals for controlling of *C. jejuni* pathogenesis will be achieved. The availability of such invaluable information will advance our current knowledge on the physiology and pathogenesis of *C. jejuni* and lead to potential strategies and drugs for detecting and eliminating this harmful human pathogen from infection.

Bibliography

Abdul-Tehrani, H., Hudson, A. J., Chang, Y-S., Timms, A. R., Hawkins, C., Williams, J. M., Harrison, P. M., Guest, J. R. and Andrews, S. C. (1999) Ferritin mutants of *Escherichia coli* are iron deficient and growth impaired and fur mutants are iron deficient. *J. Bacteriol.* **181**:1415-1428

Adrait, A., Jacquamet, L., Le Pape, L., Gonzalez de Peredo, A., Aberdam, D., Hazemann, J., Latour, J. and Michaud-Soret, I. (1999) Spectroscopic and saturation magnetization properties of the manganese- and cobalt-substituted Fur (ferric uptake regulation) protein from *Escherichia coli*. *Biochemistry* **38**:6248-6260

Ahmad, R., Brandsdal, B. O., Michaud-Soret, I. and Willassen, N. P. (2009) Ferric uptake regulator protein: binding free energy calculations and pre-residue free energy decomposition. *Proteins* **75**:373-386

Ahn, B. E., Cha, J., Lee, E. J., Han, A. R., Thompson, C. J. and Roe, J. H. (2006). Nur, a nickel-responsive regulator of the Fur family, regulate superoxide dismutases and nickel transport in *Streptomyces coelicolor*. *Mol. Microbiol.* **59**:1848-1858

Akanuma, G., Nanamiya, H., Natori, Y., Nomura, N. and Kawamura, F. (2006) Liberation of zinc-containing L31 (RpmE) from ribosomes by its paralogous gene product, YtiA, in *Bacillus subtilis*. *J. Bacteriol.* **188**:2715-2720

Alamuri, P., Mehta, N., Burk, A. and Maier, R. J. (2006) Regulation of the *Helicobacter pylori* Fe-S cluster synthesis protein Nifs by iron, oxidative stress conditions, and Fur. *J. Bacteriol.* **188**:5325-5330

Althaus, E. W., Outten, C. E., Olson, K. E., Cao, H., and O'Halloran, T. V. (1999) The ferric uptake regulation (Fur) repressor is a zinc metalloprotein. *Biochemistry* **38**:6559-6569

An, Y. J., Ahn, B. E., Han, A. R., Kim, H. M., Chung, K. M., Shin, J. H., Cho, Y. B., Roe, J. H. and Cha, S. S. (2009) Structural basis for the specialization of Nur, a nickel-specific Fur homology, in metal sensing and DNA recognition. *Nucleic Acids Res.* **37**:3442-3451

Anderson, J. E., Sparling, P. F. and Cornelissen, C. N. (1994) Gonococcal transferrin-binding protein 2 facilitates but is not essential for transferrin utilization. *J. Bacteriol.* **176**:3162-3170

Andrews, S. C., Robinson, A. K. and Rofríguez-Quiñones, F. (2003) Bacterial iron homeostasis. *FEMS Microbiol. Rev.* **27**:215-237

Bibliography

- Ariza, R. R., Li, Z., Ringstad, N. and Demple, B.** (1995) Activation of multiple antibiotic resistance and binding of stress-inducible promoters by *Escherichia coli* Rob protein. *J. Bacteriol.* **177**:1655-1661
- Ashton, F. E., Ryan, J. A., Borczyk, A., Caugant, D. A., Mancino, L. and Huang, D.** (1991) Emergence of a virulent clone of *Neisseria meningitidis* serotype 2a that is associated with meningococcal group C disease in Canada. *J. Clin. Microbiol.* **29**:2489-2493
- Bacon, D. J., Alm, R. A., Hu, L., Hickey, T. E., Ewing, C. P., Batchelor, R. A., Trust, T. J. and Guerry, P.** (2002) DNA sequence and mutational analyses of the pVir plasmid of *Campylobacter jejuni* 81-176. *Infect. Immun.* **70**:6242-6250
- Bagg, A and Neilands, J. B.** (1987a) Ferric uptake regulation protein acts as a repressor, employing iron(II) as a cofactor to bind the operator of an iron transport operon in *Escherichia coli*. *Biochemistry* **26**:5471-5477
- Bagg, A. and Neilands, J. B.** (1987b) Molecular mechanism of regulation of siderophore-mediated iron assimilation. *Microbiol. Rev.* **51**: 509-518
- Baichoo, N. and Helmann, J. D.** (2002) Recognition of DNA by Fur: a reinterpretation of the Fur box consensus sequence. *J. Bacteriol.* **184**:5826-5832
- Baichoo, N., Wang, T., Ye, R. and Helmann, J. D.** (2002) Global analysis of the *Bacillus subtilis* Fur regulon and the iron starvation stimulon. *Mol. Microbiol.* **45**:1613-1629
- Baillon, M. A., van Vliet, A. H. M., Ketley, J. M., Constantinidou, C. and Penn, C. W.** (1999) An iron-regulated alkyl hydroperoxide reductase (AhpC) confers aerotolerance and oxidative stress resistance to the microaerophilic pathogen *Campylobacter jejuni*. *J. Bacteriol.* **181**:4798-4804
- Baltes, N. Henning-Pauka, I. and Gerlach, G. F.** (2002) Both transferrin binding proteins are virulence factors in *Actinobacillus pleuropneumoniae* serotype 7 infection. *FEMS Microbiol. Lett.* **209**:283-287
- Banin, E. M., Vasil, M. L. and Greenberg, E. P.** (2005) Iron and *Pseudomonas aeruginosa* biofilm formation. *Proc. Natl. Acad. Sci. USA* **102**:11076-11081
- Barnard, F. M., Loughlin, M. F., Fainberg, H. P., Messenger, M. P., Ussery, D. W., Williams, P. and Jenks, P. J.** (2004) Global regulation of virulence and the stress response by CsrA in the highly adapted human gastric pathogen *Helicobacter pylori*. *Mol. Microbiol.* **51**:15-32

Barton, H. A. (1997) Structure and functional analysis of *Pseudomonas aeruginosa* Fur repressor. *Ph.D. thesis*, University of Colorado, Denver

Barton, H. A., Johnson, Z., Cox, C. D., Vasil, A. I. and Vasil, M. L. (1996) Ferric uptake regulator mutants of *Pseudomonas aeruginosa* with distinct alternations in the iron-dependent repression of exotoxin A and siderophores in aerobic and microaerobic environment. *Mol. Microbiol.* **21**:1001-1017

Batchelor, R. A., Pearson, B. M., Friis, L. M., Guerry, P. and Wells, J. M. (2004) Nucleotide sequences and comparison of two large conjugative plasmids from different *Campylobacter jejuni*. *Microbiology* **150**:3507-3517

Bearson, B. L., Wilson, L., and Foster, J. W. (1998) A low pH-inducible PhoPQ-dependent acid tolerance response protects *Salmonella typhimurium* against inorganic acid stress. *J. Bacteriol.* **180**:2409-2417

Beddek, A. J. and Schryvers, A. B. (2010) The lactoferrin receptor complex in gram negative bacteria. *Biometals* **23**:733-386

Beisel, C. L. and Storz, G. (2010) Base pairing small RNAs and their roles in global regulatory networks. *FEMS Microbiol. Rev.* **34**:866-882

Blaser, M. J. and Engberg, J. (2008) Clinical aspects of *Campylobacter jejuni* and *Campylobacter coli* infection. *Campylobacter*, 3rd ed., Nachamkin, I., Szymanski, C. M. and Blaser, M. J. ASM Press, Washington, DC

Bellamy, W., Takase, M., Wakabayashi, H., Kawase, K. and Tomita, M. (1992) Antibacterial spectrum of lactoferricin B, a potent bactericidal peptide derived from the N-terminal region of bovine lactoferrin. *J. Appl. Bacteriol.* **73**:472-479

Bellini, P. and Hemmings, A. M. (2006) *In vitro* characterization of a bacterial manganese uptake regulator of the *fur* superfamily. *Biochemistry* **45**:2686-2698

Bensing, B. A., Meyer, B. J. and Dunny, G. M. (1996) Sensitive detection of bacterial transcription initiation sites and differentiation from RNA processing sites in the pheromone-induced plasmid transfer system of *Enterococcus faecalis*. *Proc. Natl. Acad. Sci. USA* **93**:7794-7799

Bereswill, S., Lichte, F., Vey, T., Fassbinder, F. and Kist, M. (1998) Cloning and characterization of the *fur* gene from *Helicobacter pylori*. *FEMS Microbiol. Lett.* **159**:193-200

Berg, A. (2007) Defining the operator sequence for the Fur regulatory system in *Campylobacter jejuni*. *M. Sc. thesis*, University of Leicester, Leicester

Bradford, M. M. (1976) A rapid and sensitive method for the quantitation of microgram quantities of protein utilizing the principle of protein-dye binding. *Anal. Biochem.* **72**:248-254

Braun, V., Mahren, S. and Ogierman, M. (2003) Regulation of the FecI-type ECF sigma factor by transmembrane signalling. *Curr. Opin. Microbiol.* **6**:173-180

Brás, A. M., Chatterjee, S., Wren, B. W., Newell, D. G. and Ketley, J. M. (1999) A novel *Campylobacter jejuni* two-component regulatory system important for temperature-dependent growth and colonization. *J. Bacteriol.* **181**:3298-3302

Brickman, T. J. and McIntosh, M. A. (1992) Overexpression and purification of ferric enterobactin esterase from *Escherichia coli*. Demonstration of enzymatic hydrolysis of enterobactin and its iron complex. *J. Biol. Chem.* **267**:12350-12355

Brickman, T. J., Ozenberger, B. A. and McIntosh, M. A. (1990) Regulation of divergent transcription from iron-responsive *fepB-entC* promoter-operator regions in *Escherichia coli*. *J. Mol. Biol.* **212**:669-682

Bruns, C. M., Anderson, D. S., Vaughan, K. G., Williams, P. A., Nowalk, A. J., Mcree, D. E. and Mietzner, T. A. (2001) Crystallographic and biochemical analyses of the metal-free *Haemophilus influenzae* Fe³⁺-binding protein. *Biochemistry* **40**:15631-15637

Bruns, C. M., Nowalk, A. J., Arvai, A. S., McTigue, M. A., Vaughan, K. G., Mietzner, T. A. and Mcree, D. E. (1997) Structure of *Haemophilus influenzae* Fe³⁺-binding protein reveals convergent evolution with a superfamily. *Nat. Struct. Biol.* **4**:919-924

Bryans, J. T., Smith, A. G. and Baker, A. J. (1960) Ovine vibronic abortion caused by a new variety of *Vibrio*. *Cornell Vet.* **50**:54-59

Bou-Abdullah, F., Lewis, A. C., Le Brun, N. E., Moore, G. R. and Chasteen, H. D. (2002) Iron detoxification properties of *Escherichia coli* bacterioferritin. Attenuation of oxyradical chemistry. *J. Biol. Chem.* **277**:37064-37069

Boulton, I. C., Yost, M. K., Anderson, J. E. and Cornelissen, C. N. (2000) Identification of discrete domains within gonococcal transferrin-binding protein A that are necessary for ligand binding and iron uptake functions. *Infect. Immun.* **68**:6988-6996

Braun, V., Mahren, S. and Oglerman, M. (2003) Regulation of the FecI-type ECF sigma factor by transmembrane signalling. *Curr. Opin. Microbiol.* **6**:173-180

Bsat, N., Chen, L. and Helmann, J. D. (1996) Mutation of the *Bacillus subtilis* alkyl hydroperoxide reductase (*ahpCF*) operon reveals compensatory interactions among hydrogen peroxide stress genes. *J. Bacteriol.* **178**:6579-6586

Bsat, N. and Helmann, J. D. (1999) Interaction of *Bacillus subtilis* Fur (Ferric uptake repressor) with the *dhb* operator *in vitro* and *in vivo*. *J. Bacteriol.* **181**:4299-4307

Bsat, N., Herbig, A. F., Casillas-Martinez, L., Setlow, P. and Helmann, J. D. (1998) *Bacillus subtilis* contains multiple Fur homologues: identification of the iron uptake (Fur) and peroxide regulon (PerR) repressors. *Mol. Microbiol.* **29**:189-198

Bury-Mones, S., Thiberge, J. M., Contreras, M., Maitournam, A., Labigne, A. and De Reuse, H. (2004) Responsiveness to acidity via metal iron regulators mediates virulence in the gastric pathogen *Helicobacter pylori*. *Mol. Microbiol.* **53**:623-638

Butcher, J. and Stintzi, A. (2011) ChIP-chip characterization reveals novel regulatory roles for Fur in *Campylobacter jejuni*. *16th international workshop on campylobacter, helicobacter, and related organisms abstracts*. 182

Butzler, J. P. (2004) *Campylobacter*, from obscurity to celebrity. *Clin. Microbiol. Infect.* **10**:868-876

Butzler, J. P., Dekeyser, P., Detrain, M. and Dehaen, F. (1973) Related vibrio in stools. *J. Pediatr.* **82**:493-495

Calderwood, S. B. and Mekalanos, J. J. (1987) Iron regulation of Shiga-like toxin expression in *Escherichia coli* is mediated by the *fur* locus. *J. Bacteriol.* **169**:4759-4764

Calderwood, S. B. and Mekalanos, J. J. (1988) Confirmation of the Fur operator site by insertion of a synthetic oligonucleotide into an operon fusion plasmid. *J. Bacteriol.* **170**:1015-1017

Carpenter, B. M., Gancz, H., Benoit, S. L., Evans, S., Olsen, C. H., Michel, S. L. J., Maier, R. J. and Merrell, D. S. (2010) Mutagenesis of conserved amino acids of *Helicobacter pylori* Fur reveals residues importance for function. *J. Bacteriol.* **192**:5037-5052

Carpenter, B. M., Gancz, H., Gonzalez-Nieves, R. P., West, A. L., Whitmire, J. M., Michel, S. L. J. and Merrell, D. S. (2009a) A single nucleotide change affects Fur-dependent regulation of *sodB* in *H. pylori*. *PLoS One* **4**:e5369

Carpenter, B. M., Whitmire, J. M. and Merrell, D. S. (2009b) This is not your mother's repressor: the complex role of Fur in pathogenesis. *Infect. Immun.*

77:2590-2601

Carrillo, C. D., Taboada, E., Nash, J. H., Lanthier, P., Kelly, J., Lau, P. C., Verhulp, R., Mykytczuk, O., Sy, J., Findlay, W. A., Amoako, K., Gomis, S., Willson, P., Austin, J. W., Potter, A., Babiuk, L., Allan, B. and Szymanski, C. M. (2004) Genome-wide expression analyses of *Campylobacter jejuni* NCTC 11168 reveals coordination regulation of motility and virulence by *flhA*. *J. Biol. Chem.* **279**:20327-20338

Carswell, C. L., Rigden, M. D. and Baenziger, J. E. (2008) Expression, purification, and structural characterization of CfrA, a putative iron transporter from *Campylobacter jejuni*. *J. Bacteriol.* **190**:5650-5662

Cartron, M. L., Maddocks, S., Gillingham, P., Craven, C. J. and Andrews, S. C. (2006) Feo-Transport of ferrous iron into bacteria. *Biometals* **19**:143-157

Cawthraw, S., Park, S. F., Ketley, J. M., Ayling, R. and Newll, D. G. (1996) The chick colonization model and its role in molecular biology studies of campylobacters. *Campylobacter, Helicobacter and related organisms, 3rd ed.*, Newll, D. G., Ketley, J. M. and Feldman, R. A. Plenum Press, New York

Chan, A. C. K., Doukov, T. I., Scofield, M., Tom-Yew, A. L., Ramin, A. B., MacKichan, J. K., Gaynor, E. C. and Murphy, M. E. P. (2010) Structure and function of P19, a high-affinity iron transporter of the human pathogen *Campylobacter jejuni*. *J. Mol. Biol.* **401**:590-604

Chan, A. C. K., Lelj-Garolla, B., Rosell, F. I., Pedersen, K. A., Mauk, A. G. and Murphy, M. E. P. (2006) Cofacial heme binding is linked to dimerization by a bacterial heme transport protein. *J. Mol. Biol.* **362**:1108-1119

Chan, V. L., Louie, H. and Bingham, H. L. (1995) Cloning and transcription regulation of the ferric uptake regulatory gene of *Campylobacter jejuni* TGH9011. *Gene* **164**:25-31

Chang, C., Mooser, A., Pluckthum, A. and Wlodawer, A. (2001) Crystal structure of the dimeric C-terminal domain of TonB reveals a novel fold. *J. Biol. Chem.* **276**:27535-27540

Chaveerach, P., ter Huurne, A. A. H. M., Lipman, L. J. A. and van Knapen, F. (2003) Survival and resuscitation of ten strains of *Campylobacter jejuni* and *Campylobacter coli* under acid conditions. *Appl. Environ. Microbiol.* **69**:711-714

Chen, C. J., Elkins, C. and Sparling, P. F. (1998) Phase variation of hemoglobin utilization in *Neisseria gonorrhoeae*. *Infect. Immun.* **66**:987-993

Chen, C. Y. and Mores, S. A. (1999) *Neisseria gonorrhoeae* bacterioferritin: structural heterogeneity, involvement in iron storage and protection against oxidative stress. *Microbiology* **145**:2967-2975

Chen, L. and Helmann, J. D. (1995) *Bacillus subtilis* MrgA is a Dps(PexB) homologue: evidence for metalloregulation of an oxidative-stress gene. *Mol. Microbiol.* **18**:285-300

Chen, L., Keramati, L. and Helmann, J. D. (1995) Coordinate regulation of *Bacillus subtilis* peroxide stress genes by hydrogen peroxide and metal ions. *Proc. Natl. Acad. Sci. USA* **92**:8190-8204

Chen, Z., Lewis, K. A., Shultzaberger, R. K., Lyakhov, I. G., Zheng, M., Doan, B., Storz, G. and Schneider, T. D. (2007) Discovery of Fur binding site clusters in *Escherichia coli* by information theory models. *Nucleic Acids Res.* **35**:6762-6777

Chenier, D., Beriault, R., Mailloux, R., Baquie, M., Abramia, G., Lemire, J. and Appanna, V. (2008) Involvement of fumarase C and NADA oxidase in metabolic adaptation of *Pseudomonas fluorescens* cells evoked by aluminium and gallium toxicity. *Appl. Environ. Microbiol.* **74**:3977-3984

Chu, B. C., Garcia-Herrero, A., Johanson, T. H., Krewulak, K. D., Lau, C. K., Peacock, R. S., Slavinskaya, Z. and Vogel, H. J. (2010) Siderophore uptake in bacteria and the battle for iron with the host; a bird's eye view. *Biometals* **23**:601-611

Clarke, T. E., Braun, V., Winkelmann, G., Tari, L. W., and Vogel, H. J. (2002) X-ray crystallographic structures of the *Escherichia coli* periplasmic protein FhuD bound to hydroxamate-type siderophores and the antibiotic albomycin. *J. Biol. Chem.* **277**:13966-13972

Clarke, T. E., Ku, S. Y., Dougan, D. R., Vogel, H. J., and Tari, L. W. (2000) The structure of the ferric siderophore binding protein FhuD complexed with gallichrome. *Nat. Struct. Biol.* **7**:287-291

Cogan, T. A., Thomas, A. O., Rees, L. E. N., Taylor, A. H., Jepson, M. A., Williams, P. H., Ketley, J. M. and Humphrey, T. J. (2007) Norepinephrine increases the pathogenic potential of *Campylobacter jejuni*. *Gut* **56**:1060-1065

Cornelissen, C. N. (2003) Transferrin-iron uptake by Gram-negative bacteria. *Front. Biosci.* **8**:d836-847

Cornelissen, C. N., Biswas, G. D., Tsai, J., Paruchuri, D. K., Thompson, S. A. and Sparling, P. F. (1992) Gonococcal transferrin-binding protein 1 is required for

transferrin utilization and is homologous to TonB-dependent outer membrane receptors. *J. Bacteriol.* **174**:5788-5797

Cornelissen, C. N., Kelly, M., Hobbs, M. M., Anderson, J. E., Gannon, J. G., Cohen, M. S. and Sparling, P. F. (1998) The transferring receptor expressed by gonococcal strain FA190 is required for the experimental infection of human male volunteers. *Mol. Microbiol.* **27**:611-616

Cowart, R. E. (2002) Reduction of iron by extracellular iron reductases: implications for microbial iron acquisition. *Arch. Biochem. Biophys.* **400**:273-281

Cowart, R. E. and Foster, B. G. (1985) Differential effects of iron on the growth of *Listeria monocytogenes*: minimum requirements and mechanism of acquisition. *J. Inf. Dis.* **151**:721-730

Cox, C. D. (1986) Role of pyocyanin in the acquisition of iron from transferrin. *Infect. Immun.* **52**:263-270

Coy, M., Doyle, C., Besser, J. and Neilands, J. B. (1994) Site-directed mutagenesis of the ferric uptake regulation gene of *Escherichia coli*. *Biometals* **7**:292-298

Coy, M. and Neilands, J. B. (1991) Structural dynamics and functional domains of the Fur protein. *Biochemistry* **30**:8201-8210

Crawford, M. J. and Goldberg, D. E. (1998) Regulation of the *Salmonella typhimurium* flavohemoglobin gene. A new pathway for bacterial gene expression in response to nitric oxide. *J. Biol. Chem.* **273**:34028-34032

Crushell, E., Harty, S., Sharif, F. and Bourke, B. (2004). Enteric *Campylobacter*: purging its secrets? *Pediatr. Res.* **55**: 3-12

Danielli, A., Roncarati, D., Delany, I, Chiarini, V., Rappuoli, R. and Scarlato, V. (2006) *In vivo* dissection of the *Helicobacter pylori* Fur regulatory circuit by genome-wide location analysis. *J. Bacteriol.* **188**:4654-4662

Danielli, A. and Scarlato, V. (2010) Regulatory circuits in *Helicobacter pylori*: network motifs and regulators involved in metal-dependent responses. *FEMS Microbiol. Rev.* **34**:738-752

Davis, L. M., Kakuda, T. and DiRita, V. J. (2009) A *Campylobacter jejuni* *znuA* orthologue is essential for growth in low-zinc environments and chick colonisation. *J. Bacteriol.* **191**:1631-1640

de Lorenzo, V., Giovannini, F., Herrero, M. and Neilands, J. B. (1988a) Metal ion

regulation of gene expression. Fur repressor-operator interaction at the promoter region of the aerobactin system of pColV-K30. *J. Mol. Biol.* **203**:875-884

de Lorenzo, V., Herrero, M., Giovannini, F. and Neilands, J. B. (1988b) Fur (ferric uptake regulation) protein and CAP (catabolite-activator protein) modulate transcription of fur gene in *Escherichia coli*. *Eur. J. Biochem.* **173**:537-546

de Lorenzo, V., Wee, S., Herrero, M. and Neilands, J. B. (1987) Operator sequences of the aerobactin operon of plasmid ColV-K30 binding the ferric uptake regulation (*fur*) repressor. *J. Bacteriol.* **169**:2624-2630

Debruyne, L., Gevers, D. and Vandamme, P. (2008) Taxonomy of the family *Campylobacteraceae*. *Campylobacter*, 3rd ed., Nachamkin, I., Szymanski, C. M. and Blaser, M. J. ASM Press, Washington, DC

Dekeyser, P., Gossuin-Detrain, M., Butzler, J. P. and Sternon, J. (1972) Acute enteritis due to a related vibrio: first positive stool cultures. *J. Infect. Dis.* **125**:390-392

Delany, I., Rappuoli, R. and Scarlato, V. (2004) Fur functions as an activator and as a repressor of putative virulence genes in *Neisseria meningitidis*. *Mol. Microbiol.* **52**:1081-1090

Delany, I., Spohn, G., Pacheco, A. B. F., Leva, R., Alaimo, C., Rappuoli, R. and Scarlato, V. (2002) Autoregulation of *Helicobacter pylori* Fur revealed by functional analysis of the iron-binding site. *Mol. Microbiol.* **46**:1107-1122

Delany, I., Spohn, G., Rappuoli, R. and Scarlato, V. (2001) The Fur repressor controls transcription of iron-activated and -repressed genes in *Helicobacter pylori*. *Mol. Microbiol.* **42**: 1297-1309

Delany, I., Spohn, G., Rappuoli, R. and Scarlato, V. (2003) An anti-repression Fur operator upstream of the promoter is required for iron-mediated transcriptional autoregulation in *Helicobacter pylori*. *Mol. Microbiol.* **50**:1329-1338

Delihias, N. and Forst, S. (2001) *MicF*: an antisense RNA gene involved in response of *Escherichia coli* to global stress factors. *J. Mol. Biol.* **313**:1-12

Dian, C., Vitale, S., Leonard, G. A., Bahlawane, C., Fauquant, C., Leduc, D., Muller, C., de Reuse, H., Michaud-Soret, I. and Terradot, L. (2011) The structure of the *Helicobacter pylori* ferric uptake regulator Fur reveals three functional metal binding sites. *Mol. Microbiol.* **79**:1260-1275

Diaz-Mireles, E., Wexler, M., Sawers, R. G., Bellini, D., Tood, J. D. and Johnston, A. W. B. (2004) The Fur-like protein Mur of *Rhizobium leguminosarum* is a

Mn(2+)-responsive transcriptional regulator. *Microbiology* **150**:1447-1456

Diaz-Mireles, E., Wexler, M., Tood, J. D., Bellini, D., Johnston, A. W. B. and Sawers, R. G. (2005) The manganese-responsive repressor Mur of *Rhizobium leguminosarum* is a member of the Fur-superfamily that recognizes an unusual operator sequence. *Microbiology* **151**:4071-4078

Dombroski, A. J., Walter, W. A., Record, M. T. Jr., Siegele, D. A. and Gross, C. A. (1992) Polypeptides containing highly conserved regions of transcription initiation factor sigma 70 exhibit specificity of binding to promoter DNA. *Cell* **70**:501-512

Doukhan, L., Predich, M., Nair, G., Dussurget, O., Mandic-Mulec, I., Cole, S. T., Smith, D. R. and Smith, I. (1995) Genomic organization of the mycobacterial sigma gene cluster. *Gene* **165**:67-70

Doyle, L. P. (1948) The etiology of swine dysentery. *Am. J. Vet. Res.* **9**:50-51

Elvers, K. T., Wu, G., Gilberthorpe, N. J., Poole, R. K. and Park, S. F. (2004) Role of an inducible single-domain hemoglobin in mediating resistance to nitric oxide and nitrosative stress in *Campylobacter jejuni* and *Campylobacter coli*. *J. Bacteriol.* **186**:5332-5341

Elvers, K. T., Turner, S. M., Wainwright, L. M., Marsden, G., Hinds, J., Cole, J. A., Poole, R. K., Penn, C. W. and Park, S. F. (2005) NssR, a member of the Crp-Fnr superfamily from *Campylobacter jejuni*, regulates a nitrosative stress-responsive regulon that includes both a single-domain and a truncated haemoglobin. *Mol. Microbiol.* **57**:735-750

Endriss, F. and Braun, V. (2004) Loop deletions indicated regions important for FhuA transport and receptor functions in *Escherichia coli*. *J. Bacteriol.* **186**:4818-4825

Englesberg, E. (1961) Enzymatic characterization of 17 L-arabinose negative mutants of *Escherichia coli*. *J. Bacteriol.* **81**:996-1006

Enz, S., Mahren, S., Stroehel, U. H. and Braun, V. (2000) Surface signalling in ferric citrate transport gene induction: interaction of the FecA, FecR, and FecI regulatory proteins. *J. Bacteriol.* **182**:637-646

Ernst, F. D., Homuth, G., Stoof, J., Mäder, U., Waidner, B., Kuipers, E. J., Kist, M., Kusters, J. G., Bereswill, S. and van Vliet, A. H. M. (2005) Iron-responsive regulation of the *Helicobacter pylori* iron-Cofactored superoxide dismutase SodB is mediated by Fur. *J. Bacteriol.* **187**:3687-3692

Ernst, J. F., Bennett, R. L. and Rothfield, L. I. (1978) Constitutive expression of the

Bibliography

iron-enterochelin and ferrichrome uptake systems in a mutant strain of *Salmonella typhimurium*. *J. Bacteriol.* **135**:928-934

Escherich, T. (1886) Beiträge zur Kenntniss der Darmbakterien. III. Über das Vorkommen van Vibrionen im Darmcanak und den Stuhlgängen der Säuglinge. *Münch. Med. Wschr.* **33**:815-817

Escolar, L., Pérez-Martín, J. and de Lorenzo, V. (1998) Binding of the Fur (ferric uptake regulator) repressor of *Escherichia coli* to array of the GATAAT sequence. *J. Mol. Biol.* **283**:537-547

Escolar, L., Pérez-Martín, J. and de Lorenzo, V. (1999) Opening the iron box: transcriptional metalloregulation by the Fur protein. *J. Bacteriol.* **181**:6223-6229

Escolar, L., Pérez-Martín, J. and de Lorenzo, V. (2000) Evidence of an unusually long operator for the Fur repressor in the aerobactin promoter of *Escherichia coli*. *J. Biol. Chem.* **275**:24709-24714

Eustance, R, Bustos, R. and Schleif, R. (1994) Reaching out: locating and lengthening the interdomain linker in AraC protein. *J. Mol. Biol.* **242**:330-338

Ferguson, A. D. Chakraborty, R., Smith, B. S., Esser, L., van der Helm, D and Deisenhofer, J. (2002) Structural basis of gating by the outer membrane transporter FecA. *Science* **295**:1715-1719

Ferguson, A. D., Hofmann, E., Coulton, J. W., Diederichs, K. and Welte, W. (1998) Siderophore-mediated iron transport: crystal structure of FhuA with bound lipopolysaccharide. *Science* **282**:2215-2220

Fields, J. A. and Thompson, S. A. (2008) *Campylobacter jejuni* CsrA mediates oxidative stress responses, biofilm formation, and host cell invasion. *J. Bacteriol.* **190**:3411-3416

Fields, L. H., Headley, V. L., Payne, S. M. and Berry, L. J. (1986) Influence of iron on growth, morphology, outer membrane protein composition, and synthesis of siderophores in *Campylobacter jejuni*. *Infect. Immun.* **54**:126-132

Flaming, M. D., Romano, M. A., Su, M. A., Foernzler, D., Beier, D. R., Dietrich, W. F. and Andrews, N. C. (1998) Nramp2 is mutated in the anemic Belgrade (b) rat: evidence of a role for Nramp2 in endosomal iron transport. *Proc. Natl. Acad. Sci. USA* **95**:1148-1153

Florent, A. (1953) Isolement d'un vibron saprophyte du sperme du taureau et du vagin de la vache (*Vibrio bubulus*). *C. R. Soc. Biol.* **147**:2066-2069

Foster, J. W. (1991) *Salmonella* acid shock proteins are required for the adaptive acid tolerance response. *J. Bacteriol.* **173**:6896-6902

Fourel, G., Phalipon, A. and Kaczorek, M. (1989) Evidence for direct regulation of diphtheria toxin gene transcription by an Fe²⁺-dependent DNA-binding repressor, DtoxR, in *Corynebacterium diphtheriae*. *Infect. Immun.* **57**:3221-3225

Fouts, D. E., Mongodin, E. F., Mandrell, R. E., Miller, W. G., Rasko, D. A., Ravel, J., Brinkac, L. M., DeBoy, R. T., Parker, C. T., Daugherty, S. C., Dodson, R. J., Durkin, A. S., Madupu, R., Sullivan, S. A., Shetty, J. U., Ayodeji, M. A., Shvartsbeyn, A., Schatz, M. C., Badger, J. H., Fraser, C. M. and Nelson, K. E. (2005) Major structural differences and novel potential virulence mechanisms from the genomes of multiple *Campylobacter* species. *PLoS Biol.* **3**:e15

Fréchon, D. and Le Cam, E. (1994) Fur (Ferric Uptake Regulation) protein interaction with target DNA: comparison of gel retardation, footprinting and electron microscopy analyses. *Biochem. Biophys. Res. Commun.* **201**:346-355

Fried, M. G. and Liu, G. (1994) Molecular sequestration stabilizes CAP-DNA complexes during polyacrylamide gel electrophoresis. *Nucleic Acids Res.* **22**:5054-5059

Friedman, A. M., Fischmann, T. O. and Steitz, T. A. (1995) Crystal structure of the *lac* repressor core tetramer and its implications for DNA looping. *Science* **268**:1721-1727

Friedman, Y. E. and O'Brian, M. R. (2003) A novel DNA-binding site for the ferric uptake regulator (Fur) protein from *Bradyrhizobium japonicum*. *J. Biol. Chem.* **278**:38395-38401

Fuangthong, M. and Helmann, J. D. (2003) Recognition of DNA by three ferric uptake regulator (Fur) homologs in *Bacillus subtilis*. *J. Bacteriol.* **185**:6348-6357

Fuangthong, M., Herbig, A. F., Bsat, N. and Helmann, J. D. (2002) Regulation of the *Bacillus subtilis fur* and *perR* genes by PerR: not all members of the PerR regulon are peroxide inducible. *J. Bacteriol.* **184**:3276-3286

Furrer, J., Sanders, D., Hook-Barnard, I. and McIntosh, M. (2002) Export of the siderophore enterobactin in *Escherichia coli*: involvement of a 43 kDa membrane exporter. *Mol. Microbiol.* **44**:1225-1234

Gaballa, A. and Helmann, J. D. (2002) A peroxide-induced zinc uptake system plays an important role in protection against oxidative stress in *Bacillus subtilis*. *Mol. Microbiol.* **45**:997-1005

Gaballa, A., Wang, T., Ye, R. and Helmann, J. D. (2002) Functional analysis of the *Bacillus subtilis* Zur regulon. *J. Bacteriol.* **184**:6506-6514

Gahan, C. G. M. and Hill, C. (2000) The use of listeriolysin to identify in vivo induced genes in the Gram-positive intracellular pathogen *Listeria monocytogenes*. *Mol. Microbiol.* **36**:498-507

Galas, D. J. and Schmitz, A. (1978) DNAase footprinting: a simple method for the detection of protein-DNA binding specificity. *Nucleic Acids Res.* **5**:3157-3170

Galindo, M. A., Day, W. A., Raphael, B. H. and Joens, L. A. (2001) Cloning and characterization of *Campylobacter jejuni* iron-uptake operon. *Curr. Microbiol.* **42**:139-143

Gancz, H., Censini, S. and Merrell, D. S. (2006) Iron and pH homeostasis intersect at the level of Fur regulation in the gastric pathogen *Helicobacter pylori*. *Infect. Immun.* **74**:602-614

Ganz, T. (2009) Iron in innate immunity: starve the invaders. *Curr. Opin. Immunol.* **21**:63-67

Gao, H., Zhou, D., Li, Y, Guo, Z., Han, Y., Song, Y., Zhai, J., Du, Z., Wang, X., Lu, J. and Yang, R. (2008) The iron-responsive Fur regulon in *Yersinia pestis*. *J. Bacteriol.* **190**:3063-3075

Garner, M. M. and Revzin, A. (1986) The use of gel electrophoresis to detect and study nucleic acid-protein interactions. *Trends Biol. Sci.* **11**:395-396

Genco, C. A. and Dixon, D. W. (2001) Emerging strategies in microbial haem capture. *Mol. Microbiol.* **39**:1-11

Gerhart, E., Wagner, H. and Vogel, J. (2009) Approaches to identify novel non-messenger RNAs in bacteria and to investigate their biological functions: Functional analysis of identified non-mRNAs. *Handbook of RNA biochemistry, Student ed.*, Hartmann, R. K., Bindereif, A., Schön, A. and Westhof, E. WILEY-VCH Verlag GmbH & Co. KGaA, Weinheim

Gilbreath, J. J., Cody, W. L., Merrell, D. S. and Hendrixson, D. R. (2011) Change is food: Variations in common biological mechanisms in the epsilonproteobacterial genera *Campylobacter* and *Helicobacter*. *Microbiol. Mol. Biol. Rev.* **75**:84-132

Goh, L. L., Barkham, T. and Sim, T. S. (2005) Molecular cloning and functional characterisation of fumarase C in *Neisseria* species. *Antonie van Leeuwenhoek*

Gonzalez de Peredo, A., Pierre-Saint, C., Adrait, A., Jacquamet, L., Latour, J., Michaud-Soret, I. and Forest, E. (1999) Identification of the two zinc-bound cysteines in the ferric uptake regulation protein from *Escherichia coli*: chemical modification and mass spectrometry analysis. *Biochemistry* **38**:8582-8589

Grabowska, A. D., Wandel, M., Łasica, A. M., Nesteruk, M., Roszczenko, P., Wyszynska, A., Godlewska, R. and Jagusztyn-krynicka, E. K. (2011) *Campylobacter jejuni dsb* gene expression is regulated by iron in a Fur-dependent manner and by a translational coupling mechanism. *BMC Microbiol.* **11**:166

Grant, K. A., Park, S. F. (1995) Molecular characterization of *katA* from *Campylobacter jejuni* and generation of a catalase-deficient mutant of *Campylobacter coli* by interspecific allelic exchange. *Microbiology* **141**:1369-1376

Gray-Owen, S. D. and Schryvers, A. B. (1996) Bacterial transferrin and lactoferrin receptors. *Trends. Microbiol.* **4**:185-191

Grifantini, R., Sebastian, S., Frigimelica, E., Draghi, M., Bartolini, E., Muzzi, A., Rappuoli, R., Grandi, G. and Genco, C. A. (2003) Identification of iron-activated and -repressed Fur-dependent genes by transcriptome analysis of *Neisseria meningitidis* group B. *Proc. Natl. Acad. Sci. USA* **100**:9542-9547

Guerry, P., Ewing, C. P., Schirm, M., Lorenzo, M., Kelly, J., Pattarini, D., Majam, G., Thibault, P. and Logan, S. (2006) Changes in flagellin glycosylation affect *Campylobacter* autoagglutination and virulence. *Mol. Microbiol.* **60**:299-311

Guerry, P., Perez-Casal, J., Yao, R., McVeigh, A. and Trust, T. J. (1997) A genetic locus involved in iron utilization unique to some *Campylobacter* strains. *J. Bacteriol.* **179**:3997-4002

Guest, J. R., Miles, J. S., Roberts, R. E. and Woods, S. A. (1985) The fumarase genes of *Escherichia coli*: location of the *fumB* gene and discovery of a new gene (*fumC*). *J. Gen. Microbiol.* **131**:2971-2984

Guest, J. R. and Roberts, R. E. (1983) Cloning and mapping and expression of the fumarase gene of *Escherichia coli* K-12. *J. Bacteriol.* **153**:588-596

Gundogdu, O., Bentley, S. D., Holden, M. T., Parkhill, J., Dorrell, N. and Wren, B. W. (2007) Re-annotation and re-analysis of the *Campylobacter jejuni* NCTC11168 genome sequence. *MBC Genomics* **8**:162

Günther-Seeboth, K. and Schupp, T. (1995) Cloning and sequence analysis of the

Bibliography

Corynebacterium diphtheriae *dtxR* homologue from *Streptomyces lividans* and *S. pilosus* encoding a putative iron repressor protein. *Gene* **166**:117-119

Haigh, R. D., van Diemen, P., Hardy, S. L., Stevens, M. P. and Ketley, J. M. (2010) The complex role of iron uptake systems in *Campylobacter jejuni* virulence. *Society for General Microbiology 2010 autumn meeting Metals & Microbes abstracts*. 72

Hall, H. K. and Foster, J. W. (1996) The role of Fur in the acid tolerance response of *Salmonella typhimurium* is physiologically and genetically separable from its role in iron acquisition. *J. Bacteriol.* **178**:5683-5691

Handley, R., van Vliet, A. H. M., Mulholland, F. and le Brun, N. E. (2010) Characterisation of the *Campylobacter jejuni* metal-responsive peroxide-stress regulator PerR. *Society for General Microbiology 2010 autumn meeting Metals & Microbes abstracts*. 116

Hantke, K. (1981) Regulation of ferric iron transport in *Escherichia coli* K12: isolation of a constitutive mutant. *Mol. Gen. Genet.* **182**:288-292

Hantke, K. (1982) Negative control of iron uptake systems in *Escherichia coli*. *FEMS Microbiol. Lett.* **15**:83-86

Hantke, K. (1984) Cloning of the repressor protein of iron-regulated systems in *Escherichia coli* K12. *Mol. Gen. Genet.* **197**:337-341

Hantke, K. (1987) Ferrous iron transport mutants in *Escherichia coli* K-12. *FEMS Microbiol. Lett.* **44**:53-57

Hantke, K. (2001) Iron and metal regulation in bacteria. *Curr. Opin. Microbiol.* **4**:172-177

Hantke, K. (2005) Bacterial zinc uptake and regulators. *Curr. Opin. Microbiol.* **8**:196-202

Harrison-McMonagle, P., Denissova, N., Martínez-Hackert, E., Ebright, R. H. and Stock, A. M. (1999) Orientation of OmpR monomers within an OmpR:DNA complex determined by DNA affinity cleaving. *J. Mol. Biol.* **185**:555-566

Hassett, D. J., Howell, M. L., Ochsner, U. A., Vasil, M. L., Johnson, Z. and Dean, G. E. (1997a) An operon containing *fumC* and *sodA* encoding fumarase C and manganese superoxide dismutase is controlled by the ferric uptake regulator in *Pseudomonas aeruginosa*: *fur* mutants produce elevated alginate levels. *J. Bacteriol.* **179**:1452-1459

Hassett, D. J., Howell, M. L., Sokol, P. A., Vasil, M. L. and Dean, G. E. (1997b)

Bibliography

Fumarase C activity is elevated in response to iron deprivation and in mucoid, alginate-producing *Pseudomonas aeruginosa*: cloning and characterization of *fumC* and purification of native FumC. *J. Bacteriol.* **179**:1442-1451

Hassett, D. J., Sokol, P. A., Howell, M. L., Ma, J., Schweizer, H. T., Ochsner, U. A. and Vasil, M. L. (1996) Ferric uptake regulator (Fur) mutations of *Pseudomonas aeruginosa* demonstrate defective siderophore-mediated iron uptake, altered aerobic growth, and decreased superoxide dismutase and catalase activities. *J. Bacteriol.* **178**:3996-4003

Hentze, M. W., Muckenthaler, M. U. and Andrews, N. C. (2004) Balancing acts: molecular control of mammalian iron metabolism. *Cell* **117**:285-297

Herbig, A. F. and Helmann, J. D. (2001) Roles of metal ions and hydrogen peroxide in modulating the interaction of the *Bacillus subtilis* PerR peroxide regulon repressor with operator DNA. *Mol. Microbiol.* **41**:849-859

Higgs, P. I., Larsen, R. A. and Postle, K. (2002) Quantification of known components of the *Escherichia coli* TonB energy transduction system: TonB, ExbB, ExbD and FepA. *Mol. Microbiol.* **44**:271-281

Hinton, A. Jr. (2006) Growth of *Campylobacter* in media supplemented with organic acids. *J. Food Prot.* **69**:34-38

Hoerter, J. D., Arnold, A. A., Ward, C. S., Sauer, M., Johnson, S., Fleming, T. and Eisenstark, A. (2005) Reduced hydroperoxidase (HPI and HPII) activity in the Δfur mutant contributes to increased sensitivity to UVA radiation in *Escherichia coli*. *J. Photochem. Photobiol. B* **79**:151-157

Hofreuter, D., Tsai, J., Watson, R. O., Novik, V., Altman, B., Benitez, M., Clark, C., Perbost, C., Jarvie, T., Du, L. and Galán, J. E. (2006) Unique features of a highly pathogenic *Campylobacter jejuni* strain. *Infect. Immun.* **74**: 4694-4707

Holmes, K., Mulholland, F., Pearson, B., Pin, C., McNicholl-Kennedy, J., Ketley, J. M. and Wells, J. M. (2005) *Campylobacter jejuni* gene expression in response to iron limitation and the role of Fur. *Microbiology* **151**:243-257

Horsburgh, M. J., Ingham, E. and Foster, S. J. (2001) In *Staphylococcus aureus*, Fur is an interactive regulator with PerR, contributes to virulence, and is necessary for oxidative stress resistance through positive regulation of catalase and iron homeostasis. *J. Bacteria.* **183**:468-475

Hugdahl, M. B., Beery, J. T. and Doyle, M. P. (1988) Chemotactic behavior of *Campylobacter jejuni*. *Infect. Immun.* **56**:1560-1566

Hunt, M. D., Pettis, G. S. and McIntosh, M. A. (1994) Promoter and operator determinants for *fur*-mediated iron regulation in the bidirectional *fepA-fes* control region of *Escherichia coli* enterobactin gene system. *J. Bacteriol.* **176**:3944-3955

Imlay, J. A. (2008) Cellular defences against superoxide and hydrogen peroxide. *Annu. Rev. Biochem.* **77**:755-776

Irwin, S. W., Averil, N, Chang, C. Y. and Schryvers, A. B. (1993) Preparation and analysis of isogenic mutants in the transferrin receptor protein genes, *tbpA* and *tbpB*, from *Neisseria meningitidis*. *Mol. Microbiol.* **8**:1125-1133

Ishikawa, T., Mizunoe, Y., Kawabata, S., Takade, A., Harada, M., Wai, S. N. and Yoshida, S. (2003) The iron-binding protein Dps confers hydrogen peroxide stress resistance to *Campylobacter jejuni*. *J. Bacteriol.* **185**:1010-1017

Jabour, S. and Hamed, M. Y. (2009) Binding of the Zn^{2+} ion to ferric uptake regulation protein from *E. coli* and the competition with Fe^{2+} binding: a molecular modelling study of the effect on DNA binding and conformational changes of Fur. *J. Comput. Aided. Mol. Dos.* **23**:199-208

Jacob, F. and Monod, J. (1961) Genetic regulatory mechanisms in the synthesis of proteins. *J. Mol. Biol.* **2**:318-356

Jacobs, B. C., van Belkum, A. and Endtz, H. P. (2008) Guillain-Barré syndrome and *Campylobacter* infection. *Campylobacter*, 3rd ed., Nachamkin, I., Szymanski, C. M. and Blaser, M. J. ASM Press, Washington, DC

Jacquamet, L., Aberdam, D., Adrait, A., Hazemann, J., Latour, J. and Michaud-Soret, I. (1998) X-ray absorption spectroscopy of a new zinc site in the Fur protein from *Escherichia coli*. *Biochemistry* **37**:2564-2571

Jacquamet, L., Traoré, D. A. K., Ferrer, J. L., Proux, O., Testemale, D., Hazemann, J. L., Nazarenko, E., El Ghazouani, A., Caux-Thang, C., Duarte, V. and Latour, J. M. (2009) Structural characterization of the active form of PerR: insights into the metal-induced activation of PerR and Fur proteins for DNA binding. *Mol. Microbiol.* **73**:20-31

Jagannathan, A., Constantinidou, C. and Penn, C. W. (2001) Roles of *rpoN*, *fliA*, and *flgR* in expression of flagella in *Campylobacter jejuni*. *J. Bacteriol.* **183**:2937-2942

Jair, K. W., Yu, X., Skarstad, K., Thöny, B., Fujita, N., Ishihama, A. and Wolf, R. E. Jr. (1996) Transcriptional activation of promoters of the superoxide and multiple antibiotic resistance regulons by Rob, a binding protein of the *Escherichia coli* origin of

chromosomal replication. *J. Bacteriol.* **178**:2507-2513

Janvier, B., Constantinidou, C., Aucher, P., Marshall, Z. V., Penn, C. W. and Fauchère, J. L. (1998) Characterisation and gene sequencing of a 19-kDa periplasmic protein of *Campylobacter jejuni/coli*. *Res. Microbiol.* **149**:95-107

Lara-Tejero, M. and Galán, J. E. (2001). CdtA, CdtB, and CdtC form a tripartite complex that is required for cytolethal distending toxin activity. *Infect. Immun.* **69**: 4358-4365

Jaskula, J. C., Letain, T. E., Roof, S. K., Skare, J. T. and Postle, K. (1994) Role of the TonB amino terminus in energy transduction between membranes. *J. Bacteriol.* **176**:2326-2338

Johnson, D. S., Mortazavi, A., Myers, R. M. and Wold, B. (2007) Genome-wide mapping of *in vivo* protein-DNA-interactions. *Science* **316**:1497-1502

Johnston, A. W. B., Todd, J. D., Curson, A. R., Lei, S., Nikolaidou-Katsaridou, N., Gelfand, M. S. and Rodionov, D. A. (2007) Living without Fur: the subtlety and complexity of iron-responsive gene regulation in the symbiotic bacterium *Rhizobium* and other α -proteobacteria. *Biometals* **20**:501-511

Jones, F. S., Orcutt, M. and Little, R. B. (1931) Vibrios (*V. jejuni* n. sp.) associated with intestinal disorders in cows and calves. *J. Exp. Med.* **53**:853-863

Kammler, M., Schön, C and Hantke, K. (1993) Characterization of the ferrous iron uptake system of *Escherichia coli*. *J. Bacteriol.* **175**:6212-6219

Kanarek, L. and Hill, R. L. (1964) The preparation and characterization of fumarase from swine heart muscle. *J. Biol. Chem.* **239**:4202-4206

Karjalainen, T. K., Evans, D. G., Evans, D. J. Jr., Graham, D. Y. and Lee, C. H. (1991) Iron represses the expression of CFA/I fimbriae of enterotoxigenic *E. coli*. *Microb. Pathog.* **11**:317-323

Kehres, D. G., Janakiraman, A., Slauch, J. M. and Maguire, M. E. (2002) Regulation of *Salmonella enterica* serovar Typhimurium *mntH* transcription by H₂O₂, Fe²⁺, and Mn²⁺. *J. Bacteriol.* **184**:3151-3158

Ketley, J. M. (1997). Pathogenesis of enteric infection by *Campylobacter*. *Microbiology* **143**: 5-21

Keyer, K. and Imlay, J. A. (1996) Superoxide accelerates DNA damage by elevating free-iron level. *Proc. Natl. Acad. Sci. USA* **93**:13635-13640

King, E. O. (1957) Human infection with *Vibrio fetus* and a closely related vibrio. *J. Infect. Dis.* **101**:119-128

King, V., Wassenaar, T. M., van der Zeijst, B. A. M. and Newell, D. G. (1991) Variations in *Campylobacter jejuni* flagellin, and flagellin genes, during *in vivo* and *in vitro* passage. *Microb. Ecol. Health Dis.* **4**:135-140

Kondo, H., Nakagawa, A., Nishihira, J., Nishimura, Y., Mizuno, T. and Tanaka, I. (1996) *Escherichia coli* positive regulator OmpR has a large loop structure at the putative RNA polymerase interaction site. *Nat. Struct. Biol.* **4**:28-31

Konkel, M. E., Garvis, S. G., Tipton, S. L., Anderson, D. E. and Cieplak, W. (1997) Identification and molecular cloning of a gene encoding a fibronectin-binding protein (CadF) from *Campylobacter jejuni*. *Mol. Microbiol.* **24**: 953-963

Konkel, M. E., Kim, B. J., Rivera-Amill, V. and Garvis, S. G. (1999a) Identification of proteins required for the internalization of *Campylobacter jejuni* into cultured mammalian cells. *Adv. Exp. Med. Biol.* **473**:215-224

Konkel, M. E., Kim, B. J., Rivera-Amill, V. and Garvis, S. G. (1999b) Bacterial secreted proteins are required for the internalization of *Campylobacter jejuni* into cultured mammalian cells. *Mol. Microbiol.* **32**:691-701

Konkel, M. E., Klena, J. D., Rivera-Amill, V., Monteville, M. R., Biswas, D., Raphael, B. and Mickelson, J. (2004) Secretion of virulence proteins from *Campylobacter jejuni* is dependent on a functional flagellar export apparatus. *J. Bacteriol.* **186**:3296-3303

Kopecko, D. J., Hu, L. and Zaal, K. J. M. (2001). *Campylobacter jejuni*-microtubule-dependent invasion. *Trends Microbiol.* **9**: 389-396

Korlath, J. A., Osterholm, M. T., Judy, A., Forgang, J. C. and Robinson, R. A. (1985) A point-source outbreak of campylobacteriosis associated with consumption of raw milk. *J. Infect. Dis.* **152**:592-596

Korolik, V. and Ketely, J. M. (2008) Chemosensory signal transduction pathway of *Campylobacter jejuni*. *Campylobacter*, 3rd ed., Nachamkin, I., Szymanski, C. M. and Blaser, M. J. ASM Press, Washington, DC

Köster, W. (2001) ABC transporter-mediated uptake of iron, siderophores, heme and vitamin B₁₂. *Res. Microbiol.* **152**:291-301

Krewulak, K. D., Shepherd, C. M. and Vogel, H. J. (2005) Molecular dynamics

simulations of the periplasmic ferric-hydroxamate binding protein FhuD. *Biometals* **18**:375-386

Krewulak, K. D. and Vogel, H. J. (2008) Structural biology of bacterial iron uptake. *Biochim. Biophys. Acta.* **1778**:1781-1804

Lam, M. S., Litwin, C. M., Carroll, P. A. and Calderwood, S. B. (1994) *Vibrio cholerae fur* mutations associated with loss of repressor activity: implications for the structural-functional relationships of Fur. *J. Bacteriol.* **176**:5108-5115

Larsen, R. A., Thomas, M. G. and Postle, K. (1999) Proton motive force, ExbB and ligand-bound FepA drive conformational changes in TonB. *Mol. Microbiol.* **31**:1809-1824

Larson, C. L., Christensen, J. F., Pacheo, S. A., Minnich, S. A. and Konkel, M. E. (2008) *Campylobacter jejuni* secretes proteins via the flagellar type III secretion system that contribute to host cell invasion and gastroenteritis. *Campylobacter*, 3rd ed., Nachamkin, I., Szymanski, C. M. and Blaser, M. J. ASM Press, Washington, DC

Lavrrar, J. L., Christoffersen, C. A. and McIntosh, M. A. (2002) Fur-DNA interactions at the bidirectional *fepDGC-entS* promoter region in *Escherichia coli*. *J. Mol. Biol.* **322**:983-995

Lavrrar, J. L. and McIntosh, M. A. (2003) Architecture of a Fur binding site: a comparative analysis. *J. Bacteriol.* **185**:2194-2202

Le Brun, N. E., Crow, A., Murphy, M. E. P., Mauk, A. G. and Moore, G. R. (2010) Iron core mineralisation in prokaryotic ferritins. *Biochim. Biophys. Acta.* **1800**:732-744

Le Cam, E., Frechon, D., Barray, M., Fourcade, A. and Delain, E. (1994) Observation of binding and polymerization of Fur repressor onto operator-containing DNA with electron and atomic force microscopes. *Proc. Natl. Acad. Sci. USA* **91**:11816-11820

Ledala, N., Pearson, S. L., Wilkinson, B. J. and Jayaswal, R. K. (2007) Molecular characterization of the Fur protein in *Listeria monocytogenes*. *Microbiology* **153**:1103-1111

Lee, J. W. and Helmann, J. D. (2006) The PerR transcription factor senses H₂O₂ by metal-catalysed histidine oxidation. *Nature* **440**:363-367

Lee, J. W. and Helmann, J. D. (2007) Functional specialization within the Fur family of metalloregulators. *Biometals* **20**:483-499

Bibliography

Létoffé, S., Delepelaire, P and Wandersman, C. (2004) Free and hemophore-bound heme acquisitions through the outer membrane receptor HasR have different requirements for the TonB-ExbB-ExbD complex. *J. Bacteriol.* **186**:4067-4074

Levy, A. J. (1946) A gastroenteritis outbreak probably due to a bovine strain of vibrio. *Yale J. Biol. Med.* **18**:243

Lewin, A. C., Doughty, P. A., Flegg, L., Moore, G. R., and Spiro, S. (2002) The ferric uptake regulator of *Pseudomonas aeruginosa* has no essential cysteine residues and does not contain a structural zinc iron. *Microbiology* **148**:2449-2456

Lewinson, O., Lee, A. T., Locher, K. P., and Rees, D. C. (2010) A distinct mechanism for the ABC transporter BtuCD-BtuF revealed by the dynamics of complex formation. *Nat. Struct. Mol. Biol.* **17**:332-338

Lewis, L. A., Sung, M. H., Gipson, M., Hartman, K. and Dyer, D. W. (1998) Transport of intact porphyrin HpuAB, the hemoglobin-haptoglobin utilization system of *Neisseria meningitidis*. *J. Bacteriol.* **180**:6043-6047

Lewis, M., Chang, G., Horton, N. C., Kercher, M. A., Pace, H. C., Schumacher, M. A., Brennan, R. G. and Lu, P. (1996) Crystal structure of the lactose operon repressor and its complexes with DNA and inducer. *Science* **271**:1247-1254

Li, C. and Stocker, R. (2009) Heme oxygenase and iron: from bacteria to humans. *Redox Rep.* **14**:95-101

Li, Y. (2005) Investigating the role of ferric uptake regulator (Fur) of *Campylobacter jejuni* using the electrophoretic mobility shift assay (EMSA). *M. Sc. thesis*, University of Leicester, Leicester

Li, Y., Qiu, Y., Gao, H., Guo, Z., Han, Y., Song, J., Du, Z., Wang, X., Zhou, D. and Yang, R. (2009) Characterization of Zur-dependent genes and direct Zur targets in *Yersinia pestis*. *BMC Microbiol.* **9**:128

Lin, J., Akiba, M., Sahin, O. and Zhang, Q. (2005a) CmeR functions as transcriptional repressor for the multidrug efflux pump CmeABC in *Campylobacter jejuni*. *Antimicrob. Agents Chemother.* **49**:1067-1075

Lin, J., Cagliero, C., Guo, B., Barton, Y. W., Maurel, M. C., Payot, S. and Zhang, Q. (2005b) Bile salts modulate expression of the CmeABC multidrug efflux pump in *Campylobacter jejuni*. *J. Bacteriol.* **187**:7417-7424

Lin, J., Michel, O. and Zhang, Q. (2002) CmeABC functions as a multidrug efflux system in *Campylobacter jejuni*. *Antimicrob. Agents Chemother.* **46**:2124-2131

Litwin, C. M., Boyko, S. A. and Calderwood, S. B. (1992) Cloning, sequencing, and transcriptional regulation of the *Vibrio cholerae fur* gene. *J. Bacteriol.* **174**:1879-1903

Litwin, C. M. and Calderwood, S. B. (1993) Role of iron regulation of virulence genes. *Clin. Microbiol. Rev.* **6**:137-149

Litwin, C. M. and Calderwood, S. B. (1994) Analysis of the complexity of gene regulation by Fur in *Vibrio cholerae*. *J. Bacteriol.* **176**:240-248

Liu, Q., Wang, P., Ma, Y. and Zhang, Y. (2007) Characterization of the *Vibrio alginolyticus fur* gene and localization of essential amino acid sites in *fur* by site-directed mutagenesis. *J. Mol. Microbiol. Biotechnol.* **13**:15-21

Lloyd, A. L., Marshall, B. J. and Mee, B. J. (2005) Identifying cloned *Helicobacter pylori* promoters by primer extension using a FAM-labelled primer and GeneScan[®] analysis. *J. Microbiol. Meth.* **60**:291-298

Locher, K. P., Lee, A. T. and Rees, D. C. (2002) The *E. coli* BtuCD structure: a framework for ABC transporter architecture and mechanism. *Science* **296**:1091-1098

Logan, S. M., Harris, L. A. and Trust, T. J. (1987) Isolation and characterization of *Campylobacter* flagellins. *J. Bacteriol.* **169**:5072-5077

Logan, S. M., Kelly, J. F., Thibault, P., Ewing, C. P. and Guerry, P. (2002) Structural heterogeneity of carbohydrate modifications affects serospecificity of *Campylobacter* flagellins. *Mol. Microbiol.* **46**:587-597

MacKichan, J. K., Gaynor, E. C., Chang, C., Cawthraw, S., Newell, D. G., Miller, J. F. and Falkow, S. (2004) The *Campylobacter jejuni* DccRS two-component system is required for optimal *in vivo* colonization is dispensable for *in vitro* growth. *Mol. Microbiol.* **54**:1269-1286

Maeda, S. and Mizuno, T. (1990) Evidence for multiple OmpR-binding sites in the upstream activation sequence of the *ompC* promoter in *Escherichia coli*: a single OmpR-binding site is capable of activating the promoter. *J. Bacteriol.* **172**:501-503

Manning, G., Duim, B., Wassenaar, T. M., Wagenaar, J. A., Ridley, A. and Newell, D. G. (2001) Evidence for a genetically stable strain of *Campylobacter jejuni*. *Appl. Environ. Microbiol.* **67**:1185-1189

Marlovits, T. C., Haase, W., Herrmann, C., Aller, S. G. and Unger, V. M. (2002) The membrane protein FeoB contains an intramolecular G protein essential for Fe(II) uptake in bacteria. *Proc. Natl. Acad. Sci. USA* **99**:16243-16249

Martínez-Hackert, E. and Stock, A. M. (1997) The DNA-binding domain of OmpR: crystal structure of a winged helix transcription factor. *Structure* **5**:109-124

Massé, E. and Arguin, M. (2005) Ironing out the problem: new mechanisms of iron homeostasis. *Trends Biochem. Sci.* **30**:462-468

Massé, E., Escorcia, F. E. and Gottesman, S. (2003) Coupled degradation of a small regulatory RNA and its mRNA targets in *Escherichia coli*. *Genes Dev.* **17**:2374-2383

Massé, E. and Gottesman, S. (2002) A small RNA regulates the expression of genes involved in iron metabolism in *Escherichia coli*. *Proc. Natl. Acad. Sci. USA* **99**:4620-4625

Massé, E., Vanderpool, C. K. and Gottesman, S. (2005) Effect of RyhB small RNA on global iron use in *Escherichia coli*. *J. Bacteriol.* **187**:6962-6971

Matzanke, B. F., Anemüller, S., Schünemann, V., Trautwein, X. and Hantke, K. (2004) FhuF, part of a siderophore-reductase system. *Biochemistry* **43**:1386-1392

Mazmanian, S. K., Skaar, E. P., Gaspar, A. H., Humayun, M., Gornicki, P., Jelenska, J., Joachmiak, A., Missiakas, D. M. and Schneewind, O. (2003) Passage of Heme-iron across the envelope of *Staphylococcus aureus*. *Science* **299**:906-909

McFadyean, J. and Stockman, S. (1913) *Report of the Departmental Committee appointed by the Board of Agriculture and Fisheries to inquire into Epizootic Abortion, III, Abortion in Sheep*, His Majesty's Stationery Office, London

McHugh, J. P., Rodríguez-Quñones, F., Abdul-Tehrani, H., Svistunenko, D. A., Poole, R. K., Cooper, C. E. and Andrews, S. C. (2003) Global iron-dependent gene regulation in *Escherichia coli*. A new mechanism for iron homeostasis. *J. Biol. Chem.* **278**:29478-29486

Marchant, J., Wren, B. and Ketley, J. M. (2002). Exploiting genome sequence: predictions for mechanisms of *Campylobacter* chemotaxis. *Trends Microbiol.* **10**: 155-159

Merrell, D. S., Thompson, L. J., Kim, C. C., Mitchell, H., Tompkins, L. S., Lee, A. and Falkow, S. (2003) Growth phase-dependent response of *Helicobacter pylori* to iron starvation. *Infect. Immun.* **71**:5510-5525

Mey, A. R., Wyckoff, E. E., Kanukurthy, V., Fisher, C. R. and Payne, S. M. (2005) Iron and Fur regulation in *Vibrio cholerae* and the role of Fur in virulence. *Infect. Immun.* **73**:8167-8178

Miethke, M. and Marahiel, M. A. (2007) Siderophore-based iron acquisition and pathogen control. *Microbiol. Mol. Biol. Rev.* **71**:413-451

Mignolet, J., van der Henst, C., Nicolas, C., Deghelt, M, Dotreppe, D, Letesson, J. J. and de Bolle, X. (2010) PdhS, an old-pole-localised histidine kinase, recruits the fumarase FumC in *Brucella abortus*. *J. Bacteriol.* **192**:3235-3239

Miles, S., Carpenter, B. M., Gancz, H. and Merrell, D. S. (2010a) *Helicobacter pylori* apo-Fur regulation appears unconserved across species. *J. Microbiol.* **48**: 378-386

Miles, S., Piazuolo, M. B., Semino-Mora, C., Washington, M. K., Dubois, A., Peek, R. M. Jr., Correa, P. and Merrell, D. S. (2010b) Detailed *in vivo* analysis of the *Helicobacter pylori* Fur in colonisation and disease. *Infect. Immun.* **78**:3073-3082

Miller, C. E., Rock, J. D., Ridley, K. A., Williams, P. H. and Ketley, J. M. (2008) Utilization of lactoferrin-bound and transferrin-bound iron by *Campylobacter jejuni*. *J. Bacteriol.* **190**:1900-1911

Miller, C. E., Williams, P. H. and Ketley, J. M. (2009) Pumping iron: mechanisms for iron uptake by *Campylobacter*. *Microbiology* **155**:3157-3165

Miller, J. H. (1972) *Experiments in molecular genetics*, Cold Spring Harbour Laboratory Press, New York

Mills, S. A. and Marletta, M. A. (2005) Metal binding characteristics and role of iron oxidation in the ferric uptake regulator from *Escherichia coli*. *Biochemistry* **44**:13553-13559

Monteville, M. R. and Konkel, M. E. (2002) Fibronectin-facilitated invasion of T84 eukaryotic cells by *Campylobacter jejuni* occurs preferentially at the basolateral cell surface. *Infect. Immun.* **70**:6665-6671

Monteville, M. R., Yoon, J. E. and Konkel, M. E. (2003) Maximal adherence and invasion of INT 407 cells by *Campylobacter jejuni* requires the CadF outer-membrane protein and microfilament reorganisation. *Microbiology* **194**:153-165

Moraes, T. F., Yu, R., Strynadka, N, C. J. and Schryvers, A. B. (2009) Insights into the bacterial transferrin receptor: the structure of transferrin-binding protein B from *Actinobacillus pleuropneumoniae*. *Mol. Cell.* **35**:523-533

Morton, D. J., Seale, T. W., Madore, L. L., VanWagoner, T. M, Whitby, P. W. and Stull, T. L. (2007). The haem-haemopexin utilization gene cluster (*hxcCBA*) as a

Bibliography

virulence factor of *Haemophilus influenzae*. *Microbiology* **153**:215-224

Morton, D. J., Whitby, P. W., Jin, H., Ren, Z. and Stull, T. L. (1999) Effect of multiple mutations in the hemoglobin- and hemoglobin-haptoglobin-binding proteins, HgpA, HgpB, and HgpC, of *Haemophilus influenzae* type b. *Infect. Immun.* **67**:2729-2739

Moser, I. and Schröder, W. (1997) Hydrophobic characterization of thermophilic *Campylobacter* species and adhesion to INT 407 cell membranes and fibronectin. *Microb. Pathog.* **22**:155-164

Müller, A., Wilkinson, A. J., Wilson, K. S. and Duhme-Klair, A. K. (2006) An $[\{\text{Fe}(\text{mecam})\}_2]^{6-}$ bridge in the crystal structure of a ferric enterobactin binding protein. *Angew. Chem. Int.* **45**:5132-5136

Nagababu, E. and Rifkind, J. M. (2004) Heme degradation by reactive oxygen species. *Antioxid. Redox. Signal.* **6**:967-978

Naikare, H., Palyada, K., Panciera, R., Marlow, D. and Stintzi, A. (2006) Major role of FeoB in *Campylobacter jejuni* ferrous iron acquisition gut colonization, and intracellular survival. *Infect. Immun.* **74**:5433-5444

Neilands, J. B. (1995) Siderophores: structure and function of microbial iron transport compounds. *J. Biol. Chem.* **23**:601-611

Newman, D. L. and Shapiro, J. A. (1999) Differential *fiu-lacZ* fusion regulation linked to *Escherichia coli* colony development. *Mol. Microbiol.* **33**:18-32

Niland, P., Hühne, R and Müller-Hill, B. (1996) How AraC interacts specifically with its target DNAs. *J. Mol. Biol.* **264**:667-674

Noinaj, N., Guillier, M., Barnard, T. J. and Buchanan, S. K. (2010) TonB-dependent transporters: regulation, structure, and function. *Annu. Rev. Microbiol.* **64**:43-60

Nowalk, A. J., Tencza, S. B. and Mietzner, T. A. (1994) Coordination of iron by ferric iron-binding protein of pathogenic *Neisseria* is homologous to the transferrins. *Biochemistry* **33**:12769-12775

O'Halloran, T. V. (1993) Transition metals in control of gene expression. *Science* **261**:715-725

Occhino, D. A., Wyckoff, E. E., Henderson, D. P., Wrona, T. J. and Payne, S. M. (1998) *Vibrio cholerae* iron transport: haem transport genes are linked to one of two set of *tonB*, *exbB*, *exbD* genes. *Mol. Microbiol.* **29**:1493-1507

Ochsner, U. A., Johnson, Z., and Vasil, M. L. (2000) Genetics and regulation of two distinct haem-uptake systems, *phu* and *has* in *Pseudomonas aeruginosa*. *Microbiology* **146**:185-198

Ochsner, U. A. and Vasil, M. L. (1996) Gene repression by the ferric uptake regulator in *Pseudomonas aeruginosa*: cycle selection of iron-regulated genes. *Proc. Natl. Acad. Sci. USA* **93**:4409-4414

Ochsner, U. A., Vasil, A. I., Johnson, Z. and Vasil, M. L. (1999) *Pseudomonas aeruginosa fur* overlaps with a gene encoding a novel outer membrane lipoprotein, OmlA. *J. Bacteriol.* **181**:1099-1109

Ochsner, U. A., Vasil, A. I. and Vasil, M. L. (1995) Role of the ferric uptake regulator of *Pseudomonas aeruginosa* in the regulation of siderophores and exotoxin A expression: purification and activity on iron-regulated promoters. *J. Bacteriol.* **177**:7194-7201

Ochsner, U. A., Wilderman, P. J., Vasil, A. I. and Vasil, M. L. (2002) GeneChip[®] expression analysis of the iron starvation response in *Pseudomonas aeruginosa*: identification of novel pyoverdine biosynthesis genes. *Mol. Microbiol.* **45**:1277-1287

Oglesby, A. G., Farrow, J. M. III., Lee, J. H., Tomaras, A. P., Greenberg, E. P., Pesci, E. C. and Vasil, M. L. (2008) The influence of iron on *Pseudomonas aeruginosa* physiology: a regulatory link between iron and quorum sensing. *J. Bio. Chem.* **283**:15558-15567

Oguiza, J. A., Tao, X., Macros, A. T., Martin, J. F. and Murphy, J. R. (1995) Molecular cloning, DNA-sequence analysis, and characterization of the *Corynebacterium diphtheriae dtxR* homolog from *Brevibacterium lactofermentum*. *J. Bacteriol.* **177**:465-467

On, S. L. W. (2001). Taxonomy of *Campylobacter*, *Arcobacter*, *Helicobacter* and related bacteria: current status, future prospects and immediate concerns. *J. Appl. Microbiol.* **90**: 1S-15S.

Outten, C. E. and O'Halloran, T. V. (2001) Femtomolar sensitivity of metalloregulatory proteins controlling zinc homeostasis. *Science* **292**:2488-2492

Outten, C. E., Tobin, D. A., Penner-Hahn, J. E. and O'Halloran, T. V. (2001) Characterization of the metal receptor sites in *Escherichia coli* Zur, an alternative zinc(II) metalloregulatory protein. *Biochemistry* **40**:10417-10423

Palyada, K., Sun, Y. Q., Flint, A., Butcher, J., Naikare, H. and Stintzi, A. (2009)

Bibliography

Characterization of the oxidative stress stimulon and PerR regulon of *Campylobacter jejuni*. *BMC Genomic* **10**:481

Palyada, K., Threadgill, D. and Stintzi, A. (2004) Iron acquisition and regulation in *Campylobacter jejuni*. *J. Bacteriol.* **186**:4714-4729

Panina, E. M., Mironov, A. A. and Gelfand, M. S. (2001) Comparative analysis of Fur regulons in gamma-proteobacteria. *Nucleic Acids Res.* **29**:5195-5206

Panina, E. M., Mironov, A. A. and Gelfand, M. S. (2003) Comparative genomics of bacterial zinc regulations: enhanced ion transport, pathogenesis, and rearrangement of ribosomal proteins. *Proc. Natl. Acad. Sci. USA* **100**:9912-9917

Park, S. F. and Richardson, P. T. (1995) Molecular characterization of a *Campylobacter jejuni* lipoprotein with homology to periplasmic siderophore-binding proteins. *J. Bacteriol.* **177**:2259-2264

Park, S. J. and Gunsalus, R. P. (1995) Oxygen, iron, carbon, and superoxide control of fumarase *fumA* and *fumC* genes of *Escherichia coli*: role of the *arcA*, *fnr*, and *soxR* gene products. *J. Bacteriol.* **177**:6255-6262

Parkhill, J., Wren, B. W., Mungall, K., Ketley, J. M., Churcher, C., Basham, D., Chillingworth, T., Davies, R. M., Feltwell, T., Holroyd, S., Jagels, K., Karlyshev, A. V., Moule, S., Pallen, M. J., Penn, C. W., Quail, M. A., Rajandream, M-A., Rutherford, K. M., van Vliet, A. H. M., Whitehead, S. and Barrell, B. G. (2000) The genome sequence of the food-borne pathogen *Campylobacter jejuni* reveals hypervariable sequences. *Nature* **403**: 665-668

Patzer, S. I. and Hantke, K. (2000) The zinc-responsive regulator Zur and its control of the *znu* gene cluster encoding the ZnuABC zinc uptake system in *Escherichia coli*. *J. Biol. Chem.* **275**:24321-24332

Pawelek, P. D., Croteau, N., Ng-Thow-Hing, C., Khursigara, C. M., Moiseeva, N., Allaire, M. and Coulton, J. W. (2006) Structure of TonB in complex with FhuA, *E. coli* outer membrane receptor. *Science* **312**:1399-1402

Pearson, B. M., Gaskin, D. J. H., Segers, R. P. A. M., Wells, J. M., Nuijten, P. J. M. and van Vliet, A. H. M. (2007) The complete genome sequence of *Campylobacter jejuni* strain 81116 (NCTC 11828). *J. Bacteriol.* **189**:8402-8403

Pecqueur, L., D'Autréaux, B., Dupuy, J., Nicolet, Y., Jacquamet, L., Brutscher, B., Michaud-Soret, I. and Bersch, B. (2006) Structural changes of *Escherichia coli* ferric uptake regulator during metal-dependent dimerization and activation explored by NMR and X-ray crystallography. *J. Biol. Chem.* **281**:21286-21295

Pei, Z., Burucoa, C., Grignon, B., Baqar, S., Huang, X. Z., Kopecko, D. J., Bourgeois, A. L., Fauchere, J. L. and Blaser, M. J. (1998). Mutation in the *peb1A* locus of *Campylobacter jejuni* reduces interactions with epithelial cells and intestinal colonisation of mice. *Infect. Immun.* **66**: 938-943

Pesci, E. C., Cottle, D. L. and Pickett, C. L. (1994) Genetics, enzymatic, and pathogenic studies of the iron superoxide dismutase of *Campylobacter jejuni*. *Infect. Immun.* **62**:2687-2694

Petersen, L., Larsen, T. S., Ussery, D. W., On, S. L. and Krogh, A. (2003) RpoD promoters in *Campylobacter jejuni* exhibit a strong periodic signal instead of a -35 box. *J. Mol. Biol.* **326**:1361-1372

Phongsisay, V and Fry, B. N. (2007) Bidirectional transcription of lipooligosaccharide synthesis genes from *Campylobacter jejuni*. *Int. J. Med. Microbiol.* **297**:431-441

Pickett, C. L., Auffenberg, T., Pesci, E. C., Sheen, V. L. and Jusuf, S. D. (1992) Iron acquisition and hemolysin production by *Campylobacter jejuni*. *Infect. Immun.* **60**:3872-3877

Pohl, E., Haller, J. C., Mijovilovich, A., Meyer-Klaucke, W., Garman, E. and Vasil, M. L. (2003) Architecture of a protein central to iron homeostasis: crystal structure and spectroscopic analysis of the ferric uptake regulator. *Mol. Microbiol.* **47**:903-915

Pohl, E., Holmes, R. K. and Hol, W. G. J. (1999) Crystal structure of a cobalt-activated diphtheria toxin repressor-DNA complex reveals a metal-binding SH3-like domain. *J. Mol. Biol.* **292**:653-667

Polack, B., Dacheux, D., Delic-Attree, I., Toussaint, B. and Vignais, P. M. (1996) The *Pseudomonas aeruginosa fumC* and *sodA* genes belong to an iron-responsive operon. *Biochem. Biophys. Res. Comm.* **226**:555-560

Posey, L. E. and Gherardini, F. C. (2000) Lack of a role for iron in the Lyme disease pathogen. *Science* **288**:1651-1653

Postle, K. (1993) TonB protein and energy transduction between membranes. *J. Bioenerg. Biomembr.* **25**:591-601

Pratt, L. A. and Silhavy, T. J. (1995) Porin regulation of *Escherichia coli*. *Two-component signal transduction*, Hoch, J. A. and Silhavy, T. J. ASM Press, Washington, DC

Prince, R. W., Cox, C. D. and Vasil, M. L. (1993) Coordinate regulation of

Bibliography

siderophore and exotoxin production: molecular cloning and sequencing of the *Pseudomonas aeruginosa fur* gene. *J. Bacteriol.* **175**:2589-2598

Privalle, C. T. and Fridovich, I. (1993) Iron specificity of the Fur-dependent regulation of the biosynthesis of the manganese-containing superoxide dismutase in *Escherichia coli*. *J. Biol. Chem.* **268**:5178-5181

Ptashne, M. (2004) *A genetic switch: Phage lambda revisited. 3rd ed.*, Cold Spring Harbor Laboratory Press, Cold Spring Harbor, New York

Rahman, M., Hasan, M. R. and Shimizu, K. (2008) Growth phase-dependent changes in the expression of global regulatory genes and associated metabolic pathways in *Escherichia coli*. *Biotechnol. Lett.* **30**:853-860

Rampersaud, A., Harlocker, S. L. and Inouye, M. (1994) The OmpR protein of *Escherichia coli* binds to sites in the *ompF* promoter region in a hierarchical manner determined by its degree of phosphorylation. *J. Biol. Chem.* **269**:12559-12566

Raphael, B. H. and Joens, L. A. (2003) FeoB is not required for ferrous iron uptake in *Campylobacter jejuni*. *Can. J. Microbiol.* **49**:727-731

Rashid, R. A., Tarr, P. I. and Moseley, S. L. (2006) Expression of the *Escherichia coli* IrgA homolog adhesin is regulated by the ferric uptake regulation protein. *Microb. Pathog.* **41**:207-217

Ratledge, C. and Dover, L. G. (2000) Iron metabolism in pathogen bacteria. *Annu. Rev. Microbiol.* **54**:881-941

Rea, R. B., Gahan, C. G. and Hill, C. (2004) Disruption of putative regulatory loci in *Listeria monocytogenes* demonstrates a significant role for Fur and PerR in virulence. *Infect. Immun.* **72**:717-727

Ren, B., Robert, F., Wyrick, J. J., Aparicio, O., Jennings, E. G., Simon, I., Zeitlinger, J., Schreiber, J., Nannett, N., Kanin, E., Volkert, T. L., Wilson, C. J., Bell, S. R. and Young, R. A. (2000) Genome-wide location and function of DNA-binding proteins. *Science* **290**:2306-2309

Richardson, P. T. and Park, S. F. (1995) Enterochelin acquisition in *Campylobacter coli*: characterization of components of a binding-protein-dependent transport system. *Microbiology* **141**:3181-3191

Ridley, K. A., Rock, J. D., Li, Y. and Ketley, J. M. (2006) Heme utilization in *Campylobacter jejuni*. *J. Bacteriol.* **188**:7862-7875

Bibliography

- River-Amill, V., Kim, B. J., Seshu, J. and Konkel, M. E.** (2001) Secretion of the virulence-associated campylobacter invasion antigens from *Campylobacter jejuni* requires a stimulatory signal. *J. Infect. Dis.* **183**:1607-1616
- Rock, J. D.** (2003) Iron acquisition from host molecules by *Campylobacter jejuni*. *Ph. D. thesis*, University of Leicester, Leicester
- Rodgers, M. E. and Schleif, R.** (2009) Solution structure of the DNA binding domain of AraC protein. *Proteins* **74**:81-91
- Rodionov, D. A., Dubchak, I., Arkin, A., Alm, E. and Gelfand, M. S.** (2004) Reconstruction of regulatory and metabolic pathways in metal-reducing δ -proteobacteria. *Genome Biol.* **5**:R90
- Rodionov, D. A., Gelfand, M. S., Todd, J. D., Curson, A. R. J. and Johnston, A. W. B.** (2006) Computational reconstruction of iron- and manganese-responsive transcriptional networks in α -proteobacteria. *PLoS Comput. Biol.* **2**:e163
- Rollins, D. M. and Colwell, R. R.** (1986). Viable but nonculturable stage of *Campylobacter jejuni* and its role in survival in the natural aquatic environment. *Appl. Environ. Microbiol.* **52**: 531-538
- Romeo, T.** (1996) Post-transcriptional regulation of bacterial carbohydrate metabolism: evidence that the gene product CsrA is a global mRNA decay factor. *Res. Microbiol.* **147**:505-512
- Saito, T. and Williams, R. J. P.** (1991) The binding of the ferric uptake regulation protein to a DNA fragment. *Eur. J. Biochem.* **197**:43-47
- Saito, T., Duly, D. and Williams, R. J. P.** (1991a) The histidines of the iron-uptake regulation protein Fur. *Eur. J. Biochem.* **197**:39-42
- Saito, T., Wormald, M. R. and Williams, R. J. P.** (1991b) Some structural features of the iron-uptake regulator protein. *Eur. J. Biochem.* **197**:29-38
- Sanger, F., Nicklen, S. and Coulson, A. R.** (1977) DNA sequencing with chain-termination inhibitors. *Proc. Natl. Acad. Sci. USA* **74**:5463-5467
- Sauter, A. and Braun, V.** (2004) Defined inactive FecA derivatives mutated in functional domains of the outer membrane transport and signalling protein of *Escherichia coli* K-12. *J. Bacteriol.* **186**:5303-5310
- Saviola, B., Seibold, R. and Schleif, R.** (1998) Arm-domain interactions in AraC. *J. Mol. Biol.* **278**:539-548

Schäffer, S., Hantke, K. and Braun, V. (1985) Nucleotide sequence of the iron regulatory gene *fur*. *Mol. Gen. Genet.* **200**:110-113

Schaible, U. E. and Kaufmann, S. H. E. (2004) Iron and microbial infection. *Nat. Rev. Microbiol.* **2**:946-953

Schleif, R. (2003) The AraC protein a love-hate relationship. *Bioessays* **25**:274-282

Sebald, M. and Véron, M. (1963) Teneur en bases de l'ADN et classification des vibrions. *Ann. Inst. Pasteur* **105**:897-910

Sebastian, S., Agarwal, S., Murphy, J. R. and Genco, C. A. (2002) The gonococcal Fur regulon: identification of additional genes involved in major catabolic, recombination, and secretory pathways. *J. Bacteriol.* **184**:3965-3974

Sechasayee, A. S. H., Bertone, P., Fraser, G. M. and Luscombe, N. M. (2006) Transcriptional regulatory networks in bacteria: from input signals to output responses. *Curr. Opin. Microbiol.* **9**:511-519

Shearer, N., Haigh, R. D., Perrett, C. A., Ketley, J. M., Humphrey, T. J., van Vliet, A. H. M. and Pearson, B. M. (2009) Fur regulation of the divergent *Campylobacter jejuni* *cfrA* and *tonB3* promoters. *CampylobacterUK 2009 abstracts*. 19

Sheikh, M. A. and Taylor, G. L. (2009) Crystal structure of the *Vibrio cholerae* ferric uptake regulator (Fur) reveals insights into metal co-ordination. *Mol. Microbiol.* **72**:1208-1220

Skaar, E. P., Gaspar, A. H. and Schneewind, O. (2004) Heme-degrading enzymes in the cytoplasm of *Staphylococcus aureus*. *J. Biol. Chem.* **279**:436-443

Skirrow, M. B. (1977) *Campylobacter* enteritis: a 'new' disease. *Br. Med. J.* **2**:9-11

Skirrow, M. B. (2006) John McFadyean and the centenary of the first isolation of *Campylobacter* species. *Clin. Infect. Dis.* **43**:1213-1217

Smith, J. (2004) The physiological role of ferritin-like compounds in bacteria. *Crit. Rev. Microbiol.* **30**:173-185

Smith, M. A., Mendz, G. L., Jorgensen, M. A. and Hazell, S. L. (1999) Fumarate metabolism and the microaerophily of *Campylobacter* species. *Int. J. Biochem. Cell Biol.* **31**:961-975

Smith, T. and Taylor, M. S. (1919) Some morphological and biochemical characters of

Bibliography

the spirilla (*Vibrio fetus* n. sp.) associated with disease of the fetal membranes in cattle. *J. Exp. Med.* **310**:299-312

Snelling, W. J., Matsuda, M., Moore, J. E. and Dooley, J. S. G. (2005). *Campylobacter jejuni*. *Lett. Appl. Microbiol.* **41**: 297-302

Snyder, L. and Champness, W. (2003) Global regulatory mechanisms. *Molecular genetics of bacteria*, 2nd ed., ASM Press, Washington, DC

Soisson, T. M., MacDougall-Shackleton, B., Schleif, R. and Wolberger, C. (1997) Structural basis for ligand-regulated oligomerization of AraC. *Science* **276**:421-425

Sommerlad, S. M. and Hendrixson, D. R. (2007) Analysis of the roles of FlgP and FlgQ in flagellar motility of *Campylobacter jejuni*. *J. Bacteriol.* **189**:179-186

Song, Y. C., Jin, S., Louie, H., Ng, D., Lau, R., Zhang, Y., Weerasekera, R., Al Rashid, S., Ward, L. A., Der, S. D. and Chan, V. L. (2004) FlaC, a protein of *Campylobacter jejuni* TGH9011 (ATCC43431) secreted through the flagellar apparatus, binds epithelial cells and influences cell invasion. *Mol. Microbiol.* **53**:541-553

Staggs, T. M. and Perry, R. D. (1991) Identification and cloning of a *fur* regulatory gene in *Yersinia pestis*. *J. Bacteriol.* **173**:417-425

Stintzi, A. (2003) Gene expression profile of *Campylobacter jejuni* in response to growth temperature variation. *J. Bacteriol.* **185**:2009-2016

Stintzi, A., Marlow, D., Palyada, K., Naikare, H., Panciera, R., Whitworth, L. and Clarke, C. (2005) Use of genome-wide expression profiling and mutagenesis to study the intestinal lifestyle of *Campylobacter jejuni*. *Infect. Immun.* **73**:1797-1810

Stintzi, A., van Vliet, A. H. M. and Ketley, J. K. (2008) Iron metabolism, transport, and regulation. *Campylobacter*, 3rd ed., Nachamkin, I., Szymanski, C. M. and Blaser, M. J. ASM Press, Washington, DC

Stock, A. M., Robinson, V. L. and Goudreau, P. N. (2000) Two-component signal transduction. *Annu. Rev. Biochem.* **69**:183-215

Stoebner, J. A. and Payne, S. M. (1998) Iron-regulated hemolysin production and utilization of heme and hemoglobin by *Vibrio cholerae*. *Infect. Immun.* **56**:2891-2895

Stojiljkovic, I., Bäumlner, A. J. and Hantke, K. (1994) Fur regulon in gram-negative bacteria. Identification and characterization of new iron-regulated *Escherichia coli* by a Fur titration assay. *J. Mol. Biol.* **236**:531-545

Stojiljkovic, I., Cobeljic, M. and Hantke, K. (1993) *Escherichia coli* K-12 ferrous iron uptake mutants are impaired in their ability to colonize the mouse intestine. *FEMS Microbiol. Lett.* **108**:111-116

Stojiljkovic, I. and Hantke, K. (1994) Transport of haemin across the cytoplasmic membrane through a haemin-specific periplasmic binding-protein-dependent transport system in *Yersinia enterocolitica*. *Mol. Microbiol.* **13**:719-732

Stojiljkovic, I. and Hantke, K. (1995) Functional domains of the *Escherichia coli* uptake regulator protein. *Mol. Gen. Genet.* **247**:199-205

Stojiljkovic, I., Larson, J., Hwa, V., Anic, S. and So, M. (1996) HmbR outer membrane receptors of pathogenic *Neisseria* spp. Iron-regulated, hemoglobin-binding proteins with a high level of primary structure conservation. *J. Bacteriol.* **178**:4670-4678

Suits, M. D. L., Pal, G. P., Nakatsu, K., Matte, A., Cygler, M. and Jia, Z. (2005) Identification of an *Escherichia coli* O157:H7 heme oxygenase with tandem functional repeats. *Proc. Natl. Acad. Sci. USA* **102**:16955-16960

Szymanski, C. M. and Wren, B. W. (2005) Protein glycosylation in bacterial mucosal pathogens. *Nat. Rev. Microbiol.* **3**:225-237

Takata, T., Fujimoto, S. and Amako, K. (1992). Isolation of nonchemotactic mutants of *Campylobacter jejuni* and their colonisation of the mouse intestinal tract. *Infect. Immun.* **60**: 3596-3600

Tanaka, T., Saha, S. K., Tomomori, C., Ishima, R., Liu, D., Tong, K. I., Park, H., Dutta, R., Qin, L., Swindells, M. B., Yamazaki, T., Ono, A. M., Kainosho, M., Inouye, M. and Ikura, M. (1998) NMR structure of the histidine kinase domain of the *E. coli* osmosensor EnvZ. *Nature* **396**:88-92

Teixidó, L., Carrasco, B., Alonso, J. C., Barbé, J. and Campoy, S. (2011) Fur activates the expression of *Salmonella enterica* pathogenicity island 1 by directly interacting with the *hilD* operator *in vivo* and *in vitro*. *PLoS One* **6**:e19711

Thomas, C. E. and Sparling, P. F. (1994) Identification and cloning of a *fur* homologue from *Neisseria meningitidis*. *Mol. Microbiol.* **11**:725-737

Thompson, J. M., Jones, H. A. and Perry, R. D. (1999) Molecular characterization of the hemin uptake locus (*hmu*) from *Yersinia pestis* and analysis of *hmu* mutants for hemin and hemoprotein utilization. *Infect. Immun.* **67**:3879-3892

Thompson, S. A., Li, J. and Fields, J. A. (2009) Post-transcriptional regulation of

Bibliography

Campylobacter jejuni virulence properties. 15th international workshop on campylobacter, helicobacter, and related organisms abstracts. 36

Tiss, A., Barre, O., Michaud-Soret, I. and Forest, E. (2005) Characterisation of the DNA-binding site in the ferric uptake regulator protein from *Escherichia coli* by UV crosslinking and mass spectrometry. *FEBS Lett.* **579**: 5454-5460

Todd, J. D., Sawers, G., Rodionov, D. A. and Johnston, A. W. B. (2006). The *Rhizobium leguminosarum* regulator IrrA affects the transcription of a wide range of genes in response to Fe availability. *Mol. Genet. Genomics* **275**:564-577

Todd, J. D., Wexler, M., Sawers, G., Yeoman, K. H., Poole, P. S. and Johnston, A. W. B. (2002) RirA, an iron-responsive regulator in the symbiotic bacterium *Rhizobium leguminosarum*. *Microbiology* **148**:4059-4071

Tomomori, C., Tanaka, T., Dutta, R., Park, H., Saha, S. K., Zhu, Y., Ishima, R., Liu, D., Tong, K. I., Kurokawa, H., Qian, H., Inouye, M. and Ikura, M. (1999) Solution structure of the homodimeric core domain of *Escherichia coli* histidine kinase EnvZ. *Nat. Struct. Biol.* **6**:728-734

Tong, Y. and Guo, M. (2009) Bacterial heme-transport proteins and their heme-coordination modes. *Arch. Biochem. Biophys.* **481**:1-15

Torres, A. G., and Payne, S. M. (1997) Haem iron-transport system in enterohaemorrhagic *E. coli* O157:H7. *Mol. Microbiol.* **23**:825-833

Touati, D. (2000) Iron and oxidative stress in bacteria. *Arch. Biochem. Biophys.* **373**:1-6

Traoré, D. A. K., El Ghazouani, A., Ilango, S., Dupuy, J., Jacquamet, L., Ferrer, J. L., Caux-Thang, C., Duarte, V. and Latour, J. M. (2006) Crystal structure of the apo-PerR-Zn protein from *Bacillus subtilis*. *Mol. Microbiol.* **61**:1211-1219

Trust, T. J., Logan, S. M., Gustafson, C. E., Romaniuk, P. J., Kim, N. W., Chan, V. L., Ragan, M. K., Guerry, P. and Gutell, R. R. (1994) Phylogenetic and molecular characterization of a 23S rRNA gene positions the genus *Campylobacter* in the epsilon subdivision of the *Proteobacteria* and shows that the presence of transcribed spacers is common in *Campylobacter* spp. *J. Bacteriol.* **176**:4597-4609

Tseng, C. P. (1997) Regulation of fumarase (*fumB*) gene expression in *Escherichia coli* in response to oxygen, iron and heme availability: role of the *arcA*, *fur*, and *hemA* gene products. *FEMS Microbiol. Lett.* **175**:67-72

Tseng, C. P., Yu, C. C., Lin, H. H., Chang, C. Y. and Kuo, J. T. (2001) Oxygen- and growth rate-dependent regulation of *Escherichia coli* fumarase (FumA, FumB, and

FumC) activity. *J. Bacteriol.* **183**:461-467

Tsolis, R. M., Bäumlner, A. J., Heffron, F. and Stojiljkovic, I. (1996) Contribution of TonB- and Feo-mediated iron uptake to growth of *Salmonella typhimurium* in the mouse. *Infect. Immun.* **64**:4549-4556

Ueda, Y., Yumoto, N., Tokushige, M., Fukui, K. and Ohya-Nishiguchi, H. (1991) Purification and characterization of two type of fumarase from *Escherichia coli*. *J. Biochem.* **109**:728-733

Ueshima, J., Shoji, M., Ratnayake, D. B., Abe, K., Yoshida, S., Yamamoto, K. and Nakayama, K. (2003) Purification, gene cloning, gene expression, and mutants of Dps from the obligate anaerobe *Porphyromonas gingivalis*. *Infect. Immun.* **71**:1170-1178

van Mourik, A., Guilhabert, M. R., Heijmen-van Dijk, L., Parker, G. T., van Putten, J. P. M. and Wösten, M. M. S. M. (2009) The RacR-RacS two component system alters the energy metabolism in response to oxygen. *15th international workshop on campylobacter, helicobacter, and related organisms abstracts*. 104

van Vliet, A. H. M., Baillon, M. L. A., Penn, C. W. and Ketley, J. M. (1999) *Campylobacter jejuni* contains two Fur homologs: characterization of iron-responsive regulation of peroxide stress defense genes by the PerR repressor. *J. Bacteriol.* **181**:6371-6376

van Vliet, A. H. M., Baillon, M. L. A., Penn, C. W. and Ketley, J. M. (2001) The iron-induced ferredoxin FdxA of *Campylobacter jejuni* is involved in aerotolerance. *FEMS Microbiol. Lett.* **196**:189-193

van Vliet, A. H. M. and Ketley, J. M. (2001). Pathogenesis of enteric *Campylobacter* infection. *J. Appl. Microbiol.* **90**: 45S-56S.

van Vliet, A. H. M., Ketley, J. M., Park, S. F. and Penn, C. W. (2002) The role of iron in *Campylobacter* gene regulation, metabolism and oxidative stress defence. *FEMS Microbiol. Rev.* **26**:173-186

van Vliet, A. H. M., Rock, J. D., Medeleine, L. N. and Ketley, J. M. (2000) The iron-regulated regulator Fur of *Campylobacter jejuni* is expressed from two separate promoters. *FEMS Microbiol. Lett.* **188**:115-118

van Vliet, A. H. M., Stoof, J., Poppelaars, S. W., Bereswill, S., Homuth, G., Kist, M., Kuipers, E. J. and Kusters, J. G. (2003) Differential regulation of amidase- and formamidase-mediated ammonia production by the *Helicobacter pylori* Fur repressor. *J. Biol. Chem.* **278**:9052-9057

Bibliography

van Vliet, A. H. M., Wooldridge, K. G. and Ketley, J. M. (1998) Iron-responsive gene regulation in a *Campylobacter jejuni* *fur* mutant. *J. Bacteriol.* **198**:5291-5298

Vasil, M. L. (2007) How we learnt about iron acquisition in *Pseudomonas aeruginosa*: a series of very fortunate events. *Biomaterials* **20**:587-601

Velayudhan, J., Hughes, N. J., McColm, A. A., Bagshaw, J., Clayton, C. L., Andrews, S. C. and Kelly, D. J. (2000) Iron acquisition and virulence in *Helicobacter pylori*: a major role for FeoB, a high-affinity ferrous iron transporter. *Mol. Microbiol.* **37**:274-286

Véron, M. and Chatelain, R. (1973) Taxonomic study of the genus *Campylobacter* Sebald and Véron and designation of the neotype strain for the type species *Campylobacter fetus* (Smith and Taylor) Sebald and Véron. *Int. J. Syst. Bacteriol.* **23**:122-134

Vinzent, R., Dumas, J. and Picard, N. (1947) Septicémie grave eu cours de la grossesse, due à un vibrion. Avortement consécutif. *C. R. Acad. Med.* **131**:90

Voskuil, M. I., Voepel, K. and Chambliss, G. H. (1995) The -16 region, a vital sequence for the utilization of a promoter in *Bacillus subtilis* and *Escherichia coli*. *Mol. Microbiol.* **17**:271-279

Wai, S. N., Nakayama, K., Umene, K., Moriya, T. and Amako, K. (1996) Construction of a ferritin-deficient mutant of *Campylobacter jejuni*: contribution of ferritin to iron storage and protection against oxidative stress. *Mol. Microbiol.* **20**:1127-1134

Waidner, B., Gleinear, S., Odenbreit, S., Kavermann, H., Velayudhan, J., Stähler, F., Guhl, J., Bissé, E., van Vliet, A. H. M., Andrews, S. C., Kusters, J. G., Kelly, D. J., Haas, R., Kist, M. and Bereswill, S. (2002) Essential role of ferritin Pfr in *Helicobacter pylori* iron metabolism and gastric colonization. *Infect. Immun.* **70**:3923-3929

Waldron, K. J. and Robinson, N. J. (2009) How do bacterial cells ensure that metalloproteins get the correct metal? *Nat. Rev. Microbiol.* **7**:25-35

Wandersman, C. and Delepelaire, P. (2004) Bacterial iron sources: from siderophores to hemophores. *Annu. Rev. Microbiol.* **58**:611-647

Wang, Y. and Taylor, D. E. (1990) Natural transformation in *Campylobacter* species. *J. Bacteriol.* **172**:949-955

Wassenaar, T. M. (1997). Toxin production by *Campylobacter* spp. *Clin. Microbiol.*

Wassenaar, T. M. and Blaser, M. J. (1999). Pathophysiology of *Campylobacter jejuni* infections of humans. *Micro. Infect.* **1**: 1023-1033

Wassenaar, T. M., Bleumink-Pluym, N. M. C., Newell, D. G., Nuijten, P. J. and van der Zeijst, B. A. M. (1994). Differential flagellin expression in a *flaA flaB*⁺ mutant of *Campylobacter jejuni*. *Infect. Immun.* **62**:3901-3906

Wassenaar, T. M., Bleumink-Pluym, N. M. C. and van der Zeijst, B. A. M. (1991) Inactivation of *Campylobacter jejuni* flagellin genes by homologous recombination demonstrates that *flaA* but not *flaB* is required for invasion. *EMBO J.* **10**:2055-2061

Wassenaar, T. M., van der Zeijst, B. A. M., Ayling, R. and Newell, D. G. (1993) Colonization of chicks by motility mutants of *Campylobacter jejuni* demonstrates the importance of flagellin A expression. *J. Gen. Microbiol.* **139**:1171-1175

Wee, S., Neilands, J. B., Bittner, M. L., Hemming, B. C., Haymore, B. L. and Seetharam, R. (1988) Expression, isolation and properties of Fur (ferric uptake regulation) protein of *Escherichia coli* K12. *Biometals* **1**:62-68

Weinberg, E. D. (1997) The Lactobacillus anomaly: total iron abstinence. *Perspect. Biol. Med.* **40**:578-583

Weinberg, E. D. (2009) Iron availability and infection. *Biochim. Biophys. Acta.* **1790**:600-605

Weldon, J. E., Rodgers, M. E., Larkin, C. and Schleif, R. F. (2007) Structure and properties of a truly apo form of AraC dimerization domain. *Protein* **66**:646-654

Wexler, M., Todd, J. D., Kolade, O., Bellini, D., Hemmings, A. M., Sawers, R. G. and Johnston, A. W. B. (2003). Fur is not the global regulator of iron uptake gene in *Rhizobium leguminosarum*. *Microbiology* **149**:1357-1365

White, A., Ding, X., van der Spek, J. C., Murry, J. R. and Ringe, D. (1998) Structure of the metal-ion-activated diphtheria toxin repressor/*tox* operator complex. *Nature* **394**:502-506

Whitehouse, C. A., Balbo, P. B., Pesci, E. C., Cottle, D. L., Mirabito, P. M. and Pickett, C. L. (1998). *Campylobacter jejuni* cytolethal distending toxin causes a G₂-phase cell cycle block. *Infect. Immun.* **66**: 1934-1940

Wilderman, P. J., Sowa, N. A., FitzGerald, D. J., FitzGerald, P. C., Gottesman, S., Ochsner, U. A. and Vasil, M. L. (2004) Identification of tandem duplicate regulatory

Bibliography

small RNAs in *Pseudomonas aeruginosa* involved in iron homeostasis. *Proc. Natl. Acad. Sci. USA* **101**:9792-9797

Wilks, A. (2001) The ShuS protein of *Shigella dysenteriae* is a heme-sequestering protein that also binds DNA. *Arch. Biochem. Biophys.* **387**:137-142

Wilson, D. J., Gabriel, E., Leatherbarrow, A. J. H., Cheesbrough, J., Gee, S., Bolton, E., Fox, A., Fearnhead, P., Hart, C. A. and Diggle, P. J. (2008) Tracing the source of campylobacteriosis. *PLoS Genet.* **4**:e10000203

Woodall, C. A., Jones, M. A., Barrow, P. A., Hinds, J., Marsden, G. L., Kelly, D. J., Dorrell, N., Wren, B. W. and Maskell, D. J. (2005) *Campylobacter jejuni* gene expression in the chick cecum: evidence for adaptation to a low-oxygen environment. *Infect. Immun.* **73**:5278-5285

Wooldridge, K. G. and Ketley, J. M. (1997). *Campylobacter*-host cell interaction. *Trends Microbiol.* **5**: 96-102

Wooldridge, K. G. and Williams, P. H. (1993) Iron uptake mechanisms of pathogenic bacteria. *FEMS Microbiol. Rev.* **12**:325-348

Wooldridge, K. G., Williams, P. H. and Ketley, J. M. (1994) Iron-responsive genetic regulation in *Campylobacter jejuni*: cloning and characterisation of a *fur* homolog. *J. Bacteriol.* **176**:5852-5856

Woods, S. A. and Guest, J. R. (1988) Differential roles of the *Escherichia coli* fumarases and *fnr*-dependent expression of fumarase B and aspartase. *FEMS Microbiol. Lett.* **48**:219-224

Woods, S. A., Miles, J. S., Roberts, R. E. and Guest, J. R. (1986) Structural and functional relationships between fumarase and aspartase. *Biochem. J.* **237**:547-557

Woods, S. A., Schwartzbach, S. D. and Guest, J. R. (1988) Two biochemically distinct classes of fumarase in *Escherichia coli*. *Biochim. Biophys. Acta.* **954**:14-26

Worst, D. J., Gerrits, M. M., Vandenbroucke, G. C. and Kusters, G. (1988) *Helicobacter pylori* *ribBA*-mediated riboflavin production is involved in iron acquisition. *J. Bacteriol.* **180**:1473-1479

Wösten, M. M. S. M., Boeve, M., Koot, M. G. A., van Nuene, A. C. and van der Zeijst, B. A. M. (1998) Identification of *Campylobacter jejuni* promoter sequences. *J. Bacteriol.* **180**:594-599

Wösten, M. M. S. M., Paker, C. T., van Mourik, A., Guilhabert, M. R., van Dijk, L.

and van Puttrn, J. P. M. (2006) The *Campylobacter jejuni* PhosS/PhosR operon represents a non-classical phosphate-sensitive two-component system. *Mol. Microbiol.* **62**:278-291

Wösten, M. M. S. M., van Mourik, A. and van Putten, J. P. M. (2008) Regulation of genes in *Campylobacter jejuni*. *Campylobacter*, 3rd ed., Nachamkin, I., Szymanski, C. M. and Blaser, M. J. ASM Press, Washington, DC

Wösten, M. M. S. M, Wagenaar, J. A. and van Putten, J. P. M. (2004) The FlgS/FlgR two-component signal transduction system regulates the *flg* regulon in *Campylobacter jejuni*. *J. Biol. Chem.* **279**:16214-16222

Xiao, B., Li, W., Guo, G., Li, B., Liu, Z., Jia, K., Guo, Y., Mao, X. and Zou, Q. (2009) Identification of small noncoding RNAs in *Helicobacter pylori* by a bioinformatics-based approach. *Curr. Microbiol.* **58**:258-263

Xu, F., Zeng, X., Haigh, R. D., Ketley, J. M. and Lin, J. (2010) Identification and characterization of a new ferric enterobactin receptor, CfrB, in *Campylobacter*. *J. Bacteriol.* **192**:4425-4435

Yanatori, I., Tabuchi, M., Kawai, Y., Yasui, Y., Akagi, R. and Kishi, F. (2010) Heme and non-heme iron transporters in non-polarized and polarized cells. *BMC Cell Biol.* **11**:39

Yao, R., Burr, D. H., Doig, P., Trust, T. J., Niu, H. and Guerry, P. (1994). Isolation of motile and non-motile insertional mutants of *Campylobacter jejuni*: the role of motility in adherence and invasion of eukaryotic cells. *Mol. Microbiol.* **14**: 883-893

Yao, R., Burr, D. H. and Guerry, P. (1997). CheY-mediated modulation of *Campylobacter jejuni* virulence. *Mol. Microbiol.* **23**: 1021-1031

Yasmin, S., Andrews, S. C., Moore, G. R. and Le Brun, N. E. (2011) A new role for heme, facilitating release of iron from the bacterioferritin iron biomineral. *J. Biol. Chem.* **286**:3473-3483

Young, K. T., Davis, L. M. and DiRita, V. J. (2007) *Campylobacter jejuni*: molecular biology and pathogenesis. *Nat. Rev. Microbiol.* **5**:665-679

Zahrt, T. C., Song, J., Siple, J. and Deretic, V. (2001) Mycobacterial FurA is a negative regulator of catalase-peroxidase gene *katG*. *Mol. Microbiol.* **39**:1174-1185

Zeng, X., Xu, F. and Lin, J. (2009) Molecular, antigenic, and functional characteristics of ferric enterobactin receptor CfrA in *Campylobacter jejuni*. *Infect. Immun.* **77**:5437-5448

- Zhang, M., Xiao, D., Zhao, F., Gu, Y., Meng, F., He, L., Ma, G. and Zhang, J.** (2009) Comparative proteomic analysis of *Campylobacter jejuni* cultured at 37 °C and 42 °C. *Jpn. J. Infect. Dis.* **62**:356-361
- Zhang, X., Reeder, T. and Schleif, R.** (1996) Transcription activation parameters at *ara pBAD*. *J. Mol. Biol.* **258**:14-24
- Zhang, X. and Schleif, R.** (1998) Catabolite gene activator protein mutations affecting activity of the *araBAD* promoter. *J. Bacteriol.* **180**:195-200
- Zhao, G., Ceci, P., Ilair, A., Giangiacomo, L., Laue, T. M., Chiancone, E. and Chasteen, N. D.** (2002) Iron and hydrogen peroxide detoxification properties of DNA-binding protein from starved cells. A ferritin-like DNA-binding protein of *Escherichia coli*. *J. Biol. Chem.* **277**:27689-27696
- Zheng, L., Baumann, U. and Reymond, J.** (2004) An efficient one-step site-directed and site-saturation mutagenesis protocol. *Nucleic Acids Res.* **32**:e115
- Zheng, M., Aslund, F. and Storz, G.** (1998) Activation of the OxyR transcription factor by reversible disulfide bond formation. *Science* **279**:1718-1721
- Zheng, M., Doan, B., Schneider, T. D. and Storz, G.** (1999) OxyR and SoxRS regulation of *fur*. *J. Bacteriol.* **181**:4639-4643
- Zhu, W., Wilks, A. and Stojiljkovic, I.** (2000) Degradation of heme in Gram-negative bacteria: the product of the *hemO* gene of *Neisseriae* is a heme oxygenase. *J. Bacteriol.* **182**:6783-6790
- Ziprin, R. L., Young, C. R., Byrd, J. A., Stanker, L. H., Hume, M. E., Gray, S. A., Kim, B. J. and Konkel, M. E.** (2001) Role of *Campylobacter jejuni* potential virulence genes in cecal colonization. *Avian Dis.* **45**:549-557
- Ziprin, R. L., Young, C. R., Stanker, L. H., Hume, M. E. and Konkel, M. E.** (1999). The absence of cecal colonisation of chicks by a mutant of *Campylobacter jejuni* not expressing bacterial fibronectin-binding protein. *Avian Dis.* **43**: 586-589